UNIVERSITY OF LEEDS

Context- and Terrain-Aware Gait Analysis and Activity Recognition

John Charles Mitchell

Submitted in accordance with the requirements for the degree
of PhD in Mechanical Engineering

The University of Leeds

Faculty of Engineering

School of Mechanical Engineering

September 2024

Intellectual Property

I confirm that the work submitted is my own and that appropriate credit has been given where reference has been made to the work of others.

This copy has been supplied on the understanding that it is copyright material and that no quotation from the thesis may be published without proper acknowledgement.

This copy has been supplied on the understanding that it is copyright material and that no quotation from the thesis may be published without proper acknowledgement.

© 2024 The University of Leeds, John Charles Mitchell

Signed

Acknowledgements

This research has been carried out with the invaluable assistance and guidance of my supervisors: Professor Abbas A. Dehghani-Sanij, Professor Sheng Q. Xie, and Professor Rory J. O'Connor.

Firstly, I would like to thank Professor Dehghani-Sanij for creating the opportunity for me to undertake a PhD during our initial meetings in 2020, and for organising my involvement in several enriching and useful aspects of the PhD such as journal reading clubs, demonstrating and teaching, networking with other researchers, and contributing towards a book chapter.

Secondly, I would like to thank Professor Xie for his insight into several technical aspects of the work, for introducing me to a large network of fellow researchers, and for offering his expertise, experience, and insight into a number of journals and conferences, which has helped me develop my academic writing skills and write for IEEE journals.

Finally, I would like to thank Professor O'Connor for assisting in the various healthcare and practical aspects of the research, such as: the National Health Service (NHS) Health Research Authority (HRA) ethical review; recruiting and performing the data collection procedure with our 20 participants; and advancing my writing style to be more suited for healthcare journals.

Together, my supervisors created the perfect environment for an enjoyable and enriching 4 years, for which I am extremely grateful.

In addition to my supervisors, I would like to thank Dr. Zhenhong Li for his contributions to the systematic review. Dr. Li undertook the title, abstract, and full record screening for the fall intervention papers, helping to make our large-scale review more manageable.

Finally, I would like to thank my family for accommodating my transformation of our house into a laboratory, along with my friends Andrew Chai, David Russell, and Luke Shannon for offering opinions, advice, and guidance on multiple aspects of this project.

Abstract

The global population is ageing, causing an increase in the number of people living with age-related gait-affecting conditions that increase risk of falling. Current methods of gait analysis enable healthcare professionals to evaluate a person's fall risk and inform rehabilitation. However, gait analysis in unable to reproduce the real-world contexts in which people walk, limiting its capacity as a tool for diagnosis and prognosis with respect to falls. Wearable sensors show promise in enabling gait data to be captured outside the laboratory, but the context-labelling of this data is necessary due to the dependency of gait on walking activity and terrain. Whilst the field of Human Activity Recognition (HAR) provides successful methods of determining walking activity, recent studies have highlighted a lack of consideration for terrain variation among HAR datasets.

This work aims to produce a prototype automatic gait analysis system capable of collecting gait data and labelling it with the context — that is, the activity and terrain, in which the data was collected. Particularly, this work places a focus on producing the first dataset which enables high-accuracy terrain classification using wearable sensors to take gait analysis out of the laboratory and into the real world.

To achieve this aim, a comprehensive background and literature review is established, which finds that technologies that address the underlying spatio-temporal gait parameters have the widest reach and can be applied to both healthy and gait-impaired individuals alike. Following this background, the thesis comprises material from four research papers submitted to various journals and conferences, the first of which is a systematic review which explores the differing healthcare and technological approaches to fall prevention and highlights a lack of real-world data in many fall-related technologies, limiting the generalisation of proposed systems. Then, an exploratory analysis into existing HAR datasets and methods for achieving high activity classi-

fication accuracies finds that Support Vector Machines (SVMs) and Artificial Neural Networks (ANNs) enable the highest classification accuracies, whilst Inertial Measurement Units (IMUs) are the highest performing sensor types for activity classification. A novel sensor system is then designed, comprising IMU sensors, Force Sensing Resistor (FSR) insoles, and novel LiDAR and colour sensor implementations, which are investigated for their use in terrain recognition. This sensor system is used to collect the Context-Aware Human Activity Recognition (CAHAR) dataset, which features 7.8 hours of gait data collected from 20 participants, who each perform 38 combinations of 11 unique activities on 9 different indoor and outdoor terrains. This dataset enables novel investigations into the effects of terrain on gait, and the detectability of these changes using wearable sensors. Analysing this novel dataset shows that both the activity and terrain in which gait data was collected can be classified using SVMs with 96% accuracy for an optimised set of sensors featuring just IMU and colour sensor data only.

Overall, this thesis makes major contributions towards the fields of HAR and fall research through the identification of interdisciplinary research gaps in the fall literature, a bias-reduced analysis of existing HAR datasets, the development of a novel sensor system for both HAR and terrain classification, the collection of the first multi-terrain HAR dataset, and the demonstration of the feasibility of high-accuracy terrain classification using wearable sensors. Each of these contributions help to construct a foundation for remote gait analysis systems that can determine the full context in which gait data was captured outside the laboratory.

Contents

List of Figures

List of Tables

List of Abbreviations

ABC Activities-specific Balance Confidence Scale.

ACE-R Addenbrooke's Cognitive Examination-Revised.

AD Alzheimer's Disease.

ADL Activity of Daily Living.

ANN Artificial Neural Network.

ANOVA Analysis of Variance.

AST Alternate Step Test.

BBS Berg Balance Scale.

BIRCH Balanced Iterative Reducing and Clustering using Hierarchies.

BLS Bureau of Labour Statistics.

BT Balance training.

CAH Chapel Allerton Hospital.

CAHAR Context-Aware Human Activity Recognition.

CNN Convolutional Neural Network.

CoG Centre of Gravity.

CoM Centre of Mass.

CoP Centre of Pressure.

DALY Disability-Adjusted Life Year.

DFA Detrended Fluctuation Analysis.

DL Deep Learning.

DNN Deep Neural Network.

DRNN Deep Recurrent Neural Network.

DT Decision Tree.

DwLB Dementia with Lewy Bodies.

DwPD Dementia with Parkinson's Disease.

ECG Electrocardiogram.

EEG Electroencephalogram.

EMG Electromyography.

FDD Fall Detection Dataset.

FES Falls Efficacy Scale.

FN False Negative.

FNOW Fully Non-Overlapping Windows.

FNR False Negative Rate.

FoF Fear of Falling.

FOG Freezing of Gait.

FP False Positive.

FPR False Positive Rate.

FRT Functional Reach Test.

FSR Force Sensing Resistor.

GADS Generalized Anxiety Disorder Scale.

GB Gradient Boosting.

GRF Ground Reaction Force.

HAR Human Activity Recognition.

HMM Hidden Markov Model.

HQFS High Quality Fall Simulation.

HRA Health Research Authority.

HRQOL Health-Related Quality of Life.

HS Heel Strike.

IADL Instrumental Activity of Daily Living.

IC Initial Contact.

IDE Integrated Development Environment.

IFES Iconographical Falls Efficacy Scale.

IMU Inertial Measurement Unit.

IoT Internet of Things.

ISw Initial Swing.

KARD Kinect Activity Recognition Dataset.

KNN K-Nearest Neighbours.

LDA Linear Discriminant Analysis.

LESS Lower Extremity Strength Score.

LLA Lower-limb Amputee.

LLFDI Late Life Function and Disability Instrument.

LOSO Leave One Subject Out.

LR Loading Response.

LS Least Squares.

LSTM Long Short-Term Memory.

MAE Mean Absolute Error.

MCF Multiple Cameras Fall.

ML Machine Learning.

MoS Margin of Stability.

MPE Multi-system Physical Exercise.

MPK Microprocessor Knee.

MRI Magnetic Resonance Imaging.

MS Multiple Sclerosis.

MSt Mid-Stance.

MSw Mid-Swing.

NB Naïve Bayes.

NCC Nearest Centroid Classifier.

NHS National Health Service.

NPV Negative Predicted Value.

NRS Numeric Rating Scale.

NUCLA Northwestern-University of California.

ONS Office of National Statistics.

PCA Principal Component Analysis.

PD Parkinson's Disease.

PHQ-9 Patient Health Questionnaire 9.

PIR Pyroelectric Infrared.

PLA Polylactic Acid.

PPA Physiological Profile Assessment.

PPAS Physiological Profile Assessment Scores.

PPV Positive Predicted Value.

PRISMA Preferred Reporting Items for Systematic Reviews and Meta-Analyses.

PSw Pre-Swing.

PwMS People with Multiple Sclerosis.

PwPD People with Parkinson's Disease.

QDA Quadratic Discrimenant Analysis.

RCI Reciprocal Compensatory Index.

RCR Range Control Radar.

RF Random Forest.

RGB Red Green Blue.

RMS Root Mean Square.

RNN Recurrent Neural Network.

SAFFE Survey of Activities and Fear of Falling.

SNF Self-reported Number of Falls.

SNOW Semi Non-Overlapping Windows.

SOT Sensory Organization Test.

SPPBS Short Physical Performance Battery Scores.

SRT Sit and Reach Test.

STS Sit to stand.

SVM Support Vector Machine.

TC Terminal Contact.

TFA Transfemoral Amputee.

TFES Thai Fall Efficacy Scale.

TGDS Thai Geriatric Depression Scale.

TO Toe-Off.

TPR True Positive Rate.

TSt Terminal Stance.

TSw Terminal Swing.

TTA Transtibial Amputee.

TTS Train-Test Split.

TUG Timed Up and Go.

UI User Interface.

UoL University of Leeds.

USS Upright Stance Posturography.

VD Vascular Dementia.

VR Virtual Reality.

WBB Wii Balance Board.

WHO World Health Organisation.

WHODAS v.2.0 World Health Organisation Disability Assessment Schedule v2.0.

Chapter 1

Introduction

1.1 Introduction

Falls, defined as an unintentional event which results in a person resting on the floor or a lower level if the body cannot restore balance in time [1], are the second leading cause of unintentional injury death worldwide, with statistics from the World Health Organisation (WHO) in 2021 stating that an estimated 684,000 falls are fatal each year, while a further 37.3 million require medical attention [1]. Furthermore, people aged over 60 years old are disproportionately likely to suffer a fatal fall [1], which has severe implications given the ageing population [2], indicating that hospitals and healthcare systems could become increasingly pressured as a result of fall-related injuries.

Among the causes of falls, slips and trips are particularly prevalent [3, 4], and refer to spontaneous balance loss due to a low-friction surface or collision with a physical object. These slips and trips typically occur more frequently in people with cognitive or muscle weaknesses, which can be attributed to causes such as age and disability [5–7]. Whilst most falls occur indoors [8], a high number of falls are reported outdoors, which can be more serious due to harder surfaces, fewer opportunities to get back up, and hypothermia if the fall is unnoticed [4, 9].

In addition to environmental factors, increased fall risk is also present across a range of conditions such as age, Parkinson's disease, dementia, stroke, multiple sclerosis, amputation, etc., which affect a person's gait [10–26]. As a result, gait analysis is a useful tool for identifying a person's risk of falling, and for providing valuable metrics which can guide rehabilitation and

aid in the diagnosis of various conditions [27].

Fall prediction systems, therefore, should aim to perform gait analysis in real time whilst also collecting environmental data such as the terrain that a person is currently walking on, which may introduce slip and trip factors, or affect a person's spatio-temporal gait parameters. The fusion of these data would allow such a system to evaluate a person's incremental fall risk over time, which may result in more accurate fall prediction and forecasting whilst presenting patients with diagnostic data, such as how different terrains affecting their gait, to help them reduce risks in their daily life. Three core fields must be combined to achieve this: Human Activity Recognition (HAR), terrain identification, and remote gait analysis.

HAR is a large, diverse research area which uses analytical techniques like machine learning to determine what walking activity, such as level-ground walking, navigating ramps and stairs, sitting, standing, etc., a person is performing from collected gait data [28–34]. However, few studies to date have aimed to incorporate a range of terrain variations, with Luo et al. stating in 2020 that "there is an urgent need to create large data sets that have an exhaustive set of walking surfaces representative of the real environment outside the laboratory, preferably with wearable and non-intrusive sensors" [35]. Furthermore, in a 2020 review of gait analysis using wearable sensors by Saboor *et al.* [36], the authors highlight the effect of uneven surfaces on gait, and outline a need to identify these surfaces in future work, stating: "context awareness is an essential requirement for the applicability of gait analysis in the outdoor environment". Without this context in which the gait data is collected, healthcare professionals cannot be sure if gait abnormalities are caused by changes in motion planning due to terrain, or if they are indicative of an underlying gait-affecting condition. Many studies in recent years have used wearable sensors, such as Inertial Measurement Units (IMUs), to perform gait analysis [37], however these studies do not fully utilise the remote nature of wearable sensors, which enable data to be captured outside the laboratory on the terrains a person will be exposed to in daily life, which are known to affect gait and fall risk [4, 38, 39].

This thesis outlines the process of creating a sensor system capable of HAR, terrain identification, and gait analysis. This system is then used to collect and analyse a large, terrain-focussed HAR dataset designed to fill the recognised research gap of terrain identification in the HAR literature. Finally, the spatio-temporal parameters are extracted for each participant in the dataset and evaluated to determine the effect of terrain on gait.

1.2 Motivations

Due to the ageing population, the number of people who fall as a result of age-related gait-affecting conditions, such as Parkinson's disease, dementia, stroke, etc., is increasing. As a result, falls have the potential to occupy large amounts of time and resources in healthcare systems due to admissions to accident and emergency departments, time occupying hospital beds, performing gait analyses, and the associated follow-up appointments. Aside from some existing fall-detection systems, most of which rely on human contact, few technological interventions for falls have been adopted in recent years. Many prototype fall-intervention systems in research are extremely promising, such as exoskeletons, automatic fall detection with smartphones, and gait health monitoring devices, but these can be expensive, uncomfortable, inaccurate, and burdensome, severely limiting adoption in healthcare systems.

The 'perfect' fall-prediction system could be interpreted as one capable of predicting a fall in the strides before it occurs, where the person wearing the device still maintains enough balance and control to stop walking and rest, preventing the fall before it occurs. However, such a system would require information about a person's environment, the activity they're performing, and demographic information such as their age, weight, height, gender, history of falls, and any gait-affecting health conditions. The fusion of these aspects that contribute towards a person's risk of falling would allow such a system to monitor the wearer's incremental fall risk factors over time, which may allow the prediction of fall events or provide diagnostic data that helps people at risk of falling to avoid dangerous situations. While it's simple to collect a person's demographic information, automatically determining external fall-risk factors caused by the combination of walking activity a person is performing, and the terrain they're performing this on, presents a significant challenge.

As such, one major motivation for this research is to address the real-world aspects of fall prediction research by introducing a novel method of performing terrain identification using lightweight, convenient, and privacy-retaining sensors. Furthermore, terrain identification promises to make fall prediction and HAR technologies more robust, allowing the results of this work to help future researchers develop devices which are both accurate and convenient to accelerate the adoption of these technologies in healthcare systems.

One common procedure to determine and monitor fall risk is gait analysis, which many studies in

the literature have aimed to automate through the extraction of gait parameters using wearable sensors. Whilst this approach can enable gait analysis to be conducted remotely, it does not fully utilise the multitude of advantages that wearable sensors provide over camera technologies. As such, another motivation of this research is to bring gait analysis outside the laboratory so that the collected data is more representative of daily life than data collected in a gait analysis laboratory.

All in all, this research takes major steps towards developing implementable fall prevention systems in healthcare settings to reduce the prevalence of falls in society and improve the lives of those affected by fall-related injuries, deaths, and fears.

1.3   Aims and Objectives

This research aims to answer the primary research question: "Can the many external and internal factors that contribute towards a person's risk of falling in real-world environments be monitored using wearable sensors?". In order to answer this question, many aims and objectives must be accomplished to establish the current approaches to fall research, identify the state of HAR and how high accuracies are achieved when performing activity classification, and to design a new sensor system which is suitable for collecting a novel dataset that enables high-accuracy terrain classification. The aims of this research, therefore, are as follows:

1. To identify trends and research gaps in the large, cross-disciplinary field of fall prevention research.

2. To develop a novel wearable sensor system capable of high-accuracy HAR and terrain classification.

3. To collect and analyse a novel, terrain-labelled HAR dataset which will determine the feasibility of terrain classification using wearable sensors.

4. To determine the effect of terrain on gait in real environments.

In order to achieve these aims, a variety of objectives must be met. These objectives and the chapters which address them are as follows:

- To identify the underlying factors and gait parameters that contribute towards increased fall risk.

- To determine the current uses of sensor and machine learning technologies in fall research.

- To explore the current state of fall detection, prediction, prevention, and intervention across both technology and healthcare research.

- To analyse existing datasets and sensor types used for HAR and determine the most important sensors that contribute towards accurate HAR.

- To find the optimal parameters in the sliding window approach to feature engineering for classifying core walking activities.

- To design and manufacture a novel sensor system designed for both activity and terrain classification.

- To collect a large dataset of activities performed on a variety of different common terrains found in daily life.

- To analyse this novel dataset and determine the feasibility of accurate terrain identification using classical machine learning methods.

- To identify which sensors have the largest contributions towards high accuracy terrain identification, such that the system can be optimised for future research and implementation.

- To extract the gait parameters from the collected dataset.

- To evaluate how changes in terrain and environment affect the gait parameters.

1.4 Scope

This thesis assumes that the capacity to perform gait analysis using wearable sensors is already possible. Sensor types such as IMUs, Force Sensing Resistor (FSR) insoles, Electromyography (EMG), and goniometers are already used in some gait laboratories and, as Chapters 2 and 3 will show, these sensor types have already been shown to enable the extraction of gait events and the spatio-temporal gait parameters with high accuracy. Therefore, this research is designed with the scope of augmenting these existing systems through the novel introduction of terrain classification, which enables the full context, defined throughout this research as both activity and terrain, to be extracted.

Furthermore, this research primarily focusses on the practical limitations of adopting technologies in healthcare settings. That is, to reduce the burden placed on users of such devices, sometimes at the cost of classification accuracy, so long as the device is still usable. As such, particularly in Chapters 2 and 3, high accuracy or other performance metrics will be irrelevant in systems that are so burdensome to users that they could not feasibly be introduced in a healthcare setting. The generalisation capabilities of machine learning models are highly valued for this reason, as any system which requires a training period will automatically be more burdensome to users than a system which works 'off the shelf'. Chapter 4 highlights this scope through the use of different terrains between participants in different weathers and lighting conditions, as this will negatively impact classification accuracy, but these are necessary conditions that such a system must deal with if it is to see real-world use.

Finally, the sensor system in this project is framed as a prototype system which will be tested to evaluate it's capability to capture various fall-risk factors, such as activity, terrain, and the gait parameters. The intention is to discover where this system offers novel insights into fall-related factors, and what changes should be made to the following iterations of this system to develop a comfortable and convenient system capable of determining the internal and external fall-risk factors. As a result, various chapters in this thesis focus on reducing the number of sensors and the profile of the device, while maintaining the capabilities of the system to detect fall-risk factors in real-world settings.

1.5 Contributions

The contributions of this research are plentiful in both the fields of fall research and HAR. These contributions are as follows:

- The first cross-disciplinary systematic review of fall research, offering new insights into the field.

Firstly, a wide literature review, featuring a 10-year systematic review, is performed, covering the current state of fall-related research across both healthcare and technological fields. As a result, this review offers unique, cross-disciplinary insights into the state of fall research, and guides the direction of research in this thesis.

- A bias-reduced analysis of existing HAR datasets, which explores the contributions of

various sensor types and analytical parameters towards classification accuracy.

Secondly, a first-of-its-kind cross-analysis of existing HAR datasets is performed, offering new, more generalised conclusions on the performance of different sensor types, analytical models, and data processing methods with reduced bias due to the novel approach of achieving homogeneity between datasets.

- A novel sensor system capable of capturing relevant data to perform terrain-recognition.

A novel sensor system is developed which uses a combination of sensors known to be capable of high-accuracy HAR, along with previously unexplored sensors such as a colour sensor and body-worn LiDAR. This sensor system is shown to be capable of collecting data which enables both activity and terrain to be classified with high accuracy.

- The collection of the first, openly-accessible, terrain-labelled HAR dataset.

The Context-Aware Human Activity Recognition (CAHAR) dataset is collected and is the first terrain-labelled HAR dataset in the literature — a major step towards the real-world implementation of remote, automated gait analysis systems. This dataset will enable future researchers in the field of HAR to develop models with higher generalisation capabilities for deployment in real-world applications.

- An evaluation of the feasibility of terrain classification using wearable sensors.

The CAHAR dataset is analysed using various machine learning techniques to determine the feasibility of terrain classification and optimise the proposed sensor system to prepare for the next design iteration, which will move towards testing and implementation in a healthcare setting.

- An analysis into the effect of terrain on gait in real environments.

Finally, the CAHAR dataset, and a follow-up dataset designed to reduce variability between walking trials on different terrains, is used to compare how walking on different terrains affects the gait parameters. The results from this study are compared with those in the literature, which augments the current understanding of how terrain affects gait for a large set of walking trials captured in real-environments.

1.6 Thesis Outline

Chapter 2 of this thesis contains a background and literature review of falls, fall risk factors such as age, health conditions, and terrains, the current applications of sensor technologies in gait-related research, and the current research on terrain identification. This review highlights a wide range of wearable sensor applications, and identifies terrain classification and variety as a research gap in the area of HAR. This chapter also features a systematic literature review of fall-related research across the areas of fall detection, prediction, prevention, and intervention, spanning the fields of healthcare and technology.

Chapter 3 features an analysis of four existing datasets which are made homogenous among the number of participants, sample rate, activities, and classification methods to evaluate how different sensor types and feature engineering parameters affect classification accuracy across different datasets. These datasets are each analysed using a range of classical machine learning models present in the literature. This chapter contains material published in the MDPI Technologies journal with the title: "Analysis of Multimodal Sensor Systems for Identifying Basic Walking Activities" [40].

Chapter 4 outlines the design of a novel wireless sensor system for gait data collection, along with its use to collect the CAHAR dataset — the first terrain and activity labelled HAR dataset featuring 20 participants each performing 11 activities on 9 different terrains for a total of 38 activity-terrain combinations per participant. Additionally, the raw data is visualised to demonstrate how this sensor system and dataset are suited to gait analysis, HAR, and terrain classification.

Chapter 5 contains the analysis of the CAHAR dataset, and reports on the accuracy attainable using classical machine learning methods for activity and terrain classification in both subject-dependent, and subject-independent contexts. As a result, this chapter establishes the feasibility of terrain classification using wearable sensors, and determines the factors which enable this so that researchers can adopt terrain classification into future HAR and fall research. Furthermore, this chapter identifies the most significant sensors that contribute towards high-accuracy terrain classification, and explores the performance of the optimal configuration of sensors. This chapter contains material from the paper "Machine Learning Techniques for Context-Aware Human Activity Recognition: A Feasibility Study" which was published in the 30th IEEE International

Conference on Mechatronics and Machine Vision in Practice [41].

Chapter 6 explores the effect of terrain on gait by extracting a series of gait parameters from the CAHAR dataset, along with an additional follow-up dataset. This chapter performs an analysis on the effect of terrain on gait, finding that terrain affects the gait parameters with statistical significance, even in controlled environments in which factors like distance and pace are controlled. This chapter highlights the capabilities of the proposed sensor system to monitor gait variability, which is another fall risk factor, on real-world terrains.

Chapter 7 summarises the findings of this thesis and highlights the contributions of the work, along with demonstrating how the aims and objectives were met, and discussing the future work required to use the findings of this research to construct a fall-prediction system which monitors the internal and external fall-risk factors using wearable sensors.

Chapter 2

Background

2.1 Introduction

The fields of gait analysis and fall-related technologies incorporate many aspects from a wide range of disciplines such as: medicine and healthcare, sensors, assistive robotics, statistics, and machine learning. The following chapter first aims to establish the necessary background information to contextualise the need for such devices and explore commonly used technologies and methods in this area. Next, the relevant literature is separated based on objectives and outcomes, and each of these areas is explored and critically analysed. Finally, this review summarises each area of research to identify overall gaps in the literature which must be addressed before many of the prototype gait analysis, fall-risk assessment, and fall detection devices can see practical, clinical use.

2.2 Activities of Daily Living

An Activity of Daily Living (ADL) is a fundamental action or skill necessary to maintaining independence in daily life [42]. Examples of ADLs include eating, dressing, washing/grooming, walking/ambulation, toileting and the ability to perform various leisure tasks such as watching TV. Along with these basic ADLs, an Instrumental Activity of Daily Living (IADL) is a higher-level task such as partaking in sporting activities and the management of medication and personal finances, which are crucial skills in modern life [42]. Whilst ADLs involve both upper-limb and lower-limb actions, this section focuses on those that require healthy gait and lower-limb mobility to perform.

Inability to perform ADLs strongly correlates to decreased mental health, life satisfaction and self-perceived quality of life [42–45]. Additionally, there is a strong correlation between the age of an individual and their inability to perform both IADLs and ADLs as a result of various conditions, such as back pain and osteoarthritis along with chronic neurological conditions such as dementia, stroke, and Parkinson's Disease (PD) which decrease the sensory, motor and cognitive abilities of those affected [42, 43, 46–49]. Due to the age-related nature of many of these conditions, it is older people who primarily lack ADL independence, with National Health Service (NHS) England reporting that 28% of women and 24% of men aged 65 and over required help with at least one ADL over a one-month period, whilst 29% of women and 21% of men in the same age group needed help with at least one IADL over the same time period [47]. Furthermore, it was found that as age increased from 65-69 to 80+, the proportion of adults needing help with at least one ADL or IADL rose from 21% to 52% [47]. Regarding specific activities, multiple studies find that older people are most likely to need assistance with navigating stairs, bathing, household work, climbing in and out of chairs, and moving indoors [44, 47, 48, 50].

There is a further connection between falling and inability to perform ADLs, as demonstrated in a survey by Suzuki *et al.* [12] which found that elderly individuals who have an increased fear of falling require assistance in ADLs such as dressing, bathing, walking and toileting, as this fear typically leads to anxiety, disuse syndrome and lower-limb muscle weakness. These conditions further contribute to a sense of unease and fear when performing ADLs which, without intervention, can lead to individuals becoming completely ADL dependant [12]. Fear of falling is typically associated with the act of falling, and is reported to affect a person for up to a year after they experience a fall, which negatively impacts their quality of life for this period [10, 51].

Whilst older people are the most likely to be ADL dependent, the American Bureau of Labour Statistics (BLS), and the UK Office of National Statistics (ONS) report that sport and leisure activities were the second-largest uses of time among retirement-age people in 2019 and 2023 respectively [52, 53]. Community sport and leisure activities such as yoga, dance, and karate have shown to be effective in improving balance and reducing fall risk [54–56], highlighting a need to maintain ADL and IADL independence in this group to prevent fall-related injuries.

This overview of the prevalence and impact of ADL dependency in elderly and disabled people

highlights the need for interventions in this area, particularly with respect to performing walking activities, which will mitigate much of the mental and physical strain on the affected population [45], enabling ADL independence much later into life.

2.3 Falls: Prevalence and Impact

Whilst the risk of falling is prevalent in all people due to uneven terrain, misplaced footing, and the temporary spontaneous loss of balance, certain groups of people will exhibit greater chances of falling than others for a variety of reasons. Typically, older people are at increased risk of falling primarily due to their diminished balance, strength, and vision as well as the introduction of gait asymmetries and secondary factors such as heart disease or orthostatic hypotension [57, 58]. These primary factors are also present in a variety of other chronic diseases, such as multiple sclerosis, dementia, Parkinson's disease, stroke, and lower-limb amputation, where increased risk of falling can also be observed [19, 23, 57, 59–61].

In 2018, the World Health Organisation (WHO) reported that falls are the second most common cause of death due to injury globally, with 646,000 deaths and 37.3 million injuries caused by falls annually [1]. Most of these deaths occur in individuals over 60 years.

Various studies have also indicated that falls are more common among individuals who are isolated from their community due to similarities in risk factors, making them more vulnerable to fall-related injury and morbidities [45]. This factor is especially prevalent in older people who often cannot return to a standing position after falling, resulting in a sustained period of laying on the floor, leading to further morbidities such as hypothermia [9]. These morbidities increase mortality for people who fall with sustained periods of floor contact, with deaths occurring in half of those on the floor for more than an hour within a six-month period after the fall [9]. Survivors of falls can suffer from hip fractures, head trauma, cognitive impairment, depression, or other conditions which result in decreased quality of life and autonomy [1, 43, 46, 62].

The UK Office for Health Improvement and Disparities reported that in the 2022/2023 period, 209,989 people aged over 65 were admitted to hospital in England due to falls at a rate of 1,933 per 100,000 [63]. These figures rise dramatically to a rate of 4,845 per 100,000 in those over 80. The combination of these age-related facts highlight a growing population of older people who are increasingly ADL dependent and at risk of falling as they advance in age, whilst wishing

to stay active and engage in sporting and leisure activities, the pursuit of which will naturally reduce fall risk [47, 52–56, 63]. It is therefore in the best interest of society and healthcare systems to develop systems that swiftly detect, diagnose, and rehabilitate older people with gait-affecting conditions to maintain their ability to perform social, leisure, and sport activities which act to naturally reduce risk of falling.

2.4 Personal Factors Contributing to Falls

Falls and risk of falling cannot be attributed to a single condition as, even within a healthcare condition associated with falls, there is often large variability in the frequency, risk, and injury caused by falling [11]. Despite this, many similarities are present between groups of people at high-risk of falls with respect to unequal lower limb kinematics, spatio-temporal gait asymmetry, and impaired cognitive abilities [11, 57]. The following sections aim to identify the underlying factors leading to an increase in fall risk.

2.4.1 The Ageing Population

In 2000, 10% of the global population were aged 60 and over, which is projected to rise to 21.8% in 2050 and 32.2% by 2100 with more developed regions such as Japan, Europe, North America and China having the highest proportions of elderly people [2]. These trends can be attributed to a variety of societal improvements, including the early detection and prevention of health conditions associated with older people, such as type 2 diabetes mellitus, cancer, and cardiac disease [64, 65]. Typically, women live longer than men, but spend on average only 0.6 years longer without disability, making them one of the largest age groups at risk of falling and with decreased ability to perform ADLs [66, 67].

Despite the heterogeneity among older people due to the large variance in health and activeness [57, 68], many studies have aimed to identify commonalities in older people's movement capabilities. Typically, older people experience significantly reduced lower limb muscle force and torque, reaction times, walking speeds, ankle dorsiflexion, vision, proprioception, and balance, along with increased energy expenditure, oxygen requirements, postural instability and gait asymmetry [11, 57, 69].

Reduction in muscle mass and strength do not correlate with increased chance of falling in healthy, older people [11, 49, 69]. Rather, personal factors such as anxiety and fear from a history

of falls are more likely to be causes due to balance loss through self-adjusting gait in an attempt to mitigate falls [10–12]. Additionally, people over the age of 85 who fall have an increased chance of fatality as a result of falling, with those who survive and become hospitalised being at an increased chance of delirium, which can lead to further complications regarding treatment and increase hospital discharge time [62, 67]. In a study specific to the older population, Rikkonen *et al.* [4] monitored the causes of 1281 falls which occurred over two years among a population of 914 women with a mean age of 76.5. Of these falls, slipping and tripping were the leading causes, accounting for 457 and 425 falls respectively, highlighting balance loss and asymmetric gait as primary risk factors. Furthermore, 608 of these falls occurred on a street, floor, or otherwise even surface. This may be due to the frequency with which people are exposed to these common surfaces, although studies which demonstrate that gait is affected by the terrain underfoot [38, 39] suggest that terrain should be an area of interest when considering factors which contribute towards falls.

2.4.2 Stroke

In 2016 alone, it was reported that 5.5 million deaths resulted from stroke globally, with 13.7 million strokes resulting in 116.4 million Disability-Adjusted Life Years (DALYs) [70]. In the UK, strokes account for 75% of the deaths caused by cerebrovascular diseases, which were the 4th leading cause of death in 2018 [71]. Stroke incidence increases with age, from 100 per 100,000 people at age 40 to 1,000 at age 65 and 2,500 at age 90 [70]. Additionally, strokes are more common in men from ages 50-85, becoming more common in women at age 90 due to differences in the probabilities of risk factors such as smoking [66, 70].

Survivors of strokes typically experience impaired gait due to factors such as hemiplegia, decreased proprioception, and muscle spasticity [60, 72, 73]. These issues result in gait impairment in the form of increased stride, stance, and swing time and decreased stride length, frequency, velocity, cadence, ankle plantar flexion, and ankle dorsiflexion on the affected side, resulting in asymmetry between legs during ambulation [13–15]. A study by Patterson *et al.* [74] grouped 54 stroke survivors by the severity of their gait asymmetries. Of these participants, 30 exhibited some form of temporal asymmetry, whilst 18 were found to have spatial asymmetry in their gait. Participants in the severe asymmetry groups also demonstrated a notable drop in walking speed and large asymmetries in swing and stance time and step length, which aligns with the findings of other studies on the walking characteristics of stroke survivors [14, 15, 72–74].

2.4.3 Dementia

Dementia is an umbrella term for conditions affecting cognitive functions, the most common of which are Alzheimer's Disease (AD), Dementia with Lewy Bodies (DwLB) and Vascular Dementia (VD) [75]. The probability of developing dementia increases with age, with the World Alzheimer's Report in 2015 stating that cases rise from 3.9 per 1000 between ages 60-64 to 104.8 per 1000 over age 90, with 46 million people living with dementia globally in 2015 [76, 77]. Due to the prevalence of dementia, its incurable nature, and the ageing population, many healthcare systems are forced to spend increasing amounts of resources in this area without appropriate technological or medical intervention [77].

With respect to ambulation in people living with dementia, gait impairments vary between subtypes of dementia and much research has been conducted into whether gait analysis can be used to definitively differentiate between these subtypes to allow for early detection [75, 76, 78–80]. With respect to spatio-temporal gait parameters, all dementia types typically result in increased variation in stride length, stride velocity, stride time, swing time, stance time, double support time, and single support time compared to healthy individuals [16, 17]. When comparing between dementia subtypes, stride width is the largest indicator of AD or non-AD dementia, with non-AD dementias having a larger mean stride width [17]. As a result of this increased variability, fall prevalence is much higher in non-AD dementia types, such as Dementia with Parkinson's Disease (DwPD) and DwLB, as these affect different parts of the brain [81].

2.4.4 Multiple Sclerosis

Multiple Sclerosis (MS) is a degenerative neurological condition resulting from an immune response in the brain and spinal cord that causes progressive cognitive, sensory and motor impairments, which usually affects individuals aged 20–40 years old [82]. As a result of diminished motor skills, People with Multiple Sclerosis (PwMS) are more likely to fall than people without MS [83], with over 50% of PwMS suffering a fall over any given three-month period [84–86]. PwMS are also more likely to sustain injuries from falls [83], with up to 50% of those who fall requiring medical attention, further increasing risk of falling and fear of falling, impacting abilities to perform ADLs, and decreasing quality of life [12, 87].

PwMS typically experience increased gait variability when compared to healthy controls, with studies showing increased variability in step width, length, and time which worsen as the disease

progresses [18, 19]. This variability in gait typically results in decreased walking speed, step length and step time with an increase in step width [18].

2.4.5   Parkinson's Disease

Parkinson's Disease (PD) is a neurological condition in which the brain's capacity for producing dopamine is reduced as a result of nerve cell damage, resulting in reduced motor control [88]. People with Parkinson's Disease (PwPD) typically exhibit increased walking time due to increased time spent in the stance and swing phase and a decrease in stride length, height, velocity, ankle dorsiflexion, and ankle plantar flexion [23–26]. This reduction in the range of motion of the ankle in addition to a reduced foot clearance are major contributors towards the prevalence of falls in this group [11, 24]. A study by Wood [23] analysed the fall rates in a group of 101 PwPD over one year. The study found that 69 (68.3%) of participants had fallen, with 51 (50.5%) reporting multiple falls over the period of study. People who fell in this study typically exhibited a reduced stride length, loss of arm swing, increased time spent with the condition, and reduced cognitive abilities when compared with the people who did not fall [23]. Motor deficiencies such as gait abnormalities, rigidity, and bradykinesia in PwPD often precede diagnosis by four to six years, during which it can be difficult to distinguish between PD, Alzheimer's Disease and Dementia with Lewy Bodies as motor differences between these conditions are extremely subtle [61, 89, 90].

An additional factor towards fall prevalence in PD stems from Freezing of Gait (FOG), which is reported as the feeling of one's feet being stuck to the ground with the potential to occur spontaneously and frequently during ambulation [91, 92]. FOG events typically last less than ten seconds, but have been reported to last over 30 seconds in previous studies [93, 94]. Furthermore, FOG events commonly occur during gait initiation and turning, resulting in increased risk of falling, with events appearing more frequently in those under increased stress, whom are distracted, or those in an environment of increased spatial constraint [11, 93, 95]. In addition to FOG events, PwPD tend to experience more severe falls, resulting in greater injury when compared to other high-risk groups [67]. This results from an impaired ability to use the arms for protection as a result of bradykinesia and impaired attentiveness from reduced cognitive abilities [11].

2.4.6 Lower-Limb Amputees

Lower limb amputations may take place for a variety of reasons, with the most common being diabetes and arterial vascular disease [96]. Whilst amputations of the lower limb are carried out at many different levels, all impact gait, with the most common major lower limb amputations being transtibial and transfemoral [20, 59]. Post-operation, Lower-limb Amputees (LLAs) are given the option to utilise a prosthetic device to return to walking, however a notable deterioration in walking ability and balance still occurs despite the modern advances in Microprocessor Knees (MPKs) such as the Ottobock C-Leg [97–99].

With respect to spatio-temporal gait parameters, both Transtibial Amputees (TTAs) and Transfemoral Amputees (TFAs) experience decreased walking speed and step length along with increased step width, gait asymmetry, and variability [20–22]. Additionally, TFAs exhibit more extreme variations in these values than TTAs when compared to non-amputees. Both types of amputee will also tend to place less body weight on a prosthetic leg, indicating a lack of trust and further increasing gait asymmetry [22]. These spatio-temporal gait changes result in a drastic increase in fall risk amongst amputees, along with increased incidence of osteoarthritis due to gait loading asymmetries [100–102].

2.4.7 Summary

Based on the commonalities between affected populations, increased gait asymmetry and variability seem to be prevalent spatio-temporal gait parameters in people who are at the highest risk of falling, regardless of the source of these abnormalities. Asymmetric gait results in unequal force distribution between legs during ambulation, which causes decreased balance and increased loading on the non-affected limb, potentially resulting in joint pain and osteoarthritis [74, 100, 103]. Furthermore, conditions affecting cognitive abilities seem to cause falls of increased severity and injury probability as a result of reduced reaction speeds and reflexes, which are more likely to impair one's ability to save oneself during the fall. Interventions to prevent falls, therefore, should focus on these underlying spatio-temporal parameters, rather than individual healthcare conditions, to allow a single method of fall prevention to apply to the largest population possible.

2.5 External Factors Contributing to Falls

2.5.1 Slips and Trips

Slips and trips refer to spontaneous balance loss due to a low-friction surface or collision with a physical object. In multiple studies that consider falls in older people, slips and trips are commonly reported as a cause for falling, with 30-70% of all reported falls in these studies being attributed to these two factors [3, 4, 104]. These slips and trips typically occur more frequently in people with cognitive or muscle weaknesses, which can be attributed to causes such as age and disability [5–7]. Whilst most falls occur indoors [8], a high number of falls are reported outdoors, which can be more serious due to harder surfaces, fewer opportunities to get back up, and hypothermia if the fall is unnoticed [4, 9].

Slips and trips are a product of the environment in which a person is walking, with low light levels, temporary hazards, and frictional variations in foot contact among the reported causes for falls [104–106]. As a result, visual impairments are reported to increase the frequency of slips and trips and are an additional factor which contributes towards fall risk [104, 106].

2.5.2 Terrain

Terrain is used in varying contexts throughout the literature, with some studies using the term to refer to situations that affect walking activity classification such as ramps and stairs [107], whilst other studies are referring to common surface properties, such as grass, pavement, gravel, etc [38, 108]. For this study, the latter definition of terrain is used - referring to the surface properties of the ground underfoot.

Terrain has been shown to reduce gait speed and affect the variability of gait parameters such as step width and step time, which is more pronounced among older people [38, 39, 108–112]. Kowalsky *et al.* [38] conducted an analysis of the effect different terrains had on several gait parameters, along with metabolic rate. Ten subjects equipped with foot-mounted Inertial Measurement Units (IMUs) walked across five terrains at a fixed pace. These terrains were, in increasing metabolic cost: pavement, dirt, gravel, grass, and woodchip. Of the spatio-temporal parameters, foot clearance, stride height, and stride width were found to correlate with terrain [38]. Kang *et al.* [108] explored the effect of surface characteristics on gait parameters among 31 subjects walking on three types of surface: a levelled mat, a soft urethane mat, and a desta-

bilising rock surface. Six infrared motion capture cameras and a pressure measurement system monitored the subjects' gait parameters on each surface, and it was found that uneven surfaces decrease gait speed, shorten stride length, and vertically lower Centre of Mass (CoM) [108]. The authors comment that this may be a necessary response to ensure stability is maintained on uneven terrains. Menant *et al.* [110] recruited ten young and 26 older subjects, the latter of which had a range of health conditions, to walk seven metres on three different terrains. The control terrain consisted of linoleum, which was covered with an even layer of water for the 'wet' terrain. The third 'irregular' terrain consisted of uneven wooden blocks covered with a layer of artificial grass [110]. On the irregular terrain, subjects exhibited reduced walking velocity, cadence, step length, and double support time, with an increase in step width and toe clearance. For the wet surface, subjects exhibited reduced walking velocity, step length, and increased step width [110].

Overall, these studies highlight a general trend that, as terrain becomes uneven, people generally slow their gait, taking shorter steps, increasing their foot clearance, and lowering their centre of mass to increase stability [38, 39, 108–112]. While these studies tend to lack a wide variety of terrains, with many choosing to emulate uneven terrains rather than considering common daily terrains [108–112], these studies clearly identify how gait is dependent on the terrain underfoot.

2.6 Fall-Related Research

Fall-related research is multidisciplinary, spanning both the healthcare and technology literature. As a result, a comprehensive review of these areas is required to illustrate what progress has been made, and what the state-of-the-art healthcare approaches to falls are, to identify research gaps and ensure that appropriate sensor methods are selected for this work. The following section details the results of a systematic review on fall-related research.

2.6.1 Categories of Fall Research

Fall-related research can be divided into four categories: fall detection, fall prediction, fall prevention, and fall intervention. Figure 2.1 shows how these studies are classified. The definitions of these areas in the context of this review are as follows:

	While a fall is occurring	Before a fall occurs
Fall event identified	Fall Detection	Fall Prediction
Fall event prevented	Fall Prevention	Fall Intervention

Figure 2.1: A visualisation of how fall detection, prediction, prevention, and intervention are defined in this review.

Fall Detection

Fall detection encapsulates studies which aim to identify a fall event as it is occurring, typically before the person hits the ground. Although there are applications for fall detection after the person has hit the ground, these will not be considered in this review.

Fall Prediction

Fall prediction is the detection of a fall event before the fall occurs, enabling a fall to be prevented ahead of time. This area can include the monitoring of diagnostic gait data, such as the spatio-temporal gait parameters, which may aid in predicting the diminishing of gait health and therefore the risk of fall. Alternatively, studies may aim to determine the risk of a fall outright using novel analytical and sensing approaches.

Fall Prevention

Fall prevention is the physical prevention of a fall as the fall is occurring through external factors such as orthotics, exoskeletons, and balance-correction devices. Generally, any device which imposes a force on the wearer will be classified as fall prevention in this study.

Fall Intervention

Fall intervention includes approaches to preventing a fall before it occurs, typically through rehabilitation programs and targeted muscle-strengthening exercises. The outcomes of these programs are often measured through some form of standardised test, such as the Timed Up and Go (TUG) test, Berg Balance Scale (BBS) score, etc.

2.6.2 Eligibility Criteria

This review was performed according to the Preferred Reporting Items for Systematic Reviews and Meta-Analyses (PRISMA) guidelines. Studies were obtained from online searches spanning from January 2012 to April 2024 using the CINAHL, Embase, PubMed, IEEE Xplore, and Web of Science (Core Collection) databases. In addition to the results of these database searches, citation searches, Google Scholar, and some expanded search terms were used to obtain additional relevant papers.

2.6.3 Database Search Terms

Each database in this review varies in the formatting of a search. As such, a generic search term was formulated to encapsulate all four research areas considered in this review and was translated for all databases. This search term was:

```
((human) AND ((fall* OR trip) AND (detect* OR prevent* OR predict* OR risk* OR
reduc* OR interven*)) AND ("machine learning" OR "deep learning" OR robot* OR
sensor* OR sensing OR exoskeleton OR orthotic OR rehab* OR balance OR assist*)
NOT (Parkinson* OR stroke OR "multiple sclerosis" OR "cerebral palsy" OR
dementia)).
```

Due to the large number of results from this search, additional tagging and filtering was performed to obtain a subset of relevant studies for each of the four areas of interest in this review. As such, all records were exported and custom automation tools were created using Python to perform duplicate removal along with title, abstract, and keyword searching, and filtering to return a list of studies for each of the four areas of interest. Title, abstract, and full record screening was performed on the remaining studies to determine eligibility for inclusion in the review.

During full record screening, a scoring criteria, previously used in the literature [113], was
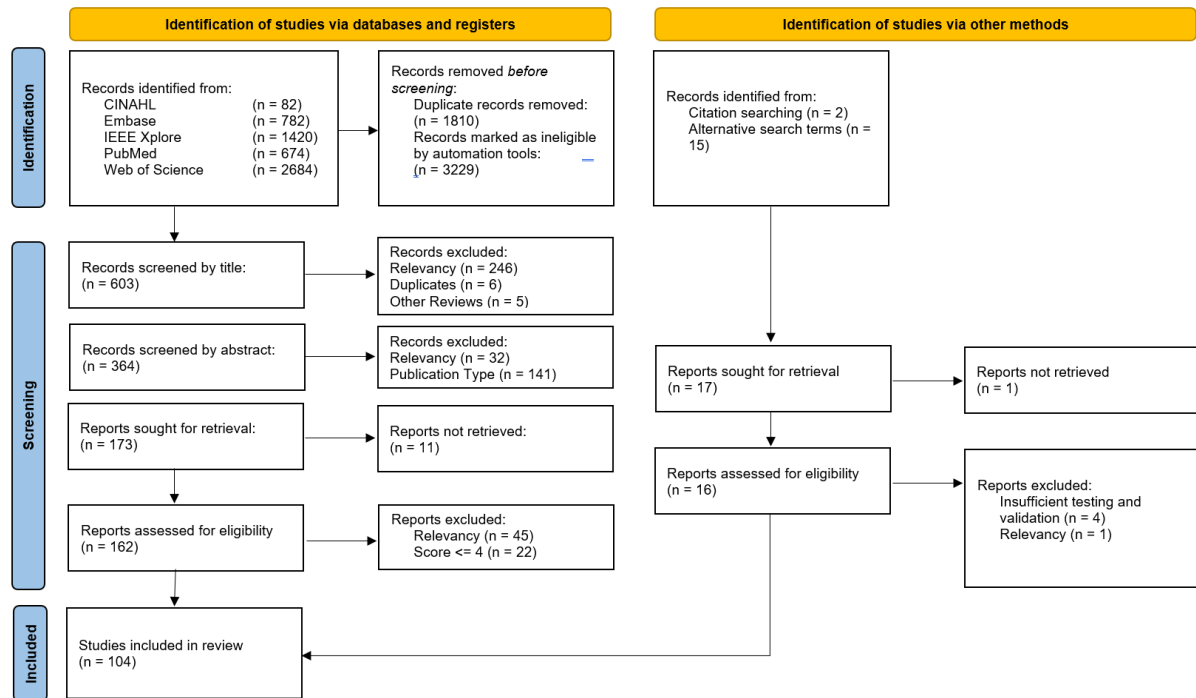
Figure 2.2: The PRISMA diagram for this review.

applied to further refine the search results. A record received up to two points for each of the following:

- Are the research question/aims and design clearly stated?

- Is the research design appropriate for the aims and objectives of the research?

- Are the methods clearly described?

- Is the data adequate to support the authors' interpretations/conclusions?

- Are the results generalizable?

Studies which scored less than five points were removed from the study. The PRISMA diagram for this study can be seen in Figure 2.2. A full list of papers included in this study can be found in Appendix A.

2.6.4 Fall Detection

Many fall detection studies draw their data from one of a variety of open access fall detection datasets, or produce a dataset for future researchers to access, the details of which can be found in Tables 2.1 and 2.2. Figure 2.4 shows the frequency with which fall detection datasets were analysed in this review. Of the available datasets, URFall and Multiple Cameras Fall (MCF)

were the most frequently analysed by a large margin. These datasets most prominently feature a Kinect and RGB cameras [114–116], with the accelerometer data from URFall typically being excluded when this dataset is analysed [117–125]. This highlights a phenomenon in which most IMU-based datasets are only analysed a single time, typically being recorded and analysed within a single study. Furthermore, these single-study datasets feature a large variation in number of participants, as seen in Figure 2.3a, which can hinder the validity of proposed fall detection approaches due to insufficient test sets. One approach to tackle this issue is seen in the FARSEEING dataset proposed by Klenk *et al.* [126], which defines a data capture procedure rather than a sensor system, resulting in a large multicentre dataset where researchers can select and analyse data based on their desired sensor type. Future studies should work to augment this dataset or produce a similar repository that allows researchers to contribute towards a collective data pool or pull from it to test novel analytical techniques with a universally recognised validation set.

Table 2.1: Fall Detection Datasets

Dataset	Year	Sensor(s)	Sensor Locations	Participants	Activities
FallFree [127]	2017	Kinect	Ambient	2 healthy participants mimicking the walking pattern of cane users.	42 true falls, 23 pseudo falls, and 14 ADL, each repeated 4 to 5 times.
SisFall [128]	2017	Accelerometer and gyroscope.	Waist	Different activities and falls performed by 2 groups: 23 healthy young adults and 1 older person, and 14 healthy people over 62 years old.	Young healthy people and 1 older person: 19 ADLs and 15 falls, healthy older people: 15 ADLs.
UMAFall [129]	2017	4x 9-axis IMUs connected to a central mobile phone acting as a data sink.	Chest, wrist, waist, and ankle.	17 participants aged 18-55 (mean: 26.9)	8 ADLs and 3 falls
UCIFall [130]	2014	6x 9-axis IMU and barometer nodes.	Head, chest, waist, right wrist, right thigh, and right ankle.	14 participants with a mean age of 22.75.	16 ADLs and 20 falls.
FallAllD [131]	2021	3x 9-axis IMU and barometer nodes.	Neck, waist, and wrist.	15 participants aged 21-53 (mean: 32)	Up to 44 ADLs and 35 falls whilst wearing protective equipment. However, participants only wore devices and completed activities convenient to them, resulting in a large variation.
Kinect Activity Recognition Dataset (KARD) [132]	2015	Kinect	Ambient	10 participants aged 20-30	Around 1 hour of data comprised of 10 gestures and 8 actions but no falls.

Table 2.2: Fall Detection Datasets — continued

Dataset	Year	Sensor(s)	Sensor Locations	Participants	Activities
Le2i [133]	2013	RGB camera	Ambient	9 participants	191 videos are captured of participants performing ADLs and falls in 4 different indoor locations. 143 of these videos contain a fall.
Northwestern-University of California (NUCLA) [134]	2014	3x Kinect cameras	Ambient	10 participants	16 activities but no falls.
MCF [116, 135]	2011	8x RGB cameras	Ambient	1 participant	24 ADLs and 22 falls with varying configurations of the cameras.
High Quality Fall Simulation (HQFS) [136]	2016	5x RGB cameras	Ambient	10 participants	Participants watched footage of real falls and re-enacted them including using different walking aids. This totalled 17 ADLs and 55 fall activities.
SDUFall [137]	2014	Kinect	Ambient	10 young participants	5 ADLs and 1 fall. The lighting, direction, and position of the Kinect was changed throughout.
Fall Detection Dataset (FDD) [115]	2012	RGB camera	Ambient	N/A	six ADLs and 3 falls in 4 different locations.
UPFall [138]	2019	1x Electroen-cephalogram (EEG) sensor, 5x nodes each consisting of an IMU and ambient light sensor, 6x infrared sensors, and 2x RGB cameras.	Neck, waist, right pocket, wrist, ankle, and ambient.	17 participants aged 18-24.	6 ADLs and 5 fall activities.
IRMTv1 [139]	2018	2x depth cameras	Ambient	2 young participants	20 ADLs and 20 falls.
TSTv2 [140]	2016	Kinect and 2x IMUs.	Ambient, wrist and waist.	11 participants aged 22-39	4 ADLs and 4 falls.
RealAct [141]	2021	Accelerometer and barometer	neck (7 subjects), wrist (9 subjects)	16 participants aged 80 or older.	Data is captured during a participant's daily life in which 2 real falls occurred over the total 400 days worth of data.
Fall360 [142]	2022	360°RGB camera	Ambient	22 young participants	4 types of falls are captured among 1327 video clips along with 5 non-fall ADLs in a further 1387 clips.
Unnamed Dataset - Medrano et al. [143]	2014	Smartphone IMU	Both pockets or both in a handbag (falls), 1 pocket or 1 phone in a handbag (non-falls)	10 participants	8 falls and a prolonged period of unlabelled ADLs
FARSEEING [126]	2016	Accelerometer, gyroscope, various additional sensors.	Various	Various	This dataset is a large growing repository of fall data. As such, activities, falls, sensor systems, and participants vary heavily. However, all sensor signals include at least an accelerometer and gyroscope, with a further 58% including a magnetometer.
UT-A3D [144]	2012	Kinect	Ambient	10 participants	10 ADLs but no fall events.
ACT4^2 [145]	2012	Kinect	Ambient	24 participants	12 ADLs and 2 falls.
URFall [114]	2014	1x/2x Kinect and 1x accelerometer	Ambient and pelvis region	5 participants	2 fall activities captured across 30 fall trials using 2 Kinects and an IMU. 40 ADL trials are also included which were recorded by just a single Kinect and IMU.

(a) Single-study datasets

(b) Multi-study datasets
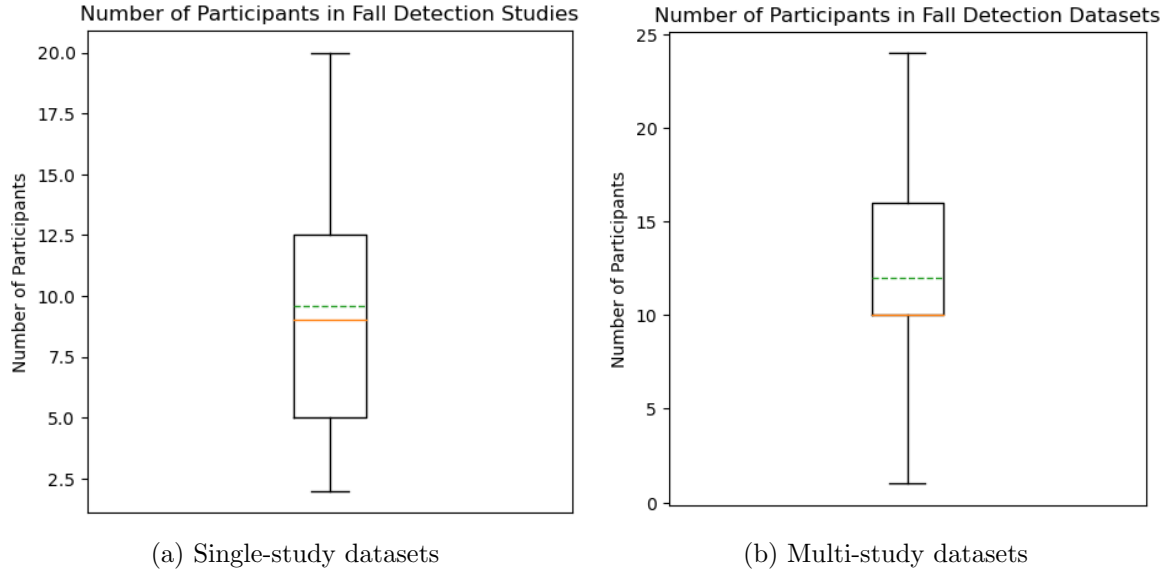
Figure 2.3: Box plots of the number of subjects in fall detection studies.

One issue with these datasets is that many studies make use of actors falling onto crash mats or otherwise simulating a fall [142, 146–151], where other studies showed this to diminish the performance of models when introduced to real-world falls [141, 152]. Datasets such as HQFS [136] and RealAct [141] have demonstrated an awareness of this factor and made an effort to improve the quality of simulated falls and capture real falls, respectively. However, there remains a need for studies which capture a large enough quantity of real falls to facilitate a sizeable dataset, something which may be unfeasible for the young healthy population, due to the infrequency of falls in this group.

Due to the wide variation in datasets, a wide range of sensor types are also present among the fall detection studies in this review. As seen in Figure 2.5, IMU, Red Green Blue (RGB) cameras, and Kinect/depth cameras are the most prevalent across both single-study and externally collected datasets. Many IMU-based studies feature either a single sensor [148, 150, 152–158] or multiple sensors [131, 141, 146, 159–161] at different combinations of the neck, chest, waist, wrists, thighs, and ankles. To address the issue of convenience in fall detection systems, some studies aimed to analyse IMU sensor data from existing body-worn devices such as smartphones [148, 154, 157] or smartwatches [156]. Ribeiro *et al.* [162] also demonstrated the versatility of IMU-based solutions by using these sensors to monitor floor vibrations in an ambient-sensing approach.

As depth cameras and Kinect sensors also capture RGB data, there is much overlap between
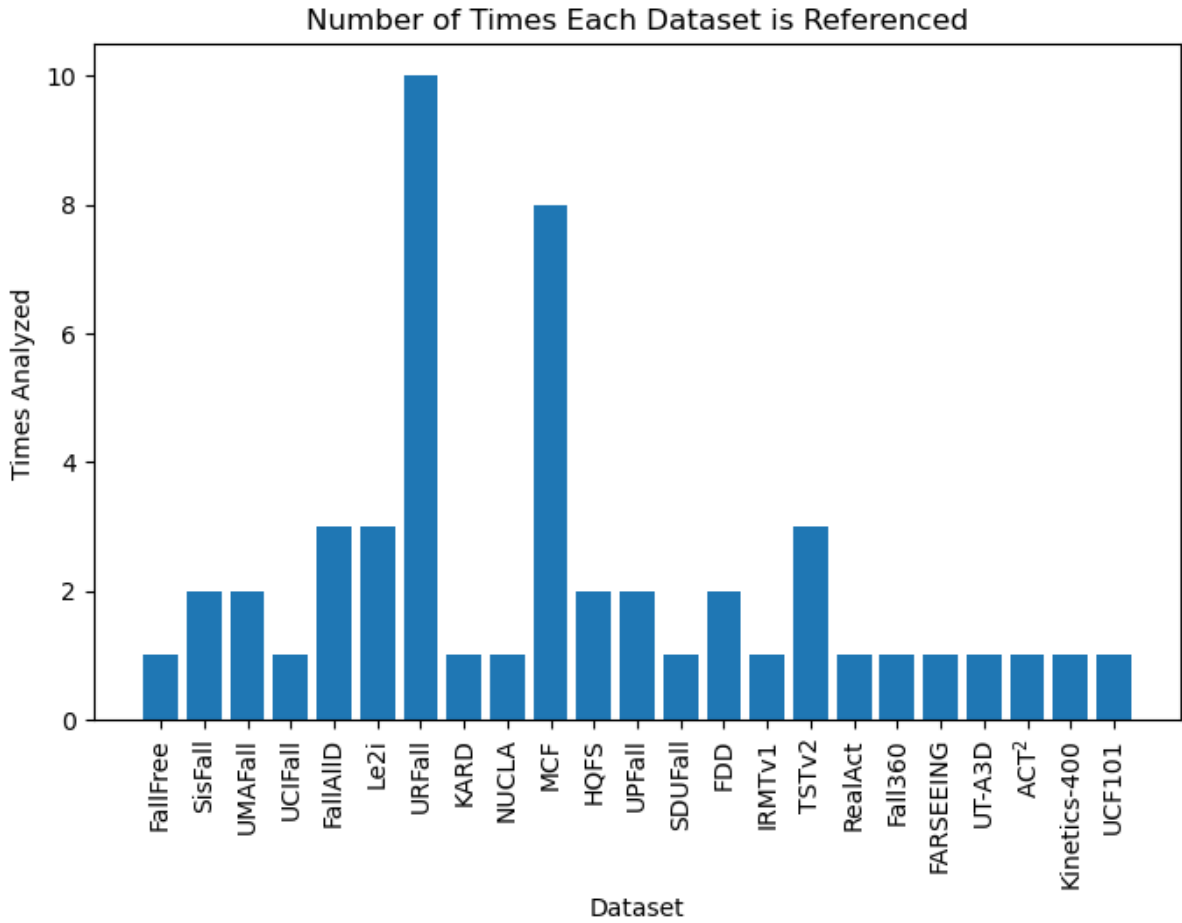
Figure 2.4: The number of times each fall detection dataset was analysed in this review.

these sensor types in regard to datasets, data preprocessing, and classification methods. As with the IMU studies, a variety of setups are considered for camera-based solutions featuring either a single [120, 125, 139, 142, 151, 163–169] or multiple [118, 119, 121–124, 170–175] cameras, typically dependent on the dataset being analysed. Two major approaches present themselves throughout the camera-based solutions, each with advantages and disadvantages. The first of these approaches is to access and monitor the skeleton data, which can be extracted from RGB [122, 125] or depth camera images [120, 163, 168, 169]. These approaches enable fast-acting threshold algorithms that monitor features extracted from the relative and absolute positions of the joints, while achieving performance metrics comparable to more complex methods [120]. However, the need for access to raw footage of the subject may raise privacy concerns [120]. On the other hand, some studies in this area choose to make use of silhouette data [119, 151, 174, 176], which reduce the amount of personal data being processed whilst maintaining high performance metrics. In addition to these manual feature extraction approaches, some studies aim to use powerful deep learning approaches such as Convolutional Neural Networks

Sensor Usage in Single-Study Fall Detection Datasets

(a) Single-Study fall detection sensor use
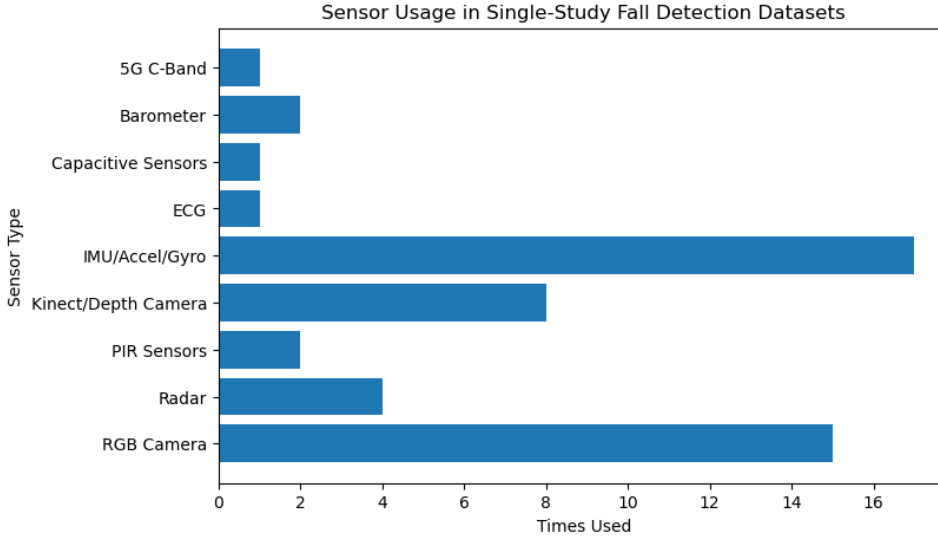
Sensor Usage in External Fall Detection Datasets
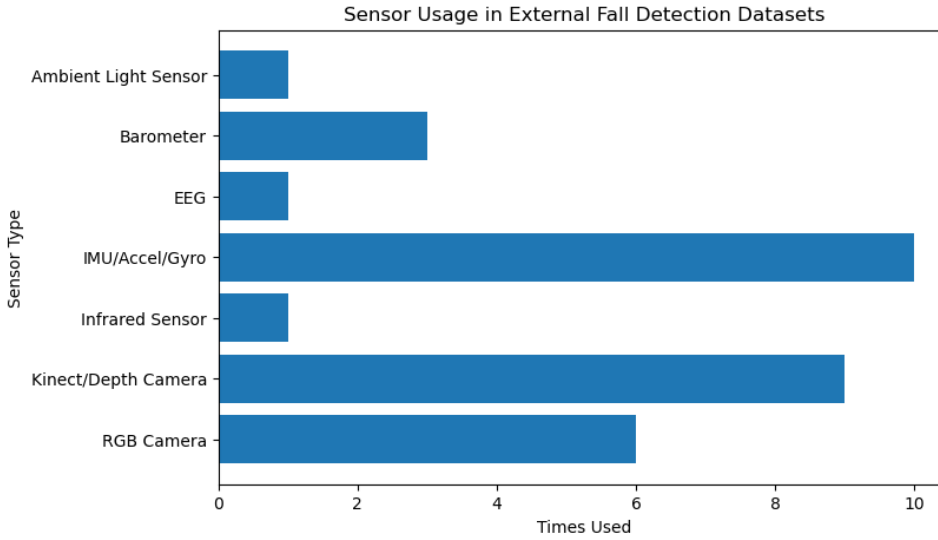
(b) Externally-referenced fall detection sensor use

Figure 2.5: Graphs of the frequency with which sensors are used in fall detection studies for single-study datasets and external datasets.

(CNNs) and Long Short-Term Memory (LSTM) models to perform automatic feature extraction and fall detection on sequences of image data [121, 142, 170, 172]. Whilst this approach has demonstrated high accuracies and versatility, it also suffers from the aforementioned privacy concerns.

Whilst IMU, RGB cameras, and depth cameras are extremely popular, several other sensor systems are adopted in the literature for the purpose of fall detection. Radar-based approaches allow researchers to create non-restrictive ambient systems that offer data rich enough to yield performance metrics up to 100% sensitivity when detecting a fall [149], while maintaining the

privacy of the subject [149, 162, 177, 178]. Butt *et al.* [147] exploited the body's reaction to a fall using Electrocardiogram (ECG) sensors with a CNN to achieve a classification accuracy of 97.36%, whilst using transfer-learning to reduce training times. Using information from the 5G C-band wireless channel, Haider *et al.* [179] obtained a kappa score of 0.98 when classifying between falls and five ADLs. Pyroelectric Infrared (PIR) sensors are also verified through the works of Liu *et al.* [180] and Luo *et al.* [181], who propose and refine novel sensor systems that rapidly detect falls with a 93.1% accuracy with four participants, and 92.2% accuracy with eight participants using Hidden Markov Models (HMMs). Another privacy-secure ambient approach is presented by Haffner *et al.* [182], who use capacitive sensors embedded in both static and portable flooring to classify falls and ADLs with accuracies of 92.6% and 100% respectively, using a Least Squares (LS) classifier.

A large variety of classification methods are adopted across the studies included in this review, with many studies testing multiple classifiers to optimise their results [117, 118, 123, 124, 131, 139, 141, 142, 152–156, 159, 161–163, 171, 172, 174, 178, 179, 182]. Figure 2.6 shows the distribution of classification methods in fall detection studies. Among all fall detection studies, Support Vector Machines (SVMs) were the most common models with 22 appearances, followed by K-Nearest Neighbours (KNN) at 13 appearances, and the equally popular CNN and Artificial Neural Network (ANN) classifiers at ten appearances. Despite their popularity, SVMs, KNN, and ANNs only outperform other models in 47.3%, 27.3%, and 20% of their appearances, respectively. In contrast, CNN-based methods, which were typically compared with classical machine learning models, appeared as the highest performing model in 60% of multimodel studies, being outperformed typically by LSTMs, another deep learning approach [161, 178]. Furthermore, some models such as Naïve Bayes, and Decision Trees (DTs), were featured five and four times respectively without a single appearance as the highest performing model. It is suggested that future research continues to validate deep learning approaches, and that more studies consider contrasting their methods with other classification approaches, as 21 of the 50 studies in this area only consider a single model.

Overall, the results acquired in this area are extremely positive, with many studies reporting performance metrics ranging from 90-100% [117–125, 131, 141, 142, 146–150, 152, 154–178, 180–182], yet many studies fail to address the limitations outlined in this section which prevent the wide scale adoption of this technology in the daily lives of those at risk of falling, such
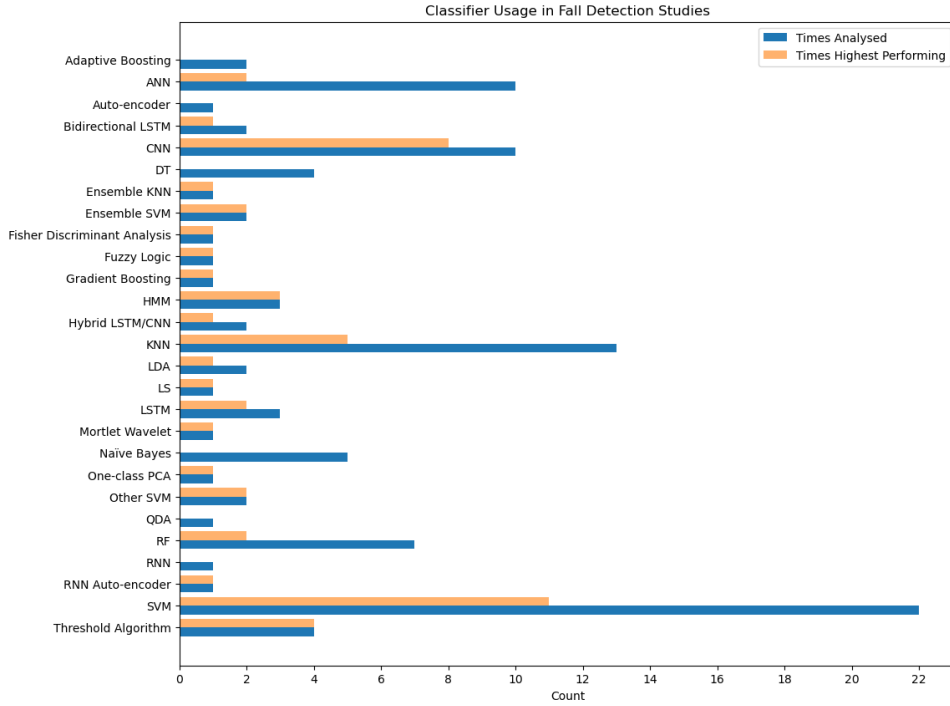
(a) All studies.
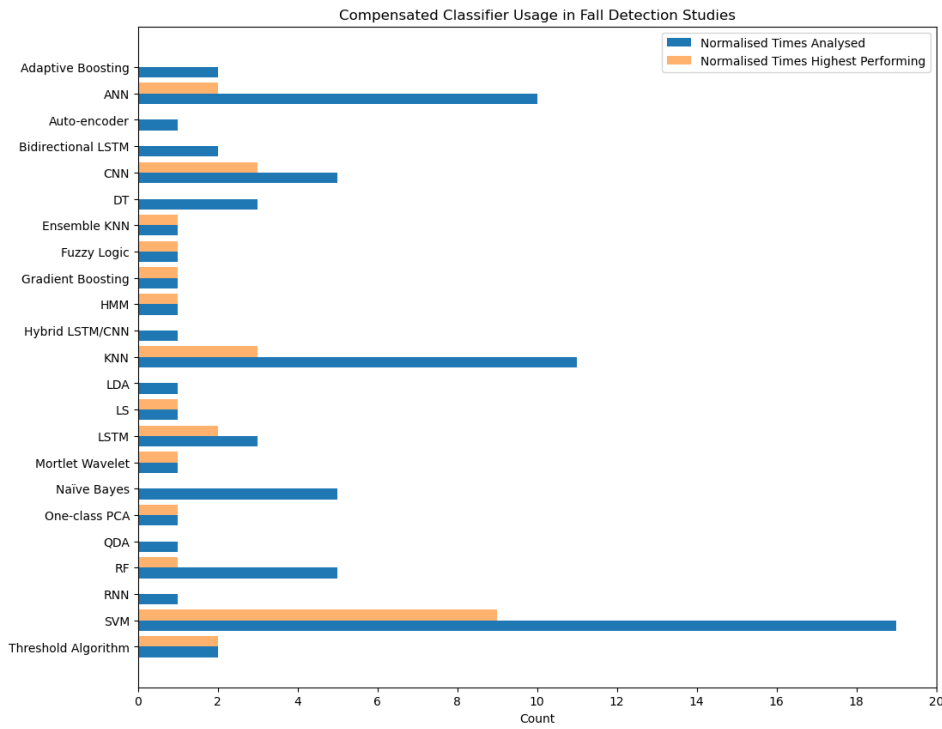
(b) Single-classifier studies removed.

Figure 2.6: The instances in which each classifier was used, and was the highest performing model, in fall detection classification.

as generalisability, convenience, and privacy concerns. These limitations must be overcome on a large scale to allow for the comparison of equally-viable approaches to fall detection, such that specific sensors and models can be identified for use in real-world implementations to help

29

reduce the impact of falls on society.

2.6.5   Fall Prediction

Fall prediction studies typically contain two approaches to identifying a person's individual fall risk. The first of these approaches is the extraction of the spatio-temporal gait parameters using a novel sensor system, allowing healthcare professionals to maintain their current approach to determining fall risk, whilst offering the advantages of increased portability, comfort, and convenience [183–195]. Many studies in this area propose a novel sensor system designed to mimic the function of commercially available systems, such as the Wii Balance Board (WBB) [183], GAITRite [194], or motion capture systems [184, 186]. Agreement measures between IMU and Force Sensing Resistor (FSR) insole devices and the existing standards are particularly high [183, 184, 186, 188, 189], highlighting these sensor types as powerful wearable alternatives to the current standards, all of which are stationary devices.

Alternatively, some studies aim to directly determine fall risk using methods such as machine learning trained on healthy and abnormal gait, to determine the risk of falls in unseen subjects [195–207]. Where in fall detection these models could be trained on fall vs non-fall data, in fall prediction, another measure must be used to determine the risk of falling. In defining the ground truth, studies tend to vary, with clinical assessments [196, 198, 199], questionnaires [200], history of falls [202], fear of falling [204], asymmetry [205], a previous step [206], and various spatio-temporal gait parameters [195, 207] all being used to determine the risk of falling. This variety of ground-truth values, input data, and outcome measures illustrate an issue with current fall prediction research in determining a measure for fall risk. Real fall events are dangerous, unpredictable events, yet the inability to capture them results in a wide variety of outcome measures. However, many of the studies in this area did achieve reasonable performance metrics, demonstrating a capacity to automate sections of fall-related healthcare work such as automatically determining fall risk from the BBS, six-minute walking test, TUG, and 30-second sit to stand tests [196, 199, 200].

Regarding fall prediction datasets, no common datasets exist among the studies in this review. Particularly with regard to direct fall risk prediction, these datasets are essential in reducing the barrier to entry for future researchers who specialise in analytical models. This is reflected in the performance metrics and chosen models in this area, with the average classification accuracy

(a) Number of subjects
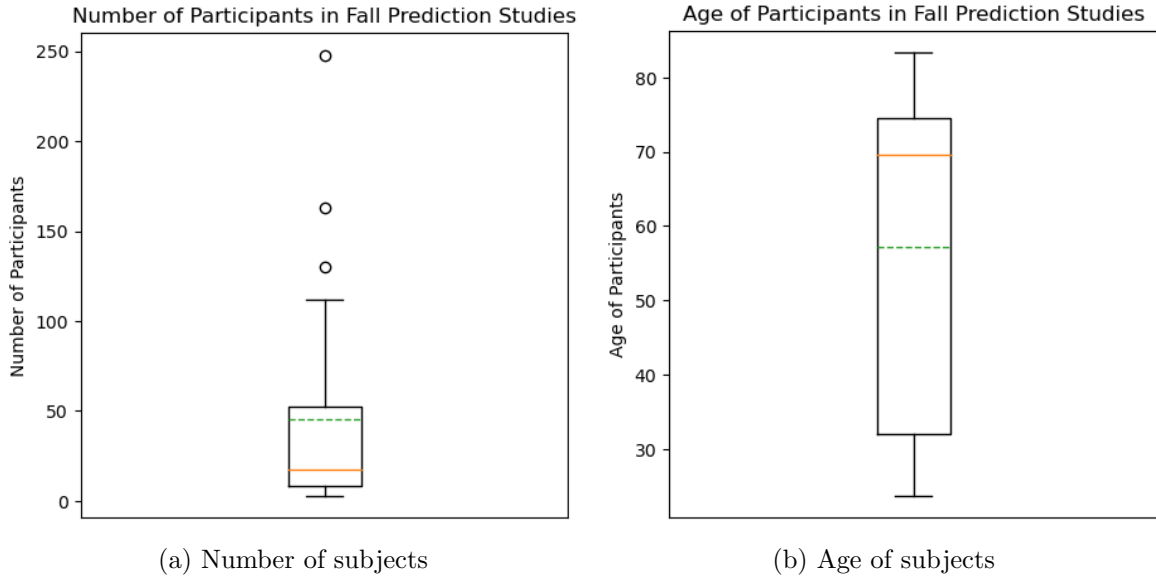
(b) Age of subjects

Figure 2.7: Box plots of the number of subjects and mean age of subjects in fall prediction studies.

across fall risk prediction studies being much lower than with fall detection, and with just a single study by Savadkoohi *et al.* [204] making use of deep learning techniques which achieved extremely high performance metrics of 99.9% specificity and 100% sensitivity on a dataset of 163 participants. Without robust, multi-study testing on collected datasets, proposed approaches cannot be adequately verified, increasing the time for such methods to be adopted in healthcare settings. Furthermore, fall prediction studies typically collect more robust datasets with an increased number, and a wider age range, of subjects when compared to fall detection datasets. As opposed to fall detection, fall risk analysis and spatio-temporal gait parameter extraction do not require a subject to risk harm when building a training set, reducing the ethical barriers to collecting data from the target population at risk of falling. Figure 2.7 shows the wide variety of reported mean subject ages in fall prediction studies.

Among the area of fall prediction, spatio-temporal gait parameters are featured in most studies, either extracting large numbers of parameters suitable for gait analysis [184, 186, 192, 194, 198, 207], calculating a more focused or limited set depending on the available hardware and intended application [183, 185, 187–191, 193, 195, 200, 202, 204], or choosing to forgo observing any spatio-temporal gait parameters in favour of a more specific approach [196, 197, 199, 201, 203, 205, 206]. Of the extracted spatio-temporal gait parameters, Figure 2.8 shows the frequency with which each parameter was referenced with respect to fall prediction for those parameters which were referenced more than once. This highlights Centre of Pressure (CoP)/CoM and

step length as the parameters most relevant to fall prediction, which reflects the most popular

sensors found in Figure 2.9, of IMUs, depth cameras, and force sensing insoles.
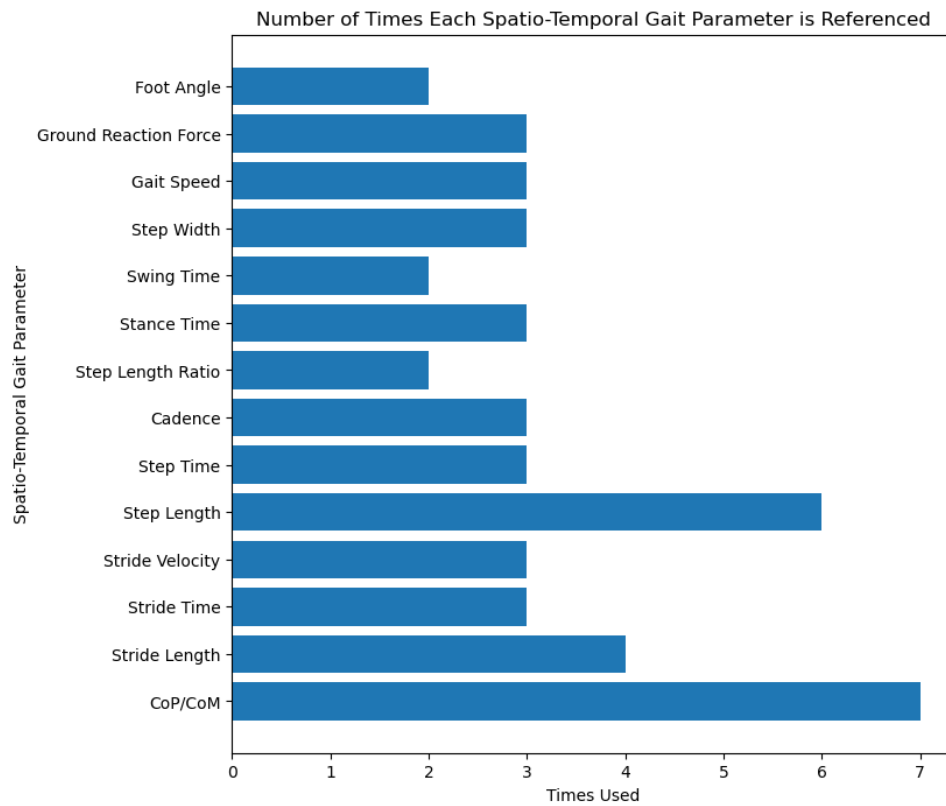
Figure 2.8: The instances in which each spatio-temporal gait parameter was used in fall prediction for those parameters which were referenced more than once.
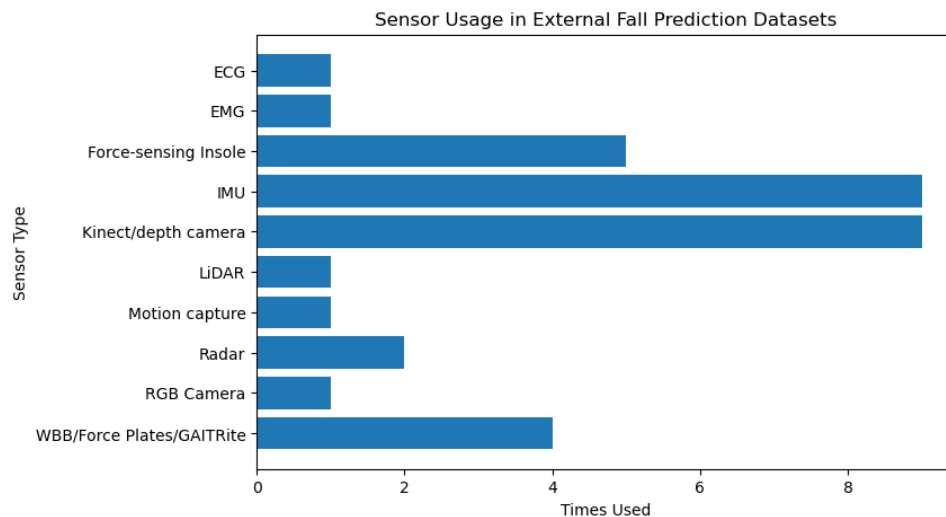
Figure 2.9: The frequency with which each sensor type is used in fall prediction.

2.6.6   Fall Prevention

Fall prevention studies are extremely varied in their devices, sensors, participant numbers, and results [208–219]. Box plots of the mean number of participants in fall prevention studies can be seen in Figure 2.10a. Regarding devices, most studies in this review featured exoskeletons [208, 209, 212, 214, 218–220]. These were primarily active lower-limb exoskeletons which supplied additional torques to the hip [209, 219], knee [209, 218], and ankle joints [208, 212, 214]. The goal of these external torques vary between studies and include reducing gait variability [208, 212], improving balance [209], aiding recovery after a slip or perturbation [218, 219], and increasing foot clearance [214]. These active exoskeletons are tested on small populations of subjects which, whilst insufficient if the device is to be adopted in a healthcare setting, is less important at the prototype stage than in areas such as fall detection, where the training set directly affects the performance of the proposed solution. Another method of applying corrective forces to maintain balance was proposed by Romtrairat *et al.* [215], who proposed a device that used the gyroscopic procession forces of two flywheels in a backpack worn by the subject to counteract postural sway and maintain balance. Unfortunately, this device was only tested on a simulated subject. Some devices are external, user-held devices designed to intelligently offer support and prevent a fall event once it is detected [210, 211, 213, 216, 217]. Robotic walking frames augmented with various sensors, such as force sensors [210], IMUs [211], and depth sensors [217], monitor a subject whilst they walk and intelligently provide support and enact preventative measures when a fall is detected. These devices are typically extremely large, and were only tested on limited datasets of one [210, 211], and four [217] healthy subjects. A more portable alternative is found in robotic walking canes [213, 216], which reposition themselves to maximise the user's stability. Similar to robotic walkers, robotic walking canes feature very small datasets of healthy participants and highlight a need for such devices to be tested on those who will adopt the device, such as older people. Furthermore, these devices demonstrate an application for fall detection and fall prediction research, particularly relating to the use of the smaller sensors embedded in walking canes like IMUs and force sensors.

2.6.7   Fall Intervention

Like fall prevention, fall intervention studies feature a wide array of methods with varying outcome measures [221–231]. As such, this section will explore the approaches and methods of a handful of studies to establish how healthcare studies approach fall impact reduction and

(a) Fall Prevention

(b) Fall Intervention
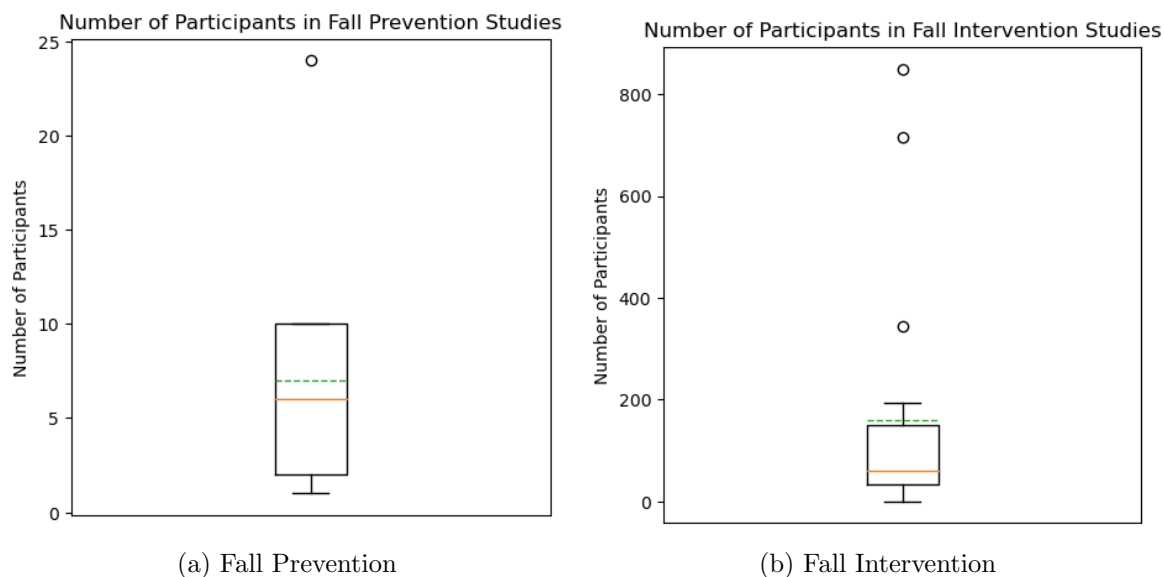
Figure 2.10: Box plots of the number of subjects and mean age of subjects in fall prevention and fall intervention studies.

identify how these can benefit from recent technological advances.

Fall intervention studies in this review include yoga [221], dance [223], elastic-band resistance exercises [227], karate and fitness training [4, 228, 232], Otago training [230], and various Balance training (BT) programmes [222, 224–226, 229, 231, 233, 234]. Participants underwent these programs for 4–52 weeks, before having their fall risk or fear of falling tested through a variety of methods such as the Illinois Fear of Falling (FoF) measure, BBS, TUG, Self-reported Number of Falls (SNF), Falls Efficacy Scale (FES) etc.

Schmid *et al.* [221], Duque *et al.* [222], and Phu *et al.* [231] propose interventions to tackle fear of falling along with improving balance parameters. Schmid *et al.* [221] provided 14 participants aged 65 and older with a 12-week yoga program. Participants were issued a yoga mat, block, and resistance band which were each incorporated into the classes, which required participants to mimic postures whilst sitting in a chair or standing and using the chair as a support. After the 12-week program, participants exhibited a 6% decrease in fear of falling, and an increase in static balance by 4% and lower-body flexibility by 34% [221]. Duque *et al.* [222] instead make use of Virtual Reality (VR) in a randomised controlled trial for the purpose of decreasing fear of falling and improving balance parameters. In this study, 60 participants aged 65 years and older underwent a six-week programme using a custom balance rehabilitation unit that combines variable somatosensory, visual and vestibular conditions to assess and train balance. After the program, participants who underwent training with the balance rehabilitation unit exhibited

improved Survey of Activities and Fear of Falling (SAFFE) scores, along with significantly improved balance parameters, which were associated with a reduction in falls and fear of falling [222]. Finally, Phu *et al.* [231] demonstrated improvements in fear of falling in 195 participants with a mean age of 78. This was achieved through dividing participants into three groups: an exercise group who underwent modified Otago exercises; a VR-based BT group; and a control group. After six weeks, both the Otago and VR BT group demonstrated improved scores on the FES, Sit to stand (STS), Upright Stance Posturography (USS) and TUG tests, along with improved gait speed and handgrip strength [231].

Regarding postural sway methods, Koceja and Greiwe [224] required a single, 63-year-old participant to undergo a balance training program for a month using a self-developed apparatus consisting of a stable platform and free-floating handles which allow for postural sway control during the provided exercises [224]. Similarly, Schwenk *et al.* [225] recruited 33 participants with a mean age of 84.6 to undergo a month of balance training, such as weight shifting and performing specific movements, with data captured from IMUs to establish virtual obstacles and provide visual feedback of the training exercises. This approach reduced CoM, ankle, and hip sway, improved gait speed, and improved Alternate Step Test (AST) and TUG scores [225]. Freyler *et al.* [226] compared the effects of sensorimotor training and reactive balance training over a one-month program on a population of 38 participants with a mean age of 23.5. This study found that, whilst both methods were effective in improving balance and neuromuscular activation, the reactive balance training group showed larger improvements when using a swinging platform and in situations featuring cognitive interference [226]. Coubard *et al.* [223] trialled the effects of contemporary dance on the CoP of 38 subjects with a mean age of 71.6 who were asked to participate in contemporary dance sessions for four weeks. Participants had their CoP recorded before and after the process using a Techno-Concept platform, and Detrended Fluctuation Analysis (DFA) was performed on the time series of CoP displacements. In the contemporary dance group, the alpha component of the DFA increased, indicating higher postural confidence in this group [223]. Together, these studies demonstrate a variety of successful methods for reducing fall risk by improving CoM-related parameters. Finally, Dehzangi *et al.* [235] investigated the effect of vibrotactile feedback devices positioned on the chest and ankle of 12 older people, which alerted the wearer when their postural sway become too high. The device was tested on a population of 12 older people at risk of falls, who were split into a control and experimental group. Use of the device was shown to counteract the degradation of gait

health in the experimental group and improved lateral sway and posture control [235].

Another approach to fall intervention aims to reduce falls by targeting step-related spatio-temporal gait parameters such as step time, frequency, and length [228]. Pliske *et al.* [228] split 68 participants with a mean age of 68 into groups who underwent a 20-week program of either karate or fitness training, along with a control group. Both the karate and fitness training groups demonstrated improved spatio-temporal gait parameters such as reduced single step time, increased step frequency and step length, and improved cognitive performance which was tested using a dual-task gait test in which subjects counted backwards in intervals of three from a given number [228].

Many studies use a series of standardised balance/fall scales to determine the success of a fall intervention whilst featuring a wide variety of methods such as BT, elastic-band resistance exercises, and Otago training [220, 225, 227, 229–233]. Kwak *et al.* [227] split 45 participants aged 65 or older into two groups, one of which received elastic-band resistance exercises, whilst the other was issued general physical therapy for an eight-week period. After the exercise program, participants were evaluated using various scales such as the Functional Reach Test (FRT), BBS, TUG, Sit and Reach Test (SRT), and Activities-specific Balance Confidence Scale (ABC). Subjects showed significant improvements in both groups, with the elastic band resistance group showing more effectiveness [227]. Allison *et al.* [229] issued 20 participants aged 70 or older and who had a history of falls with an eight-week program of sensory-challenge balance training using a SMART Balance Master device. After the program concluded, participants exhibited significant improvements in the ABC, BBS, Sensory Organization Test (SOT), and Lower Extremity Strength Score (LESS) scales, along with improved CoM gain and phase [229]. Liu-Ambrose *et al.* [230] conducted a large study in which 345 participants with a mean age of 81.6 at risk of falling were either issued a series of Otago exercises, or were part of a control group who received their usual care. After 52 weeks, participants were evaluated using the Physiological Profile Assessment Scores (PPAS), TUG, Short Physical Performance Battery Scores (SPPBS), and SNF, which identified no significant improvements in physical performance, despite an increase in the SNF, which reflects a decrease in fear of falling. Verrusio *et al.* [220] propose a passive exoskeleton designed to improve cognitive and motor function in 150 people with a mean age of 64.85, who demonstrated improved scores in the Tinetti Gait and Balance Test, Tinetti Balance, SPPBS, a Numeric Rating Scale (NRS) for pain, and SF-36 QoL. Chittrakul

et al. [232] propose a Multi-system Physical Exercise (MPE) program targeting proprioception, muscle strength, reaction times, and balance in a randomised controlled trial on 72 participants aged 65 and above, 36 of whom received the MPE. After 12 and 24 weeks, these participants underwent several standardised assessments targeting fall risk, fear of falling, depression, and quality of life. Among the MPE group, all assessment scores were observed to improve after 12 weeks, with depression and quality of life scores returning to their baseline values after the 24-week assessment. Finally, Zahedian-Nasab *et al.* [233] measure improvements in FES, TUG, and BBS scores of the control group from a 60-participant cohort with balance disorders aged over 60 years using a Kinect. The Kinect group performed two, 30-45 minute exercise sessions a week for six weeks using the penalty, goalkeeping, ski, and darts activities from the "Kinect Sports" games. After the course, TUG and FES test scores decreased whilst BBS scores increased, indicating improved balance and a reduction in fear of falling.

Finally, two studies by Rikkonen *et al.* [4] and Sturnieks *et al.* [234] perform year-long studies in which the outcome measure is the frequency of falls between the control group and the intervention group. Rikkonen *et al.* [4] split a cohort of 914 women into two groups, one of which was the control whilst the other was given complimentary access to their city's exercise facilities for a year, and were subscribed to a six-month program comprising a one-hour circuit gym session and one-hour of Tai Chi, with warms ups and 50 minutes of training, each week. In a follow-up after 24 months, the intervention group exhibited a 14.3% reduction in fall rate and improvement in TUG speed when compared to the control group. Similarly, Sturnieks *et al.* [234] perform a randomised controlled trial of 716 participants in which 231 participants were assigned Exergame training, 239 were assigned cognitive training, and the remaining 246 were the control group. The Exergame and cognitive group were assigned eight games to play for 120 minutes a week using either their feet or a keyboard, respectively, as inputs for the game. Participants spent an average actual time of 79.7 minutes per week performing the tasks, and a decrease in falls occurred among the Exergame group when compared to the cognitive and control groups. Furthermore, the Exergame group exhibited improvements among some cognitive and general health aspects of the Patient Health Questionnaire 9 (PHQ-9), Iconographical Falls Efficacy Scale (IFES), and Late Life Function and Disability Instrument (LLFDI).

These studies outline a wide variety of methods and outcomes, which demonstrate many forms of exercise and balance training that can have a positive impact on balance and reduce the

likelihood and fear of falls. Studies generally make use of large cohorts of appropriately-aged participants, as seen in Figure 2.10b, and use a variety of established scales, tests, and spatio-temporal parameters related to falls to determine their success. This approach immediately validates proposed methods in the context of established or current methods, which can more easily communicate the successes of such methods, creating opportunities for adoption in health-care settings.

2.6.8 Summary of Fall-Related Research

This review offers an insight into the wide range of literature that shares the goal of reducing the impact of falls in society. Whilst developments, trends, and future research in each of the four core areas have been identified, this cross-disciplinary approach to fall literature searching highlights broader research gaps which, when addressed, will help to accelerate the adoption of all fall-related technologies in healthcare settings.

Fall Detection

Fall detection research, despite being the largest area of research in this review, has shown very little change in direction over the past ten years. These studies employ a formulaic approach of capturing limited datasets using novel configurations of a narrow range of sensor types, without consideration for the user experience or the implementation complexities involved in adopting such a solution in a real-world healthcare setting. This approach to fall detection lies in stark contrast to fall intervention, and as such is insufficient in producing results which can be adopted in real-world scenarios, leaving this area stagnant for many years. Future research in this area should be designed with implementation, rather than analytical results, as the research outcome, such that the large variety of high-performing fall detection methods in this study are exposed to the nuances of real-world falls in subjects at risk of falling. Furthermore, novel sensor systems must be designed with the input of those at risk of falling, as privacy concerns, the comfort of having such a system equipped, and the convenience of charging and maintaining the device are factors more likely to affect the adoption of this technology than small variations in accuracy. Future research in this area must introduce larger, more realistic datasets consisting of subjects at risk of falls, perform qualitative studies into the needs and feasibility of the current successful methods, and take additional steps to design infrastructure such as mobile apps or alarm systems which act upon the detected fall.

Fall Prediction

Fall prediction features a wide variety of approaches to automate several aspects of what would be a traditional gait analysis procedure. This involves either extracting the spatio-temporal gait parameters in novel ways, or skipping this process and determining a person's risk of fall directly. As such, these studies have a lower potential impact than fall detection, prevention, or intervention, but do help to improve and standardise the existing fall-related healthcare pipeline. For this reason, these studies are much more healthcare-focussed than fall detection and prevention studies, typically already featuring large datasets of appropriate subjects and looking to implement their systems in real gait-analysis settings. Fall prediction studies which aim to replace some existing tools used in gait analysis, such as the GAITRite, WBB, and motion capture systems, with simpler portable systems, have demonstrated the feasibility of IMUs and force-sensing insoles as powerful wearable alternatives to the existing stationary approaches. Future research should take full advantage of these methods and enrich gait analysis with data captured outside the laboratory, as studies have demonstrated a dependency on gait performance with terrain [38, 39]. With regard to direct fall risk assessment, many studies used just a single physiotherapist as the ground truth value for determining if a subject was at risk of falling, which introduces bias into these datasets. The future work of these studies, therefore, should be to improve their models and datasets with additional physiotherapist evaluations of a subject's fall risk, such that risk assessment can be reliably automated. Furthermore, given the frequency with which fall-related standardised scales, such as the BBS, are used in fall intervention, fall prediction studies, such those of Colagiorgio *et al.* [196], Eichler *et al.* [199], and Haescher *et al.* [200], which aim to automate fall-risk analysis through the automated scoring with these scales are shown to augment existing healthcare approaches to fall intervention, and should be further pursued.

Fall Prevention

Fall prevention studies feature a broad range of approaches to preventing a fall through inducing forces or providing feedback to the user during walking. These devices are generally complex and in the prototype stage, with several proposed systems being tested on just a single subject. As such, one large requirement in this area is the need to consider activities other than walking. It can be seen, therefore, how dependent the future of fall prevention is on the current developments in fall detection and prediction, with each of these fields containing crucial developments which

fall prevention approaches must incorporate before they can be adopted. With respect to fall detection, fall prevention systems must be capable of determining when a fall is occurring, when activities other than walking are being performed, and accurately differentiating between common daily activities and falls, so that these systems know when to activate and prevent a fall. This lack of consideration for other walking activities can also be seen in the type of device being proposed, as many of the exoskeletons, walking canes, and robotic walkers are unusable or untested outside of walking on level ground. Furthermore, many fall prediction methods offer the capabilities to monitor the spatio-temporal gait parameters and determine fall risk, which are also crucial variables when controlling a fall prevention device. Fall detection and fall prediction make heavy use of IMUs and force-sensing insoles, respectively, each of which is prominently featured in many of the fall prevention methods in this review. Future studies in this area should continue to develop systems with these sensor types, and investigate the effectiveness of combining fall detection and fall prediction methods to augment and contextualise the devices proposed for the purpose of fall prevention.

Fall Intervention

Fall intervention studies typically aim to swap existing fall intervention and rehabilitation programs with novel exercises which offer increased benefits such as balance training or more general exercise like yoga, karate, dance, etc. Some of these studies make use of technology such as VR, IMUs, Kinect, and the SMART balance training device, however most studies make use of traditional exercises and manual fall risk assessment methods. This reflects a lack of impact in fall prediction studies, particularly of those that automatically determine the spatio-temporal gait parameters or directly assess fall risk. Furthermore, fear of falls only appears as an outcome in fall intervention studies, despite being relevant to all areas of fall research. Fall intervention studies also feature the most appropriate datasets of each area in this study, with large cohorts of older people at risk of falling being commonplace among fall intervention studies. This could be due to a variety of reasons, such as an increased difficulty in obtaining ethical approval to explore novel technologies on vulnerable populations, or reduced trust by potential participants in these technologies.

2.7 Human Activity Recognition

The field of Human Activity Recognition (HAR) involves the use of classification methods, such as Machine Learning (ML) and Deep Learning (DL), to determine the activity a person is performing from data collected using a wide variety of sensors [236]. Whilst some studies and datasets aim to classify activities involving the upper limbs [236, 237], this review focusses on lower-limb HAR, such as walking, navigating stairs and ramps, and non-ambulation activities like sitting and standing [238–246]. Due to the nature of the detected activities, wearable sensors have shown to be effective in enabling high-accuracy activity recognition whilst maintaining a high level of portability, leading many modern studies to use sensory data from smartphones [247–249]. However, another application of HAR is in the control systems of microprocessor knees, which must determine user intent with high accuracy in extremely short times [244, 250].

HAR studies feature a multitude of sensor systems, datasets, and classification techniques, resulting in large between-study variations in reported performance metrics. Attal *et al.* [28] used nine IMUs placed on the chest, right thigh, and left ankle and a variety of classical ML models to classify between 12 classes of human activities. The study found that KNN and Random Forest (RF) were the most accurate models, and that all supervised ML methods performed better than the unsupervised methods. However, this paper was limited by cumbersome wearables, a lack of participants and a biased training set where over 30% of the data belonged to a single activity. Sok *et al.* [30] use HMMs to increase the accuracy of HAR classification algorithms by preventing the model from switching between states that did not make logical sense (for example, rapid alternations between lying down and walking) which resulted in an increased accuracy of up to 2.6%. Asim *et al.* [31] proposed a system to perform context-aware HAR, where data collected from a smartphone was assigned classes for both the activity and the context (such as: lying down — watching TV, and lying down — sleeping). The researchers state that this approach would increase utility due to the variety of different situations associated with a given activity. After performing feature extraction and training various models, RFs demonstrated the highest accuracy and only a small accuracy drop was reported between the six-class, context-independent data and the 15-class, context-dependant data. This paper is a good initial step into HAR for real-environment activities, however, this study is limited by the lack of terrain variation [31].

HAR models can be trained subject-dependently or subject-independently, where accuracy or

generalisation are prioritised, respectively [246, 251]. Subject-dependent models are trained using data gathered from the end user, which typically involve lengthy training programmes for each individual using the system and attain high accuracies, whilst subject independent models use a large database for training, striving for 'off the shelf', pre-trained systems at the cost of subject-specific accuracy [246]. Some studies combine these approaches, adding a small amount of subject-specific data to a large database, which yields further accuracy improvements [33, 246, 252].

With respect to DL methods, Bianchi *et al.* [32] demonstrate the potential accuracy of CNNs by achieving accuracies of 92.5% and 97% on two popular datasets, whilst Lawal and Bano [33] convert sensor signals from the RealWorld Human Activity Recognition dataset into images for analysis with a CNN, which can perform automatic feature extraction and classification. The model utilised decision fusion to combine individual predictions from each of the two sensors to increase accuracy. Despite this technique, a relatively low accuracy of 78% was reported when classifying between all eight activities due to the confusion between the 'walking' and 'climbing up' activities. This factor was also identified by Murad and Pyun [34], who found that their Deep Recurrent Neural Network (DRNN) could not differentiate between the 'elevator' classes of the USC-HAD dataset, despite achieving an accuracy of 97.8% and outperforming SVMs, KNN, RFs, and CNNs across five datasets. In summary, the potential accuracy gains of LSTM and CNN seem to depend on the application, presenting a need for further investigation into the contexts in which these models excel.

HAR datasets offer a large range of different sensor configurations and modalities. [35, 238–241, 253, 254]. However, due to class imbalances, differences in subject numbers, varying sample rates, different sensor modalities, and the use of a wide range of classification models, it can be difficult to determine what factors result in high-accuracy HAR [255, 256]. Furthermore, generalisation can be a concern, with datasets typically using a single staircase or ramp, resulting in the models learning only a single step height and ramp incline. Camargo *et al.* [254] manage to mitigate some of these issues by using ramps and stairs of varying heights, which helps to increase model generalisation. However, this dataset utilised an extremely cumbersome sensor system which would not be viable for daily usage. In 2020, a novel dataset was proposed by Luo *et al.* [35], with a focus on under-explored, real-environment HAR. However, this dataset is still limited due to a lack of activities as, although ten were collected, eight were simply level-

ground walking on different terrains, with two remaining stair ascent classes. This approach is too minimal to produce a model that sufficiently generalises when considering the number of permutations of terrain and walking activity in daily life.

In summary, RF classifiers seem to provide extremely high accuracies for HAR, often outperforming other classical ML algorithms when acting on the same dataset [28, 30, 31, 248, 257]. On the other hand, DL methods can further increase accuracies, particularly with respect to CNN and LSTM models, which have consistently exhibited high accuracies and reasonable decision times [32–34, 258, 259]. HAR datasets lack terrain and real environment data, despite the large number of publicly available datasets which, in recent years, demonstrate a focus on Internet of Things (IoT) applications, telemedicine, remote monitoring and identification of activities among vulnerable populations [32, 247]. HAR is an application of sensor technologies somewhat removed from reducing the impact of falls, and may be best suited to the labelling of remotely collected gait data such that the healthcare professionals who analyse these data are aware of the context in which it was collected. As this gait data can be used in multiple areas of diagnosis and prognosis, this context is crucial to prevent misdiagnoses and allow healthcare specialists to select which activities they want to analyse the data from. Furthermore, HAR can be used to detect bouts of walking in unobserved subjects for the purpose of remotely monitoring the gait parameters to evaluate fall risk in real-time. With these applications in mind, the lack of real-environment datasets severely limits the potential for healthcare applications of HAR.

2.8 Gait Event Detection

Human gait is considered to be symmetrical and composed of eight phases separated by whether the foot is contacting the ground or is not in contact with the ground [36, 260, 261]. These eight phases of gait are as follows: the Stance Phase consisting of Initial Contact (IC)/Heel Strike (HS), Loading Response (LR), Mid-Stance (MSt), Terminal Stance (TSt), and Pre-Swing (PSw)/Toe-Off (TO), and the Swing Phase consisting of Initial Swing (ISw), Mid-Swing (MSw) and Terminal Swing (TSw). Gait event detection typically involves classifying the gait phase using sensor data and threshold algorithms or ML models [36, 262–269], with some studies additionally aiming to identify a general activity or 'gait mode' such as walking or climbing [243–245]. Applications of gait phase and gait mode detection typically relate to

control systems for prosthetic limbs, which restore natural ambulation to amputees [243, 246], or for use in diagnostics along with spatio-temporal gait parameter estimation [25, 270–272]. In all of these areas, three methods are traditionally used for classification: rule-based algorithms, user-dependant ML models and user-independent ML models [246, 266, 273].

Rule-based gait phase detection algorithms typically involve identification of the HS and the TO events by monitoring when sensor signals or calculated variables, such as CoP, cross a threshold or reach a specific value [265, 266, 274]. One example of the benefits of such algorithms can be seen in the work of Maqbool *et al.* [267], where peak detection is used to find the HS and TO events with 100% accuracy on both a healthy control and multiple amputees, regardless of the worn prosthetic. Whilst demonstrating a high accuracy, problems arise when considering the order in which detection of events occurs, resulting in detection issues during the initial stride [267]. Additionally, as all data was collected in a laboratory environment, the accuracy in real-world settings is unknown. Many threshold based algorithms are simple to implement and reliable in systems where only HS and TO events are required, but generally lack the capacity to accurately identify additional gait phases [266]. The use of machine learning techniques is more applicable for higher resolution gait phase detection with high accuracy at the cost of increased decision time, as shown by Farah *et al.* [275], Heng *et al.* [276], and Ding *et al.* [277], the latter of which additionally demonstrates that DL methods such as LSTMs can further increase accuracies over classical ML models. Furthermore, the sequential, cyclical nature of gait enables certain techniques, such as finite state machines and HMMs, to improve classification accuracy through the inclusion of state probabilities [30, 263, 278]. Once the HS and TO events are identified, data from individual strides can be processed to extract the spatio-temporal parameters such as stride length, stride width, velocity, and cadence, which hold clinical relevancy in diagnosis, prognostication, and rehabilitation [271].

2.9 Terrain Identification

Terrain identification is not uniquely applicable to human fall-related research, with stroke research [279], walking robot control systems [280–282], exoskeletons [283], and prosthetics [284] all benefitting from knowledge of the terrain underfoot. However, in the context of human gait and fall research, as stated by Das *et al.* [285], "Identification of the type of terrain (e.g., grass, flat ground, sand, gravel, etc.) is scarcely covered in the current literature.", highlighting

a need for additional terrain identification systems. The following section explores studies and research trends in recent years which aim to address this issue.

Moore *et al.* [286] created a dataset of online videos recorded from a range of indoor and outdoor terrains from YouTube videos. They then created three CNN-based models to classify the video frames and determine whether the scene is indoor/outdoor, if the floor is visible, and whether the terrain was asphalt, concrete blocks, grass, gravel, sand, snow, or woodland. The model was tested on two subjects and performed well under certain conditions, with accuracies of 45-80% when tested on 720p-resolution video, which increased to 70-90% when the quality was increased to 1080p [286]. Similarly, Nouredanesh *et al.* [287] used a belt-mounted wearable camera to collect a novel dataset from nine subjects walking on eight terrains: pavement, gravel/stone, soil, grass/foliage, high-friction materials, indoor tiles, and wood. Several models were trained, and classification scores were high, with the outdoor and indoor models achieving accuracies of 99.23% and 85.26%, respectively. However, not all subjects walked on all possible terrains, with subjects OA2 and OA9 walking exclusively on indoor terrains [287]. Diaz *et al.* [284] attached a Samsung S6 smartphone camera to a subject's prosthetic with the aim of identifying terrain for use in the control system of these devices to increase safety and comfort. The subject walked for four minutes on six different terrains: asphalt, carpet, cobblestone, grass, mulch, and tile. A bag of words classifier was then used to identify each terrain, and achieved a mean accuracy of 86%, although this appears to be inflated due to large class imbalances, with grass being classified with less than 50% accuracy [284]. Zhong *et al.* [288] compared the locations of two wearable cameras: a custom device placed on the leg, and the Tobii Pro Glasses 2 eye tracker for the purpose of terrain classification. Seven participants wore both systems while walking at a self-selected pace on tile, grass, brick, cement, upstairs, and downstairs. A Bayesian neural network was then trained to predict the terrain a participant was about to walk on within the next one to two seconds. Of the tested model architectures, the Bayesian gated recurrent unit model achieved the highest accuracy at 91.30%. When combining features from the glasses and the leg-mounted device, this accuracy increased to 95.36% [288]. Finally, Das *et al.* [285] had two subjects walk on concrete, cobblestone, sand, and gravel while equipped with IMUs on the feet, lower legs, upper legs, lumbar, and sternum, along with GoPro Hero 4 cameras placed on the ankle, chest, and head. The researchers built two CNN models for terrain classification using either camera or IMU data. Whilst the camera-based classification achieved an accuracy of 97.79%, this study demonstrates the capacity to predict terrain with IMU data, with 1D CNN

models trained on this data achieving accuracies of 94.90%-97.00% depending on the position of the IMU, with the sternum being the position that achieved the highest accuracy [285].

Regarding IMU-only studies, Hashmi *et al.* [289], Dixon *et al.* [290], and Hu *et al.* [291] aim to classify terrain using data from one to two IMUs. Hashmi *et al.* [289] attached a smartphone to the chest and lower back of 40 subjects who walked on six terrains separated into soft (carpet, grass, and soil) and hard (concrete, asphalt, and tiles) surfaces. Features were extracted from the data, which were then processed by a SVM and RF model. Of the sensors and models, the highest accuracy was obtained by the RF using data from the sensor on the lower back, which classified between the six terrains with 88.7% accuracy [289]. Dixon *et al.* [290] collected data from 29 participants, each of which wore a 3-axis accelerometer on the lower back and the right tibia, while running on three surfaces: concrete, synthetic, and woodchip. CNN and Gradient Boosting (GB) models were then trained on the data from these sensors. The highest performing combination of model and sensor used GB with both accelerometers, which identified terrain with 97.0% accuracy [290]. Hu *et al.* [291] had 17 older, and 18 younger subjects walk over flat and uneven brick surfaces while equipped with a IMU on the trunk [292]. These data were then used to train an LSTM model, which classified terrain with 96.3% accuracy [291]. Whilst accurate, all of these studies consider only subject-dependent cross validation, which impedes the generalisation of these models.

Whilst these studies show the current state of terrain classification for human subjects, this field is not limited to this application, with some studies demonstrating the capacity for depth cameras like the Microsoft Kinect V2 to classify terrain for robot walkers with accuracies of 94-99% across 10-12 classes [280–282]. Additionally, LiDAR technologies have proven useful in classifying terrain in the context of robotics [293, 294]. However, due to the size and weight of devices like the Kinect V2, these do not see applications for terrain classification with human subjects.

2.10 Notable Sensor Types In Fall-Related Research

Each area of this chapter highlights different sensor types as being effective towards the associated application. The following section explores the most promenade sensor types in different areas of fall-related research.

IMUs appear throughout almost all areas of technology-related fall research. These sensors comprise an accelerometer, gyroscope, and magnetometer, the data from which are fused to identify movements in 3D space [247, 295]. IMUs are also small, lightweight devices which can easily be attached to the body, resulting in their popularity among gait analysis [36, 37] and HAR [35, 238–241, 253, 254, 296].

FSR insoles appear frequently among fall prediction research, as demonstrated in Figure 2.9, and are suited to extracting the CoP/CoM [186, 188–190] and identifying the gait phase [265, 297–299]. These sensors are also convenient, comfortable, and subtle when equipped by simply placing them inside the shoes.

Finally, while camera technologies are effective across most areas of fall-related research, the area where they offer unique capabilities in the literature is through effective terrain classification. However, to preserve the privacy of subjects, alternative methods must be investigated to replicate these successes without capturing images. Das *et al.* [285] demonstrated the capability for IMUs to achieve high accuracy terrain classification, however it is possible that a combination of LiDAR and colour sensor could capture depth and low-dimensionality visual data, which reflect the success of depth cameras in terrain classification while protecting the wearer's privacy.

2.11 Gaps in the Literature

Current studies into gait analysis lack environmental context [35, 36, 300] and focus too heavily on specific conditions, despite the medical literature suggesting that many people who are at high risk of falling share certain spatio-temporal gait abnormalities such as increased variability and asymmetry, as noted by Li *et al.* [13] and Fasano *et al.* [11]. If projects were more tailored to these underlying properties of gait, a more general utility could be created to aid in the rehabilitation and recovery process of those with hip replacements, new prosthetics, or gait-affecting injuries, whilst also monitoring progressive conditions such as MS and PD.

Existing fall research, particularly fall prediction research, can use variations in the spatio-temporal parameters to assess a person's risk of falling. However, these parameters are subject to variations caused by internal and external factors, such as health conditions and the terrain underfoot. As such, it is crucial for data collection systems designed for use in real-world

scenarios to collect contextual data about the environment and activity being performed. Furthermore, terrain itself has been shown to contribute towards a person's risk of falling through introducing slip and trip hazards, and inducing changes in gait to accommodate the reduction in balance on these surfaces. To address this issue, some studies have aimed to perform terrain classification using wearable sensors, such as body-mounted cameras and IMUs. However, there are privacy concerns with systems that use body-mounted cameras [236], whilst the IMU-based approaches are not tested using subject-independent cross validation, meaning that a training period would be required if implementing these in healthcare systems. Furthermore, many IMU-based approaches do not consider a wide range of common indoor and outdoor terrains. This highlights a need for a privacy-retaining sensor system which collects data from subjects walking on a range of indoor and outdoor terrains to explore the contributions of unexplored sensor types.

Finally, the areas of gait analysis and fall-risk detection lack real-environment devices and applications, as the spatio-temporal gait parameters have been shown to differ greatly in real environments when compared to laboratory conditions [301]. This has significant clinical implications when considering that currently, gait analysis occurs in a confined area of laboratory-like conditions when using systems such as the GAITRite [302]. Furthermore, the effect of terrain on gait is largely separated into smooth and uneven terrain [108–112], without consideration for the effect of individual real-world terrains on gait. As a result, the future of automatic gait analysis must account for realistic terrains, which can augment data collected using methods such as IMUs in real environments to better represent the context in which the data were captured, and offer insights into the effect of terrain on fall risk [300].

These areas highlight a gap in the literature for the development of a terrain-identification system which incorporates the sensor types required for remote gait analysis, fall prediction, and HAR, such as IMUs and FSR insoles. Furthermore, due to the successes in the literature of using depth cameras for terrain identification in robotic applications, a combination of LiDAR and colour sensors may be capable of emulating this success by extracting depth and basic visual information about the terrain underfoot, without capturing image data to maintain the privacy of the wearer. Such a system will be capable of monitoring the incremental internal and external fall-risk factors that occur during natural walking on a range of terrains throughout a person's daily life for the purpose of real-time fall prediction.

2.12 Summary

This chapter introduces the multidisciplinary research field of falls and fall-impact reduction research such as the various internal and external fall risk factors, how the technological and healthcare literature address falls through detection, prediction, prevention, and intervention, HAR, gait event detection, and terrain classification. These areas highlight the many conditions encountered in daily life which can contribute towards a person's fall risk. While a 'perfect' fall prediction system would be able to detect a fall in the steps before it occurs, this capability does not exist at present. As such, a more useful approach in the current landscape of fall research may be to monitor a person's individual risk of falling in real-time, which is calculated by combining knowledge of how various health conditions affect gait, along with automatically-detected external risk factors such as terrain. This thesis outlines the design of a prototype system capable of monitoring these changing real-time fall-risk factors such that a person's fall risk can be monitored and estimated throughout the various different terrains and walking activities encountered in daily life.

Chapter 3

Analysis of Existing Datasets

3.1 Introduction

The development of a device which can monitor incremental risk factors first requires the ability to differentiate walking from other activities. Once the subject is determined to be walking, the spatio-temporal gait parameters can be extracted from this data and used to monitor gait health and risk of falling, as covered in Chapter 2. This prevents the system from attempting to determine the spatio-temporal parameters during activities which will affect the gait cycle, such as ramps and stairs. Many studies have been conducted in the field of Human Activity Recognition (HAR) with respect to analysing existing datasets, offering a large range of classifiers, results, and preprocessing parameters [29, 303–306]. Among this wide variety of approaches to activity classification, Semi Non-Overlapping Windows (SNOW) and Fully Non-Overlapping Windows (FNOW) are a popular approach in converting time-series data to individual samples, which can be used to train Machine Learning (ML) models [307–311]. This approach is also used, although is not necessary, with many deep learning techniques such as Convolutional Neural Networks (CNNs), Deep Neural Network (DNN), and Long Short-Term Memory (LSTM) models [312–314]. Due to the wide array of sliding window parameters used in these studies, some researchers have aimed to analyse the effects of changing these parameters on the classification accuracy of ML and Deep Learning (DL) models [313, 315].

Dehghani *et al.* [315] explore the effects of window size on the classification accuracy of two datasets by Baños *et al.* [316] and Morris *et al.* [317]. This study finds that window size does not correlate with classification accuracy, as one dataset decreases in accuracy with window size

whilst the other increases. Rather, this study concludes that use of SNOW correlates with the underperforming of subject-dependent (Train-Test Split (TTS)) cross-validation, whilst having no effect on subject-independent (Leave One Subject Out (LOSO)) cross-validation despite increasing the computational costs during training. However, this study is limited by the choice of classification method as, while K-Nearest Neighbours (KNN), Decision Tree (DT), and Naïve Bayes (NB) are somewhat prevalent in the literature, Nearest Centroid Classifiers (NCCs) are rarely seen, and all of these methods are shown to be less popular or effective than Random Forests (RFs), Artificial Neural Networks (ANNs), and Support Vector Machines (SVMs) [318–320]. Furthermore, a limited feature set is used, each dataset contains only Inertial Measurement Unit (IMU) sensors, and there are large variations in activity type, number of activities, and number of subjects between datasets. Banos *et al.* [311] studied the effect of window size on classification performance for a single dataset featuring accelerometers placed on each thigh, shank, upper arm, forearm, and the back [256]. This work highlights the need for a balance between high accuracy and rapid decision times, and finds that larger window sizes do not correlate to increased classification performance, with the optimal window sizes occurring below two seconds using DTs, KNN, naïve bayes, and a NCC. Similarly, Niazi *et al.* [321] analysed the codependency of window size and sample rate to determine what parameters enable the highest classification accuracy using RFs and a single hip-worn accelerometer. This study found that window sizes of two to ten seconds are optimal, contrasting the results of Banos *et al.* [311]. Both of these studies highlight that future work is needed to consider additional technologies and sensor types. Li *et al.* [322] discuss the difficulty of determining an optimal window size for a given application, instead choosing to use different window sizes for each activity based on the temporal properties of that activity, which increases classification performance. Jaén-Vargas *et al.* [313] collect a novel dataset from ten healthy participants using an IMU and motion capture system. Participants performed three core movement activities: walking, squatting, and sit-to-stand. Using various window sizes ranging from 200 samples down to just 50, the study found that larger window sizes increased model performance across all models for both the motion capture and IMU data. Whilst accounting for the introduction of bias, this study is limited by the use of a single dataset and a limited range of activities and sensors. Furthermore, the use of automatic feature extraction in deep learning limits the scope of these results for researchers wishing to use more lightweight wearable devices who may wish to use classical ML algorithms, as the use of human-extracted features may change these results.

Regarding sensor placement, Duan and Fujinami [255] placed seven accelerometers on the upper arm, wrists, thighs, and chest to determine how sensor location affects classification accuracy. This study found that sensors placed on the subject's dominant side, the right side in all cases for this study, exhibited increased performance with the right wrist being the highest-performing sensor type when used alone. Furthermore, this study evaluated the use of RF models along with deep learning techniques such as convolutional neural networks, transformers, and long short-term memory models, with the latter. Kulchyk and Etemad [323] analysed the performance of sensors positioned on the sternum, left thigh, right ankle, and right shoulder using a convolutional neural network for both subject-dependent and subject-independent cross-validation. This study found the right ankle to be the optimal sensor location, with multiple pairs of sensors including the ankle sensor resulting in 100% classification accuracy [323]. Fianlly, Khan *et al.* [324] place five sensor nodes consisting of accelerometers and gyroscopes on each forearm, the waist, and each ankle and perform HAR using simple logistic regression, naïve bayes, and sequential minimal optimization classifiers. The study found that individual sensor performance was dependent on activity type, with sensors on the chest and thigh being optimal for stationary tasks, whilst sensors on the thigh, lower back, and ankle performed better at movement tasks [324]. Many studies which consider sensor placement for HAR consider only accelerometers or IMUs [255, 323–326], leaving much room for sensor position analysis using additional technologies which can capture motion data.

In summary, due to contrasting results across these analyses, there exists a need to analyse the sliding window feature extraction parameters across multiple datasets whilst accounting for variations in subject number, sample rate, and activities. This analysis will help to eliminate the effect of variations in datasets on reported model performances, which may introduce classification bias, affecting the results and conclusions of these analyses. Furthermore, both subject-dependent and subject-independent cross-validation must be considered to verify the findings of Dehghani *et al.* [315], and different sensor types must be explored such that this analysis is applicable to a larger number of sensor systems and datasets found in the literature. This chapter outlines the homogenisation and subsequent analysis of four multi-sensor HAR datasets in the literature to identify these trends and verify the findings of existing studies in this area, along with identifying the optimal sensor locations and analytical methods for the development of a system capable of monitoring incremental fall risk.

3.2 Methods

Four datasets were selected for this study which feature a wide variety of sensor systems, an appropriate number of participants for sufficient model generalisation, and walking activities comparable between datasets. A description of each dataset along with the reasons it was chosen for this analysis follows.

3.2.1 Dataset 1: USC-HAD

The USC-HAD dataset [238] was published in 2012 and features 14 participants with a mean (standard deviation; std) age, height and weight of 30.1 (std: 7.2) years, 170 (std: 6.8) cm and 64.6 (std: 12.1) kg respectively. Each subject was equipped with a single 'MotionNode' IMU containing a 3-axis accelerometer, gyroscope, and magnetometer, totalling nine data channels. The IMU was mounted to the participants' anterior right hip in a pouch designed for mobile phones. Data was recorded using a laptop which was held under the arm, pressed to the waist by the subject and connected to the IMU via a cable.

The USC-HAD dataset features 12 activities which were performed at the participant's own pace [238]. These activities were: walking forwards, left, and right, walking upstairs and downstairs, running, jumping, sitting, standing, sleeping, and going up and down in a lift.

USC-HAD was chosen because this dataset has been well explored in the literature since its publication [34, 327, 328]. Therefore, this dataset will act as a control for the newer datasets to validate the chosen methods and models.

3.2.2 Dataset 2: HuGaDB

The HuGaDB dataset [239] was published in 2017 and features 18 participants with a mean age, height, and weight of 23.67 (std: 3.69) years, 179.06 (std: 9.85) cm, and 73.44 (std: 16.67) kg respectively. The sensor system worn by each participant consisted of IMU sensors placed at the thigh, shank and foot, and an Electromyography (EMG) sensor placed on the vastus lateralis, each of which are sampled at around 60Hz. This setup was mirrored on each leg, for a total of six IMUs and two EMG sensors.

Participants were asked to perform the following 12 activities at a usual pace: walking, running, navigating stairs, sitting (stationary), sitting down, and standing up, standing (stationary),

cycling, going up and down in a lift, and sitting in a car [239].

3.2.3   Dataset 3: Camargo et al.

Camargo *et al.* [254] created an open-source dataset for the study of lower-limb biomechanics in 2021, featuring 22 healthy participants with a mean age, height, and weight of 21 (std: 3.4) years, 170 (std: 7.0) cm and 68.3 (std: 10.83) kg respectively. Subjects were equipped with 11 EMG sensors, three goniometers and four, 6-axis IMUs on their right side only. Sensor locations and sample rates can be found in Table 3.1.

Table 3.1: The sensor type, position, and sample rate of each sensor in the Camargo et al. dataset.

Sensor	Position	Sample Rate
Goniometer	Hip Knee Trunk	1000Hz
Inertial Measurement Unit	Trunk Thigh Shank Foot	200Hz
Electromyography Sensor	Gastrocnemius Medialis Tibialis Anterior Soleus Vastus Medialis Vastus Lateralis Rectus Femoris Biceps femoris Semitendinosus Gracilis Gluteus Medius Right External Oblique	1000Hz

Whilst participants only performed six basic activities, the transition states have also been labelled, raising the activity count to 19 [254]. With the 'idle' class removed as no activities were being performed, 18 walking activities remain, consisting of six core activities and the transitions between them. These core activities were ramp ascent, ramp descent, stair ascent, stair descent, stand, turning, and walking.

3.2.4 Dataset 4: CSL-SHARE

CSL-SHARE is a dataset published in 2021 for the purpose of exploring activity recognition for common sport-related movements [240]. The sensor system is a multimodal, knee-mounted system featuring two, 6-axis IMUs placed on the thigh and shank, four EMG sensors placed on the vastus medialis, tibialis anterior, biceps femoris, and gastrocnemius, a goniometer placed on the lateral knee, and an airborne microphone. Like the Camargo et al. dataset, these sensors were placed on the right leg only. The CSL-SHARE dataset features 22 activities, and was upscaled to 1000Hz due to differing sample rates for the various sensors [240].

3.2.5 Summary of Datasets

The datasets chosen for this study cover a variety of environments, activities, and sensor configurations. Analysis of the datasets with the same ML models and pre-processing methods will provide insight into how sensor configuration and type affect classification accuracy in HAR. A comparison of these datasets can be found in Table 3.2.

Table 3.2: A Summary of the Properties of Each Dataset in This Analysis

Dataset Features	USC-HAD	Camargo et al.	HuGaDB	CSL-SHARE
Participants	14	22	18	20
Mean Age (Years)	30.1	21	23.67	30.5
Mean Height (cm)	170	170	179.06	N/A
Mean Weight (kg)	64.6	68.3	73.44	N/A
IMU Sensors	1	4	6	2
EMG Sensors	0	11	2	4
Goniometers	0	3	0	1
Acoustic Sensors	0	0	0	1
Activities	12	18	12	22
Sample Rate	100Hz	200Hz/ 1000Hz	60Hz	100Hz/ 1000Hz

3.2.6 Dataset Preprocessing

Normalisation Between Datasets

As this study focuses on the sensor types in the HAR datasets, steps were taken to reduce the differences in bias and variation in the datasets. Of the variables in Table 3.2, participant numbers, activity types, and sample rates were normalised. To achieve this, the number of participants in each dataset was limited to the minimum number available across all datasets, which was 14, with additional participants being excluded from the datasets where appropriate

to maintain a fair comparison between the datasets. For example, in CSL-SHARE, participants 2, 11, and 16 contained different data due to varying protocol versions, device communication issues, and a participant stopping early due to knee pain. As such, these three participants were removed, before cropping the number of participants down to 14. Of the activities included in the four datasets, only walking, standing, stair ascent, and stair descent were common across datasets, and are activities of interest with respect to fall-related research [329, 330]. Therefore, the additional activities were removed from each dataset. Finally, 100Hz was chosen as the common sample rate, resulting in the sample rate for the Camargo et al., and CSL-SHARE datasets being subsampled to 100Hz, whilst HuGaDB was interpolated up to 300Hz with fifth-order polynomial interpolation, before being subsampled to 100Hz.

Filtering

Before data can be presented to the machine learning models, a series of pre-processing steps must be performed to prepare the data for use by the machine learning models. This process begins with a fourth-order low-pass Butterworth filter with a cut-off frequency of 7Hz before windowing and feature extraction occur. This cut-off frequency was chosen through testing and lies around the 10Hz mark, which is typical for analyses using inertial sensors [331].

3.2.7   Feature Extraction

As is typical for performing classification with time-series data, semi-overlapping sliding windows are used to extract statistical features such that a single sample represents a larger time window of raw data. The size of these windows and the amount of overlap varies between studies, with lower window sizes being preferable for real-time classification, whilst larger window sizes consider more of the gait cycle per sample and can result in higher classification accuracies. For this study, a search is performed to identify trends in accuracy from a one second to ten-second window size, with a 75% window overlap for each window size. This overlap is chosen to combine co-dependent window parameters and reduce computation times.

For each window of time-series data, a wide array of statistical features is extracted to enable the ML models to make accurate predictions. There is little consensus on which features are necessary for accurate HAR, with many studies considering a mean of 15 features [327, 332–338]. This analysis includes 22 features from each sensor, including commonly chosen features from existing research [327, 334–337, 339]. Feature selection methods are then used to eliminate noisy

features before classification. This combination of increased feature numbers with appropriate feature selection techniques to accommodate this ensures that relevant data from each sensor is present to allow a sensor-focussed analysis. The list of included features is as follows:

- Maximum value
- Minimum value
- Mean
- Median
- Standard Deviation
- Mean Absolute Deviation
- Median Absolute Deviation
- Number of Zero Crossings
- Root Mean Square
- Maximum Gradient
- Kurtosis

- Skewness
- Variance
- Interquartile Range
- Entropy
- Energy
- Maximum Frequency Amplitude
- Mean Frequency Amplitude
- Maximum Power Spectral Density
- Mean Power Spectral Density
- Frequency Kurtosis
- Frequency Skewness

After feature extraction, the data is split into train and test data by leaving out the data from a single subject. Scikit-Learn's 'MinMaxScaler' function is then fit to the train set and applied separately to the train and test sets to scale each feature between 0 and 1. Principal Component Analysis (PCA) is performed to reduce the number of features whilst retaining the amount of variance they represent. As with the scaler, the PCA is fit to the train set and applied separately to the train and test sets. The number of selected principal components varies for each dataset due to the different features which were dependent on the sensors but is controlled by choosing the minimum amount required to retain 95% of the variance of the full feature set. Finally, another round of scaling is performed to prepare the data for the machine learning algorithms.

3.2.8   Cross-Validation and Test Data

As mentioned by Dehghani *et al.* [315], two methods of cross-validation and testing are prevalent in the literature for gait- and fall-related studies: subject-dependent analysis using TTS cross-validation and subject-independent analysis using LOSO cross-validation. TTS cross-validation uses a set percentage of the total data from all subjects as test and validation data, whilst

LOSO leaves out the data from a specific subject. Each of these methods of cross-validation offers differing advantages and disadvantages, with TTS creating models with higher accuracies at the cost of poor generalisation, whilst LOSO typically creates models with lower accuracies that perform better with data from new subjects. This enables researchers and engineers to choose whether the subject should undergo a training period to build a higher accuracy model, or if the system should work 'off the shelf' at the risk of reduced accuracies when performing HAR on the new subject. For this study, both TTS and LOSO cross-validations are used to make the results applicable to both types of device, and to be more comparable with existing and future studies.

3.2.9 Models

For classification, KNN, SVM, DT, RF, ANN, an ensemble Voting classifier, and an ensemble Stacking classifier are chosen due to their prevalence in the literature. Ensemble models are constructed from each of the individual models (KNN, SVM, DT, RF, and ANN), with either a voting or a logistic regression classifier fusing the decisions. This inclusion of a variety of ML models reduces bias that could be introduced due to the various properties of each model, such as how prone they are to overfitting and how dataset size affects their classification performance.

Each type of model in this analysis features various tunable hyperparameters, which affect the classification capabilities of that model. For example, the parameter k in KNN models affects how prone the model is to overfitting, with a k of 1 resulting in the model labelling a sample with the same class as the single closest data point, whilst a k of 100 will consider the most occurring class among the closest 100 samples. The other models in this analysis contain similar parameters, which affect overfitting and generalisation, such as the box constraint C for SVMs, the number of neurons in each layer in ANNs, the number of estimators and tree constraints in RFs, and the splitting criterion in DTs, to name just one parameter for each model. Due to the different cross-validation methods, parameters relating to both higher and lower levels of generalisation will be required in different circumstances. Furthermore, due to the large number and range of these parameters, an unrealistic number of parameter combinations exist to manually search through. As such, hyperparameter optimisation is employed to identify a good set of hyperparameters for each model with each cross-validation method.

Hyperparameter tuning typically consists of employing search algorithms to train a model, and

use a validation set to obtain a validation score, which can then be used to determine how the hyperparameters should be changed. In a typical grid or randomised search, this process is iterated until either all possible combinations have been exhausted, or for a set number of random combinations, respectively. However, the former of these methods is not possible for the large number of parameters in this analysis, and the latter is not guaranteed to yield a good set of hyperparameters. As such, Bayesian hyperparameter tuning was implemented, which compares the predictions of model performance with the actual performance after training, using Bayes theorem, to iteratively improve the model performance by intelligently adjusting the hyperparameters between iterations. Hyperparameter tuning, therefore, is performed using 25 iterations of the Scikit-Optimize Bayesian hyperparameter search. All models are trained on a computer with 32GB of RAM, a 12th Generation Intel i9-12900K processor, and a 12GB Nvidia RTX 3060 GPU using the Scikit-Learn library for Python.

3.3 Results

To determine the optimal window size for sliding window feature extraction, each model is trained using all the extracted features for each window size, ranging from one to ten seconds. Ten seconds was selected as the maximum time due to issues with class distributions and the number of samples in each class at larger window sizes. This process is repeated three times for each model to reduce the impact of random initialisations, which can lead to models getting stuck in local minima during training. The results for subject-dependent cross-validation can be seen in Figures 3.1 and 3.2, whilst the results for subject-independent cross-validation can be found in Figures 3.3 and 3.4.

3.3.1 Subject-Dependent Cross-Validation

Determining Optimal Window Sizes

Figure 3.1 shows the mean performance of each model over the three repeat trials for each window size. The trend lines present in these figures demonstrates a clear increase in accuracy with window size for subject-dependent cross-validation using TTS across all models and all datasets. The exceptions to this trend suggest that overfitting may be occurring as the number of samples decreases, with some models decreasing in accuracy with nine- and ten-second window sizes, where the amount of data from each class is at a minimum. This issue is most prevalent

(a) USC-HAD

(b) Camargo et al.

(c) HuGaDB

(d) CSL-SHARE

Figure 3.1: Trend graphs showing the mean accuracy across all models and window sizes for the four datasets in this analysis when using TTS cross-validation.

with the ANNs among the smaller datasets, whilst the Camargo et al. dataset is the only one in which ANN accuracy does not drop at higher values of window size. Although accuracy generally trends upwards with window size, all datasets except for CSL-SHARE, which exhibited 100% accuracy for most models at all window sizes, plateau at around four to five seconds. Furthermore, CSL-SHARE appears to exhibit overfitting at higher window sizes for both ANN and SVM, likely due to a lack of data.

Figure 3.2 shows the average highest performing model among all window sizes, along with the average accuracy at each window size across all models. These figures highlight SVM and the stacking ensemble classifier as the most capable models across all window sizes, and that a peak in model performance occurs in the range of four- to seven-second window sizes.

Regarding the individual (non-ensemble) highest performing model, all models perform fairly similarly between datasets, with SVM being the only model that performs significantly higher than others with average accuracies of 99.5%, 83.7%, 99.8%, and 100.0% on each of the USC-HAD, Camargo et al., HuGaDB, and CSL-SHARE datasets respectively. However, these results
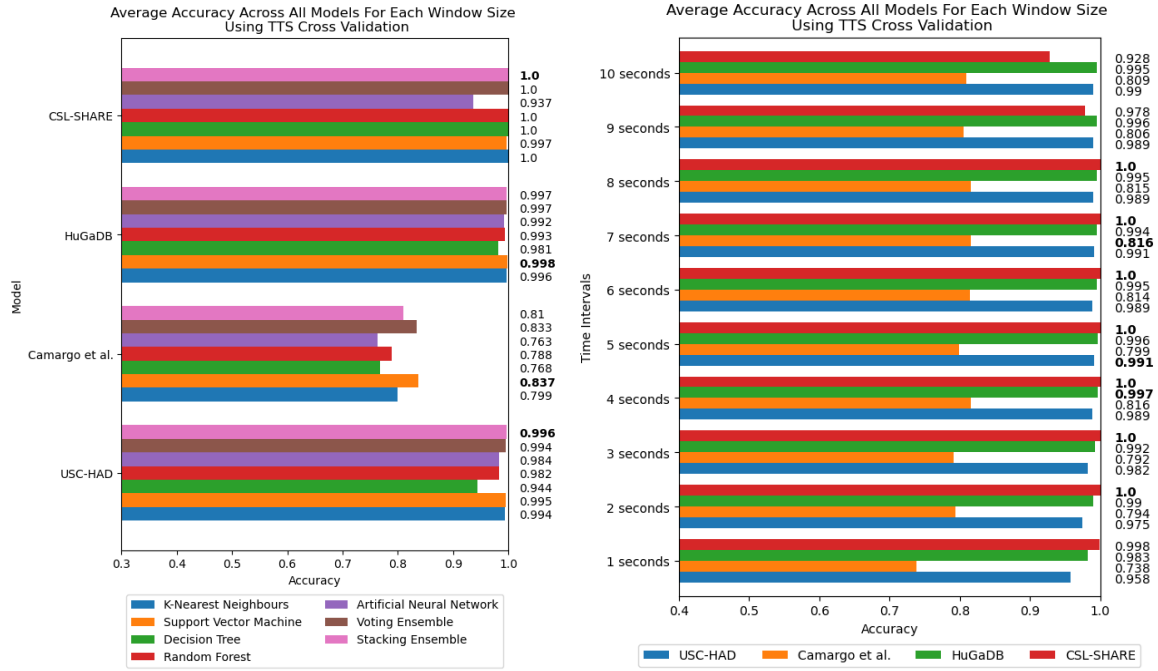
(a) Average accuracy for each model across all window sizes for each dataset.

(b) Average accuracy across all models at each window size from 1 to 10 seconds for each dataset.

Figure 3.2: Model and window size effect on classification accuracy across all four datasets using TTS cross-validation.

also suggest an issue with the Camargo et al. dataset, as the average accuracies for all models and window sizes is far reduced for this dataset when compared with the others. An overview of the highest performing individual models can be found in Table 3.9.

Individual Sensor Analysis

The optimal window sizes for each dataset are used to determine the sensor importance for achieving high accuracies among the four core activities. As USC-HAD contained just a single sensor, it was excluded from this analysis. Due to its high performance across all datasets, and due to the SVM failing to converge on these reduced datasets, an ANN is trained to classify between the four activities using data from individual sensors.

Tables 3.3, 3.4, and 3.5 show the precision, recall, f1 score, and accuracy of the ANN trained from features extracted from each sensor in the Camargo et al., HuGaDB, and CSL-SHARE datasets respectively. These tables highlight IMUs as the most effective individual sensor, providing accuracies of 87%-100% across all datasets. Goniometers also appear as a high performing sensor, with the 3-axis goniometers of at the hip and ankle of the Camargo et al. dataset exhibiting accuracies comparable to IMUs at 86.8% and 97.4% respectively. Following the 3-axis

goniometers, both the Camargo et al. and CSL-SHARE datasets feature 2-axis goniometers at the knee, which enable accuracies of 74.2% and 99.6% respectively. Finally, EMG sensors exhibit the lowest accuracies across all datasets. Among the EMG sensors, placement heavily affects classification accuracy, with the vastus lateralis and biceps femoris performing extremely poorly, whilst the tibialis anterior, soleus, gastrocnemius, and gracilis generally appear to outperform sensors placed on other muscles. However, even the highest performing EMG sensors in each dataset are 5%-30% less accurate than the IMUs.

Table 3.3: Subject-Dependent Performance Metrics of Each Individual Sensor in the Camargo et al. Dataset

Sensor	Precision	Recall	F1 Score	Accuracy
Trunk IMU	0.801	**0.798**	**0.799**	**0.897**
Thigh IMU	0.753	0.751	0.744	0.874
Shank IMU	0.778	0.769	0.772	0.881
Foot IMU	**0.814**	0.787	0.774	0.894
Gastrocnemius Medialis EMG	0.716	0.630	0.621	0.758
Tibialis Anterior EMG	0.636	0.547	0.523	0.755
Soleus EMG	0.676	0.620	0.629	0.774
Vastus Medialis EMG	0.459	0.493	0.470	0.652
Vastus Lateralis EMG	0.158	0.256	0.169	0.458
Rectus Femoris EMG	0.185	0.252	0.212	0.374
Biceps Femoris EMG	0.296	0.348	0.302	0.561
Semitendinosus EMG	0.216	0.296	0.242	0.423
Gracilis EMG	0.763	0.460	0.456	0.652
Gluteus Medius EMG	0.348	0.357	0.316	0.577
Right External Oblique EMG	0.372	0.372	0.336	0.594
Ankle Goniometer	0.741	0.747	0.708	0.874
Knee Goniometer	0.410	0.500	0.445	0.742
Hip Goniometer	0.753	0.744	0.742	0.868

Table 3.4: Subject-Dependent Performance Metrics of Each Individual Sensor in the HuGaDB Dataset

Sensor	Precision	Recall	F1 Score	Accuracy
Right Thigh	0.990	0.994	0.992	0.995
Left Thigh	0.993	0.996	0.995	0.997
Right Shank	**0.995**	**0.997**	**0.996**	**0.998**
Left Shank	0.989	0.990	0.989	0.993
Right Foot	0.973	0.979	0.976	0.987
Left Foot	0.978	0.984	0.981	0.991
Right Vastus Lateralis EMG	0.669	0.509	0.506	0.775
Left Vastus Lateralis EMG	0.597	0.478	0.457	0.783

Table 3.5: Subject-Dependent Performance Metrics of Each Individual Sensor in the CSL-SHARE Dataset

Sensor	Precision	Recall	F1 Score	Accuracy
Vastus Medialis EMG	0.691	0.699	0.695	0.661
Tibialis Anterior EMG	0.659	0.648	0.644	0.592
Biceps Femoris EMG	0.430	0.383	0.391	0.367
Gastrocnemius EMG	0.582	0.550	0.534	0.475
Airborne Microphone	0.550	0.536	0.534	0.454
IMU Upper	**1.000**	**1.000**	**1.000**	**1.000**
IMU Lower	**1.000**	**1.000**	**1.000**	**1.000**
Goniometer	0.997	0.996	0.997	0.996

3.3.2 Subject-Independent Cross-Validation

Determining Optimal Window Sizes

Figure 3.3, shows the performance trends of each model at each window size for the four datasets in this study using LOSO cross-validation. The maximum accuracy for USC-HAD occurs at a ten-second window size with an SVM exhibiting an accuracy of 91.9%, whilst the Camargo et al. dataset achieves a maximum accuracy of 80.8% at nine seconds using an ANN. Both the CSL-SHARE and HuGaDB datasets achieve 100% classification accuracy with multiple model types at one and two seconds respectively, which is maintained up to a window size of ten seconds. The DT, RF, and KNN models perform erratically across all datasets and window sizes, which causes the stacking and voting ensemble methods to underperform when compared to ANN and SVM.

Figure 3.4 shows the mean accuracies across all time windows and models. From Figure 3.4a, SVMs and ANNs appear as the classifiers with the highest classification accuracy where there is a statistically significant difference between classifier performances, with SVMs achieving 79.1%, 68.4%, 98.8%, and 99.9% accuracy, whilst ANNs achieve 75.4%, 73.6%, 99.9%, and 100% accuracy on each of the USC-HAD, Camargo et al., HuGaDB, and CSL-SHARE datasets respectively. As such, ANN and SVM can clearly be identified as the highest performing model types across all datasets, as seen in Table 3.9. Concerning window size, each dataset presents a different window size at which the maximum mean accuracy occurs. For USC-HAD, the highest mean accuracy across all models occurs at a three-second window size, whilst for the Camargo et al. dataset it occurs at five seconds, both of which are similar to the time at which model accuracy plateaus using subject-dependent cross-validation. Both HuGaDB, and CSL-SHARE

achieved accuracies of 100% on several models, but due to the lower accuracies of other models, their highest mean performances occur at eight seconds for HuGaDB, and any value from three to ten seconds for CSL-SHARE.

(a) USC-HAD
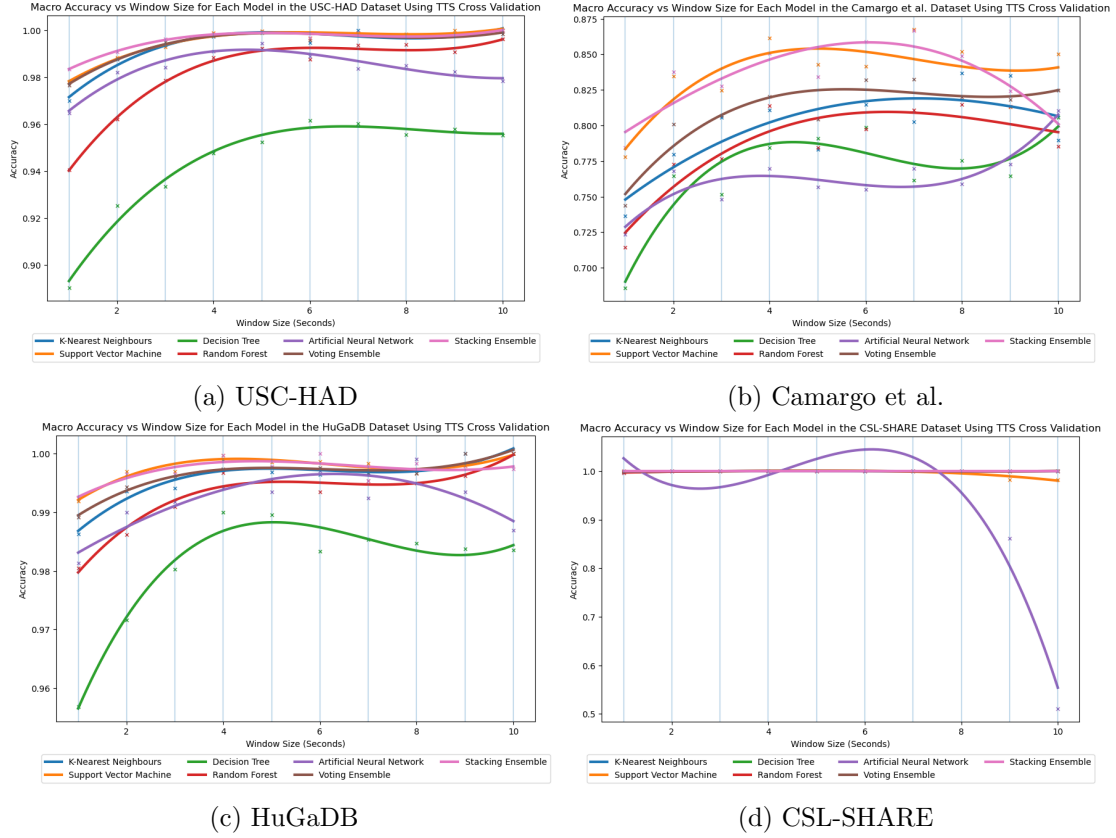
(b) Camargo et al.

(c) HuGaDB

(d) CSL-SHARE
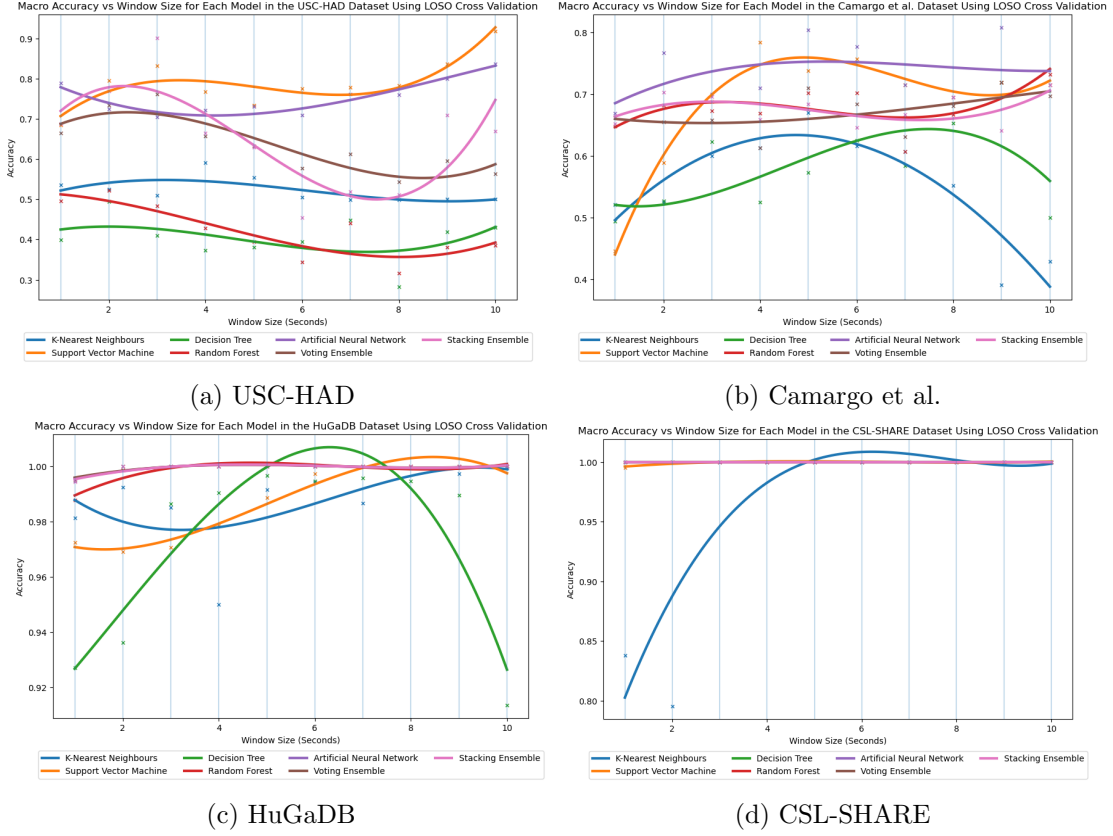
Figure 3.3: Trend graphs showing the mean accuracy across all models and window sizes for the four datasets in this analysis when using LOSO cross-validation.

Individual Sensor Analysis

As with the subject-dependent individual sensor analysis, an ANN is trained on the features extracted from each individual sensor. Tables 3.6, 3.7, and 3.8 show the performance metrics for each sensor used in the Camargo et al., HuGaDB, and CSL-SHARE datasets respectively. Like with the subject-dependent analysis, IMUs achieve the highest accuracies across all three datasets, whilst EMG sensors exhibit consistently poor performances. In this scenario, performance metrics are drastically reduced, with only the EMG sensors placed on the soleus, tibialis anterior, and gastrocnemius medialis for the Camargo et al. dataset, and the vastus medialis for the CSL-SHARE dataset achieving performance metrics above 50%. The 3-axis goniometers on the ankle and hip from the Camargo et al. dataset exhibit high performance metrics, comparable to those of the IMUs, whilst the 2-axis goniometers positioned on the knee in the
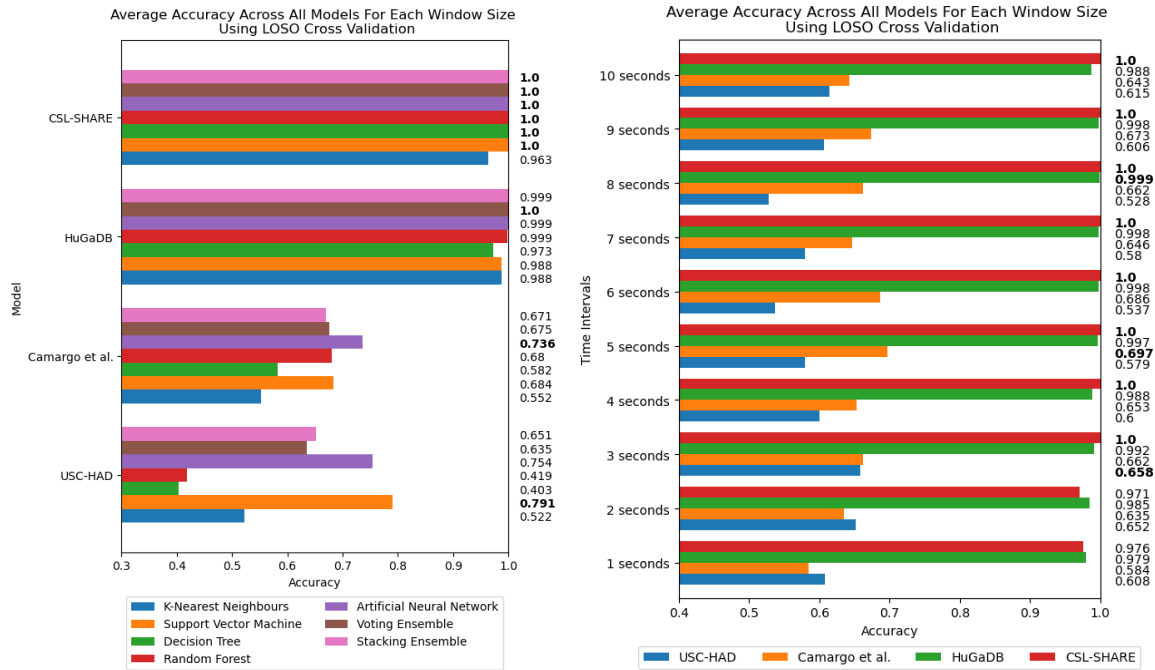
(a) Average accuracy for each model across all window sizes for each dataset.

(b) Average accuracy across all models at each window size from 1 to 10 seconds for each dataset.

Figure 3.4: Model and window size effect on classification accuracy across all four datasets using LOSO cross-validation.

Camargo et al. and CSL-SHARE datasets exhibit much lower performance metrics.

Overall, the trends among these sensors were largely the same as with the subject-dependent analysis, with the main difference being an overall reduction in accuracy for the EMG sensors, further highlighting the volatility of performance when using these sensors.

3.4 Discussions

The results of the window size analysis do not exhibit a consistent peak or plateau, with accuracies appearing volatile across the four datasets for each window size, and trend lines displaying misaligned peaks. Furthermore, the averaging of accuracies across all models at each window size shows no clear single optimal window size across the four datasets and methods of cross-validation.

Before any further discussions, it must be noted that the performance metrics of the Camargo et al. dataset do not align with the other multimodal datasets in terms of overall classification accuracy. These systems all make use of the same 6-axis IMU positioned on the thigh, yet the Camargo et al. dataset achieves significantly reduced accuracies when trained on only this

Table 3.6: Subject-Independent Performance Metrics of Each Individual Sensor in the Camargo et al. Dataset

Sensor	Precision	Recall	F1 Score	Accuracy
Trunk IMU	0.801	**0.798**	**0.797**	**0.897**
Thigh IMU	0.753	0.751	0.744	0.874
Shank IMU	0.778	0.769	0.772	0.881
Foot IMU	**0.814**	0.787	0.774	0.894
Gastrocnemius Medialis EMG	0.716	0.630	0.621	0.758
Tibialis Anterior EMG	0.636	0.547	0.523	0.755
Soleus EMG	0.676	0.620	0.629	0.774
Vastus Medialis EMG	0.459	0.493	0.470	0.652
Vastus Lateralis EMG	0.158	0.256	0.169	0.458
Rectus Femoris EMG	0.185	0.252	0.212	0.374
Biceps Femoris EMG	0.296	0.348	0.302	0.561
Semitendinosus EMG	0.216	0.296	0.242	0.423
Gracilis EMG	0.763	0.460	0.456	0.652
Gluteus Medius EMG	0.348	0.357	0.316	0.577
Right External Oblique EMG	0.372	0.372	0.336	0.594
Ankle Goniometer	0.741	0.746	0.708	0.874
Knee Goniometer	0.410	0.500	0.445	0.742
Hip Goniometer	0.753	0.744	0.742	0.868

Table 3.7: Subject-Independent Performance Metrics of Each Individual Sensor in the HuGaDB Dataset

Sensor	Precision	Recall	F1 Score	Accuracy
Right Thigh	**1.000**	**1.000**	**1.000**	**1.000**
Left Thigh	0.970	0.966	0.966	0.984
Right Shank	**1.000**	**1.000**	**1.000**	**1.000**
Left Shank	0.976	0.997	0.986	0.992
Right Foot	0.953	0.960	0.952	0.982
Left Foot	0.874	0.824	0.779	0.923
Right Vastus Lateralis EMG	0.211	0.290	0.229	0.478
Left Vastus Lateralis EMG	0.428	0.330	0.330	0.726

Table 3.8: Subject-Independent Performance Metrics of Each Individual Sensor in the CSL-SHARE Dataset

Sensor	Precision	Recall	F1 Score	Accuracy
Vastus Medialis EMG	0.846	0.634	0.624	0.757
Tibialis Anterior EMG	0.475	0.375	0.332	0.456
Biceps Femoris EMG	0.366	0.361	0.270	0.417
Gastrocnemius EMG	0.300	0.458	0.354	0.573
Airborne Microphone	0.525	0.517	0.475	0.427
Thigh IMU	**0.992**	**0.993**	**0.992**	**0.990**
Shank IMU	0.935	0.931	0.924	0.903
Knee Goniometer	0.884	0.767	0.706	0.738

Table 3.9: Maximum Accuracy, Precision, Recall, and F1 Score for Each Dataset,
Non-Ensemble Model, and Method of Cross-Validation

Dataset	Model	Window Size(s)	Acc(%)	Prec(%)	Rec(%)	F-Score(%)
USC-HAD TTS	SVM	5	99.90	99.73	99.90	99.81
USC-HAD LOSO	SVM	10	91.89	79.29	91.89	81.17
Camargo et al. TTS	SVM	4	86.15	92.56	92.52	92.51
Camargo et al. LOSO	ANN	5	80.41	86.66	86.06	85.19
HuGaDB TTS	SVM	4	99.97	99.82	99.97	99.90
HuGaDB LOSO	ANN	2	100	100	100	100
CSL-SHARE TTS	ALL	2	100	100	100	100
CSL-SHARE LOSO	ALL	3	100	100	100	100

sensor when compared to HuGaDB and CSL-SHARE. Given the large number of controlled variables in this study, this indicates a difference in experimental procedure or activity data distribution, which is negatively affecting the results of the Camargo et al. dataset. Figures 3.5a and 3.5b show the confusion matrix for an SVM trained on the Camargo et al. dataset, which shows the misclassifications to be between the stair ascend and stair descend classes. This is also shown to not be caused by sample weighting, as Figures 3.5c and 3.5d show the confusion matrices for the HuGaDB and CSL-SHARE datasets respectively, which feature more extreme sample weightings than the Camargo et al. dataset whilst achieving 100% accuracy. As such, the accuracy differences in this dataset for high accuracies, i.e. above the $\tilde{7}5\%$ of samples that belong to the walking and standing classes which are typically classified correctly, cannot be relied upon due to the error introduced for these samples.

Figure 3.9 highlights SVMs as the most effective individual model for HAR using subject-dependent cross-validation, with ANNs proving more effective when using subject-independent cross-validation. This is likely due to the tendency for ANNs to overfit, which is further pronounced by the use of a TTS in creating test data for subject-dependent cross-validation, whereas SVMs typically perform well in these scenarios due to the maximisation of the margin when creating a decision boundary.

For subject-dependent cross-validation, peak accuracies occur at smaller window sizes, ranging from 2–5 seconds. The trend lines in Figures 3.1 and 3.3 also exhibit rises in accuracy for some models as they approach a 10-second window size, indicating that, if the dataset contains enough samples in each class for this to be viable, larger window sizes offer more rich features which lead to higher classification accuracies. For subject-independent cross-validation, the highest performing models occur at 2, 3, 5, and 10 seconds for the HuGaDB, CSL-SHARE, Camargo

(a) Camargo et al. Vastus Lateralis

(b) Camargo et al. Vastus Medialis

(c) HuGaDB Vastus Lateralis

(d) CSL-SHARE Vastus Medialis EMG
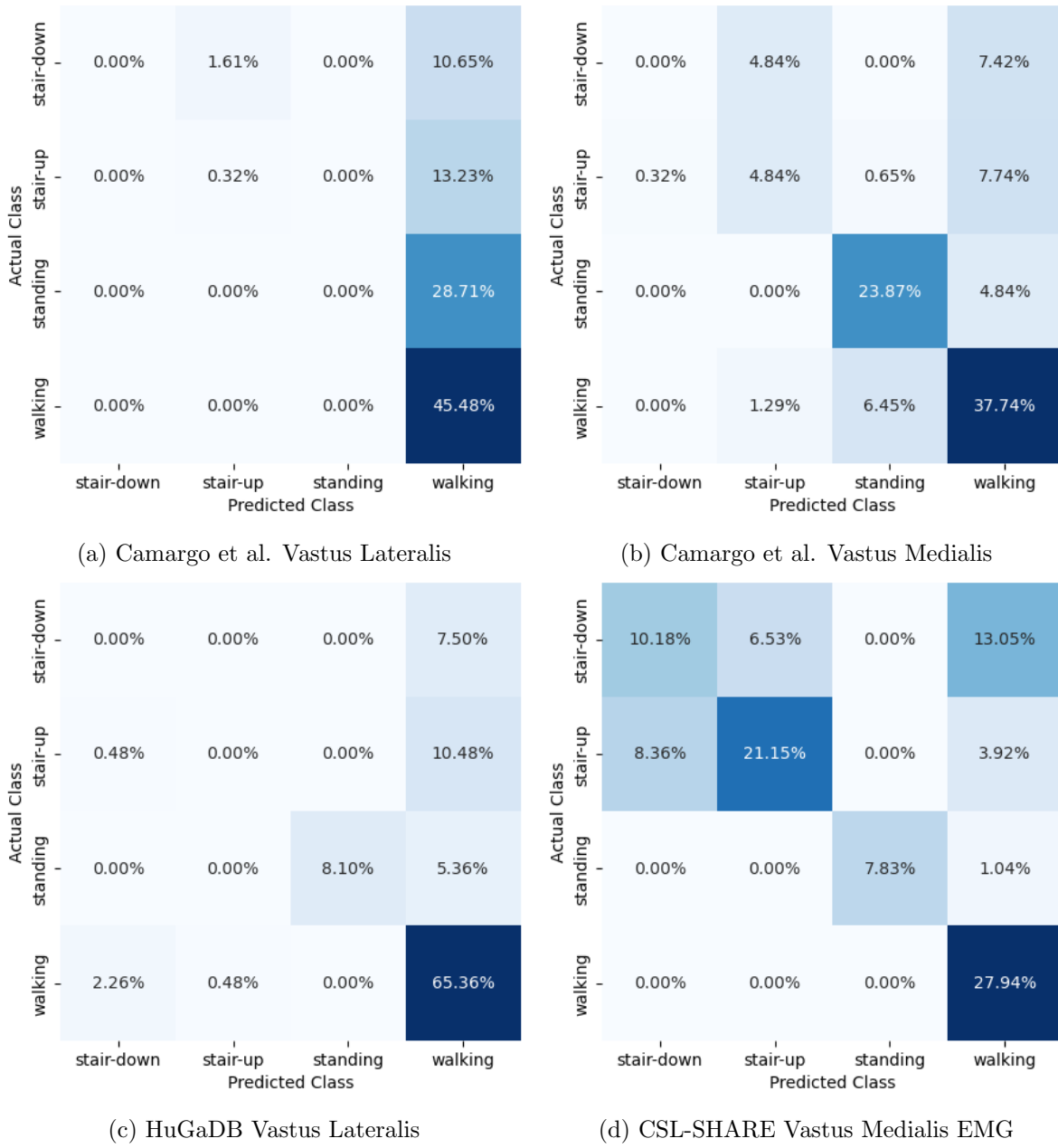
Figure 3.5: Confusion matrices of a SVM trained on data from a single EMG sensor using LOSO cross-validation.

et al., and USC-HAD datasets respectively. Apart from USC-HAD, this further highlights the range of 2–5 seconds as an effective range of window sizes in achieving high classification accuracy for the core activities of HAR.

Aside from the Camargo et al. dataset, the multimodal datasets achieve much higher classification accuracies when using the same models and window sizes, which allows high accuracies to be obtained with much smaller windows sizes. This has significant implications when considering the delay time, portability, and convenience of systems, as increasing the number of sensors can

enable high accuracy HAR using very computationally inexpensive methods such as DT. These computationally low-cost methods can also allow designers of real-time HAR systems to incorporate low-power computational devices with reduced size profiles and battery consumption, therefore increasing the comfort and convenience of the device. Additionally, the fact that high accuracies can be obtained in multimodal systems with low window sizes means much faster response times for real-time HAR systems, as some models trained on the CSL-SHARE dataset achieve 100% accuracy using just 1 second windows with a 0.25s fixed delay time caused by the step size. Whilst it is shown that accuracy at each window size is dependent on the sensor types used in each dataset, further work is needed to identify how model performance varies with window size for each individual sensor type. This will enable the building of a knowledge database to help future researchers choose a window size given a sensor system without the need for lengthy, brute-force approaches to finding the most appropriate window size, combination of sensors, and choice of model for each novel dataset produced in this field.

Regarding individual sensor types, IMUs exhibit the highest accuracies across all datasets, followed by goniometers, and finally EMG sensors. Among IMU locations, accuracy varies among the different locations, with no clear ranking between all datasets. Only the Camargo et al. and CSL-SHARE dataset feature goniometers, with the 3-axis goniometers at the thigh and ankle of the Camargo et al. dataset showing large performance improvements over the 2-axis goniometers located on the knee in both the Camargo et al. and CSL-SHARE datasets. Goniometers are low power devices with fewer data dimensions than IMUs which can be incorporated into smart clothing devices to improve comfort and convenience. Given the competitive performance of goniometers in this study, 3-axis goniometers should be considered in future datasets and HAR systems. On the other hand, EMG sensor performance is volatile between locations and datasets, which may be due to differences in filtering methods, varying placements on muscles, or changes in experimental procedures. As such, it is not currently possible to compare the locations of these sensors, particularly with so few datasets for reference. More datasets are required to accurately rank the locations of these sensors so that the impact of differences in experimental setup can be minimised.

The results of this chapter align with the findings of Banos *et al.* [311], who found that increased window size does not necessarily increase activity classification performance across many datasets. However, this new study offers insight into the reason for this assumption,

with subject-dependent cross-validation demonstrating this pattern until accuracy begins to reduce at larger values of window size due to insufficient sample sizes. Crucially, this work considers both subject-dependent and subject-independent methods of cross-validation, which highlights how the choice of cross-validation method impacts the selection of an optimal window size, which was not considered in their study [311]. Niazi *et al.* [321] considered the effect of window size and sample rate on classification accuracy using a RF classifier, where it was reported that window sizes could appear optimal between two to ten seconds using subject-dependent cross-validation. The results of this chapter support these findings, and demonstrate that this also applies to additional classical machine learning models such as ANN, SVM, KNN, and DT. Duan and Fujinami [255] considered the optimal placement of sensors using deep learning techniques for a single dataset, finding that sensors placed on the right leg exhibited increased performance. Those results align with the findings of the current study, with the HuGaDB dataset demonstrating that, when subject-independent cross-validation is used, the performance metrics of the right leg are higher than the left. Finally, Khan *et al.* [324] report that sensor performance is dependent on the activities being performed in the dataset. By removing the variation between datasets, this new study controls for this factor, resulting in a reliable ranking of sensor locations that achieve high performances and offer future researchers the necessary information to build effective HAR systems.

It is important to note that the results of this study do not necessarily suggest that EMG is an ineffective method for HAR. EMG extracts unique physiological signals which are known to be suited for detecting user intent in the context of controlling exoskeletons and prosthetics [340]. When combined with IMUs, it is possible that these sensors can augment classification accuracies, as has been shown in previous research [341]. However, in the context of this study, issues with repeatability and difficulty obtaining comparable EMG readings between participants [340] may have resulted in significant accuracy drops when assessing the test set. For the purpose of developing a system for assessing incremental fall risk however, these issues also need to be avoided, so EMG sensors remain unattractive for use in the proposed sensor system.

Regarding the sample rates of each dataset, no correlation is present between the native sample rates of each dataset and the final classification accuracy, with the HuGaDB dataset exhibiting far higher accuracies than USC-HAD and the Camargo et al. dataset, despite having the lowest

native sample rate of 60Hz. As such, whilst sample rate is expected to have an effect at even lower values, 60Hz can be considered a sufficient sample rate for high-accuracy HAR, and will act as a minimum for the sensor system designed in this thesis.

Finally, this study features several limitations due to the computational cost of performing this analysis. The first of these limitations was the lack of investigation into the effects of step size, which was set to 25% of the window size for the duration of the study. This could have been set to a fixed time value for all window sizes, or have been individually analysed to explore the co-dependent effects of step size and window size. Furthermore, the choice of datasets which feature a sufficiently large number of participants and sensors, along with the core activities included in this study was limited, resulting in the inclusion of just four datasets. Finally, the co-dependencies and combinations of sensor types and locations was not explored. As mentioned, combinations of IMU and EMG have been shown to improve accuracies in the past [341]. Each sensor, even if incapable of accurate HAR on its own, may offer high classification accuracies on classes where another lacks the appropriate data to do so. However, incorporating these factors into such a large analysis is extremely computationally expensive across all four datasets, and would not offer much additional information in the scope of selecting the optimal sensor types and positions for accurate HAR in the context of identifying walking activities for the extraction of gait parameters and other incremental fall risk factors.

3.5 Contributions

This chapter outlines the analysis of four existing datasets using a novel approach of achieving homogeneity across several dataset properties such as number of subjects, activities, and sample rate, which reduces bias when determining the most effective sensors and classification methods across these different datasets. Furthermore, this chapter performs both a subject-dependent and subject-independent analysis of the effect of window size on classification accuracy in the sliding window approach to feature engineering, finding that a window size of two to five seconds is optimal for obtaining high accuracies, which will help to guide future researchers when performing analyses on future HAR datasets without the need for lengthy, brute-force computational procedures. Finally, this chapter offers new insights into 3-axis goniometer sensors for HAR which, despite being under-explored in the literature, have shown to be competitive with IMU sensors and should be further explored in future research.

3.6   Summary

This study addresses the research objectives of exploring and analysing existing HAR datasets, and finding the optimal parameters for sliding window feature engineering. Furthermore, this study is the first of its kind in providing a bias-reduced, normalised, cross-dataset analysis of HAR datasets. First, ANNs and SVMs are found to be the highest-performing models across multiple multimodal HAR datasets, with the optimal window size used to create samples for these models being in the range of two to five seconds when using the semi non-overlapping sliding window approach to feature engineering with a 75% overlap. Where datasets are large enough to reduce the impact of class imbalance, or models are sufficiently powerful to generalise with smaller sample numbers, accuracies are also shown to trend upwards with larger window sizes of nine to ten seconds. Regarding the contributions of individual sensor types to classification accuracy, IMUs and 3-axis goniometers are the overall largest contributors to high-accuracy HAR, whilst EMG sensors are largely incapable of performing HAR on the basic mobility activities that underpin human functioning. It remains appropriate for researchers collect large HAR datasets, and to investigate alternative methods of HAR using multimodal sensor systems and smart clothing to investigate how the size and inconvenience of these systems can be minimised whilst maintaining high accuracy using low-computational complexity classification methods.

The findings of this chapter align with those of Chapter 2 in highlighting IMUs as a powerful sensor type for both HAR and fall risk assessment using wearable sensors, which will guide the development of the sensor system in this thesis to ensure that high-accuracy HAR can be attained. Furthermore, there was no correlation between sample rate and classification accuracy in this study, with HuGaDB, the lowest sample rate dataset, exhibiting much higher accuracies than the USC-HAD and Camargo et al. datasets, which were sampled at 100Hz, and 200Hz, respectively. As such, 60Hz will form the lower bound of acceptable sample rates in the design of the sensor system used to collect the dataset in the upcoming chapters. By designing a sensor system with the limitations of this study in mind, high-accuracy HAR can be achieved, allowing a system to determine when a person is walking so that the spatio-temporal gait parameters can be estimated for the purpose of fall prediction. When combined with accurate terrain identification, this will form the basis for a novel system capable of determining a person's incremental fall risk factors in their daily life.

This study was limited by the scarcity of open multimodal gait datasets with large numbers

of sensors and common activities. As a result, future research on this topic should include more datasets, activities, and sensor types to investigate how classifier performance in HAR is affected by these properties. Additionally, elements such as step size, proportion of data for each activity, features, and sample rate should be investigated for their contribution towards achieving efficient and convenient high-accuracy HAR.

Chapter 4

A Real-Environment Gait Dataset

4.1 Introduction

As outlined in Chapter 2, terrain affects fall risk through the introduction of slip and trip hazards, along with affecting the gait parameters in such a way that increases variability - a factor commonly found in people at increased risk of falling [4, 38, 39]. When designing a sensor system capable of detecting incremental risk factors for falling, terrain is a significant factor which must be automatically identified by the system, along with the current activity, to determine the external fall risk factors. Many research projects in recent years have achieved high-accuracy Human Activity Recognition (HAR) with lightweight, convenient, and power-efficient sensor systems. However, studies which consider the terrain in which the gait data were collected are both rare and limited [36, 284, 289–291, 342], largely due to the lack of terrain-labelled datasets [35].

Where studies do attempt to classify terrain in the context of human activities, gait activity is typically limited to walking or running [284, 289–291], and some approaches raise potential privacy concerns through the use of camera technologies [284, 342]. Dixon *et al.* [290] classify between three terrains using Gradient Boosting (GB) and Convolutional Neural Network (CNN) classifiers on data collected from two Inertial Measurement Units (IMUs) placed on the lower-back and right tibia while a participant is running. GB is found to be the highest performing sensor on data from both sensors combined with an accuracy of 97.0%, whilst CNN is the highest performing classifier on a single sensor, with an accuracy of 96.1% on data from the tibia alone. Similarly, Hashmi *et al.* [289] aims to classify between six terrains using IMUs on

the chest and lower-back, and obtain an 88.7% accuracy using Random Forest (RF) on data from the lower-back alone.

To address the limitations in the field of terrain classification in the context of HAR, this study aims to collect a new context- and terrain-aware gait dataset with a novel sensor system that builds on the current state-of-the-art activity classification systems. This dataset will enable researchers to develop and train machine learning models for real-world HAR and terrain classification, advancing the field of gait analysis by enabling the contextual labelling of gait data collected outside the lab, and allowing the identification of external fall risk factors caused by the terrain. Furthermore, there exists a need to explore the contributions of additional sensing methods for terrain classification. While IMU and camera technologies have been shown to achieve high accuracies [284–291], other sensing methods used in fall prediction like Force Sensing Resistor (FSR) insoles, and those used in terrain classification for robotic walkers, such as LiDAR, should be explored. If these additional sensor types are effective at performing terrain classification, this may enable future terrain-classification systems to reduce costs, improve privacy, or exploit data collected for other aspects of the system.

With the goal of this research being to develop a system that can identify the incremental risk factors which contribute towards a person's instantaneous fall risk, the following chapter outlines the design of a sensor system and experimental procedure used to collect a dataset which enables the classification of terrain - a significant external fall-risk factor. The development of this sensor system, collection of the dataset, and subsequent analysis to determine the feasibility of terrain classification, will form the foundation for a system which can identify both internal and external fall risk factors.

4.2 Sensor System Design

4.2.1 Sensor Types and Locations

To collect a dataset of real-environment gait data, a novel sensor system comprising existing sensor types that are known to enable high-accuracy HAR, along with new sensor types which are unexplored for terrain identification, is designed. As this is a feasibility study into the capacity to perform both activity and terrain identification, the sensor system featured in this project is a prototype, with the aim being to remove redundant sensors through the analysis of

the collected data.

Existing HAR datasets feature IMUs frequently [35, 238–240, 254, 343] and analyses of these datasets typically yield high performance metrics with both traditional machine learning and deep learning approaches [344–347]. As such, an InvenSense ICM-20948 9-DoF IMU is positioned on the waist of the subject and on the top of each foot. This IMU was chosen due to the inclusion of a magnetometer for additional data dimensionality, for its low power requirements, and for the inclusion of a digital motion processor which helps to reduce drift [348].

Whilst the use of IMUs is expected to enable accurate HAR, it is not feasible to incorporate the depth cameras or body-mounted Red Green Blue (RGB) cameras shown to be successful in Chapter 2 for this application due to size, weight, and privacy issues. As such, this study aims to combine the data from colour sensors and LiDARs to function as a one-dimensional depth camera, providing the colour and distance to a single point on the ground over time, while maintaining the privacy of the wearer. The colour sensor used in this system is a TCS34725 colour sensor [349] positioned on the outside of the heel and facing the ground. This sensor provides contextual information in multiple forms, such as the red, green, and blue components of the colour of the ground directly underfoot, as well as the ambient light levels [349]. This should allow analytical methods to easily identify constant-colour terrains such as grass and paving slabs, along with helping to determine if the terrain is indoor or outdoor. As the TCS34725 monitors the colour of the reflections when shining a light on an object [349], the operating range is low, resulting in the need for the sensor to be placed on the side of the foot, and as low to the ground as possible.

Whilst the colour sensor may be capable of differentiating grass from paving slabs, the existence of multicolour carpets, gravel, and tarmac adds more complexity to the problem, and results in a need to identify additional separating factors about the terrain underfoot. For this reason, a VL53L1X LiDAR [350] is placed at the back of the shank, pointing towards the ground. Variation in the distance between the sensor and the ground should aid in determining the gait cycle when considering the low frequency data, and in building a noise profile of the ground underfoot when considering the high frequency data. These noise profiles of the ground can be used to separate terrains which are similarly coloured, but vary in texture. It is for this reason that a LiDAR was chosen over an ultrasonic distance sensor, as the LiDAR can be sampled at a much higher rate. The VL53L1X has a minimum operating distance of 40mm [350], meaning

that it cannot be mounted with the colour sensor, and must be separately attached higher up on the shank.

Finally, as covered in Chapter 2, force-sensing insoles are an effective sensor type in studies that propose novel wearable devices for remote gait analysis and fall risk analysis [351, 352]. Whilst many FSR insoles are available on the market, these are expensive [353, 354] and typically do not accommodate different shoe sizes [355, 356], with the intended solution to this problem being to remove excess material at the top and bottom of the device. However, this approach does not properly scale the device to differently-sized feet so that the sensors remain in the same relative position [355, 356]. Furthermore, when a participant requires a larger shoe size than the provided insole, these devices may move around in the shoe and no longer represent the force exerted by a specific part of the foot. To avoid these issues, low-cost insoles are manufactured consisting of 13 Interlink 402 FSRs [357] each. These insoles consist of a 0.6mm thick layer, which is 3D printed using Polylactic Acid (PLA) at a chosen shoe size, where resizing the 3D model automatically adjusts the locations of the markings that denote where the FSRs should be placed, allowing the insoles to properly scale with differently-sized feet. The 3D model used to print these insoles can be seen in Figure 4.1. This allows the insole to be manufactured to various different shoe sizes whilst maintaining the relative position of the FSRs on the feet. The FSRs are attached to the insole via a silicone-based adhesive, which is then covered by a 1mm thick layer of silicone to protect both the FSRs and the wearer's feet. A layer of flexible prototyping board is adhered to the underside of the PLA layer, to which the FSRs are soldered. Simple potential divider circuits are needed to obtain voltage readings from the changes in resistance that the FSRs exhibit, and the location of these circuits changes between two versions of the insoles. Version 1 insoles feature the potential divider circuits on the base of the insole. This has the advantage of reducing the number of wires from the insole down to 15: 13 data channels along with a positive and ground wire. However, this also introduces the weakness of having a power and ground wire which, if either break, will cause the loss of readings from all 13 FSRs. The version 1 insoles can be seen in Figure 4.2. Each insole was worn by participants of that size and the size above to reduce manufacturing times, and because of inconsistencies in the size of the provided shoes.
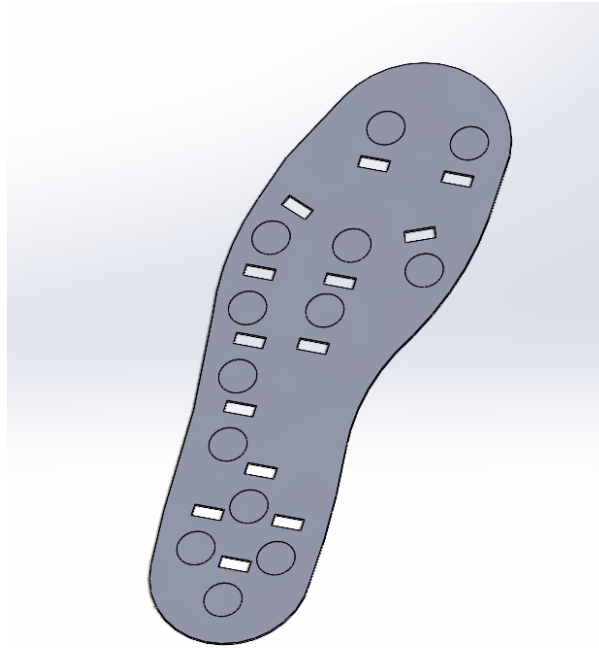
Figure 4.1: The 3D models of the insole.
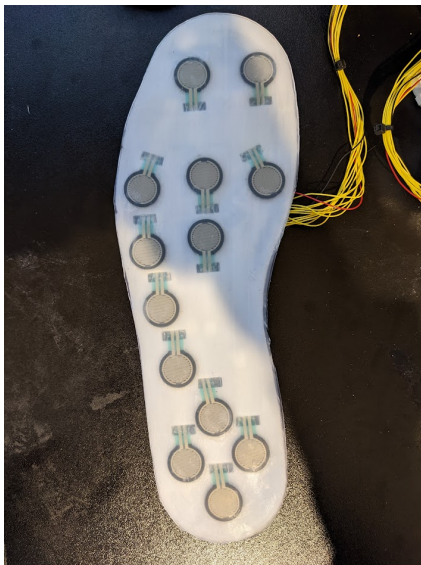
(a) The top side of the insole.
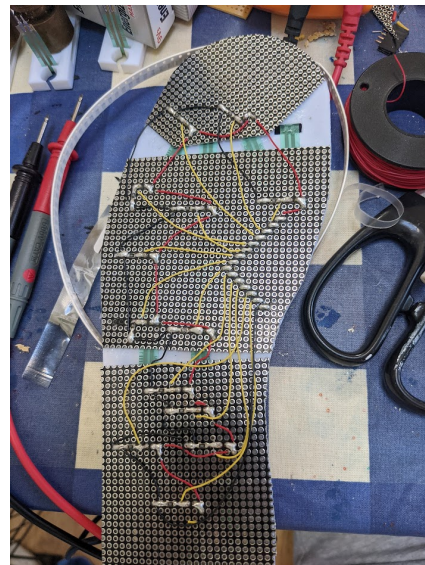
(b) The circuitry on the bottom of the insole.

Figure 4.2: The version 1, size 9 insoles.

As the wires from the sensor system to the insole are somewhat loose, the subject would oc-
casionally catch them on an object during a trial, or due to the insole breaking through wear,
insoles needed to be replaced several times over the course of the data collection sessions. As
a result, a second version of the insole was manufactured, which moved the potential divider
circuits off the insole. This has the advantage of speeding up insole manufacturing speed and
robustness as there was no longer a power or ground wire, at the cost of needing 26 wires to

connect the insole to the sensor system, which may affect the convenience of the device. Testing and subject feedback suggested that there was no increase in discomfort, resulting in version 2 insoles being used for most trials. Both versions feature an additional layer of 1mm thick silicone beneath the circuitry layer, and a multiplexer is used to reduce the number of inputs from 13 down to 5 before connecting to the microprocessors.

4.2.2 System Control and Synchronisation

To take readings and control the system, each sensor is connected to one of three Arduino Nano BLE 33 microcontrollers positioned on the waist, left leg, and right leg, which sample the data and store them on a micro-SD card via a HW-125 micro-SD adaptor. The Arduino Nano BLE 33 was chosen due to its high clock speed (64MHz) and low profile of 45×18mm [358]. To ensure that the data is synchronised in time between the waist, left leg, and right leg subsystems, three pairs of HC-05 Bluetooth modules broadcast the global time and commands from a central Arduino Mega to each of the subsystems.

All data sent from the central Arduino Mega to each subsystem is formatted as a string of 11 digits. The first digit tells the subsystems whether to start recording, stop recording, or delete a file, whilst digits two and three contain the two-digit activity number, digits four and five contain the two-digit trial number, and digits 6-11 contain the six-digit time elapsed since the start of the trail in milliseconds. Each subsystem captures a new sample from each sensor upon receiving a new time value from the central Arduino Mega, and each sample is labelled with the timestamp from the received string. All data is saved as a text file, which is named with the four-digit activity and trial number. A laptop is used to enter the five digit control and naming command, which is then sent to the Arduino Mega, which subsequently broadcasts the full 11 digit command to all three subsystems at the chosen sample rate. An overview of the system can be seen in Figure 4.3.
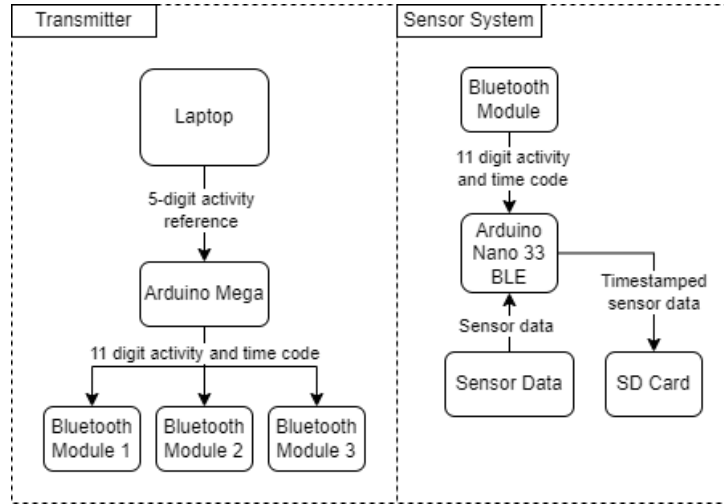
Figure 4.3: An overview of the sensor system design.

Because the subsystems read a sample when they receive a new string of digits via Bluetooth, the sample rate is consistent across the entire system and can be set to any value on the Arduino Mega. However, whilst many of the sensors are capable of high sample rate data capture, data was captured with a delay of 16ms, resulting in a sample rate of 62.5Hz. This value was determined via experimentation, as delays lower than 16ms resulted in insufficient time for the subsystems to write the data to the SD card before the next command to take a sample was issued.

The algorithms for the transmitting Arduino Mega and the receiving Arduino Nano 33 BLEs can be found in Figures 4.4 and 4.5 respectively. Whilst the transmitting Arduino Mega features fairly simple data processing and transmitting via serial, the receiver algorithm features multiple validation checks to ensure that the sensor data does not get corrupted or captured in error due to data losses over Bluetooth. Hence, the algorithm for receiving data checks to ensure that the received command is the expected 11 digits long, along with updating the transmitter with the current status of the data capture. In order to maximise the sample rate, SD card data is written to a buffer before being transmitted to the SD card in a single operation, as write operations are time expensive and will severely limit sample rates if performed after each reading is taken. This buffer, and therefore all the data for a single trial, is then written to the SD card upon receiving a stop command from the transmitter. Due to the importance of this operation, and the computational cost of performing it, it is vital to know if the command was successful, and the receivers accommodate this by transmitting the status of the data capture back to the laptop after a stop command is issued. This can also be used to check if files exist

on the SD card prior to recording to ensure that no files get overwritten and to help mitigate human errors which ultimately help to prevent subjects from being taken back to locations to perform trials again, and to prevent data loss. Finally, a delete command is available to allow the removal of files remotely, which acts to speed up the data collection process in the case of human errors. All algorithms were written in C/C++ using the Arduino Integrated Development Environment (IDE).
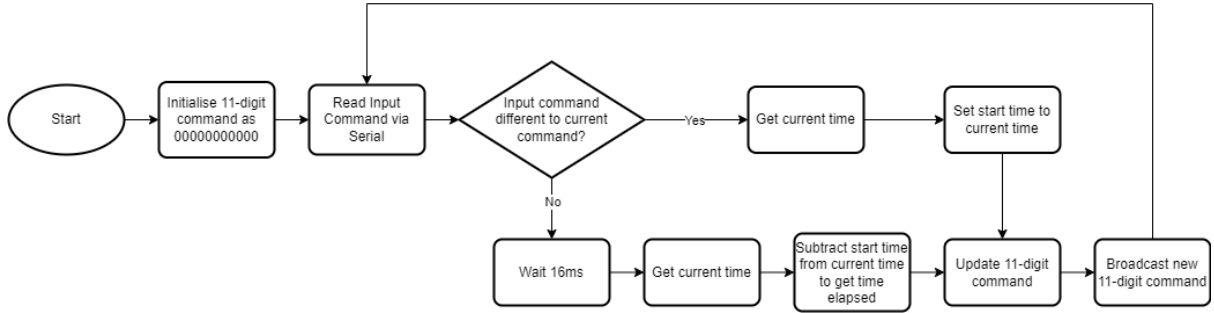
Figure 4.4: Flowchart of the Arduino Mega algorithm.
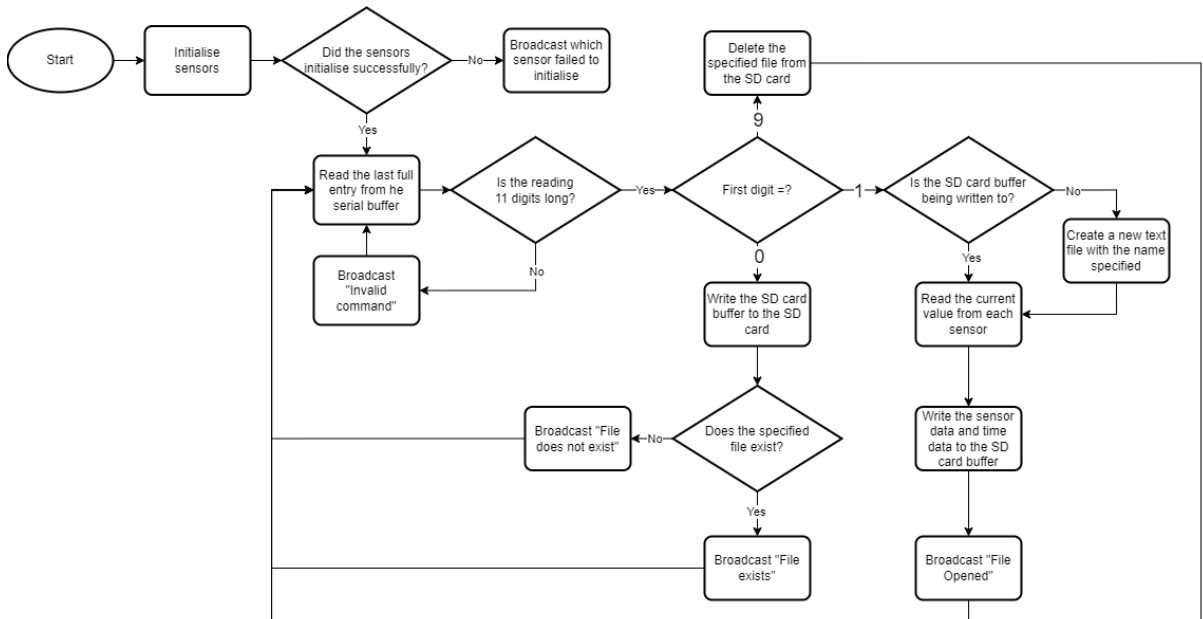
Figure 4.5: Flowchart of the Arduino Nano 33 BLE algorithm.

Data capture commands are issued to the transmitter via a laptop with a custom User Interface (UI) made using Python with the PyUI and PySerial libraries. This increases the efficiency of data collection by reducing the number of digits needed from the user to just four — the activity and trial numbers. The UI also features two data input boxes, which can be used for opposing actions such as sit-to-stand and stand-to-sit or ramp ascend and ramp descend, speeding up the

process of capturing multiple trials. The UI design can be found in Figure 4.6
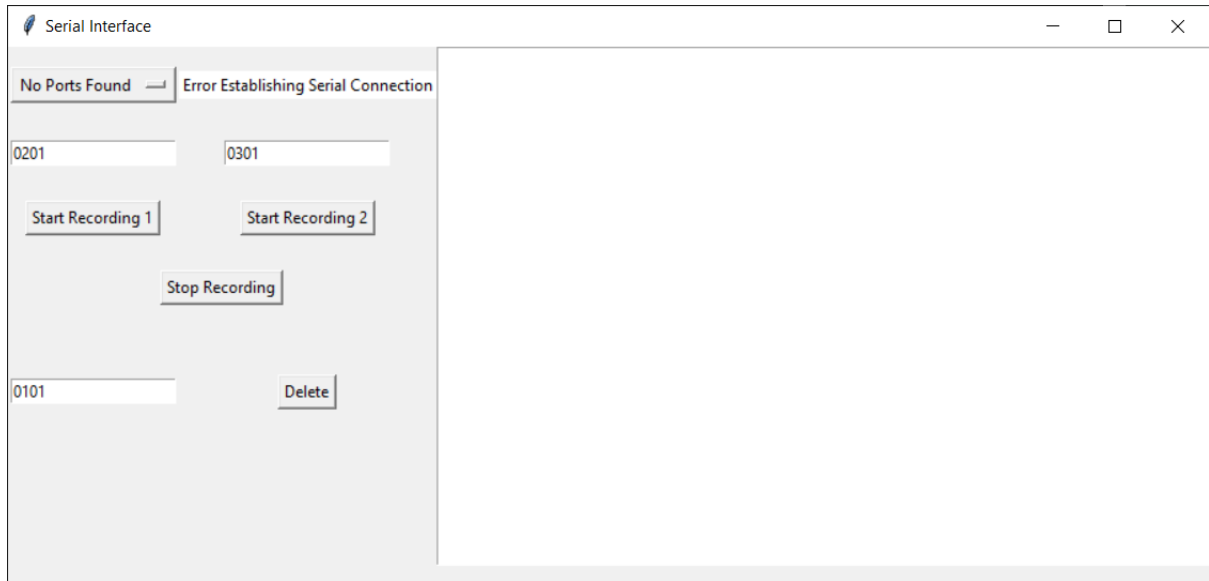
Figure 4.6: The UI design for the data capture laptop.

The sensor system is attached to the body through multiple methods. Subjects are provided with plain canvas-style shoes which were augmented with a small, 3D-printed box on the outer lateral side of the foot. This box contained the multiplexer for the insoles and the colour sensor. The foot IMU was also attached to the shoe by threading the shoelaces through another box containing the IMU. This method of attachment ensured that the inertial sensors remained in the same location relative to the foot for each subject, that the attachment was comfortable, and that noise generated by a loose attachment was minimised. A large box containing the Arduino Nano 33 BLE, a 9V battery, the SD card adaptor, and wiring was attached to the outer lateral side of the shank via two elastic straps. The LiDAR is then positioned in another small box and attached to the lower of these straps at the back of the leg on the frontal plane, facing the ground. All sensors in the various locations around the leg are wired together using I2C communications. For the waist sensor, the IMU is embedded into the same box as the Arduino Nano 33 BLE, 9V battery, SD card adaptor, and wiring, which was attached to the back of the subject's trousers via a clip. The various 3D models and final versions of the sensor attachments can be found in Figure 4.7.
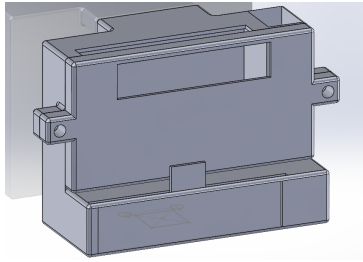
(a) The multiplexer box CAD.
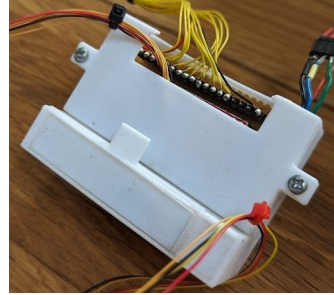
(b) The 3D printed multiplexer box.
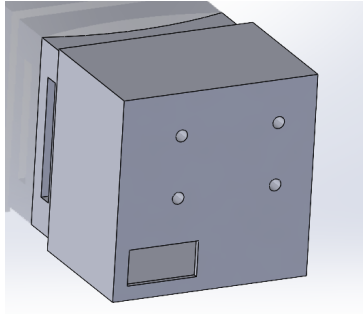
(c) The foot IMU holder CAD.
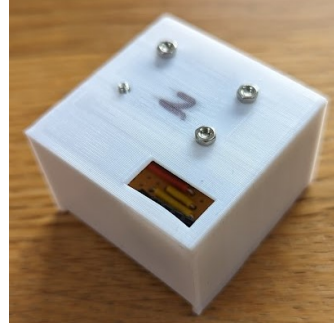
(d) The 3D printed foot IMU holder.
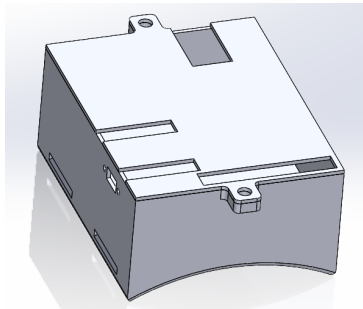
(e) The Arduino and circuitry housing CAD.
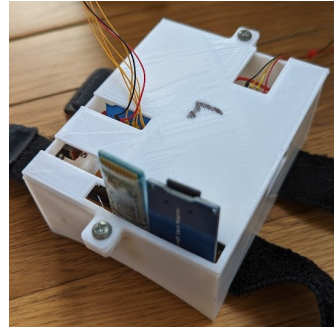
(f) The 3D printed Arduino and circuitry housing.
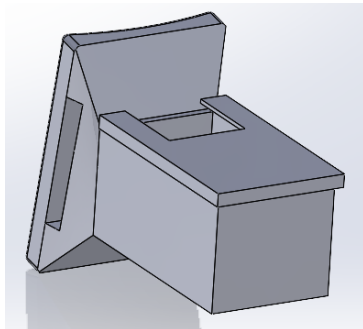
(g) The LiDAR box CAD.
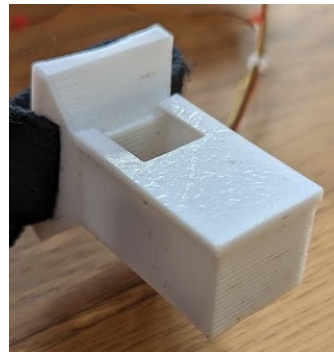
(h) The 3D printed LiDAR box.
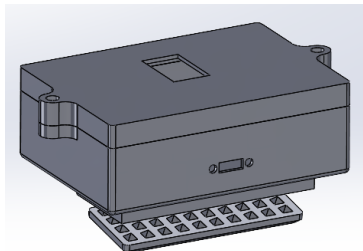
(i) The waist box CAD.

(j) The 3D printed waist box.

Figure 4.7: The various CAD elements, and their real counterparts, of the sensor system.

The circuitry for the sensor system comprised potential divider circuits for the insoles, and a voltage regulator for the Arduino Nano 33 BLE microprocessors. For the insoles, changes in force applied to the force sensors cause a reduction in resistance across the sensor [357], allowing a simple potential divider circuit to convert from variable resistance to variable voltage. This circuit can be found in Figure 4.8
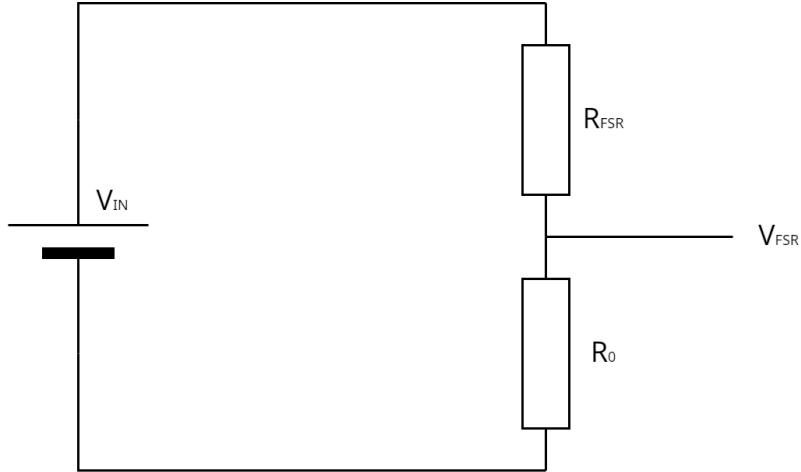
Figure 4.8: A simple potential divider circuit for converting FSR resistance changes to voltage changes.

The Arduino Nano 33 BLE can only accept and output voltages in the range of 0-3.3V, with these values being interpreted as values in the range of 0-1023 internally when reading from the analogue pins. Force applied to the FSR is inverse-logarithmically proportional to the resistance of the FSR [357], meaning that choosing a value for R_0 is crucial for setting the range, and sensitivity with which we will be able to detect changes in pressure. With participants expected to weigh between 50kg and 120kg, the maximum force exerted on a sensor would be expected to be around 500-1200N when stationary, and could be much higher when the user is walking. As such, a value of 330Ω was chosen for R_0, which results in the force-to-input graph found in Figure 4.9. This sensor should offer large changes in value within the most common operating range of around 0-1200N, whilst also enabling enough headroom that higher forces are distinguishable from noise.

The potential divider equation for calculating the voltage across the FSR can be found in Equation 4.1:

$$V_{FSR} = \frac{R_0}{R_0 + R_{FSR}} V_{IN} \tag{4.1}$$
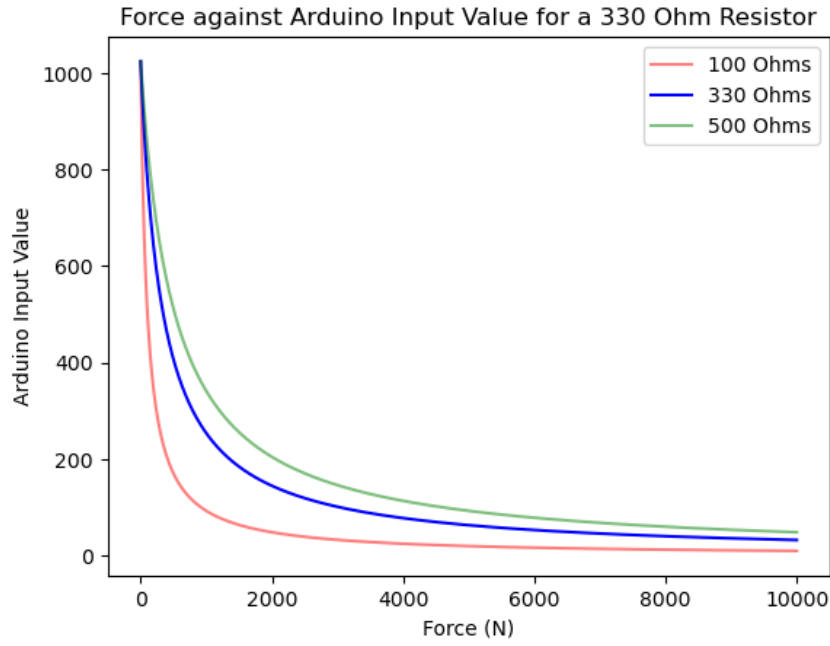
Figure 4.9: A graph showing how the resolution of the analogue values on the Arduino change when the fixed resistor is changed, and a range of forces are applied to the FSR.

Aside from the potential divider circuits, most other circuitry involved simply connecting devices and regulating voltages, as all sensors were chosen to operate at 3.3V, whilst the SD card adaptor and Bluetooth modules required an input of 5V. The internal view of the multiplexers, waist, and shank sensors can be found in Figure 4.10
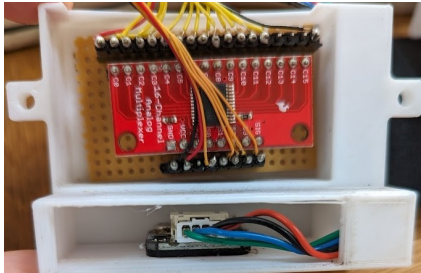
(a) The multiplexer box circuitry.
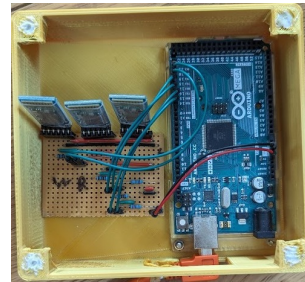
(b) The transmitter circuitry.
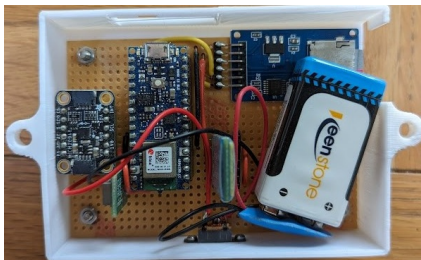
(c) The waist sensor hub circuitry.
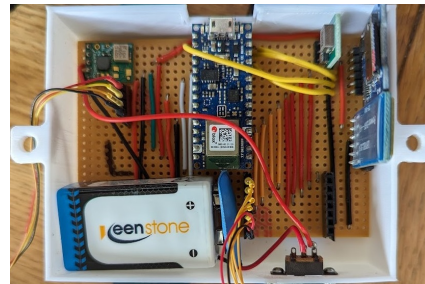
(d) The shank sensor hub circuitry.

Figure 4.10: The circuitry of the multiplexer, transmitter, waist sensor hub, and shank sensor hub.

4.3 Data Collection

Ethics was received from Leeds University EPS Research Ethics in May 2022 (reference: MEEC 21-016) for data to be collected from 20 healthy participants, which took place from November 2022 to February 2024. Data were collected from one to two subjects per week each Friday between 11am and 4pm, with some weeks being cancelled, and some subjects being split between two weeks due to rain or snow. As this dataset was designed to be a real-environment dataset, the spacing of the trials ensured that data was captured at regular intervals through all seasons, which is crucial for a dataset with a focus on real-world applications. Appendix B contains the ethical approval documentation and files given to participants before the study.

4.3.1 Participant Recruitment

Participants were recruited through obtaining verbal interest from healthy people at Chapel Allerton Hospital (CAH) with a range of ages, weights, heights, shoe sizes, and from diverse ethnic backgrounds. The inclusion and exclusion criteria for recruitment was as follows:

Inclusion Criteria:

- Age $\geq$ 18

- Able to walk indoors and outdoors without a walking aid.

Exclusion Criteria:

- Age $<$ 18

- Unable to walk indoors and outdoors without a walking aid.

- Inability to consent to the study

- Confirmed diagnosis of Parkinson's disease, dementia, acquired brain injury (stroke, cerebral palsy, etc.), multiple sclerosis, or have had a lower limb amputation.

- Unable to walk safely with provided shoes (need for specialist shoes)

- Allergy to materials used in the study, such as silicone and elastic fibres

A participant information sheet was provided before the study, and informed consent to participate was obtained in writing before the trials began. Anonymised participant demographic information was collected for those properties that affect gait, and can be found in Table 4.1

(a) Weight

(b) Height

(c) Age
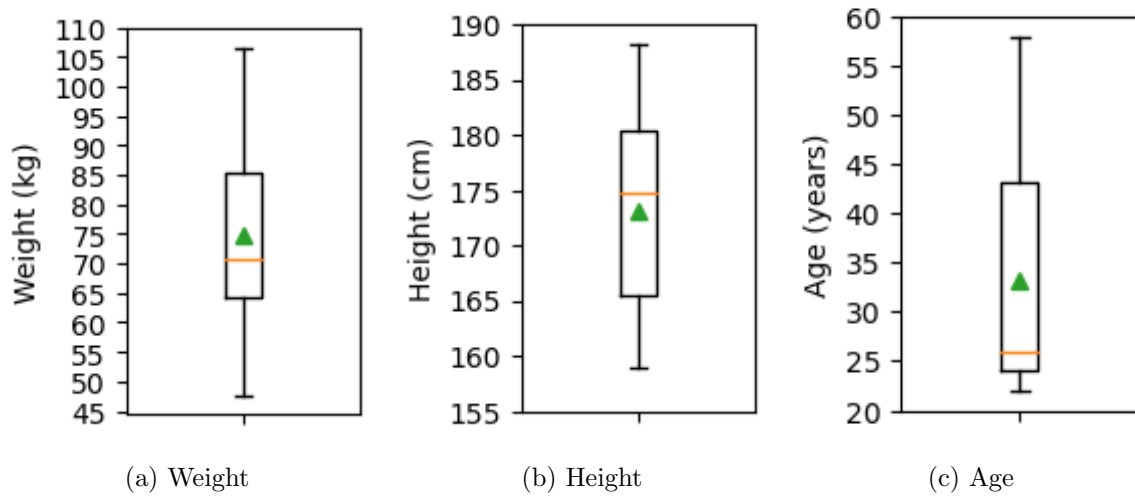
Figure 4.11: Box plots of demographic data for the 20 participants, along with the median (orange) and mean (green) values.

and Figure 4.11. It should be noted that participant 15 reported plantar fasciitis of the left foot, and arthritis in the right foot, but still met the inclusion criteria, and was the only participant with a gait-affecting condition.

Table 4.1: Participant demographic information.

Subject	Sex	Age	Weight (kg)	Height (cm)	UK Shoe Size	UK Shoe Size Provided
1	M	25	86.0	182.5	9	10
2	M	22	67.6	184.0	10	10
3	M	50	64.4	175.0	9	10
4	M	24	94.1	177.0	10	10
5	M	25	82.5	188.2	10	10
6	M	26	97.9	179.6	10	10
7	M	43	97.5	182.5	10	10
8	F	44	72.4	170.5	7	7
9	F	39	59.1	162.5	5	7
10	F	35	85.0	165.0	6	7
11	F	50	62.0	159.0	5.5	7
12	F	48	63.9	167.5	6.5	7
13	F	22	69.0	159.0	6	7
14	F	28	47.4	166.0	4	7
15	F	58	75.6	164.5	5.5	7
16	M	26	106.4	178.5	10	10
17	M	24	66.6	176.0	9	9
18	F	23	65.7	174.5	6.5	7
19	M	26	78.9	183.0	10	10
20	F	24	51.8	165.5	6	7

4.3.2 Experimental Procedure

After consent is obtained from each participant, participants were equipped with the sensor system with aid from the research team. Each participant was offered the shoe size that felt the most comfortable to them, which is reported in Table 4.1. Weight and height were measured after the system was equipped.

Regarding the activities, the data collection procedure was mapped out such that one continuous route could be taken through CAH with various stops in different locations to capture data. These activities and locations were chosen to be representative of common real life scenarios. This route can be seen in Figure 4.12, and an activity matrix and full list of activities and their activity codes can be found in Figure 4.13 and Table 4.2 respectively.

OT Bathroom	
Sit to Stand	Toilet
Stand to Sit	Toilet
Sitting	Toilet

Outside 2	
Stair Ascend	Paving Slabs
Stair Descend	Paving Slabs
Ramp Ascend (low incline)	Paving Slabs
Ramp Descend (low incline)	Paving Slabs
Ramp Ascend	Asphalt
Ramp Descend	Asphalt
Walking	Asphalt
Standing	Asphalt

Other	
Elevator Up	Lift
Elevator Down	Lift
Walking	Carpet
Standing	Carpet
Sit to Stand	Carpet
Stand to Sit	Carpet
Sitting	Carpet
Stair Ascend	Hospital Stairs
Stair Descend	Hospital Stairs

Gym (Outdoors)	
Walking	Paving Slabs
Standing	Paving Slabs
Walking	Gravel
Standing	Gravel
Sit to Stand	Outdoor Chair
Stand to Sit	Outdoor Chair
Sitting	Outdoor Chair

Gym (Indoors)	
Walking	Laminate
Standing	Laminate
Stair Ascent	Laminate
Stair Descent	Laminate
Sit to Stand	Chair
Stand to Sit	Chair
Sitting	Chair

Outside 1 (start)	
Ramp Ascend	Grass
Ramp Descend	Grass
Walking	Grass
Standing	Grass

Figure 4.12: The location of each trial and the planned route through CAH.

	Walking	Standing	Ramp Ascend	Ramp Descend	Stair Ascend	Stair Descend	Sit to Stand	Stand to Sit	Sitting	Elevator Up	Elevator Down
Grass	1	4	2	3							
Paving Slabs	5	7	24	25	22	23	9	10	11		
Gravel	6	8									
Laminated Flooring	12	13			17	18	14	15	16		
Toilet							19	20	21		
Asphalt	28	29	26	27							
Lift										30	31
Carpet	32	33					34	35	36		
Hospital Stairs					37	38					

Figure 4.13: The matrix showing all combinations of activities and locations. Activity codes correspond to those found in Table 4.2.

A total of 38 real-world activity-terrain combinations were recorded for each participant, resulting in 7.8 hours of captured gait data. Each walking activity consisted of two sets of walking anticlockwise, then clockwise, around the researcher recording the data, for 30 seconds each. Participants were instructed to walk in straight lines where possible, but also to prevent pivoting on the spot at the corners. This was to ensure that walking data would not contain one singular turn for the entire duration of the trial. The exception to this was the gravel and paving slab walking, where participants walked along a straight track three times. This was due to limitations in the availability of large gravel and paving slabs areas. Ramp ascend, ramp descend, stair ascend, stair descent, sit to stand, and stand to sit trials were performed three times each to ensure that enough data was present for analysis with these short activities. For standing and sitting, participants were simply instructed to remain relaxed and still whilst the activity was recorded. The final two activity types involve travelling up and down in a lift. This was captured from the lower ground floor to the second floor of CAH where possible. In some instances, this trial would be interrupted due to a member of the public joining or leaving the lift early. In these cases, less data may be available for the lift activities.

Table 4.2: The full activity list for data collection.

Index	Activity	Terrain	Location	Exercise
1	Walking	Grass	Outside 1	2x – Walk for 30 seconds
2	Ramp Ascend	Grass	Outside 1	3x – Walk up the ramp
3	Ramp Descend	Grass	Outside 1	3x – Walk down the ramp
4	Standing	Grass	Outside 1	1x – Stand still for 10 seconds
5	Walking	Paving Slabs	Gym (Outdoors)	3x – Walk for 10 seconds (straight line)
6	Walking	Gravel	Gym (Outdoors)	3x – Walk for 10 seconds (straight line)
7	Standing	Paving Slabs	Gym (Outdoors)	1x – Stand still for 10 seconds
8	Standing	Gravel	Gym (Outdoors)	1x – Stand still for 10 seconds
9	Sit to Stand	Paving Slabs	Gym (Outdoors)	3x – Stand up from an outdoor chair
10	Stand to Sit	Paving Slabs	Gym (Outdoors)	3x – Sit down on an outdoor chair
11	Sitting	Paving Slabs	Gym (Outdoors)	1x – Stay sitting for 10 seconds
12	Walking	Laminated Flooring	Gym (Indoors)	2x – Walk for 30 seconds
13	Standing	Laminated Flooring	Gym (Indoors)	1x – Stand still for 10 seconds
14	Sit to Stand	Laminated Flooring	Gym (Indoors)	3x – Stand up from an indoor chair
15	Stand to Sit	Laminated Flooring	Gym (Indoors)	3x – Sit down on an indoor chair
16	Sitting	Laminated Flooring	Gym (Indoors)	1x – Stay sitting for 10 seconds
17	Stair Ascend	Laminated Flooring	Gym (Indoors)	3x – Walk up a set of stairs
18	Stair Descend	Laminated Flooring	Gym (Indoors)	3x – Walk down a set of stairs
19	Sit to Stand	Toilet	OT Bathroom	3x – Stand up from a toilet
20	Stand to Sit	Toilet	OT Bathroom	3x – Sit down on a toilet
21	Sitting	Toilet	OT Bathroom	1x – Stay sitting for 10 seconds
22	Stair Ascend	Paving Slabs	Outside 2	3x – Walk up a set of stairs
23	Stair Descend	Paving Slabs	Outside 2	3x – Walk down a set of stairs
24	Ramp Ascend	Paving Slabs	Outside 2	3x – Walk up the ramp
25	Ramp Descend	Paving Slabs	Outside 2	3x – Walk down the ramp
26	Ramp Ascend	Asphalt	Outside 2	3x – Walk up the ramp
27	Ramp Descend	Asphalt	Outside 2	3x – Walk down the ramp
28	Walking	Asphalt	Outside 2	2x – Walk for 30 seconds
29	Standing	Asphalt	Outside 2	1x – Stand still for 10 seconds
30	Elevator Down	Lift	Lift	1x – Travel down in the lift
31	Elevator Up	Lift	Lift	1x – Travel up in the lift
32	Walking	Carpet	Chapel	2x – Walk for 30 seconds
33	Standing	Carpet	Chapel	1x – Stand still for 10 seconds
34	Sit to Stand	Carpet	Chapel	3x – Stand up from an indoor chair
35	Stand to Sit	Carpet	Chapel	3x – Sit down on an indoor chair
36	Sitting	Carpet	Chapel	1x – Stay sitting for 10 seconds
37	Stair Ascend	Hospital Stairs	Hospital Stairs	3x – Walk up a set of stairs
38	Stair Descend	Hospital Stairs	Hospital Stairs	3x – Walk down a set of stairs

Some variation was introduced between data collection sessions due to a variety of reasons, from human error to environmental factors. Some of the more notable elements that introduced variation were the inconsistent availability of the chapel on Friday afternoons, and the presence of a mobile Magnetic Resonance Imaging (MRI) machine in the hospital car park, which appeared to affect the sensor system. The most common variation was to change the room in which the experimental setup, and therefore the "flat smooth", activities occurred based on their availability. Room 1 was a communal room, room 2 was an office, and room 3 was a hydrotherapy pool changing room. A list of experimental variations can be found in Table 4.3. Most variations simply involved moving to different areas around the hospital with the same

terrain, however there are some instances where files were missing. These files are usually one of a set of three trials such as sit to stand, stand to sit, ramp, or stair activities, however there is one instance where activity 12 - walking in the setup room, was missing. In this instance, our participant was time pressured and was not able to perform the activity again. Additionally, due to errors in the first few trials, subjects 1 and 3 had their data recollected in 2024, where it was originally collected in late 2022, and early 2023 respectively.

For many of the early subjects, data from the waist sensor is limited and inconsistent. This was caused by a couple of electrical issues which could not be diagnosed until the later trials. The first issue found was with the SD card adapter, which was damaged, preventing the SD card from fixing in place. This made the SD card connection inconsistent as the device was being moved around, which would corrupt the data from the waist sensor. Once this issue was fixed, data was no longer being corrupted, but the waist sensor still remained inconsistent when compared to the relatively more complicated leg subsystems. During a later trial, the waist sensor power wire snapped and was reattached with an increased amount of slack. This reparation fixed the issues with the waist sensor, suggesting that the issue was the loose wiring.

In addition to the issues with the waist sensor, the insoles broke on multiple occasions. Before switching to the version 2 insoles, this would cause a loss of data from all sensors on the insole when this occurred. Both of the size-nine version 1 insoles broke after subject 7's trial, and the size-six version 1 right insole broke during subject 10's trial. The breakage of the latter of these insoles was not noticed until subject 14's trial was complete. Additionally, one of the FSR wires snapped on the size-six version 2 right insoles during subject 20's trial.

Table 4.3: Experimental procedure variations.

Subject	Variation(s)
1	Setup in room 3, version 2 insoles.
2	Setup in room 1, MRI interference, trials split into 2 sessions due to darkness, version 1 insoles.
3	Setup in room 1, version 2 insoles.
4	Setup in room 2, MRI interference, version 1 insoles.
5	Setup in room 2, paving slab and asphalt ramp and stairs moved to front car park, version 1 insoles.
6	Setup in room 3, office carpet used, paving slab and asphalt ramp and stairs moved to front car park, only 10 seconds of walking data recorded, version 1 insoles.
7	Setup in room 3, office carpet used, paving slab and asphalt ramp and stairs moved to front car park, left multiplexer ground wire snapped during final trials, but data doesn't appear to be affected, version 1 insoles.
8	Setup in room 3, paving slab, asphalt, and grass ramps and stairs moved to front car park, 0202 missing, version 1 insoles.
9	Setup in room 3, paving slab, asphalt, and grass ramps and stairs moved to front car park, very light rain during outdoor activities, version 1 insoles.
10	Setup in room 1, paving slab, asphalt, and grass ramps and stairs moved to front car park, split into 2 sessions due to rain, version 1 insoles.
11	Setup in room 1, paving slab, asphalt, and grass ramps and stairs moved to front car park, split into 2 sessions due to rain, version 1 insoles.
12	Setup in room 1, paving slab, asphalt, and grass ramps and stairs moved to front car park version 1 insoles.
13	Setup in room 1, version 2 insoles, trials split into 2 sessions due to rain.
14	Setup in room 3, paving slab, asphalt, and grass ramps and stairs moved to front car park, 1202 missing, version 1 insoles.
15	Setup in room 3, paving slab, asphalt, and grass ramps and stairs moved to front car park, version 2 insoles.
16	Setup in room 3, 0202 missing, version 2 insoles.
17	Setup in room 3, version 2 insoles.
18	Setup in room 3, meeting room carpet used, version 2 insoles.
19	Setup in room 3, 1001 missing, meeting room carpet used, version 2 insoles.
20	Setup in room 3, 0903 missing, FSR 1 wire snapped in chapel, version 2 insoles.

Despite these issues with some of the sensors during data collection, the high data dimensionality of the system and the nature of soft computing methods such as machine learning means that this should not be an issue when performing activity classification or terrain identification. Furthermore, this dataset contains lengthy trials with difficult terrains and a complex sensor system, resulting in an increased likelihood for breakages and increased difficulty in diagnosing these issues. These factors should be mitigated in future research into terrain classification by constructing more robust or less complex systems.

4.4 Processing and Visualisation

Despite some issues with data collection, a complete dataset was produced from each of the 20 healthy participants, with 85-86 activity files produced for each subsystem. For each leg, these files contain 29 channels of data, whilst the waist data contains nine, resulting in 67 total data channels for each activity file. Files are organised into folders for each subject and sensor

subsystem, and are named with the two-digit activity code, which can be found in Table 4.2, and two-digit trial number. Due to errors thought to be caused by the MRI interference, in early trials some additional files were recorded with invalid activity codes. Most of these occurred during the original recordings of subject 1 and subject 3, which were later recollected, but some of these still appear, such as "0000.txt" in the data from subject 4. These files are left in the dataset in the case that they can be useful with unsupervised learning.

4.4.1 Additional Activities

For subjects 1 and 3, additional activities were recorded for testing purposes. These activities can be found in Table 4.4.

Table 4.4: The bonus activity list for subjects 1 and 3.

Index	Activity	Terrain	Location	Exercise
39	Sit to Stand	Gravel	Outside 2	3x – Stand up from an outdoor chair
40	Stand to Sit	Gravel	Outside 2	3x – Sit down on an outdoor chair
41	Sitting	Gravel	Outside 2	1x – Sit still for 10 seconds
42	Sit to Stand	Grass	Outside 1	3x – Stand up from an outdoor chair
43	Stand to Sit	Grass	Outside 1	3x – Sit down on an outdoor chair
44	Sitting	Grass	Outside 1	3x – Sit still for 10 seconds
45	Standing	Toilet	OT Bathroom	1x – Stand still for 10 seconds
46	Ramp Ascend	Laminated Flooring	Hospital Corridor	3x – Walk up the ramp
47	Ramp Descend	Laminated Flooring	Hospital Corridor	3x – Walk down the ramp

These activity and terrain combinations were chosen to be relevant, yet less common than the main dataset. Models constructed to perform activity and terrain classification can utilise these activities in testing to ensure that their models have generalised well. It is speculated that, due to certain activities only being performed in certain locations, some bias may be introduced. For example, a model that determines the activity is stair ascent will never consider that gravel or the bathroom could be valid locations, just as a model that determines the activity is grass will never consider sit to stand or stand to sit. These additional activities will allow researchers the opportunity to demonstrate the generalisation capabilities of their models.

4.4.2 Data Reformatting and Visualisation

When plotting the data, the reformatted data is input and filtered down to the chosen sensor. A 10Hz, 4th order Butterworth low-pass filter is then applied to the data to remove high-frequency noise. Figure 4.14 shows the unfiltered and filtered data from the gyroscope X axis during file "3201" from subject 20.
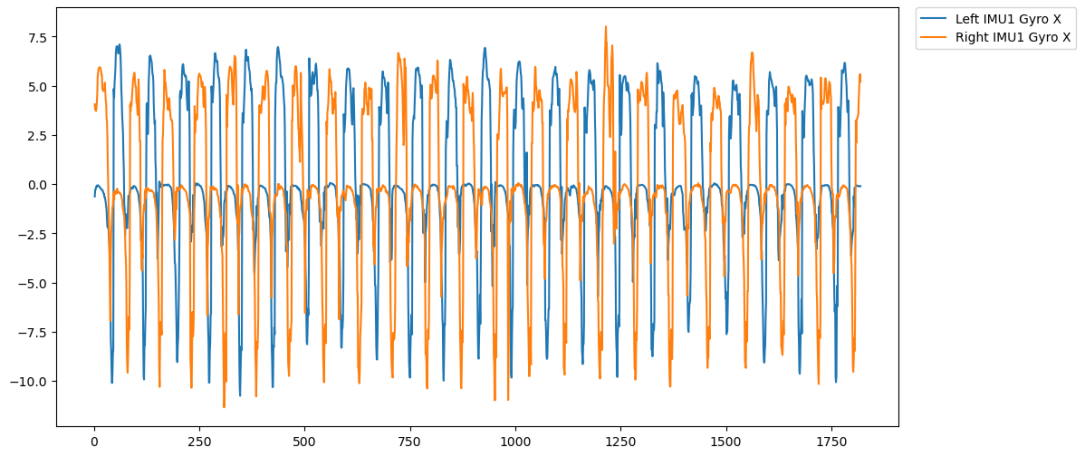
(a) Unfiltered.
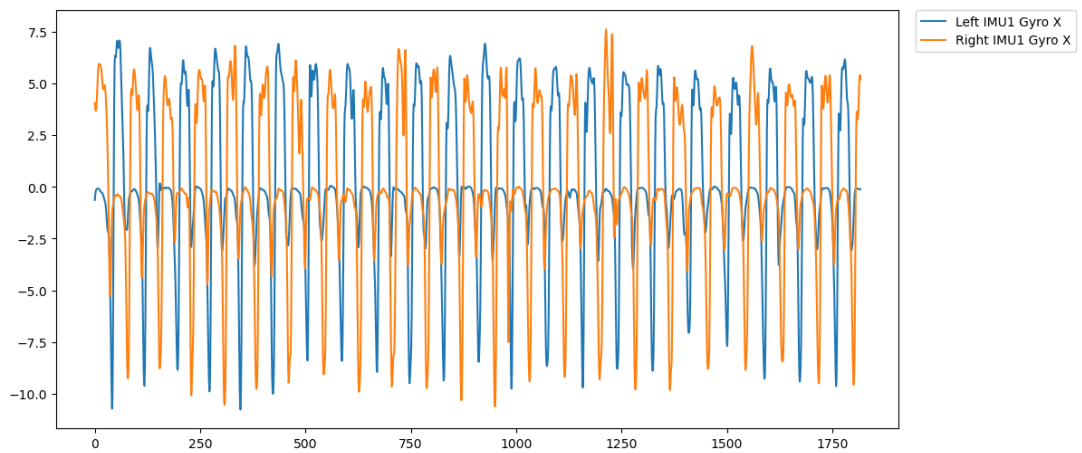
(b) Filtered.

Figure 4.14: Gyroscope X-axis data from file "3201.txt" from subject 20.

Due to the large number of FSR data channels, plotting this data in its raw or unfiltered form is not useful. As such, the FSR data from each insole is summed and normalised to display the total force on each foot. The plot of this data for subjects 1 and 20 can be found in Figure 4.15.
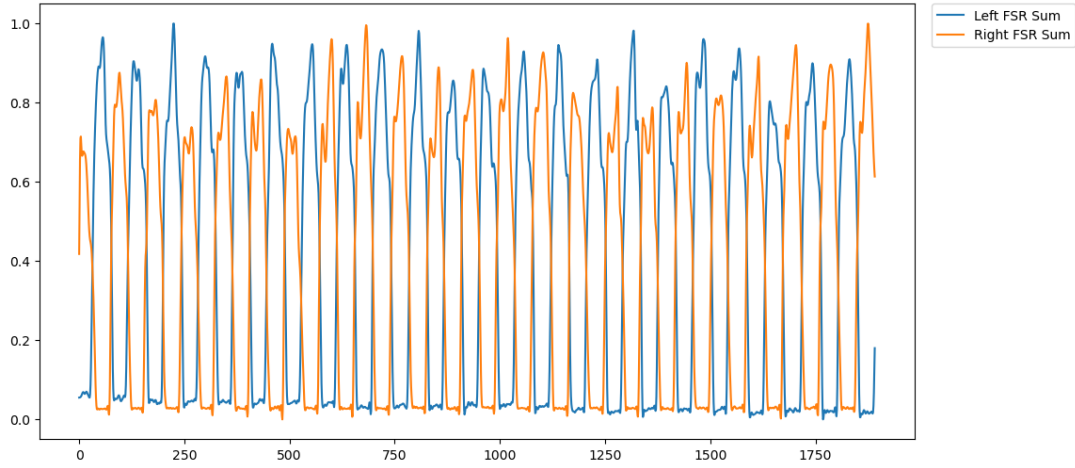
(a) Subject 1.
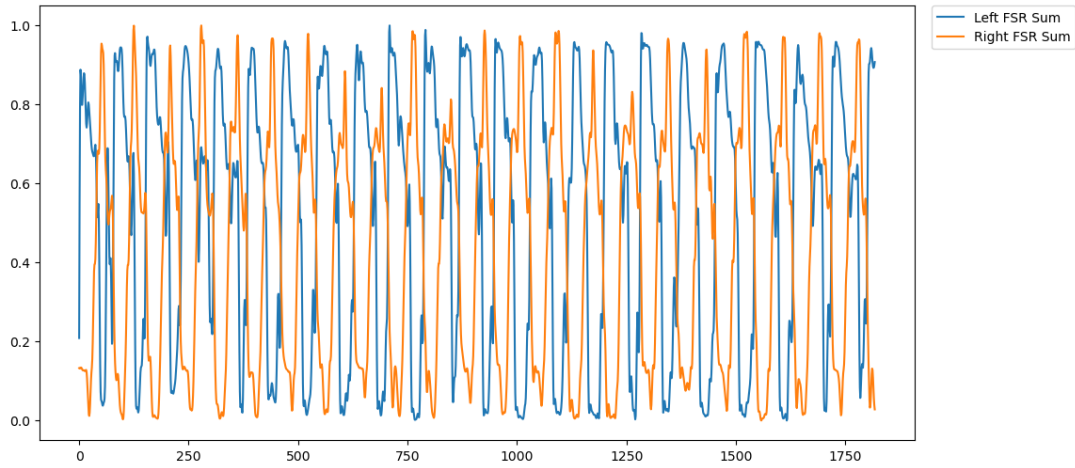
(b) Subject 20.

Figure 4.15: The summed and normalised FSR data from the file "3201.txt" from subjects 1 and 20.

Another method of visualisation for the collected data is presented in the form of short heatmap videos of the force on each sensor in the insole over time. Through these videos, the pattern of force on a foot can be observed over the course of any captured activity. As seen in Figure 4.16, these heatmaps can offer insight into the force distribution of the foot, and therefore the Centre of Pressure (CoP), over the course of each activity in this dataset.

While these various figures demonstrate the capability of this dataset for gait analysis by offering insights into the spatio-temporal gait parameters, it is crucial that this dataset also enables accurate classification of the activity being performed, along with the terrain that the activity is being performed on. Various datasets have already demonstrated the potential to enable high-accuracy activity classification using data from as little as a single smartphone IMU [343–347]. As such, this dataset collected with a large, multimodal sensor system, including a waist-

(a) 480ms	(b) 640ms	(c) 800ms
(d) 960ms	(e) 1120ms	(f) 1280ms
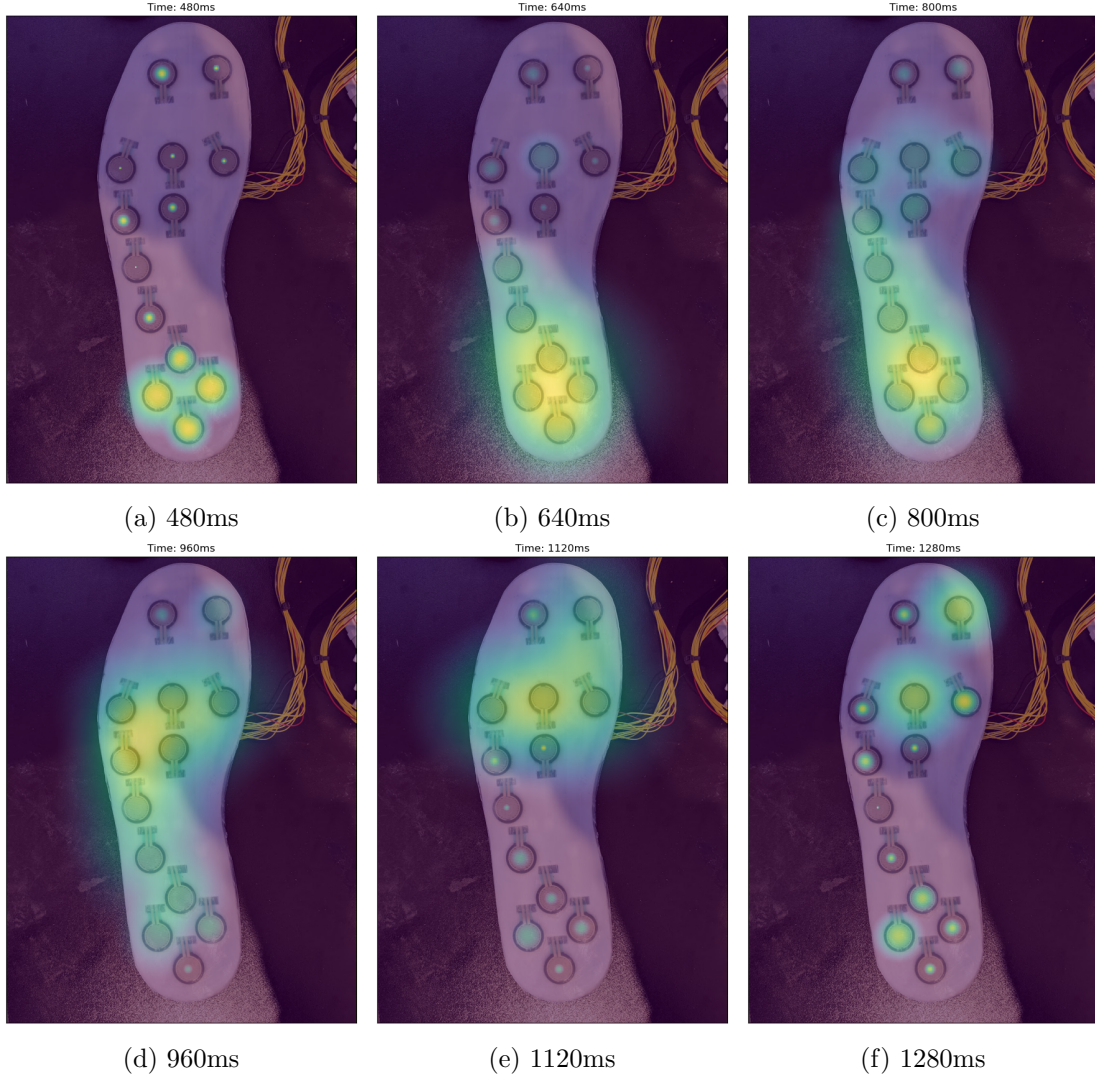
Figure 4.16: Heat maps of the FSR data 160ms apart during subject 1's walking on carpet trial.

mounted IMU to mimic the capabilities of these smartphone-based studies, should enable high-accuracy activity classification. Regarding terrain classification, the colour sensor and LiDAR generate data that enables the various terrains to be distinguished from one another. Figure 4.17 shows the combined red, green, and blue colour channels captured from the colour sensor on various terrains. From this figure, it can be seen that the colour sensor data reflects the colour of the terrain underfoot, along with the ambient light, which can be seen when the foot is lifted and is white for the outdoor terrains, and much darker for the gravel captured in the shade, and laminated flooring captured inside the hospital. It is also notable that the indoor terrain colour maps are extremely dark, which may indicate that the colour sensor was mounted too far from the ground for these indoor trials, resulting in insufficient light being reflected from the floor to the sensor to produce a more accurate reading.

(a) Grass

(b) Gravel

(c) Asphalt

(d) Laminated Flooring
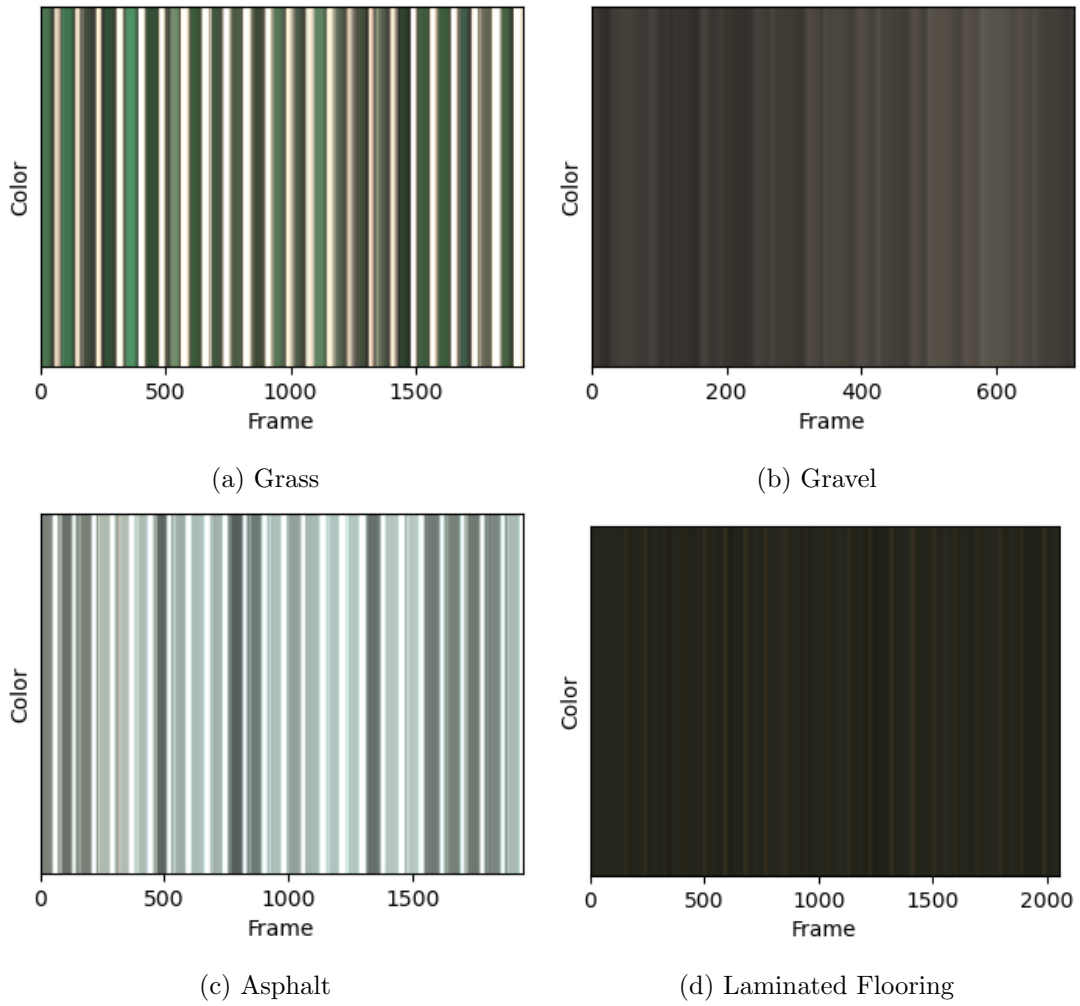
Figure 4.17: Colour over time captured from the left leg during walking on 4 different flooring types.

Alongside colour, the data from the LiDAR was theorised to provide insight into the coarseness of the terrain underfoot. However, some preprocessing is required, as the LiDAR data primarily reflects the large changes in distance from the shank to the ground during a stride, as seen in Figure 4.18a. Taking only the high-frequency data, the low-frequency strides are removed, leaving fluctuations in distance which represent the coarseness of the ground underfoot. Examples of the unprocessed and processed LiDAR data can be found in Figure 4.18, in which the large variation in coarseness can be seen between grass and laminated flooring.
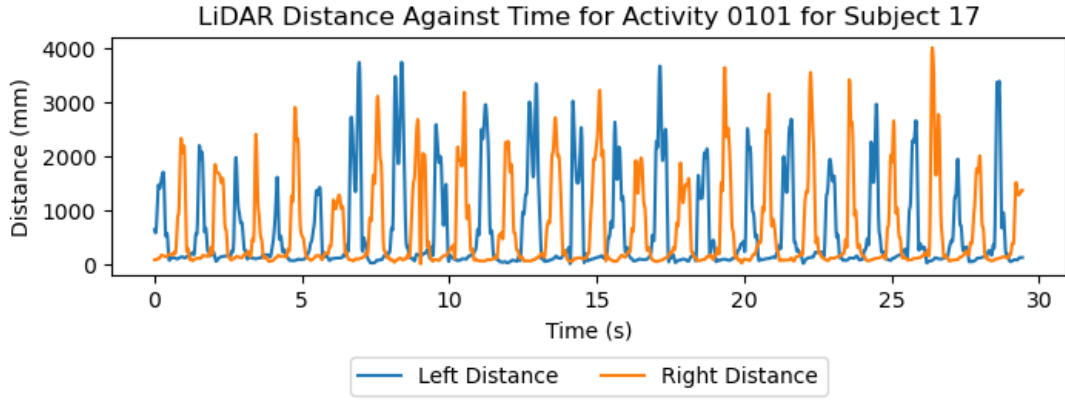
(a) Raw LiDAR data
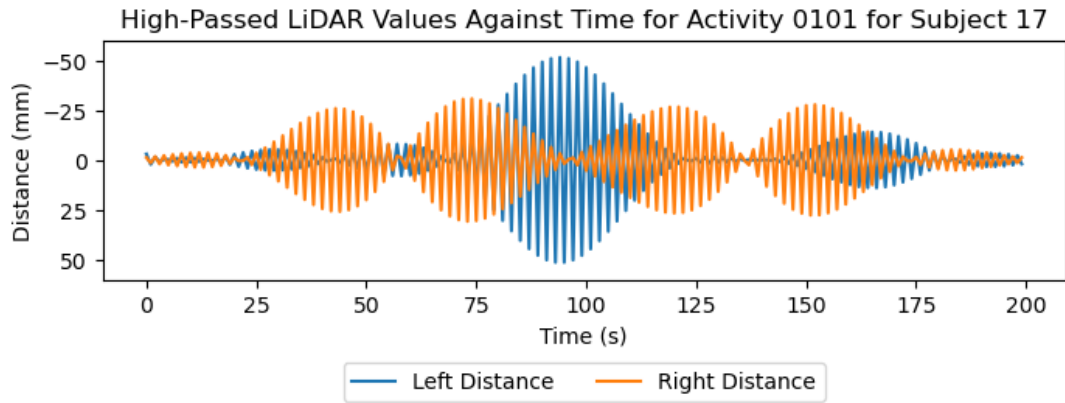
(b) High-Passed on Grass
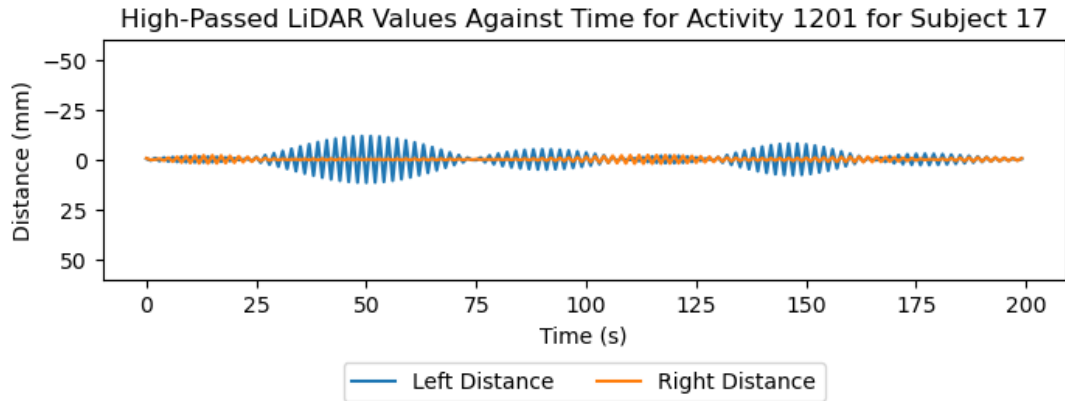
(c) High-Passed on Laminated Flooring

Figure 4.18: Raw LiDAR readings along with high-pass filtered LiDAR data at a cut-off frequency of 30Hz for the walking activity on grass and laminated flooring for subject 17.

The final dataset was uploaded to the IEEE DataPort data repository, and is dubbed the Context-Aware Human Activity Recognition (CAHAR) dataset [241]. A comparison of the properties of the CAHAR dataset compared to other recent real-environment datasets can be found in Table 4.5, while a comparison to other terrain-identification studies can be seen in Table 4.6.

Table 4.5: A Comparison of Real-Terrain Activity Recognition Datasets.

Dataset	Subjects	Sensors	Activities	Terrains	Activity-Terrain Combinations	Locations
Luo *et al.* [35]	30	6x IMUs	5	9	9	9 outdoor, 0 indoor
Losing and Hasenjäger [359]	20	17x IMUs & barometer nodes, 2x insoles with 8x FSRs each, 1x eye tracker	9	5	12	12 outdoor, 0 indoor
Proposed Dataset	20	3x IMUs, 2x LiDARs, 2x colour sensors, 2x insoles with 13x FSRs each	11	9	38	19 outdoor, 19 indoor

Table 4.6: A Comparison of This Study to Existing Terrain-Identification Studies with Human Subjects.

Dataset	Subjects	Sensors	Terrains	Locations
Nouredanesh *et al.* [287]	9	1x camera	8	4 outdoor, 3 indoor
Diaz *et al.* [284]	1	1x camera	6	4 outdoor, 2 indoor
Moore *et al.* [286]	2	A diverse range of individual cameras used to capture YouTube videos	7	0 indoor, 7 outdoor, though indoor/outdoor binary classification was implemented.
Zhong *et al.* [288]	7	2x cameras	5	0 indoor, 5 outdoor
Das *et al.* [285]	2	8x IMUs and 3x cameras	4	0 indoor, 4 outdoor
Hashmi *et al.* [289]	40	2x IMUs	6	2 indoor, 4 outdoor
Dixon *et al.* [290]	29	2x accelerometer	3	0 indoor, 3 outdoor
Hu *et al.* [291]	35	1x IMU	2	0 indoor, 2 outdoor
Proposed Dataset	20	3x IMUs, 2x LiDARs, 2x colour sensors, 2x insoles with 13x FSRs each	9	4 outdoor, 5 indoor

4.5 Discussions

HAR datasets are prevalent in the literature, with each proposing novel sensor systems, enabling additional analytical methods, or increasing the generalisation capabilities of models through various means [35, 238–240, 254, 360]. However, HAR datasets are yet to focus on the combination of activities and terrains, with terrain in particular being overlooked in existing datasets. As such, this chapter outlines the design of a novel sensor system, experimental procedure, and dataset which enables future researchers to perform context-aware HAR through the capture of gait data on a range of terrains.

With respect to terrain-classification studies, Table 4.6 compares the protocol of this study to that used to collect datasets for terrain classification. This highlights the number of terrains and diversity of sensing methods as particularly novel aspects of the CAHAR dataset, while the

inclusion of 20 participants ensures that the results of the analysis are sufficiently generalisable. Furthermore, this study considers a range of both indoor and outdoor terrains which is suited to daily living, avoiding terrains like sand, snow, woodland, and woodchip which are present in existing studies [285, 286, 290], but are rarely encountered in daily life for most people and would likely be avoided by those at risk of falling due to their extreme irregularity.

The sensor system used to collect this dataset combines known and unexplored sensor types, the latter of which are shown to be capable of extracting the colour and coarseness of the terrain underfoot, which will aid classification models in determining both terrain with high accuracy. These novel sensor types also prove useful in determining aspects of the gait cycle, with the low frequency LiDAR information reflecting individual strides, as seen in Figure 4.18, along with the colour sensor, which displays the ambient light during the swing phase, as seen in Figure 4.17. Regarding the sensors known to be effective in HAR, three IMUs are positioned on the legs and waist, which are common in existing HAR datasets [35, 238–240, 254, 343], along with force-sensing insoles which are known to be effective in wearable gait analysis devices [351, 352, 361–363]. These sensor types outline a system capable of collecting data relevant to both activity and terrain classification, whilst also being suited to the application of remote gait analysis for monitoring the effect of terrain on gait and fall risk.

Although this dataset offers a large, novel selection of activities and terrains, limitations are still present in this study. Primarily these limitations are sourced from the sensor system, which was susceptible to wear over the lengthy data collection process, resulting in some damage to the system throughout the trials. This issue was mitigated through the two-way communications between the Arduino Mega and the Arduino Nano 33 BLE sensors, ensuring that no data was lost for either of the leg sensor subsystems. However, some waist sensor data was lost in the first 12 trials due to these issues. Another limitation of this dataset is related to the sit to stand activities. These activities are extremely quick to perform, resulting in much fewer data from these trials than others, such as the 30 seconds of walking, which could lead to large class imbalances when performing classification. This was mitigated by asking participants to repeat this trial three times but, in future, activities should be performed for equal times to ensure that classification models have sufficient data to train on.

4.6 Contributions

This chapter outlines the development of a novel sensor system comprised of known and unexplored sensor types with regards to HAR, which is capable of collecting inertial, force, colour, and distance data which relate to both the wearer's gait and the terrain underfoot. This sensor system is used to collect the CAHAR dataset, which features a greatly expanded scope when compared to existing datasets in the literature, containing 38 combinations of 11 activities performed on nine different terrains, with a dedicated test set comprising nine additional combinations of activity and terrain. By containing activities repeated on multiple terrains, this dataset offers unique insights into the effect of terrain on gait, along with enabling terrain classification which was not previously possible with the existing HAR datasets in the literature. As such, this chapter takes a large step towards producing a system capable of collecting gait data which can be labelled with the appropriate context, forming the basis for a prototype system capable of monitoring internal and external factors that contribute towards fall risk.

4.7 Summary

This study proposes a novel HAR dataset comprised of 38 combinations of 11 walking activities performed on nine terrains by 20 healthy subjects, totalling 7.8 hours of continuous activity data. As the first HAR dataset to label activity and terrain separately, this dataset enables new developments in determining the full context surrounding a person's gait data to enable the design of analytical techniques required for implementing remote gait analysis using wearable sensors, and enables researchers to perform terrain classification, along with HAR, on a variety of indoor and outdoor surfaces. Furthermore, when compared with other real-world HAR and terrain-identification datasets in the literature, the CAHAR dataset features a much larger number of activity-terrain combinations which are evenly divided between indoor and outdoor surfaces, as shown in Tables 4.5 and 4.6, offering greater capacity for the generalisation of models trained on this dataset. A novel sensor system is designed to collect this dataset which combines popular, proven HAR, terrain-identification, and gait analysis sensors in the literature, such as IMUs and force-sensing insoles, with previously unexplored colour and LiDAR sensors, that are shown to be capable of determining properties such as colour and coarseness of the terrain underfoot. This novel sensor system produces a high-dimensional dataset suited for analysis with powerful machine learning techniques to attain the high accuracy, precision, and

generalisability needed to enable the detection of real-world fall-risk factors, such as terrain and its effect on the gait parameters.

The following chapters detail the analysis of the CAHAR dataset to demonstrate the feasibility of terrain-classification using wearable sensors, along with investigations into the contributions of individual sensors towards classification accuracy to optimise future iterations of this sensor system and improve the comfort and convenience of the device through removing redundant or low-performing sensors.

Chapter 5

Analysis of the CAHAR Dataset

5.1 Introduction

Whilst Chapter 4 outlines the creation of the necessary dataset to perform both activity and terrain classification, an analysis of this dataset is still required to determine the feasibility of terrain classification, and therefore the identification of external fall risk factors, in real-environments. As such, this chapter explores the proposed Context-Aware Human Activity Recognition (CAHAR) dataset [241] using the classical Machine Learning (ML) models and sliding window parameters from Chapter 3, with the intention of guiding future researchers on the potential for terrain classification. Particularly, this analysis will function as a baseline analysis for this dataset, enabling future researchers to validate and verify novel Deep Learning (DL) models against the performance of a range of classical ML models, with optimised parameters.

Furthermore, as this study focusses on the optimisation of a prototype system for identifying internal and external fall risk factors, an exploration of the contributions of each sensor type towards terrain classification will be conducted, highlighting which sensors can be removed from the system, and which sensors may be of interest in future terrain classification studies.

5.2 Methods

As covered in Chapter 4, the CAHAR dataset [241] features data captured from participants equipped with a novel sensor system performing common walking activities on a variety of

terrains, both indoor and outdoor. 20 participants (ten male, ten female) with a mean weight of: 74.69 ± 15.63kg, height: 173.02 ± 8.71cm, and age: 33.10 ± 11.34 performed 38 unique combinations of 11 activities on nine terrains. Participants performed these activities over the course of 17 months, capturing a wide variety of outdoor light levels, temperatures, and weather conditions.

Participants performed these activities while equipped with a novel sensor system featuring an Inertial Measurement Unit (IMU) on the waist, and each foot, a colour sensor on each foot, a LiDAR on each shank, and a custom force-sensing insole which contain 13 Force Sensing Resistors (FSRs). Fig. 5.1 shows the sensor system when equipped by a participant, while Fig. 5.2 shows the insoles placed within each shoe. Data was captured at 62.5Hz and is synchronised by a central data sink that broadcasts the time to each of the leg and the waist subsystems, which is then embedded into the sample captured at that time.

Figure 5.1: The various sensor system components and their locations when equipped to a participant.
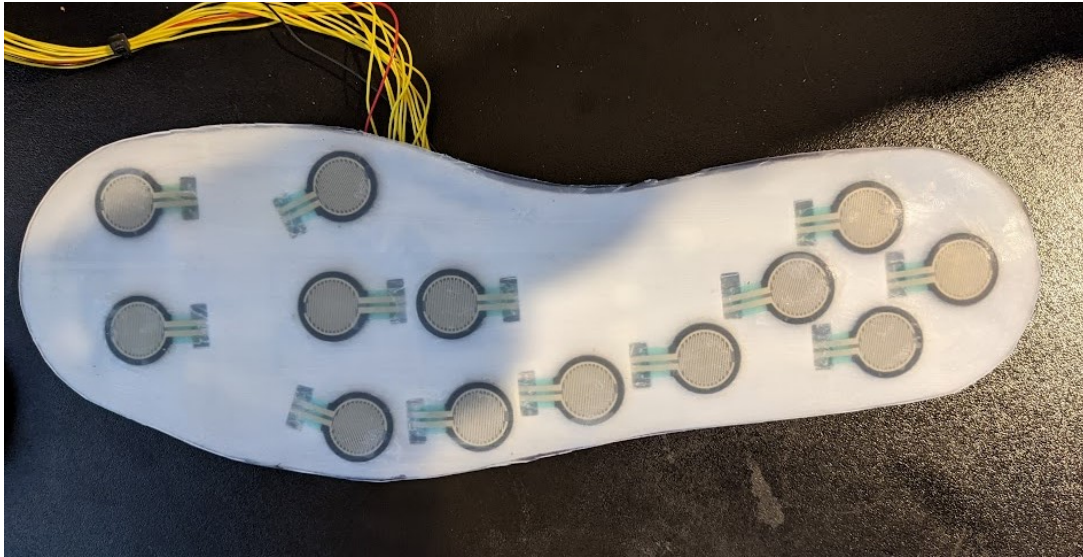
Figure 5.2: The custom insole, showing the position of the 13 FSRs.

5.2.1 Data Preprocessing

Data Cleaning and Filtering

The data from the CAHAR dataset is initially cleaned by removing any irrelevant files and labelling each sample with the activity, terrain, and activity-terrain combination, which can later be used as classes for supervised machine learning. A fourth-order, low-pass, zero-phase Butterworth filter with a cut-off frequency of 20Hz is then applied to the data from the IMUs, LiDAR, and force-sensing insoles, to remove any high-frequency noise which may have been introduced through loose clothing or momentum causing excessive oscillations during motion. This value of cut-off frequency was chosen in line with recommendations from previous studies in this area [325, 364]. An investigation into the raw LiDAR data demonstrated a relationship between the high-frequency information and the coarseness of the terrain underfoot, as shown in Fig. 5.3. As such, a second set of LiDAR data, which is high-passed using a fourth-order Butterworth filter with a cut-off frequency of 30Hz, is added to the raw data. Finally, due to the inconsistent data from the waist IMU, only data from the legs was considered in this study.

Sliding Window Feature Engineering

Sliding windows are a common approach to generating samples for machine learning from time-series data [344, 365]. Furthermore, as discussed in Chapter 3, window sizes of around two to five seconds are preferential when performing Human Activity Recognition (HAR) on a subset of activities, all of which are included in this dataset. However, windows of 1.2 seconds with a 75%
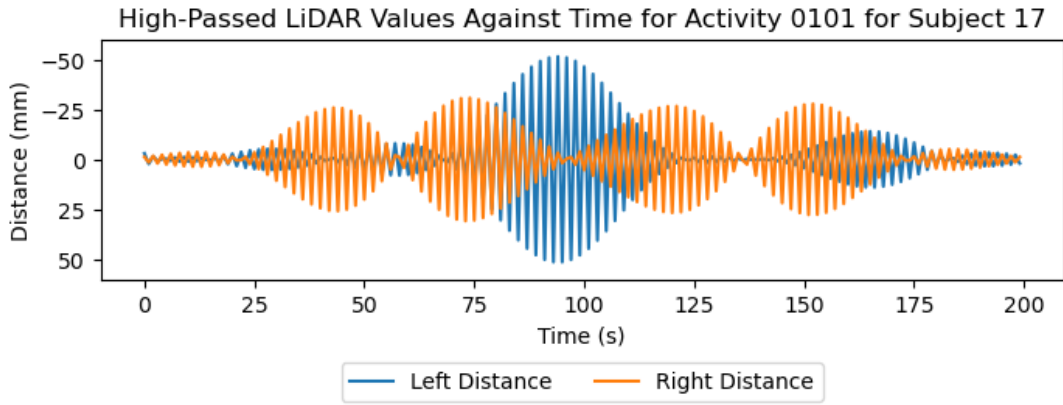
(a) Grass
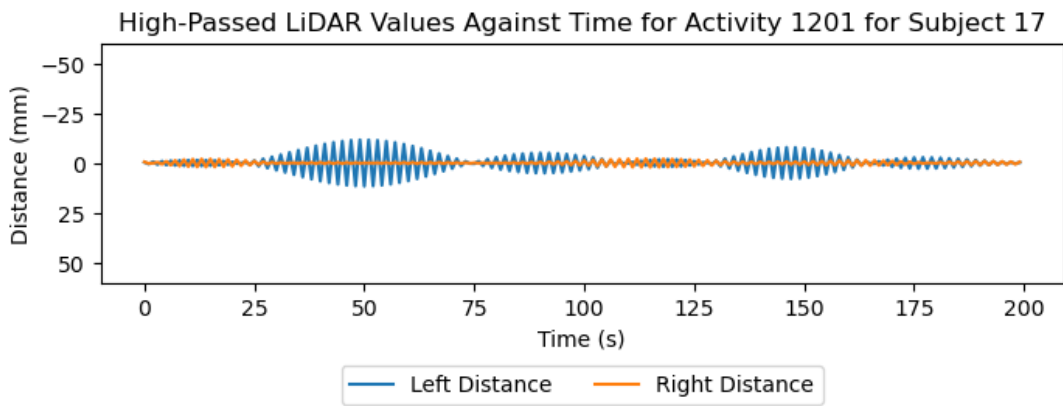
(b) Laminated Flooring

Figure 5.3: High-frequency LiDAR readings high-pass filtered at a cut-off frequency of 30Hz for the walking activity on grass and laminated flooring for participant 17.

overlap were experimentally determined to return the highest accuracies with the full dataset. For the individual sensor analysis, three-second windows were used with an 80% overlap, which were experimentally determined to give the highest accuracies in this context.

Twenty-two features are extracted from each data channel, resulting in a total of 1276 features. These features are: maximum, minimum, mean, median, standard deviation, mean absolute deviation, median absolute deviation, number of zero crossings, root-mean-square, maximum gradient, kurtosis, skewness, variance, interquartile range, entropy, energy, maximum frequency amplitude, mean frequency amplitude, maximum power spectral density, mean power spectral density, frequency kurtosis, and frequency skewness. Some features failed to generate from the raw data due to low variance or noise caused by broken wires for the FSRs, resulting in 1260 total features.

Undersampling

Due to large class imbalances, undersampling is employed to reduce the computational burden of training a model on such a large dataset. The implementation of this undersampling involves selecting a random number of samples from each class equal to the number of samples in the smallest class — sit to stand on carpet, multiplied by three. This allows the training set to contain a reasonable number of data points for generalisation where they are available, without wasting computation time or risking overfitting on the extremely large walking classes.

Feature Selection

Due to the large number of features, feature selection was employed to reduce the number of features whilst maintaining the variance needed to enable high-accuracy classification. To achieve this, Principal Component Analysis (PCA) is performed to reduce the dimensionality of the data by determining and selecting the most relevant principal components. This value was determined through selecting the minimum number of principal components needed to retain 95% of the variance in the original feature set.

Train-test Splits

Two major approaches can be employed when generating a set of data with which to test models for this type of study, depending on the desired application. A standard, randomised, Train-Test Split (TTS) removes a selected percentage of the data for use as a test set at random. This test set contains some bias due to the models being trained on data from all participants, improving the classification performance in the context of this study, at the cost of poor generalisation. On the contrary, Leave One Subject Out (LOSO) leaves out the entire dataset from a single subject as the test set, improving generalisation at the cost of lower classification accuracies due to the lack of overfitting. TTS—trained models, when deployed, are usable if the participant undergoes a training period, whilst a LOSO-trained model enables high accuracies 'off the shelf'. Both of these methods will be explored.

5.2.2 Model Classification

A variety of classical machine learning and deep learning models are prevalent in the literature for HAR. In this study, K-Nearest Neighbours (KNN), Support Vector Machines (SVMs), Random Forests (RFs), and Artificial Neural Networks (ANNs) will be explored to evaluate how

each model performs at both activity and terrain classification. Furthermore, due to the effect of various model parameters on classification accuracy, Bayesian hyperparameter optimization is performed for 25 iterations per model. Models are implemented and trained using the Scikit-learn library for Python. For each model, two methods of activity and terrain classification will be explored.

Single-model classification uses the combined activity-terrain labels as the classes, limiting the classifier to select from just 38 possible activity-terrain combinations. This model is expected to be more accurate at the cost of needing a dataset which captures all possible activities and terrains that a person could encounter in their daily lives.

Multimodel classification involves training two separate models for activity and terrain classification for each model type. When testing the combined performance of these models, the prediction of each model will be combined and compared to the original activity-terrain combination labels for samples in the test set. This approach has the benefit of generalising more suitably to a real-world environment, due to the capacity to classify a sample as any of the 99 possible combinations of activity and terrain, despite the original dataset containing data from only 38 activity-terrain combinations. Furthermore, this multimodel approach can be tested with the bonus activities included in the dataset for participants 1 and 3, which feature unseen activity-terrain combinations, to determine how well the model has generalised.

5.3   Results

5.3.1   Single-Model Classification

Train-test Split

When training a single model using a randomised TTS, all model types achieve a weighted average accuracy, precision, recall, and F1-score of 94% as seen in Table 5.1. Furthermore, the classification reports for each model show identical performances on each class, indicating that a fixed 6% of samples from the dataset are unable to be classified correctly. Misclassified samples were distributed among most classes, except for sitting and standing, which were typically classified with 100% accuracy.

Leave One Subject Out

As with the TTS analysis, the LOSO approach yielded identical results for all models, as seen in Table 5.2, indicating that, again, a fixed subset of samples is unable to be classified. The classification metrics of each model show an accuracy of 50%, precision of 52%, recall of 50%, and F1-score of 46%. Contrary to the TTS results, misclassified samples typically belonged to the sitting and standing classes, most of which exhibited 0% accuracy, with all samples being classified as the correct activity on the incorrect terrains.

Table 5.1: Single-Model performance using TTS.

Model	Accuracy	Precision	Recall	F1-Score
KNN	0.94	0.94	0.94	0.94
SVM	0.94	0.94	0.94	0.94
RF	0.94	0.94	0.94	0.94
ANN	0.94	0.94	0.94	0.94

Table 5.2: Single-Model performance using LOSO.

Model	Accuracy	Precision	Recall	F1-Score
KNN	0.50	0.52	0.50	0.46
SVM	0.50	0.52	0.50	0.46
RF	0.50	0.52	0.50	0.46
ANN	0.50	0.52	0.50	0.46

Table 5.3: Multimodel performance using TTS.

Model	Accuracy	Precision	Recall	F1-Score
KNN	0.82	0.82	0.82	0.82
SVM	**0.85**	**0.86**	**0.85**	**0.85**
RF	0.82	0.83	0.82	0.82
ANN	0.84	0.84	0.84	0.84

Table 5.4: Multimodel performance using LOSO.

Model	Accuracy	Precision	Recall	F1-Score
KNN	0.31	0.34	0.31	0.28
SVM	0.42	0.47	0.42	0.37
RF	0.21	0.28	0.21	0.17
ANN	**0.43**	**0.47**	**0.43**	**0.42**

5.3.2   Multimodel Classification

Train-test Split

When using multimodel classification with a TTS, performance metrics are much lower across all models, with SVM exhibiting the highest performance metrics with an accuracy of 85%, precision of 86%, recall of 85%, and F1-score of 85%, followed by ANN with scores of 84% across all performance metrics, as seen in Table 5.3. Investigations into the highest-performing SVM models show that sit to stand and stand to sit were the most misclassified activities, whilst gravel was the most misclassified terrain, as seen in Fig. 5.4. Despite these misclassifications, the SVM achieved weighted average performance metrics of 97.94% for activity classification, and 99.57% for terrain classification.

However, as expected due to the low generalisation of TTS-trained models, the performance metrics of the TTS multimodel SVM on the dedicated test set of unseen activity and terrain combinations were extremely poor, with a weighted average precision of 2%, recall of 1%, and F1-score of 1%.

Leave One Subject Out

As with the TTS implementation, performance metrics using LOSO are lower when using a multimodel approach compared to a single-model approach. However, LOSO classification results are much more similar between the single-model and multimodel implementations, with ANNs exhibiting the highest accuracy of 43%, precision of 47%, recall of 43%, and F1-score of 42%. The performance of the individual models for activity and terrain classification can be seen in Fig. 5.5, which highlight the lift, sit to stand, and stand to sit activities, and gravel, hospital stairs, and paving slab terrains as those which are most frequently misclassified.

Regarding the dedicated test set, the LOSO multimodel implementation outperformed the TTS implementation with an accuracy of 7%, precision of 29%, recall of 7%, and F1-score of 10% due to the increased generalisation capabilities of a model trained in this way. However, these metrics are still extremely low, indicating that more powerful classification techniques are required to enable this level of generalisation.

(a) Activity
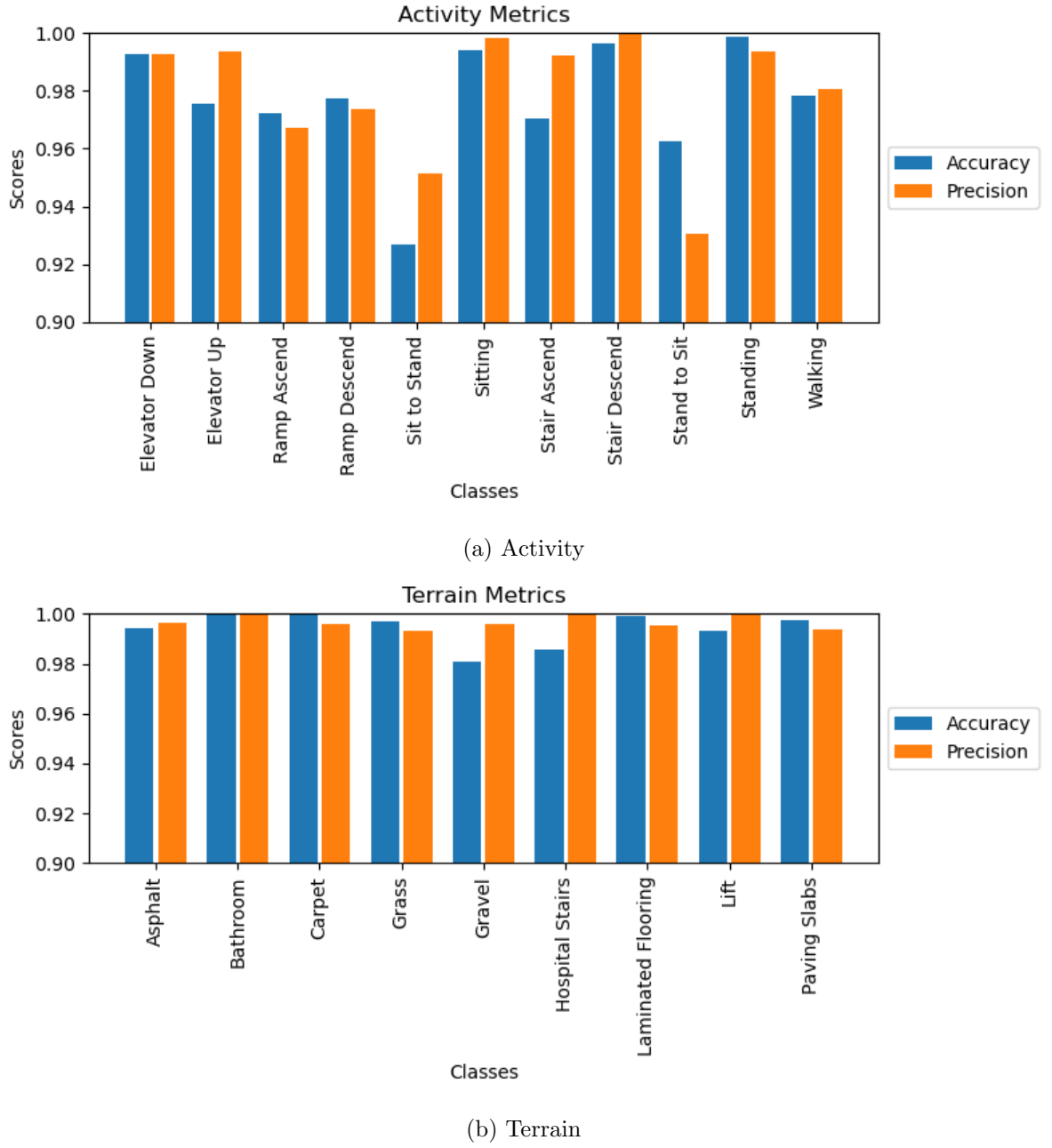
(b) Terrain

Figure 5.4: Accuracy and precision of each individual class for activity and terrain classification using multimodel SVMs and a TTS.

5.3.3 Individual Sensor Analysis

Following the analysis of the full dataset, an individual sensor analysis was conducted to evaluate how the weight, size, and computational complexity of the system can be reduced whilst maintaining the capacity for high-accuracy terrain and activity classification. Furthermore, this analysis will determine the success of the colour and LiDAR sensors introduced in the CAHAR dataset.
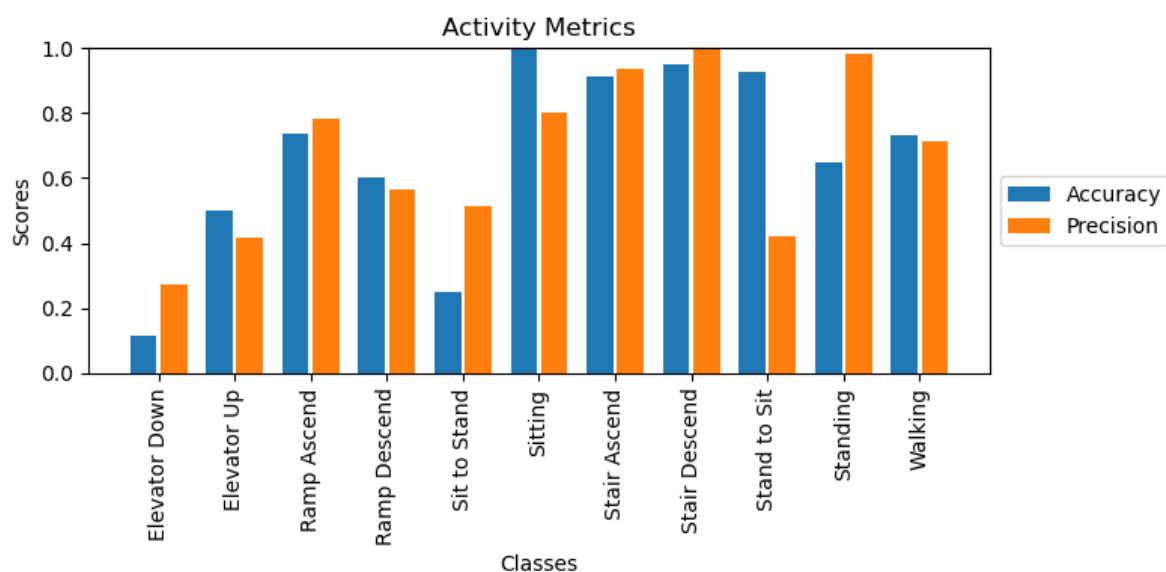
(a) Activity
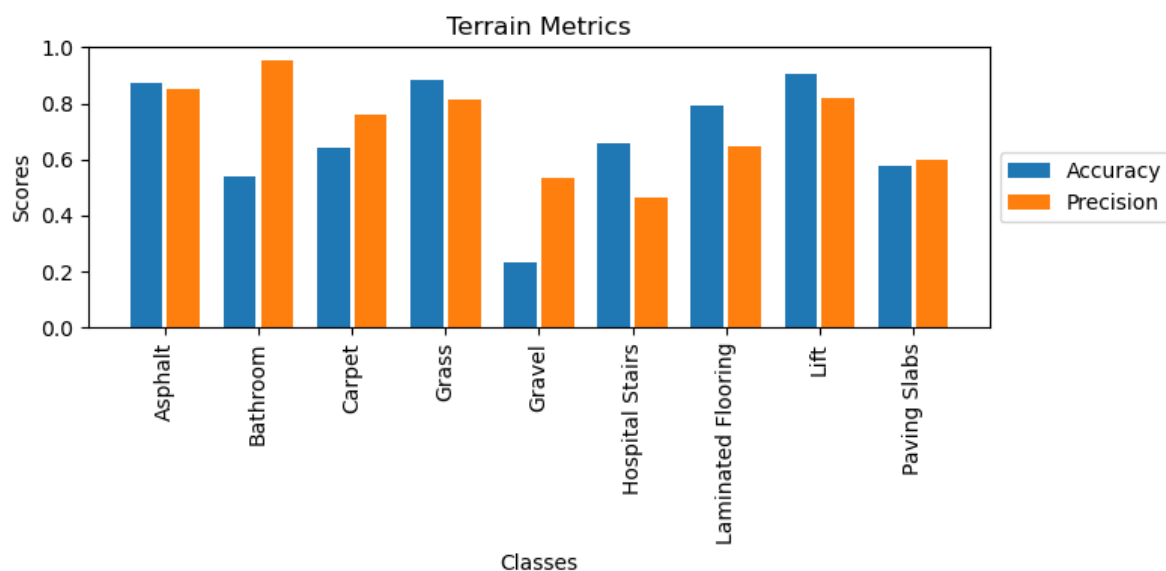
(b) Terrain

Figure 5.5: Accuracy and precision of each individual class for activity and terrain classification using multimodel ANNs and LOSO.

Figures 5.6 and 5.7, along with Table 5.5, show the performance metrics for a SVM trained on each individual sensor type. Both activity and terrain classification were highest when using data from the IMUs, with terrain classification accuracy at 89%, activity classification at 91%, and both activity and terrain classification at 86% using TTS cross validation and data from the right, left, and left IMU respectively. For LOSO cross validation, classification accuracy was lower at 63% for terrain classification, 71% for activity classification, and 49% for activity and terrain classification using data from the right, left, and right IMUs respectively.
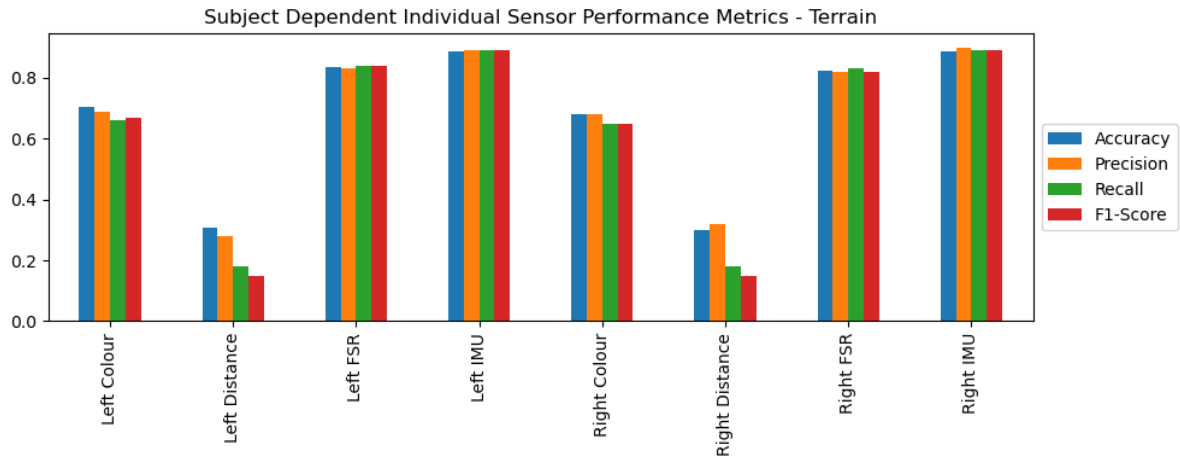
(a) Terrain
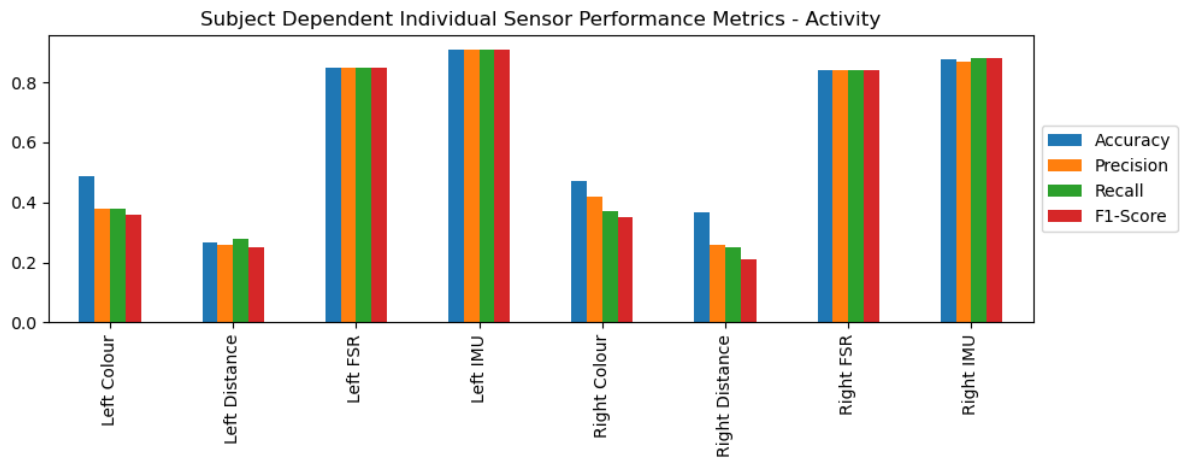
(b) Activity
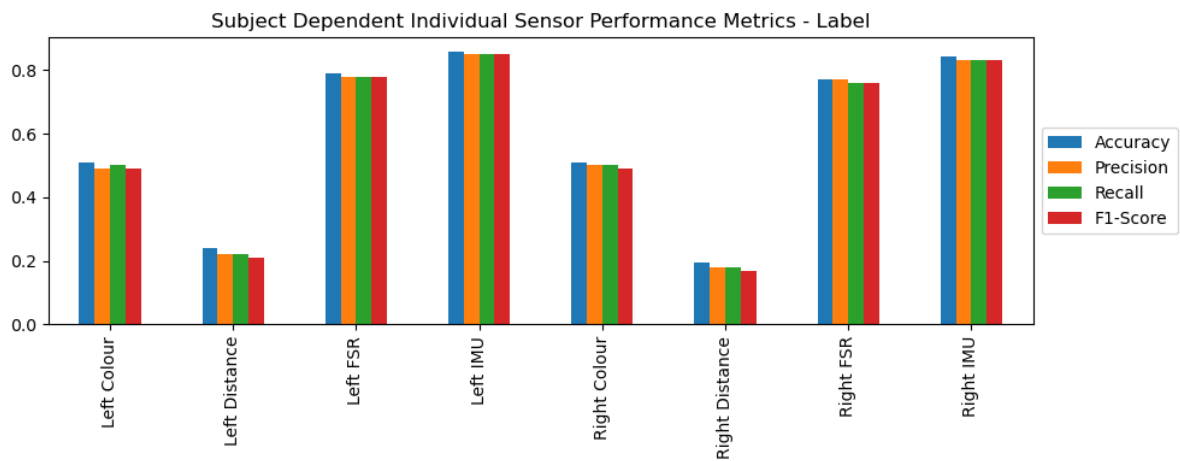
(c) Terrain and Label

Figure 5.6: Individual sensor classification metrics using TTS cross validation.

Data from the FSR insoles appear as the second-highest performing sensor when using TTS, but exhibit extremely low accuracies when performing subject-independent training using LOSO. As expected, the colour sensor performs poorly for activity classification, but contributes heavily

towards terrain classification, achieving 71% and 66% accuracy when using TTS and LOSO respectively. Furthermore, the colour sensor matches the IMU as the highest performing sensor for terrain classification when using LOSO.
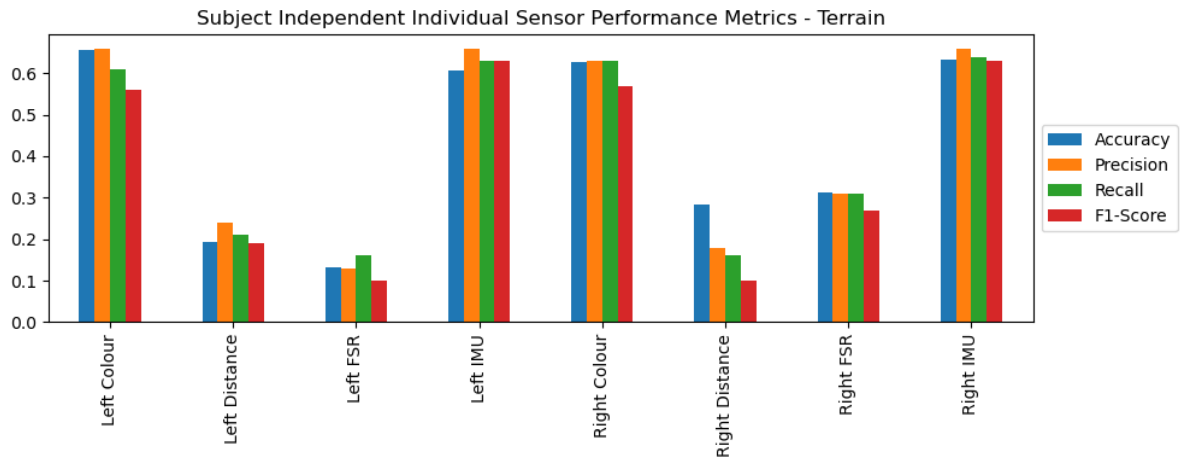
(a) Terrain
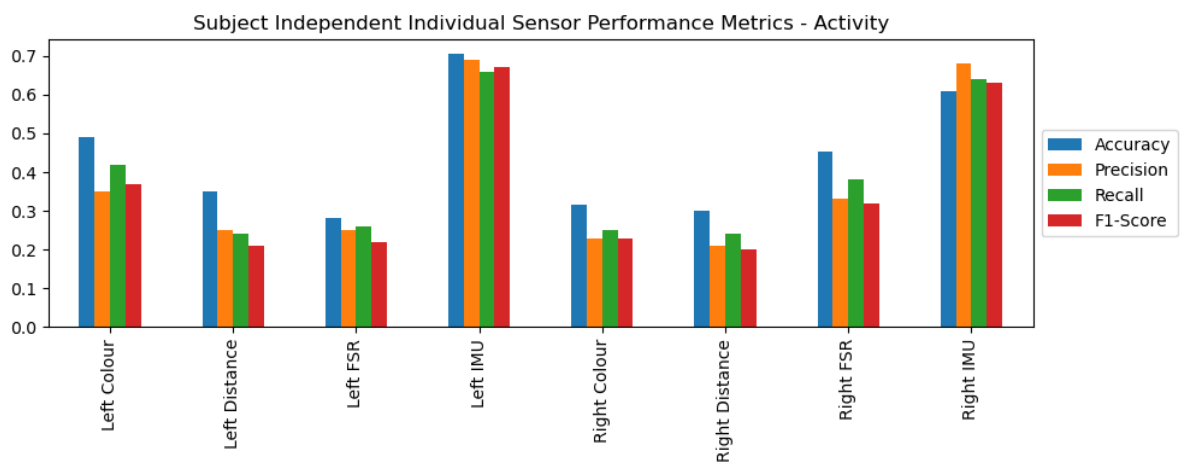
(b) Activity
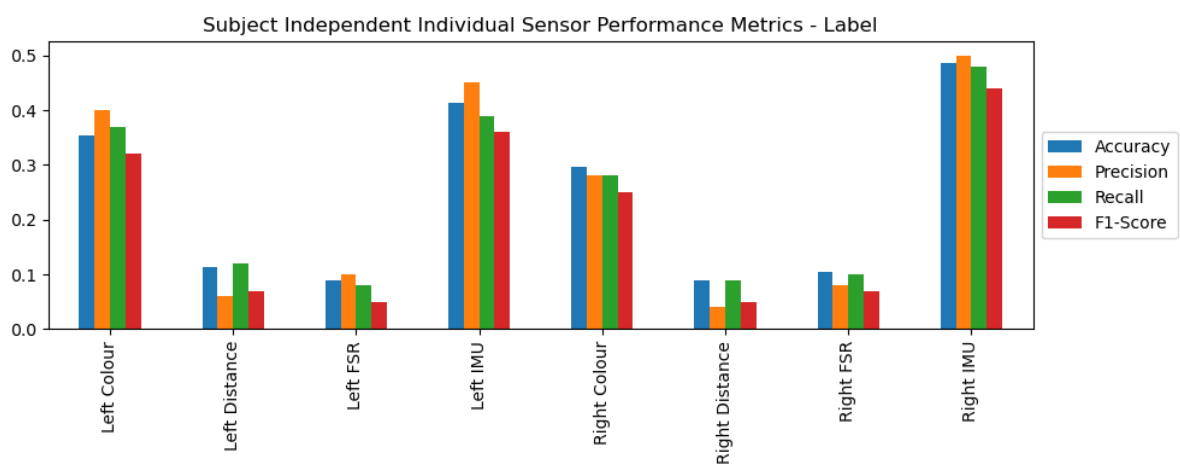
(c) Terrain and Label

Figure 5.7: Individual sensor classification metrics using LOSO cross validation.

	Sensor	Accuracy	Precision	Recall	F1-Score
Terrain - TTS	Left Colour	0.71	0.69	0.66	0.67
	Left Distance	0.31	0.28	0.18	0.15
	Left FSR	0.84	0.83	0.84	0.84
	Left IMU	0.89	0.89	0.89	0.89
	Right Colour	0.68	0.68	0.65	0.65
	Right Distance	0.30	0.32	0.18	0.15
	Right FSR	0.82	0.82	0.83	0.82
	Right IMU	**0.89**	**0.90**	**0.89**	**0.89**
	Sensor	Accuracy	Precision	Recall	F1-Score
Activity - TTS	Left Colour	0.49	0.38	0.38	0.36
	Left Distance	0.27	0.26	0.28	0.25
	Left FSR	0.85	0.85	0.85	0.85
	Left IMU	**0.91**	**0.91**	**0.91**	**0.91**
	Right Colour	0.47	0.42	0.37	0.35
	Right Distance	0.37	0.26	0.25	0.21
	Right FSR	0.84	0.84	0.84	0.84
	Right IMU	0.88	0.87	0.88	0.88
	Sensor	Accuracy	Precision	Recall	F1-Score
Activity and Terrain - TTS	Left Colour	0.51	0.49	0.50	0.49
	Left Distance	0.24	0.22	0.22	0.21
	Left FSR	0.79	0.78	0.78	0.78
	Left IMU	**0.86**	**0.85**	**0.85**	**0.85**
	Right Colour	0.51	0.50	0.50	0.49
	Right Distance	0.19	0.18	0.18	0.17
	Right FSR	0.77	0.77	0.76	0.76
	Right IMU	0.84	0.83	0.83	0.83
	Sensor	Accuracy	Precision	Recall	F1-Score
Terrain - LOSO	**Left Colour**	**0.66**	**0.66**	0.61	0.56
	Left Distance	0.19	0.24	0.21	0.19
	Left FSR	0.13	0.13	0.16	0.10
	Left IMU	0.61	0.66	0.63	0.63
	Right Colour	0.63	0.63	0.63	0.57
	Right Distance	0.28	0.18	0.16	0.10
	Right FSR	0.31	0.31	0.31	0.27
	Right IMU	0.63	**0.66**	**0.64**	**0.63**
	Sensor	Accuracy	Precision	Recall	F1-Score
Activity - LOSO	Left Colour	0.49	0.35	0.42	0.37
	Left Distance	0.35	0.25	0.24	0.21
	Left FSR	0.28	0.25	0.26	0.22
	Left IMU	**0.71**	**0.69**	**0.66**	**0.67**
	Right Colour	0.32	0.23	0.25	0.23
	Right Distance	0.30	0.21	0.24	0.20
	Right FSR	0.45	0.33	0.38	0.32
	Right IMU	0.61	0.68	0.64	0.63
	Sensor	Accuracy	Precision	Recall	F1-Score
Activity and Terrain - LOSO	Left Colour	0.35	0.40	0.37	0.32
	Left Distance	0.11	0.06	0.12	0.07
	Left FSR	0.09	0.10	0.08	0.05
	Left IMU	0.41	0.45	0.39	0.36
	Right Colour	0.30	0.28	0.28	0.25
	Right Distance	0.09	0.04	0.09	0.05
	Right FSR	0.10	0.08	0.10	0.07
	Right IMU	**0.49**	**0.50**	**0.48**	**0.44**

Table 5.5: Model Performance Metrics by Sensor Location.

Figure 5.8 shows the contributions of the colour sensor and IMU towards classifying each terrain using LOSO cross validation. The colour sensor is shown to be largely incapable of classifying the lift and gravel terrains, likely due to the similar colour of these surfaces, but exhibits much higher performance metrics on the other terrains. The IMU, however, determines the lift class with high accuracy, highlighting the role each sensor plays in the towards accurate terrain classification in the analysis of data collected from the full sensor system.
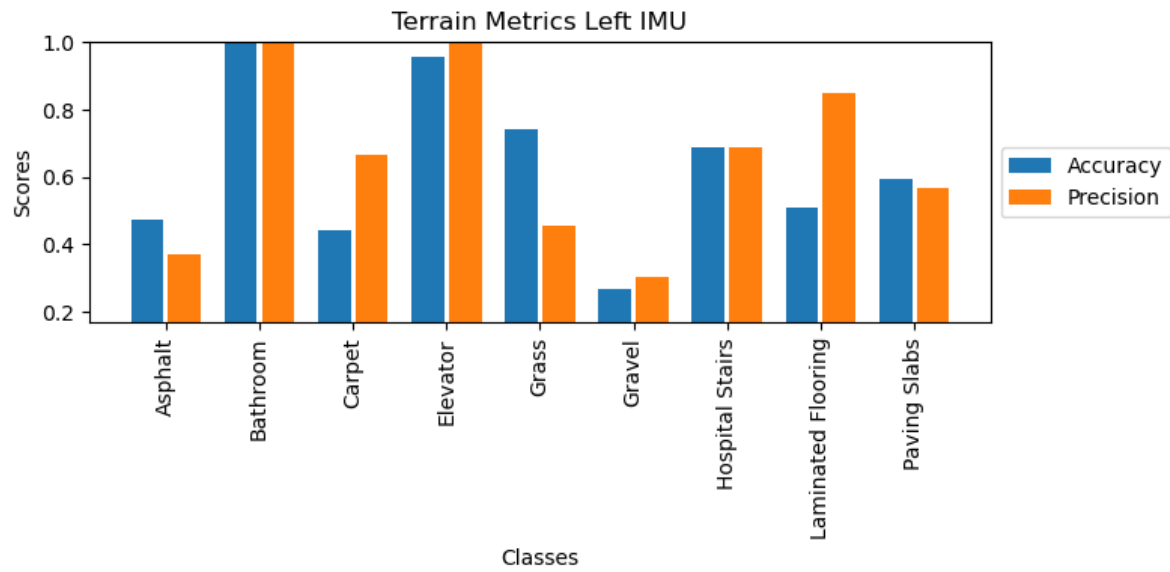
(a) Left IMU
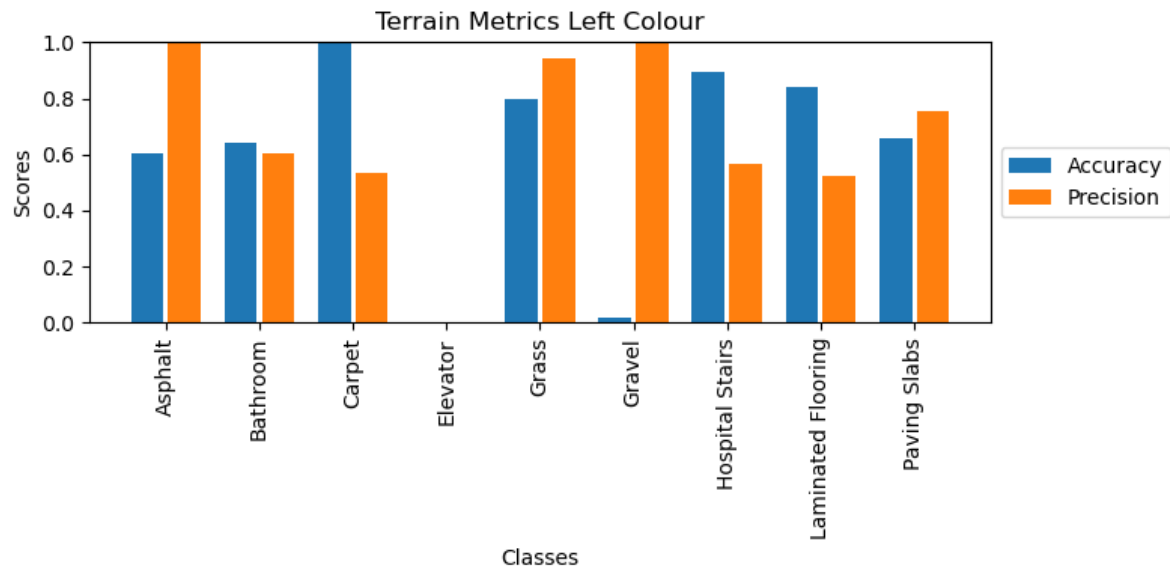
(b) Left Colour Sensor

Figure 5.8: Classification accuracy and precision per terrain using LOSO cross validation.

5.3.4 Optimised System Metrics

Following the high performance metrics of individual IMUs and colour sensors for terrain classification, another set of SVMs were trained on the combined data from these sensors for each leg. Using TTS, this combination yielded 98%, 93%, and 94% accuracy for activity, terrain, and combined activity and terrain classification respectively on the left leg, which were higher than the metrics of the right leg. When considering both legs, these metrics rise to 99%, 96%, and 96% for terrain, activity, and combined activity and terrain, respectively. These parameters are significantly reduced when using LOSO, even with data from both legs, at 86%, 74%, and 69% for activity, terrain, and combined activity and terrain, respectively. Notably, these performance metrics are higher than when the full dataset is used, indicating that the lower-performing sensors, such as the LiDAR, may contain noisy features which impede the classification accuracy of the full feature set. Tables 5.6, 5.7, and 5.8 show the performance metrics for the terrain, activity, and combined terrain and activity, respectively, for the IMU and colour sensor combination on different legs.

Table 5.6: Terrain classification performance using combined IMU and colour sensor.

Settings	Accuracy	Precision	Recall	F1-Score
Left leg — TTS	0.98	0.98	0.98	0.98
Right leg — TTS	0.97	0.97	0.98	0.97
Both legs — TTS	**0.99**	**0.99**	**0.99**	**0.99**
Left leg — LOSO	0.84	0.86	0.84	0.82
Right leg — LOSO	0.78	0.82	0.81	0.79
Both legs — LOSO	0.86	0.89	0.84	0.83

Table 5.7: Activity classification performance using combined IMU and colour sensor.

Settings	Accuracy	Precision	Recall	F1-Score
Left leg — TTS	0.93	0.93	0.93	0.93
Right leg — TTS	0.92	0.91	0.92	0.92
Both legs — TTS	**0.96**	**0.96**	**0.96**	**0.96**
Left leg — LOSO	0.69	0.69	0.66	0.64
Right leg — LOSO	0.66	0.65	0.65	0.63
Both legs — LOSO	0.74	0.74	0.73	0.71

Table 5.8: Combined activity and terrain classification performance using combined IMU and colour sensor.

Settings	Accuracy	Precision	Recall	F1-Score
Left leg — TTS	0.94	0.93	0.93	0.93
Right leg — TTS	0.93	0.91	0.92	0.91
Both legs — TTS	**0.96**	**0.96**	**0.96**	**0.96**
Left leg — LOSO	0.63	0.56	0.59	0.53
Right leg — LOSO	0.63	0.54	0.58	0.53
Both legs — LOSO	0.69	0.63	0.65	0.60

5.4   Discussions

This study performs the first investigation into terrain classification using the CAHAR dataset consisting of data from IMUs, FSR insoles, colour sensors, and LiDAR sensors. Multiple approaches present in the literature are applied to this dataset to produce classification metrics that indicate the potential for context- and terrain-aware HAR, and the detection of external fall-risk factors.

Regarding subject-dependent models, this study finds that high classification accuracies are possible when potential users of the device undergo a training period on a complete set of terrains and activities which represent those they expect to encounter in daily life. Single-model classification resulted in a consistent 94% for each performance metric, though the removal of the noisy LiDAR and FSR sensor data improves this accuracy to 96%. Reasonable performance metrics were also present in the multimodel approaches, which demonstrated performance metrics around 85% for the SVM. However, despite these performance metrics on existing activity-terrain combinations when using a multimodel approach, interpolation of predictions to identify unseen activity-terrain combinations on TTS-trained models was found to be infeasible.

For implementation in real-world settings such as healthcare applications, subject-independent models are desirable to prevent lengthy training periods which may be susceptible to human error or require specialist training to perform. However, this approach exhibits drastically reduced classification accuracies, as observed in this study. Despite this, the constituent models in the multimodel implementation exhibited reasonable performance on terrain and activity classification independently, indicating that alternative approaches to fusing the predictions of individual models may be an effective approach to improve overall performance of multi-model implementations. As expected, the subject-independent implementation outperformed

the subject-dependent implementation with regard to the dedicated test set of unseen activity-terrain combinations. However, whilst promising for the future direction of this research area and implementations using more powerful deep learning techniques, these performance metrics are still far too low at this stage for consideration in a real-world setting.

The individual sensor analysis exhibited reduced accuracies when compared to the full sensor array, although the IMU alone was able to achieve high performance metrics, which were comparable to the full system in the case of the single-model combined activity and terrain classification. The FSR insoles proved to be useful in the case of subject-dependent model training, which has positive implications given how convenient these sensors can be, but lacked accuracy in the subject-independent case. This may have been caused by the issues reported in Chapter 4, where the insoles broke for some participants, which would affect subject-independent training disproportionately. Of the novel colour and LiDAR sensors, the colour sensors exceeded expectations by exhibiting similar performances to the IMU sensors with respect to terrain classification. Furthermore, given the difference in which terrains were accurately classified from the data of each sensor, it can be seen that the colour sensor and IMU sensors complement one another, enabling a much higher classification accuracy when combined. On the contrary, the LiDAR sensor, despite the raw data exhibiting a visual separability of terrains, does not appear to contribute towards the classification accuracy of the system and should either be processed more heavily to extract useful terrain information or discarded in future systems. Furthermore, the combination of IMU and colour sensor outperforms the full dataset at 96% accuracy, indicating the prevalence of noisy features produced by other sensors. Additionally, a classification accuracy of 96% is high in the context of the literature for HAR, which ranges from 78%-100% accuracy [28–34], despite the increased number of 38 classes in this dataset due to the combinations of activity and terrain.

The appearance of the IMU as the most useful sensor for terrain classification could reflect one of two possibilities: that the dataset has overfit to specific activities, as the activities and terrains are fundamentally linked in the collected data, or that subtle changes in motion planning due to the different terrain types were captured by the IMUs, which can then be used to determine the terrain. For some terrains, such as the elevator, the IMUs are able to detect that the user is not performing an activity, yet is accelerating upwards, which is a property unique to the elevator activity and terrain. Equally, the bathroom activities contained only sit to stand and

stand to sit, again enabling the IMU to primarily use the activity to determine the terrain. The high accuracies with which these activity-specific terrains are classified can be seen in Figure 5.8a. Of the terrains with multiple activities, classification accuracy is still higher than random chance, indicating that some degree of motion planning is being captured in the IMU data. To some extent, this potential overfitting issue is acceptable given that activity and terrain are expected to be dependent on one another in real-world settings. For example, walking in a lift or bathroom are unlikely to occupy large amounts of a person's daily activities, and some activities such as stair ascent will likely never occur in these locations, highlighting how terrain and activity are co-dependent in these settings. For this reason, despite potential bias added by these activities, the results of terrain classification using IMUs are still reliable and relevant for the application of classifying gait activity context in a person's daily life.

Overall, the results of this analysis indicate that a system comprising shoes instrumented with an IMU and colour sensor would be suitable to determine the fall-risk introduced by the terrain that a person is walking on in real-world scenarios, given a short training period and a single-model solution. Gait data from the other sensors, particularly the FSR insole, may prove useful for gait analysis, but have not been shown to be suited to terrain or activity classification in this study. Future work is needed to improve these accuracies such that context-labelling can be performed 'off the shelf', and to enable multimodel approaches capable of interpolating classifications such that unseen activity-terrain combinations can be accurately identified. Furthermore, the waist sensor was excluded from this study due to an incomplete feature set but, with appropriate analytical methods, this sensor should be analysed to determine the feasibility of terrain classification using smartphones and other waist-mounted IMU systems, due to the convenience of using these sensors as opposed to instrumented shoes.

In the context of this thesis and incremental fall risk factors, these results identify the most effective sensors capable of identifying fall risk factors introduced by the environment in which a person is walking, such as slip and trip hazards and increased gait variability caused by uneven terrains. The system designed to collect the CAHAR dataset was developed with the intention of containing many sensing modalities to explore the relevance of these sensors in terrain identification. This study identifies the IMU and colour sensor as being capable of identifying the terrain underfoot, and future work in which the CAHAR sensor system is refined should reduce the system to just an IMU and colour sensor on each foot. This future version

will have a reduced profile, making it more convenient and comfortable to wear, while offering high-accuracy HAR and terrain-classification in real-time, thereby enabling the monitoring of contextual fall-risk factors that a person encounters in their daily life.

5.5 Contributions

This chapter offers the first analysis of the CAHAR dataset, and therefore the first investigation into the feasibility of terrain classification across multiple activities using wearable sensors and machine learning. IMUs placed on the foot are found to be capable of terrain classification alone, indicating that future HAR datasets should label data with the terrain it was captured from, as existing sensor systems may be capable of terrain classification due to the popularity of IMUs in the literature. Furthermore, this chapter clearly demonstrates the feasibility of terrain classification using wearable sensors, answering the primary research question in this thesis, and prompting future researchers to integrate terrain recognition into automatic gait analysis systems to add context to the collected data.

5.6 Summary

This study addresses the research aim of determining the feasibility of terrain classification using wearable sensors by offering the first analysis of the CAHAR dataset — the first activity and terrain-labelled HAR dataset. Commonly-used preprocessing steps, such as the sliding window feature engineering technique, along with popular methods in the field of HAR, such as SVMs and ANNs, are investigated to determine the feasibility of terrain classification using wearable sensors. An accuracy of 99% is obtained for terrain classification, while 96% is obtained for combined activity and terrain classification when using an optimised feature set and subject-dependent training. These accuracies are high-performing in the context of reported accuracies in the literature for HAR, despite the large number of classes in the CAHAR dataset. The contributions of individual sensors are analysed, and it is found that IMUs are capable of collecting sufficient data for acceptable terrain classification, but are augmented by the inclusion of a colour sensor. In either case, this study demonstrates that terrain and activity classification is feasible using wearable sensors, therein highlighting the capability of this system to monitor the external factors which contribute towards fall risk in real-world settings. Future studies should aim to produce more powerful models and optimised sensor systems towards the final

goal of accurate context-aware HAR and terrain classification for monitoring the internal and external fall-risk factors encountered in daily life for the purposes of fall prediction.

Chapter 6

The Effect of Terrain on Gait

6.1 Introduction

As discussed in Chapter 2, many internal and external factors affect the gait parameters such as health conditions and the terrain underfoot. Particularly, a range of studies highlight that coarser terrains cause those walking on them to exhibit reduced cadence, step length, stride length, double support time, Centre of Mass (CoM) height, and overall gait speed, whiles step width and foot clearance increased [38, 39, 108–112]. Additionally, metabolic rate is shown to correlate with terrain coarseness [38], highlighting the burden that coarse terrains have on those navigating them. In Chapter 4, a novel sensor system is developed with the goal of monitoring these gait-affecting factors, and therefore assessing the wearer's incremental fall risk factors. To this end, Chapter 5 demonstrates the capability of this system to accurately identify both walking activity and the terrain underfoot from nine different commonly-encountered indoor and outdoor surfaces such as grass, asphalt, and laminated flooring.

Each person's gait kinematics are unique to that person [366, 367], meaning that this system cannot simply compare a person's gait parameters to a database of walking on various terrains to establish if they are at risk of falling. Rather, the system should be capable of extracting a person's gait parameters on each terrain to compare gait-related responses within the context of that person. These changes can then be analysed by clinicians, or by a future version of this system, to assess the incremental fall risk factor associated with the terrain underfoot. However, there may also be general trends This chapter evaluates the effect of terrain on various gait parameters in the Context-Aware Human Activity Recognition (CAHAR) dataset.

6.2 Methods

6.2.1 Sensor Selection

As mentioned in Chapter 4, the insoles were damaged during some of the subject trials, affecting the reliability of data from these sensors for those subjects. Whilst soft computing methods like machine learning can adapt to these conditions for the Human Activity Recognition (HAR) and terrain-identification aspects of this work, spatio-temporal parameters are typically extracted using threshold- and peak-detection-based algorithms [368, 369], meaning that sensors with missing data cannot be utilised in this study. This eliminates the insole and waist sensor due to damage and missing data in a small number of trials. Furthermore, the LiDAR and colour sensor were chosen to assess the coarseness and colour of the terrain underfoot, limiting their usefulness for extracting the spatio-temporal gait parameters.

This leaves the foot-mounted Inertial Measurement Unit (IMU) on each foot as the most appropriate sensor for estimating the spatio-temporal gait parameters across all participants in the CAHAR dataset. Many previous studies have used foot-mounted IMUs to estimate the gait parameters, demonstrating high levels of agreement between this approach and measurements from motion capture systems [368–373].

6.2.2 Gait Parameter Estimation

Gait Event Detection

To calculate the gait parameters, it is required to identify gait events such as Initial Contact (IC), Mid-Stance (MSt), Terminal Contact (TC), and Mid-Swing (MSw). For this aspect, this work follows the methods of Sabatini *et al.* [374], who used a single IMU on the foot to obtain estimations for the IC and TC during walking. This method involves using peak-detection algorithms on the mediolateral gyroscope axis data from each IMU, where small negative peaks correspond to IC events, while large negative peaks correspond to TC events. The following algorithm is implemented using Python.

For the CAHAR dataset, the gyroscope data from each foot is first filtered using a second- order low-pass filter with a cut-off frequency of 2Hz. While this value for cut-off frequency is much lower than the algorithms used by Sabatini *et al.* [374], it was found that the uneven terrain, particularly gravel which caused movement while the foot was in contact with the ground,
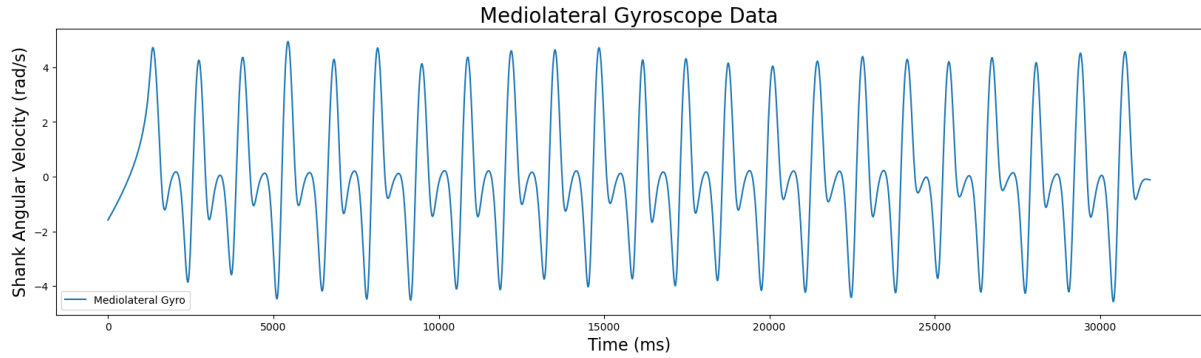
Figure 6.1: Mediolateral gyroscope data from the left foot-mounted IMU filtered with a second-order low-pass filter with a cut-off frequency of 2Hz.
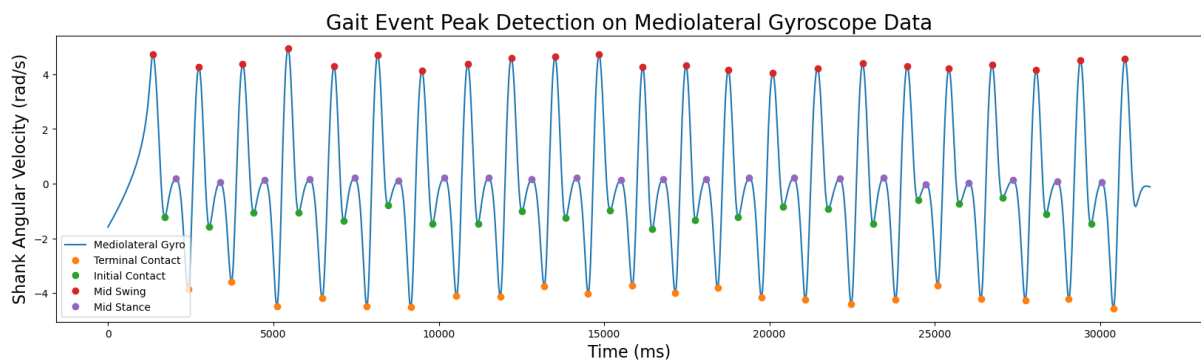
Figure 6.2: Low-pass filtered mediolateral gyroscope data from the left foot-mounted IMU with gait events identified using the peak-detection algorithm.

introduced additional peaks that needed to be filtered out using a much lower cut-off frequency. A cut-off of 2Hz was found to produce the most reliable results. The filtered gyroscope data can be seen in Figure 6.1.

After filtering, the "find_peaks" algorithm from the "Scipy" library for Python is used to obtain the peaks associated with each gait event. First, this algorithm is applied to the positive values with a "prominence" of one, which reliably obtains the peaks relating to MSw. Then, the data from between each of these peaks is extracted, and peak detection is again performed on the positive peaks to obtain MSt. Finally, the data is inverted, and the negative peaks are identified. These peaks are then compared, with the smallest peak being labelled as IC, and the largest peak being labelled as TC. The results of this method can be found in Figure 6.2.

Step Verification

While this algorithm successfully identifies the gait parameters, in some instances, potentially caused by uneven terrains, one or more of these peaks can be difficult to identify, as seen in
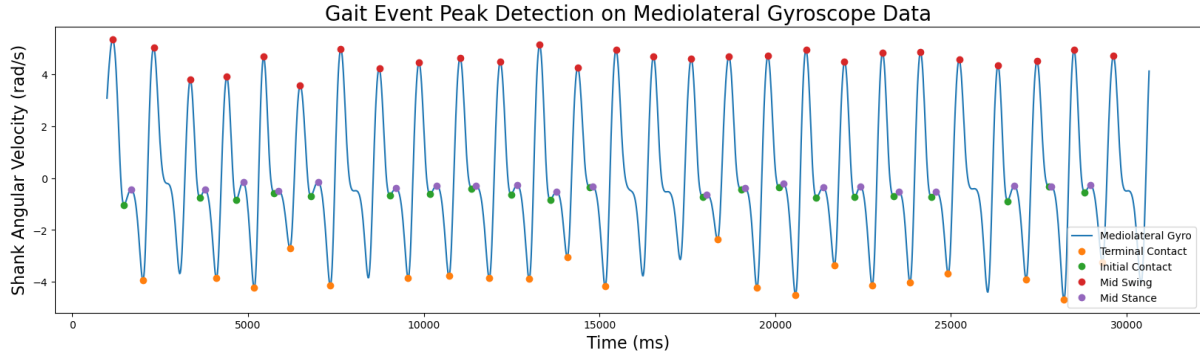
Figure 6.3: The performance of the gait event detection algorithm on subject 7.

Figure 6.3. If the steps are determined to simply be the data between subsequent IC and TC events, and left unvalidated, this will introduce steps that are too long or too short. To prevent this, a simple check is performed to ensure that between each IC event, exactly one MSw, MSt, and TC event occurs. However, this only validates strides from a single leg. When dealing with steps, calculated between legs, pairs of valid strides are identified and stored. At the end of this stage, a list of validated steps and strides have been identified, and the gait parameters can now be calculated.

Gait Parameter Estimation

As discussed in Chapter 2, many fall prediction studies discuss the importance of step and stride length as clinical parameters related to falls. However, these parameters are difficult to calculate accurately using IMUs due to issues such as gyroscope drift, accelerometer noise, and placement on the foot [370, 375, 376]. Furthermore, as the CAHAR dataset was designed for HAR and terrain recognition, no validation data is available to test the accuracy of spatial gait parameters such as step and stride length. As a result, this analysis will focus on applying validated methods, such as those proposed by Sabatini *et al.* [374], to obtain the temporal parameters such as step time, stride time, swing time, and stance time, which were shown to be relevant to fall prediction in Chapter 2, Figure 2.8. Furthermore, while it would be beneficial to show the effect of terrain on the spatial parameters, the scope of this study is to monitor the effect of terrain on gait, which can still be done using temporal parameters. Future studies should look into establishing outdoor motion capture systems to validate the spatial gait parameters on real terrains.

With timestamps for the gait phases established, each of the temporal parameters can be

determined by calculating the time difference between each event. The definition of each of the temporal parameters in this study in terms of IC and TC is as follows:

$$\text{Stride Time} = t(IC^{(n+1)}) - t(IC^{(n)})$$

$$\text{Step Time} = t(IC_R^{(n)}) - t(IC_L^{(n)}) \quad \text{or} \quad t(IC_L^{(n)}) - t(IC_R^{(n)})$$

$$\text{Single Stance Time} = \frac{t(IC^{(n)}) - t(TC^{(n)})}{\text{Stride Time}} \times 100\%$$

$$\text{Single Swing Time} = \frac{t(IC^{(n+1)}) - t(TC^{(n)})}{\text{Stride Time}} \times 100\%$$

6.3 Results

6.3.1 Analysis of the CAHAR Dataset

Each temporal parameter is extracted for all trials of the walking activities performed on each of the 6 terrains that participants walked on: grass, flat laminated indoor flooring, carpet, asphalt, paving slabs, and gravel. Bar charts of the mean stride time, step time, single stance percentage, and single swing percentage can be found in Figure 6.4, and Tables 6.1-6.4.

(a) Mean stride time

(b) Mean step time

(c) Mean single stance percentage

(d) Mean single swing percentage

Figure 6.4: Bar charts showing the mean and standard deviations of each gait parameter for all subjects on each of the terrains in the CAHAR dataset.

Table 6.1: Mean and standard deviation of stride time across each terrain

Terrain	Left Leg ($\mu \pm \sigma$)	Right Leg ($\mu \pm \sigma$)
Grass	1.330 ± 0.121	1.328 ± 0.119
Flat	1.418 ± 0.139	1.415 ± 0.136
Carpet	1.332 ± 0.120	1.333 ± 0.121
Asphalt	1.236 ± 0.106	1.235 ± 0.108
Paving	1.144 ± 0.072	1.144 ± 0.066
Gravel	1.182 ± 0.082	1.185 ± 0.081

Table 6.2: Mean and standard deviation of step time across each terrain

Terrain	Left Leg ($\mu \pm \sigma$)	Right Leg ($\mu \pm \sigma$)
Grass	0.663 ± 0.063	0.666 ± 0.061
Flat	0.710 ± 0.072	0.704 ± 0.064
Carpet	0.663 ± 0.063	0.668 ± 0.059
Asphalt	0.619 ± 0.062	0.616 ± 0.049
Paving	0.574 ± 0.041	0.573 ± 0.026
Gravel	0.594 ± 0.041	0.593 ± 0.044

Table 6.3: Mean and standard deviation of single swing across each terrain

Terrain	Left Leg ($\mu \pm \sigma$)	Right Leg ($\mu \pm \sigma$)
Grass	50.236 ± 2.434	50.177 ± 2.663
Flat	48.550 ± 2.445	48.744 ± 2.265
Carpet	49.660 ± 2.609	49.420 ± 2.631
Asphalt	51.201 ± 2.292	51.063 ± 2.744
Paving	52.573 ± 2.208	52.602 ± 1.700
Gravel	52.112 ± 2.164	52.266 ± 2.760

Table 6.4: Mean and standard deviation of single stance across each terrain

Terrain	Left Leg ($\mu \pm \sigma$)	Right Leg ($\mu \pm \sigma$)
Grass	49.764 ± 2.434	49.823 ± 2.663
Flat	51.450 ± 2.445	51.256 ± 2.265
Carpet	50.340 ± 2.609	50.580 ± 2.631
Asphalt	48.799 ± 2.292	48.937 ± 2.744
Paving	47.427 ± 2.208	47.398 ± 1.700
Gravel	47.888 ± 2.164	47.734 ± 2.760

While these results indicate that terrain has a significant effect on the gait parameters, there remains a large standard deviation, particularly in terrains where the location data was collected from was changed between subjects, such as grass, flat laminated indoor flooring, carpet, and asphalt. Gait, and therefore the gait parameters, are known to be unique to each person [366, 367], meaning that additional parameters like age, gender, and height may also be factors contributing towards differences in the gait parameters between subjects. To account for this, a repeated measures Analysis of Variance (ANOVA) was performed across all subjects for each

Table 6.5: The repeated measures ANOVA results for each gait parameter across both legs.

Gait Parameter	Left (F-value)	Left (p-value)	Right (F-value)	Right (p-value)
Stride Time	74.086	0.000	72.838	0.000
Step Time	60.753	0.000	66.727	0.000
Single Swing	32.326	0.000	31.161	0.000
Single Stance	32.326	0.000	31.161	0.000

Figure 6.5: The paving slab and gravel terrains in the CAHAR dataset.

leg using the "AnovaRM" function from the "statsmodels" library for Python. The test is set up such that the null hypothesis is that terrain has no effect on the mean of each gait parameter. The results of this analysis can be found in Table 6.5.

These results suggest that coarser terrains like gravel reduce stride time and step time when compared with smoother terrains like the flat indoor surface and carpet. The exception to this is with the paving slabs, which would be expected to be relatively smooth, particularly when compared to grass. However, as seen in Figure 6.5, the paving slabs and gravel terrains were positioned next to one another, with small plants and obstacles that require attention underfoot. It follows that participants in the CAHAR dataset walked similarly between these terrains.

However, it should be noted that, as these terrains were selected to be as natural as possible in the CAHAR dataset, participants encountered a different amount of corners in each of these settings. For the paving slab and gravel terrains, no corners were encountered, which may result

in an increased average walking speed of the participants. Furthermore, the indoor terrains required participants to walk around the edge of a room, and was the first activity participants performed, which may result in an increased stride time due to slower walking caused by being unfamiliar with the equipment. Additionally, when navigating the paving slabs and gravel terrain, the researcher walked with the participant to keep the wireless connection stable due to the walkway being linear, whilst participants walked around the researcher at a constant distance in the grass, flat laminated indoor flooring, carpet, and asphalt trials. Figures 6.4c and 6.4d suggest that these factors may be affecting the results, with reductions in the stance phase for the paving and gravel terrains suggesting an increase in walking speed when compared to the flat laminated flooring terrain. As a result, whilst these results appear to agree with the literature, these additional factors in the data suggest that capturing natural walking in natural environments is a complex, multifaceted issue which requires a much more diverse dataset, or a more specific experimental protocol that reduces the impact of human behaviour when navigating different environments.

6.3.2 Follow-up Analysis

To mitigate these issues with the protocol of the CAHAR dataset for the purpose of extracting the temporal gait parameters, a follow-up study was conducted in which participants 1, 3, 5, 8, and 12 participated in a second data collection procedure. In this new procedure, participants walked for four repetitions of a fixed distance of 20 metres in a straight line on a flat laminated flooring surface, along with the gravel and paving slab terrains from the original analysis. This time, the flat surface was the corridor outside the room used for the original flat surface with the same surface properties, and the researcher walked with the participants in all trials, removing the effect of corners and other variations between terrains which may affect the walking speed of the participants. These surfaces were chosen to verify the findings of the analysis using the CAHAR dataset, as these were the terrains with the largest difference in gait parameters. The results for the follow-up analysis can be seen in Figure 6.6 and Tables 6.6-6.9.

Another repeated measures ANOVA was performed for the gait parameters in the follow-up analysis, which can be found in Table 6.10, showing that terrain has a statistically significant impact on gait.

(a) Mean stride time

(b) Mean step time
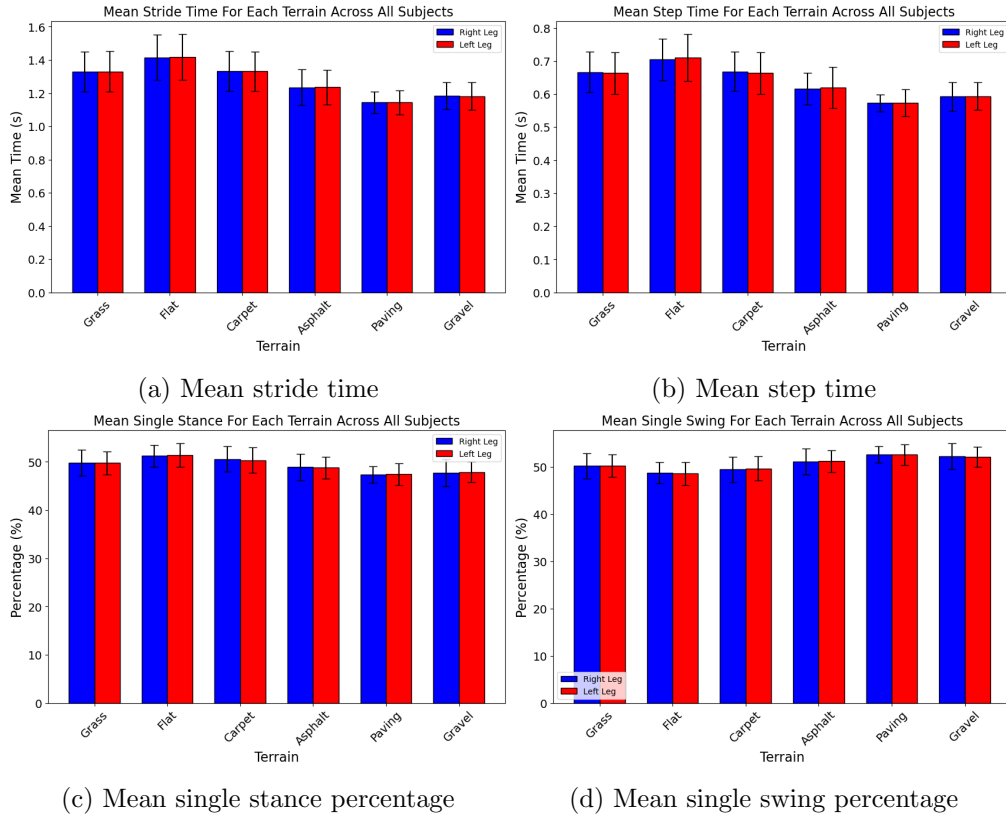
(c) Mean single stance percentage

(d) Mean single swing percentage
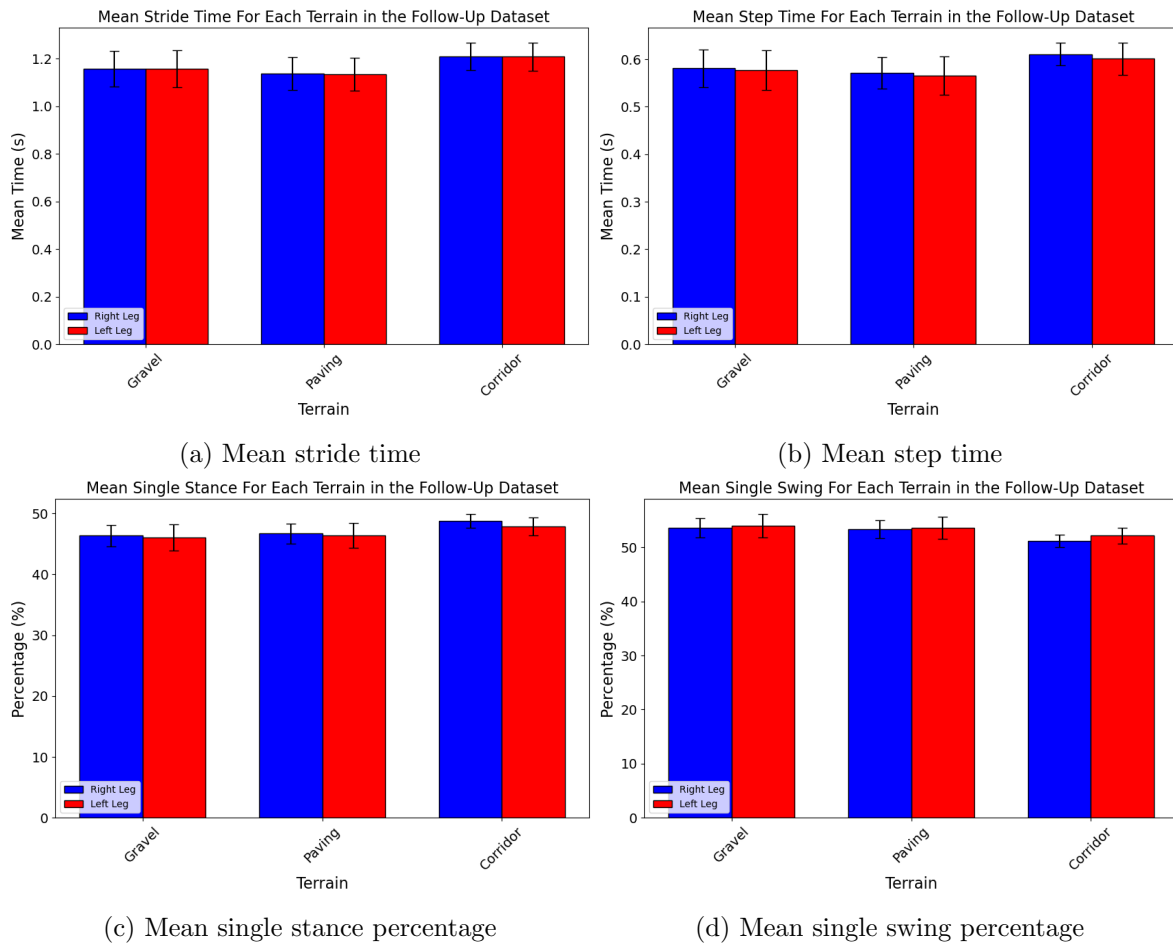
Figure 6.6: Bar charts showing the mean and standard deviations of each gait parameter for all subjects on each of the terrains in the follow-up dataset.

Table 6.6: Mean and Standard Deviation of stride time across the terrains in the follow-up dataset

Terrain	Left Leg ($\mu \pm \sigma$)	Right Leg ($\mu \pm \sigma$)
Gravel	1.157 ± 0.077	1.156 ± 0.075
Paving	1.134 ± 0.069	1.137 ± 0.069
Corridor	1.208 ± 0.058	1.209 ± 0.057

Table 6.7: Mean and Standard Deviation of step time across the terrains in the follow-up dataset

Terrain	Left Leg ($\mu \pm \sigma$)	Right Leg ($\mu \pm \sigma$)
Gravel	0.577 ± 0.042	0.581 ± 0.039
Paving	0.565 ± 0.040	0.571 ± 0.033
Corridor	0.601 ± 0.034	0.610 ± 0.024

Table 6.8: Mean and Standard Deviation of single swing across the terrains in the follow-up dataset

Terrain	Left Leg ($\mu \pm \sigma$)	Right Leg ($\mu \pm \sigma$)
Gravel	53.993 ± 2.166	53.637 ± 1.776
Paving	53.621 ± 2.032	53.323 ± 1.685
Corridor	52.156 ± 1.456	51.245 ± 1.144

Table 6.9: Mean and Standard Deviation of single stance across the terrains in the follow-up dataset

Terrain	Left Leg ($\mu \pm \sigma$)	Right Leg ($\mu \pm \sigma$)
Gravel	46.007 ± 2.166	46.363 ± 1.776
Paving	46.379 ± 2.032	46.677 ± 1.685
Corridor	47.844 ± 1.456	48.755 ± 1.144

Table 6.10: The repeated measures ANOVA results for each gait parameter across both legs with the follow-up dataset.

Gait Parameter	Left (F-value)	Left (p-value)	Right (F-value)	Right (p-value)
Stride Time	6.418	0.022	6.888	0.018
Step Time	5.791	0.028	7.287	0.016
Single Swing	4.747	0.044	12.717	0.003
Single Stance	4.747	0.044	12.717	0.003

6.4 Discussions

The results of this analysis highlight the effect of terrain on the temporal gait parameters such as stride and step time, along with single stance and single swing as a percentage of a single stride. Both the data from the CAHAR dataset, along with a focussed follow-up study are analysed to evaluate the effect of terrain on gait.

The results of the study on the CAHAR dataset, and the difference between those results and that of the follow-up study, highlight the effect that environment and context have on gait. Participants in the CAHAR dataset walked under specific conditions for each terrain, such as walking with a researcher, or walking in a confined room, to keep these environments as natural as possible. The gait parameters reflect these conditions, but this analysis does not enable a fair comparison between terrains with respect to the gait parameters. As a result, a follow-up study was performed, and under these normalised conditions, the difference between the gait parameters was reduced, but the trends remained, with the effect of terrain on the gait parameters in this controlled setting being found to be statistically significant.

Existing studies on the effect of terrain on gait highlight that coarser terrains generally result

in shorter, slower steps [38, 39, 108–112]. The findings in this study agree with the literature, finding that coarse terrains like gravel induce shorter steps with increased variability than smooth terrains like the flat corridor. Variability was also exaggerated in the non-dominant leg of each participant in the follow-up trial, which translated to increased step and stride time standard deviations.

There are some limitations to this study, primarily due to the fact that the CAHAR dataset was not designed for the extraction of the spatio-temporal gait parameters. As a result, the dataset lacks validation data for any algorithm which estimates the spatial parameters. While an existing, validated algorithm could be applied to the dataset to mitigate this, these algorithms are not validated for use on the range of terrains featured in the CAHAR dataset, which would limit the reliability of these results [36, 262–269]. The temporal parameters are much simpler to extract, relying on peak detection rather than the integrals of accelerometer and gyroscope signals over time, which are susceptible to drift and noise [375, 376]. The follow-up dataset eliminated many of the environmental issues caused by the context in which the CAHAR dataset was captured, but future work should consider implementing and validating algorithms that extract the spatial gait parameters across multiple real-world terrains.

6.5 Contributions

This chapter performs an analysis of the effect of multiple terrains and surfaces on gait by extracting the temporal gait parameters from the CAHAR dataset. The results of this study validate the findings in the literature regarding the effect of terrain on gait using a novel sensor system in real environments. A repeated measures ANOVA demonstrates a statistical significance when evaluating if terrain has an effect on the temporal gait parameters, highlighting the need for future studies to consider variation in terrain when performing remote gait analysis using wearable sensors. Furthermore, the effect of the environment on gait is highlighted, giving insight into how our surroundings and being accompanied whilst walking can affect the gait parameters, which may be significant for future datasets and experimental protocols in this area.

6.6   Summary

This chapter addresses the aim of investigating the effect of terrain on gait, along with the objectives of extracting the gait parameters and observing how changes in terrain and environment affect the gait parameters. A validated methodology for identifying the gait phases using inertial data from the foot is implemented for the CAHAR dataset, enabling the temporal gait parameters to be extracted from the walking data. A repeated measures ANOVA is then used to determine the effect of terrain on gait, which is found to be statistically significant. Coarse and uneven terrains are found to cause a reduction in step and stride time, which is mirrored in the literature in which rough terrain has been shown to cause shorter steps.

With respect to the aims of this thesis, the sensor system used to collect the CAHAR dataset is shown to be capable of determining the walking activity a person is performing, the terrain they're performing that activity on, and monitoring the gait parameters on these terrains. Each of these capabilities allows the system to monitor one of the incremental fall-risk factors encountered in daily life, whether it's an irregular activity like ascending a ramp or stairs, the introduction of trip and slip hazards via the terrain underfoot, or an increase in gait variability caused by uneven terrains such as grass and gravel. As such, with these capabilities, this system is shown to be an effective prototype for monitoring the various incremental fall risks that people encounter in daily life, answering the primary research question of this thesis.

Chapter 7

Summary, Conclusions, and Future Work

7.1 Summary

7.1.1 Contributions

- The first cross-disciplinary systematic review of fall research, offering new insights into the field.

Despite fall research spanning multiple disciplines, many literature reviews only address small subsections of healthcare or technological approaches to fall prevention [377–381]. By performing a novel cross-disciplinary systematic review spanning over 10 years, this research contributes many new insights into the current state of fall research, particularly with regard to the large disparity in dataset quality between technological interventions and rehabilitation approaches, and through the identification of interdisciplinary research gaps such as the application of fall detection research to fall prevention, and how fall prediction studies can be integrated into fall intervention programmes. Furthermore, this contribution fulfils the aim of identifying trends and research gaps in the large, cross-disciplinary field of fall prevention research, along with the research objective of exploring the current state of fall detection, prediction, prevention, and intervention across both technology and healthcare research.

- An analysis of normalised, existing Human Activity Recognition (HAR) datasets, which explores the contributions of various sensor types and analytical parameters towards clas-

sification accuracy.

Many HAR dataset analyses have been performed in the literature. However, the analysis in this study contributes a novel insight into the performance of sensors and machine learning classifiers between multiple datasets by reducing the classification biases that would normally be introduced through the differences between these datasets. This bias reduction is performed by homogenising several aspects of each dataset, such as the number of participants, sample rate, and activity types. Furthermore, this study finds two to five seconds is an optimal range of values for window size when performing the sliding window technique — an extremely common approach to time-series classification in HAR datasets, which provides future researchers with evidence to base their choice of window size on in future analyses. This contribution also addresses the research objectives of finding the sensors and sliding window parameters which contribute the most towards high-accuracy HAR, which contribute towards the development of the sensor system — another research aim.

- A novel sensor system capable of capturing relevant data to perform terrain-recognition.

The sensor system proposed in this research is capable of high-accuracy HAR, whilst also achieving accurate terrain identification through the introduction of the colour sensor, which augments the Inertial Measurement Unit (IMU) data from the feet. Compared to HAR sensor systems in the literature, the proposed system features fewer sensors [35, 239, 240, 254], resulting in a more lightweight and convenient system to wear, whilst still capturing sufficient data to enable novel terrain recognition and competitive HAR accuracies.

- The collection of the first, openly-accessible, terrain-labelled HAR dataset.

The proposed Context-Aware Human Activity Recognition (CAHAR) dataset is a major contribution towards the field of HAR, directly addressing the need for a large dataset with an exhaustive set of walking surfaces representative of the real environment outside the laboratory, outlined by Luo *et al.* [35]. Furthermore, whilst extremely high accuracies are achieved in the analysis of this dataset using subject-dependent training in Chapter 5, future researchers may succeed in improving the subject-independent accuracies using powerful deep learning methods which are popular in the literature. Additionally, the dedicated test data included in this dataset from participants 1 and 3 issues a further challenge for researchers to build models capable of combining individual activity and terrain classifications, enabling 99 possible com-

binations of activity and terrain to be classified from a training set of just 38. This dataset meets the research aim and objective of collecting a novel HAR dataset on a range of different terrains commonly encountered in daily life.

- An evaluation of the feasibility of terrain classification using wearable sensors.

This thesis demonstrates that terrain classification is possible using IMU data alone, but that accuracy is significantly improved through the addition of a colour sensor, with overall accuracies of 99% and 96% for terrain and combined terrain-activity classification respectively, using classical machine learning techniques. These accuracies are extremely competitive with the literature for HAR, which range from 78%-100% accuracy [28–34] across far fewer activities than the CAHAR dataset, due to the repetition of each activity on multiple terrains. Furthermore, this research demonstrates a terrain classification accuracy of 99% across nine terrains, compared to existing studies which achieve 97% on three terrains [290], and 88.7% on six terrains [289], with a more limited range of activities. With these results, activity and terrain classification, and therefore the external fall risk factors considered in this study, are demonstrated to be identifiable with the proposed wearable sensing system, addressing a large aspect of the main research question for this work.

- Analysing the effect of terrain on the gait parameters.

This thesis highlights the effect of both terrain, and walking context, on the gait parameters, finding that subjects walked with a reduced step and stride time on coarser terrains such as gravel and natural paving slabs. Many studies in the literature have reported similar findings when considering changes to the gait parameters between uneven terrains and smooth terrains [38, 39, 108–112]. However, many of these studies consider terrains as being only smooth or uneven, rather than discussing the effect of specific terrains on gait [108–112]. As such, this thesis analyses the temporal parameters using validated methods from the literature [374] across each of the six terrains that featured walking activities in the CAHAR dataset, along with a follow-up dataset with more controlled variables. These findings demonstrate that coarser terrains like gravel have a statistically significant effect on the gait parameters when compared to the flat laminated indoor terrain.

7.1.2 Discussions

This research project aims to investigate the feasibility of, and take crucial steps towards, developing a prototype system capable of monitoring fall-risk factors such as activity, terrain, and changes in the gait parameters. The following section summarises the developments and findings in this thesis towards answering the primary research question: "Can the many external and internal factors that contribute towards a person's risk of falling in real-world environments be monitored using wearable sensors?"

Chapter 2 of this thesis highlights the current progress made to date by researchers across many disciplines, which aim to reduce the frequency and impact of falls through a wide variety of technological and rehabilitation approaches. Studies which monitor the spatio-temporal gait parameters of people with a variety of conditions known to cause falls, such as Parkinson's disease, dementia, stroke, multiple sclerosis, lower-limb amputation, and ageing, show an increase in gait asymmetry and variability, resulting in reduced balance when walking. These factors are also prevalent in the literature for the effect of terrain on gait, along with fall interventions in healthcare research, where balance training is commonplace and parameters such as postural sway, gait speed, and Centre of Mass (CoM)/Centre of Pressure (CoP) are frequently used to monitor the success of an intervention. These areas highlight how demographic and environmental factors can contribute towards fall risk.

Fall-related research can be categorised in to four areas: detection, prediction, prevention, and interventions. Each of these areas is independently capable of reducing the impact of falls, whether through rapidly alerting family members, automating parts of the healthcare pipeline, physically preventing a fall, or improving fall-related factors like balance. However, despite advancements in each of these areas, falls remain as largely unpredictable events in the steps that precede them. While a perfect fall prediction system would be able to alert a person of an upcoming fall so that they can stop walking and prevent the incident, this is a multifaceted issue comprising the real-time monitoring of many internal and external risk factors.

This research, therefore, aims to build the foundations of a remote, wearable gait data collection system, which can automatically monitor incremental fall risk factors like activity, terrain, and the gait parameters. Such a system should be capable of identifying all the known factors which contribute towards fall risk while maintaining the privacy of the wearer, with the goal of being optimised in future iterations by reducing the number of sensors needed to perform this task.

The following sections highlight how each chapter in this thesis contributes towards this goal, resulting in a validated prototype sensor system capable of monitoring the fall risk factors that a person encounters in their daily life.

The sensor system in this research project is constructed following the results of an analysis of existing datasets to identify sensor types, locations, and sample rates which enable high-accuracy HAR. This preliminary study finds that a single IMU is sufficient to attain high performance metrics on HAR tasks alone, leaving room for new sensor modes to be explored for the purpose of terrain classification. Regarding the classifiers suited for activity classification, Support Vector Machines (SVMs) and Artificial Neural Networks (ANNs) consistently exhibit higher accuracies than the other single-model classifiers: Decision Tree (DT), Random Forest (RF), and K-Nearest Neighbours (KNN), whilst combining these models using stacking and voting ensemble methods can further help to increase performance. Data was prepared for these models using the sliding window approach to time-series feature engineering, for which it was found that window sizes in the range of two to five seconds are preferable when performing HAR. This finding led to the decision to repeat certain activities in the experimental procedure for the collection of the CAHAR dataset to ensure that at least two seconds of data would be available for the shortest activities: sit to stand and stand to sit.

With the experimental procedure and sensor system confinements determined in Chapter 3 to ensure that high-accuracy HAR would be possible with the novel dataset, a focus is placed on using the remaining Force Sensing Resistor (FSR) insoles, LiDAR, and colour sensor to improve HAR accuracies and introduce sufficient data for performing terrain classification. Camera sensors are popular in the literature for terrain recognition, particularly depth cameras such as the Microsoft Kinect, due to their high data dimensionality. However, these approaches introduce privacy concerns when attached to the body, or when observing a person in their daily life. Many studies use silhouetting to circumvent this issue, but this approach is not suitable when colour is a significant factor in determining a type of terrain. Therefore, the use of a colour and LiDAR sensor function together as a low-information depth camera which obtains the basic colour and coarseness of the ground underfoot, whilst maintaining the privacy of the wearer. This was found to be successful, with the merged red, green, and blue data channels accurately reflecting the colour and light levels of many terrains, whilst the high-frequency information of the LiDAR sensor generated coarseness plots which enable the visual

separation of terrains. Regarding the capacity of the system for extracting the spatio-temporal gait parameters, the FSR insoles gather valuable information for determining the gait phase, step time, cadence, and CoM/CoP, the IMU on the foot enables the calculation of gait phase, step width, step length, and step height, and the IMU on the waist enables the calculation of postural sway, each of which were reoccurring parameters of interest in the fall intervention studies of Chapter 2.

With regard to the data collection process, 20 participants were recruited for this study who each performed 38 combinations of 11 activities on nine different terrains, resulting in a novel dataset comprising over 7.8 hours of gait data. This makes the dataset suited for data mining approaches such as deep learning, which require large datasets to obtain high performance metrics. As such, the reach of this dataset has been tailored for researchers to test powerful, novel approaches to classification tasks, such as Convolutional Neural Networks (CNNs), transformers, and other deep learning architectures. Regarding the generalisability and robustness of this dataset, the data collection process occurred over the course of 15 months from November 2022 to February 2024, resulting in a range of ambient light levels, weather conditions, surface properties, and temperatures to ensure that this dataset reflects real-world conditions. Furthermore, some terrains, such as the carpet, grass, and laminated flooring were changed between participants to maximise the generalisation of models trained on these data. Whilst this approach may have impacted the terrain classification accuracy of models, particularly when using Leave One Subject Out (LOSO) cross validation due to the changes occurring between participants, it allows the resulting analyses of this dataset to more accurately reflect a real-world implementation of terrain recognition.

An investigatory study is performed on the collected dataset to determine the feasibility of performing terrain classification using existing methods such as those used in Chapter 3. Here it is found that terrain can be classified with 99% accuracy when using a SVM trained on terrain-labelled data only. When considering both activity and terrain, a single model achieves 96% accuracy with a feature set extracted from just the IMU and colour sensor. This highlights the success of the proposed dataset, along with a clear path for future research in this area, as multimodel approaches to terrain and activity classification can enable the interpolation of individual classifications such that models can accurately identify a combination of activity and terrain outside the scope of the train set. These multimodel approaches resulted in extremely

low accuracies in this study when tested with the dedicated test data of the CAHAR dataset. However, given the initial findings of this study, and the potential to implement much more advanced classification algorithms such as CNNs, Long Short-Term Memory (LSTM) models and transformers, a new challenge and direction of this research area is presented, as high-generalisability multimodel solutions to context classification will enable this technology to be adopted without a training period and with the capacity to detect a much wider range of activity and terrain combinations.

Finally, Chapter 6 studies the effect of terrain on the gait parameters, therein demonstrating the capacity for this system to monitor how terrain affects gait and how these changes reflect an increased fall risk. A validated algorithm for extracting the temporal parameters of gait using a foot-mounted IMU is applied to calculate the stride time, step time, single stance, and single swing phases on each of the six terrains which featured a walking activity in the CAHAR dataset. Terrain is found to have a significant impact on gait in these conditions, however the context in which the data was collected could be seen as an additional factor affecting the gait parameters. Whilst this is also relevant to fall risk, a follow-up dataset is collected which eliminates these contextual differences between walking bouts for the flat laminated indoor flooring, paving slabs, and gravel terrains. In this controlled comparison of the gait parameters, statistically significant changes are still present between the terrains, highlighting how terrain can induce gait parameters which reflect those in groups at high risk of falling, as highlighted in Chapter 2.

This Thesis outlines the development and validation of a sensor system suited to monitor the internal and external fall-risk factors. By implementing a system like this, wearers could have their incremental fall-risk factors communicated to them in real time, allowing them to respond to increases in fall risk and act to prevent falls in the steps before they occur. Such a system brings the field of fall prediction closer to the development of a 'perfect' fall prediction system which informs users that they are about to fall in the steps preceding a fall.

7.1.3 Limitations of This Research

This study features several limitations due to the scope of the project. Whilst minor limitations are outlined in each chapter, this section explores the greater limitations and how these affect the results of this research project.

Firstly, the scope of the exploration of optimal window sizes in existing datasets had to be controlled due to the limitless combinations of both window size and step size. For this study, it was determined that window size would be the independent variable, whilst all other variables such as model types, model hyperparameters, and step size were controlled to ensure a fair comparison. However, by limiting the step size to 25% of the window size, this variable became dependent on the window size. This was chosen due to the computational cost of training many models, as larger step sizes mean fewer samples and therefore less training time, and due to the idea that step size should scale with window size. This is because large windows with small step sizes will contain largely the same values as the previous window, whereas the approach in this study ensures that 25% of the values in each window are different. However, the resulting co-dependency means that the results of Chapter 3 should be considered to be the model performance at a given window size and step size. Whilst this is still a useful study in recommending parameters to other researchers for this task, identifying high-performing sensors, and removing the classification bias that affects the results in other works of the same kind, the generalisation of the results is diminished compared to a study in which both window size and step size are independent variables.

Another major limitation for this work is in the prototypic nature of the sensor system. This research was primarily a feasibility study for detecting a range of internal and external fall-risk factors using a single wearable sensor system. However, given the success of the project, it is regrettable that the sensor system was not suited to perform a full, out-of-lab clinical trial due to issues with the battery life and robustness of the device. As such, future research in this area will require the development of a new sensor system using the results of this research which is less obtrusive, and has improved battery life and durability. Given the results of the analysis in Chapter 5, the removal of the waist and LiDAR sensors would be justified due to their incompleteness and poor performance respectively, which would improve battery life and convenience.

Another issue presented by the nature of this work being a feasibility study is that insufficient validation measures existed when calculating the spatio-temporal gait parameters, restricting the study to the implementation of a pre-validated algorithm for estimating the temporal parameters only. This does not affect the conclusions of the relevant chapter, but knowledge of the CoP/CoM, step length, and stride length would have given a more complete understanding

of the effect of terrain on balance and gait.

Finally, the classification methods in this research, while capable and well-used in the literature, are no longer the cutting-edge analytical techniques in this field, with transformers and large CNNs being more popular in recent years. This does not affect the results of this project, perhaps even highlighting the success of the dataset to obtain such high accuracies without these powerful models, however it does mean that future work is needed to determine the true potential of terrain classification using the CAHAR dataset with multimodel solutions that achieve high accuracies with the dedicated test set.

7.2 Conclusions

This thesis finds that falls can typically be attributed to detectable factors such as gait abnormalities and terrains which cause slips and trips, with gait analysis being a useful tool to identify factors that increase a person's fall risk. However, while the impact of terrain on gait and fall risk is known, the literature on fall prediction is yet to incorporate these factors to build a system capable of monitoring incremental fall-risk factors in real time and on real terrains. This work addresses that research gap.

The analysis of existing datasets finds that a single IMU is sufficient for accurate HAR, which led to the inclusion of IMUs in the novel sensor system outlined in Chapter 4. Furthermore, here it is found that Electromyography (EMG) sensors are largely unreliable with respect to HAR, with accuracies appearing volatile between subject-dependent and subject-independent training, and never reaching the heights of IMU sensors. In addition to these common methods, goniometers are also found to be capable sensors with regard to HAR, and should be explored further in future research.

The findings in Chapters 2 and 3 guide the design of a novel sensor system comprised of IMUs, FSR insoles, colour sensors, and LiDARs, which is suited to the collection of a terrain-recognition HAR dataset. Upon the evaluation of this system, the IMUs and colour sensors were found to be the largest contributors towards terrain classification, with the FSR insoles proving useful only in the case that subject-dependent training was performed. This could be due to a variety of factors, such as the need for more robust calibration procedures, the damage caused to the insoles throughout some of the trials, or the presence of sensor saturation occurring at

different stages in the gait cycle for different participants. Additionally, the LiDAR proved to be inadequate for both terrain and activity classification, despite the visual separability of the high frequency information when comparing coarse and smooth terrains, which could indicate that alternative signal processing methods are required to extract useful information from these sensor types.

The CAHAR dataset, collected with the novel sensor system, features 38 combinations of 11 activities performed on nine unique terrains. The problems with existing datasets outlined in Chapter 2 are mitigated via this dataset through the recruitment of 20 participants with a wide range of age, weight, height, ethnicity, and shoe size, along with a 1:1 ratio of males and females which, in combination with the alternating locations of carpet and grass trials, ensures that the generalisation of models built using this dataset is maximised. Through these considerations, and the inclusion of a dedicated test set taken from participants 1 and 3, this dataset will enable future researchers to develop and test powerful machine learning classifiers which further the field of HAR.

Chapter 5 addresses the research goal of determining the feasibility of terrain classification using the CAHAR dataset. For subject-dependent analysis, the full sensor system obtains accuracies of 94% when classifying between the 38 combined activity and terrain classes, which is increased to 96% when reduced to just the foot IMU and colour sensor of both legs. Furthermore, individual classifications of activity and terrain were achieved with 96% and 99% respectively. When performing subject-independent classification, these accuracies drop to 50% using the full dataset, and 69% when using data from just the IMU and colour sensor. Given these results, the proposed sensor system can be reduced in future iterations to just an IMU, colour sensor, and FSR insole on each foot, which can be conveniently implemented into intelligent shoes for comfort.

Finally, Chapter 6 addresses how the terrain underfoot affects the gait parameters, finding that coarser terrains result in shorter steps which aligns with the findings in the literature. As such, this thesis outlines the design of a prototype sensor system capable of monitoring the current activity a person is performing, the terrain they're performing the activity on, and the gait parameters if that activity is walking. These factors enable the system to evaluate the external and internal fall-risk factors, answering the primary research question of this thesis.

7.3 Future Work

Whilst the aims of this research project were met, much room remains for future work to extend this work from a feasibility study, to the development of a prototype incremental fall-risk analysis system and its adoption in healthcare settings. Immediately following this research, the findings of Chapter 5 should be used to refine the proposed sensor system by removing the LiDAR sensors, along with reducing the profile of the device to increase convenience and comfort. An Internet of Things (IoT) approach would be suited to this device, and should also be investigated at this next stage to allow wireless communications from the device to the cloud, which will enable the telehealth monitoring of fall-risk factors. Additional minor hardware and software modifications are needed to enable the analysis of risk factors in real-time, either onboard the sensor system, or on the cloud, using the classification techniques from Chapter 5. Finally, validated algorithms should be developed and implemented to extract the full set of spatio-temporal gait parameters from the gait data collected by the system, and process them to determine fall-risk.

Following the finalisation of the system, this device must be tested in collaboration with health-care professionals to ensure it offers an effective solution for reducing the prevalence of falls in society. This will involve measuring the agreement between the device and existing fall-risk measures across multiple healthcare centres, along with obtaining user feedback to iterate upon and improve the system. The foundational research performed in this project towards the identification of fall-risk factors addresses the individual challenges of identifying external and internal fall risks, bringing fall prediction and its vast benefits, closer to adoption in healthcare systems globally.

References

[1] WHO, World Health Organization: "Falls," *World Health Organization: WHO*, Apr. 2021. [Online]. Available: `https://www.who.int/news-room/fact-sheets/detail/falls`.

[2] W. Lutz, W. Sanderson, and S. Scherbov, "The coming acceleration of global population ageing," en, *Nature*, vol. 451, no. 7179, pp. 716–719, Feb. 2008.

[3] A. J. Blake *et al.*, "Falls by elderly people at home: Prevalence and associated factors," *Age and Ageing*, vol. 17, no. 6, pp. 365–372, 1988, ISSN: 1468-2834. DOI: `10.1093/ageing/17.6.365`. [Online]. Available: `http://dx.doi.org/10.1093/ageing/17.6.365`.

[4] T. Rikkonen, R. Sund, H. Koivumaa-Honkanen, J. Sirola, R. Honkanen, and H. Kröger, "Effectiveness of exercise on fall prevention in community-dwelling older adults: A 2-year randomized controlled study of 914 women," *Age and Ageing*, vol. 52, no. 4, Apr. 2023, ISSN: 1468-2834. DOI: `10.1093/ageing/afad059`. [Online]. Available: `http://dx.doi.org/10.1093/ageing/afad059`.

[5] S. I. Sharif, A. B. Al-Harbi, A. M. Al-Shihabi, D. S. Al-Daour, and R. S. Sharif, "Falls in the elderly: Assessment of prevalence and risk factors," *Pharmacy Practice*, vol. 16, no. 3, p. 1206, Sep. 2018, ISSN: 1886-3655. DOI: `10.18549/pharmpract.2018.03.1206`. [Online]. Available: `http://dx.doi.org/10.18549/PharmPract.2018.03.1206`.

[6] P. N. Matsuda, A. M. Verrall, M. L. Finlayson, I. R. Molton, and M. P. Jensen, "Falls among adults aging with disability," *Archives of Physical Medicine and Rehabilitation*, vol. 96, no. 3, pp. 464–471, 2015, ISSN: 0003-9993. DOI: `https://doi.org/10.1016/j.apmr.2014.09.034`. [Online]. Available: `https://www.sciencedirect.com/science/article/pii/S0003999314011599`.

[7] Q. Xu, X. Ou, and J. Li, "The risk of falls among the aging population: A systematic review and meta-analysis," *Frontiers in Public Health*, vol. 10, Oct. 2022, ISSN: 2296-2565. DOI: `10.3389/fpubh.2022.902599`. [Online]. Available: `http://dx.doi.org/10.3389/fpubh.2022.902599`.

[8] B. L. Moreland, R. Kakara, Y. K. Haddad, I. Shakya, and G. Bergen, "A descriptive analysis of location of older adult falls that resulted in emergency department visits in the united states, 2015," *American Journal of Lifestyle Medicine*, vol. 15, no. 6, pp. 590–597, Aug. 2020, ISSN: 1559-8284. DOI: `10.1177/1559827620942187`. [Online]. Available: `http://dx.doi.org/10.1177/1559827620942187`.

[9] D. Wild, U. S. Nayak, and B. Isaacs, "How dangerous are falls in old people at home?" en, *BMJ*, vol. 282, no. 6260, pp. 266–268, Jan. 1981.

[10] W.-C. Chen, Y.-T. Li, T.-H. Tung, C. Chen, and C.-Y. Tsai, "The relationship between falling and fear of falling among community-dwelling elderly," en, *Medicine (Baltimore)*, vol. 100, no. 26, e26492, Jul. 2021.

[11] A. Fasano, M. Plotnik, F. Bove, and A. Berardelli, "The neurobiology of falls," *Neurological Sciences*, vol. 33, no. 6, pp. 1215–1223, Jun. 2012, ISSN: 1590-3478. DOI: `10.1007/s10072-012-1126-6`. [Online]. Available: `http://dx.doi.org/10.1007/s10072-012-1126-6`.

[12] M. Suzuki, N. Ohyama, K. Yamada, and M. Kanamori, "The relationship between fear of falling, activities of daily living and quality of life among elderly individuals," en, *Nurs. Health Sci.*, vol. 4, no. 4, pp. 155–161, Dec. 2002.

[13] M. Li, S. Tian, L. Sun, and X. Chen, "Gait analysis for post-stroke hemiparetic patient by multi-features fusion method," en, *Sensors (Basel)*, vol. 19, no. 7, p. 1737, Apr. 2019.

[14] G. Chen, C. Patten, D. H. Kothari, and F. E. Zajac, "Gait differences between individuals with post-stroke hemiparesis and non-disabled controls at matched speeds," en, *Gait Posture*, vol. 22, no. 1, pp. 51–56, Aug. 2005.

[15] C. K. Balasubramanian, R. R. Neptune, and S. A. Kautz, "Variability in spatiotemporal step characteristics and its relationship to walking performance post-stroke," en, *Gait Posture*, vol. 29, no. 3, pp. 408–414, Apr. 2009.

REFERENCES

[16] A.-M. De Cock *et al.*, "Comprehensive quantitative spatiotemporal gait analysis identifies gait characteristics for early dementia subtyping in community dwelling older adults," en, *Front. Neurol.*, vol. 10, p. 313, Apr. 2019.

[17] G. Allali *et al.*, "Gait phenotype from mild cognitive impairment to moderate dementia: Results from the GOOD initiative," en, *Eur. J. Neurol.*, vol. 23, no. 3, pp. 527–541, Mar. 2016.

[18] M. J. Socie, B. M. Sandroff, J. H. Pula, E. T. Hsiao-Wecksler, R. W. Motl, and J. J. Sosnoff, "Footfall placement variability and falls in multiple sclerosis," en, *Ann. Biomed. Eng.*, vol. 41, no. 8, pp. 1740–1747, Aug. 2013.

[19] M. J. Socie and J. J. Sosnoff, "Gait variability and multiple sclerosis," *Multiple Sclerosis International*, vol. 2013, pp. 1–7, 2013, ISSN: 2090-2662. DOI: 10.1155/2013/645197. [Online]. Available: http://dx.doi.org/10.1155/2013/645197.

[20] M. J. Highsmith, B. W. Schulz, S. Hart-Hughes, G. A. Latlief, and S. L. Phillips, "Differences in the spatiotemporal parameters of transtibial and transfemoral amputee gait," en, *J. Prosthet. Orthot.*, vol. 22, no. 1, pp. 26–30, Jan. 2010.

[21] S. Beausoleil, L. Miramand, and K. Turcot, "Evolution of gait parameters in individuals with a lower-limb amputation during a six-minute walk test," en, *Gait Posture*, vol. 72, pp. 40–45, Jul. 2019.

[22] L. Nolan, A. Wit, K. Dudziñski, A. Lees, M. Lake, and M. Wychowañski, "Adjustments in gait symmetry with walking speed in trans-femoral and trans-tibial amputees," en, *Gait Posture*, vol. 17, no. 2, pp. 142–151, Apr. 2003.

[23] B. H. Wood, "Incidence and prediction of falls in parkinson's disease: A prospective multidisciplinary study," *Journal of Neurology, Neurosurgery &; Psychiatry*, vol. 72, no. 6, pp. 721–725, Jun. 2002, ISSN: 0022-3050. DOI: 10.1136/jnnp.72.6.721. [Online]. Available: http://dx.doi.org/10.1136/jnnp.72.6.721.

[24] J. C. M. Schlachetzki *et al.*, "Wearable sensors objectively measure gait parameters in parkinson's disease," en, *PLoS One*, vol. 12, no. 10, e0183989, Oct. 2017.

[25] N. Muthukrishnan, J. J. Abbas, and N. Krishnamurthi, "A wearable sensor system to measure step-based gait parameters for parkinson's disease rehabilitation," en, *Sensors (Basel)*, vol. 20, no. 22, p. 6417, Nov. 2020.

[26] M. Pistacchi, "Gait analysis and clinical correlations in early parkinson's disease," *Funct. Neurol.*, vol. 32, no. 1, p. 28, 2017.

[27] M. W. Whittle, "Clinical gait analysis: A review," *Human Movement Science*, vol. 15, no. 3, pp. 369–387, 1996, ISSN: 0167-9457. DOI: `https://doi.org/10.1016/0167-9457(96)00006-1`. [Online]. Available: `https://www.sciencedirect.com/science/article/pii/0167945796000061`.

[28] F. Attal, S. Mohammed, M. Dedabrishvili, F. Chamroukhi, L. Oukhellou, and Y. Amirat, "Physical human activity recognition using wearable sensors," *Sensors*, vol. 15, no. 12, pp. 31 314–31 338, Dec. 2015, ISSN: 1424-8220. DOI: `10.3390/s151229858`. [Online]. Available: `http://dx.doi.org/10.3390/s151229858`.

[29] A. A. Badawi, A. Al-Kabbany, and H. Shaban, "Multimodal human activity recognition from wearable inertial sensors using machine learning," in *2018 IEEE-EMBS Conference on Biomedical Engineering and Sciences (IECBES)*, IEEE, Dec. 2018. DOI: `10.1109/iecbes.2018.8626737`. [Online]. Available: `http://dx.doi.org/10.1109/IECBES.2018.8626737`.

[30] P. Sok, T. Xiao, Y. Azeze, A. Jayaraman, and M. V. Albert, "Activity recognition for incomplete spinal cord injury subjects using hidden markov models," *IEEE Sensors Journal*, vol. 18, no. 15, pp. 6369–6374, Aug. 2018, ISSN: 2379-9153. DOI: `10.1109/jsen.2018.2845749`. [Online]. Available: `http://dx.doi.org/10.1109/JSEN.2018.2845749`.

[31] Y. Asim, M. A. Azam, M. Ehatisham-ul-Haq, U. Naeem, and A. Khalid, "Context-aware human activity recognition (cahar) in-the-wild using smartphone accelerometer," *IEEE Sensors Journal*, vol. 20, no. 8, pp. 4361–4371, Apr. 2020, ISSN: 2379-9153. DOI: `10.1109/jsen.2020.2964278`. [Online]. Available: `http://dx.doi.org/10.1109/JSEN.2020.2964278`.

[32] V. Bianchi, M. Bassoli, G. Lombardo, P. Fornacciari, M. Mordonini, and I. De Munari, "Iot wearable sensor and deep learning: An integrated approach for personalized human activity recognition in a smart home environment," *IEEE Internet of Things Journal*, vol. 6, no. 5, pp. 8553–8562, Oct. 2019, ISSN: 2372-2541. DOI: `10.1109/jiot.2019.2920283`. [Online]. Available: `http://dx.doi.org/10.1109/JIOT.2019.2920283`.

[33] I. A. Lawal and S. Bano, "Deep human activity recognition using wearable sensors," ser. PETRA '19, Rhodes, Greece: Association for Computing Machinery, 2019, pp. 45–

48, ISBN: 9781450362320. DOI: `10.1145/3316782.3321538`. [Online]. Available: `https://doi.org/10.1145/3316782.3321538`.

[34] A. Murad and J.-Y. Pyun, "Deep recurrent neural networks for human activity recognition," *Sensors*, vol. 17, no. 11, p. 2556, Nov. 2017, ISSN: 1424-8220. DOI: `10.3390/s17112556`. [Online]. Available: `http://dx.doi.org/10.3390/s17112556`.

[35] Y. Luo, S. M. Coppola, P. C. Dixon, S. Li, J. T. Dennerlein, and B. Hu, "A database of human gait performance on irregular and uneven surfaces collected by wearable sensors," *Scientific Data*, vol. 7, no. 1, Jul. 2020, ISSN: 2052-4463. DOI: `10.1038/s41597-020-0563-y`. [Online]. Available: `http://dx.doi.org/10.1038/s41597-020-0563-y`.

[36] A. Saboor *et al.*, "Latest research trends in gait analysis using wearable sensors and machine learning: A systematic review," *IEEE Access*, vol. 8, pp. 167 830–167 864, 2020.

[37] R. Caldas, M. Mundt, W. Potthast, F. Buarque de Lima Neto, and B. Markert, "A systematic review of gait analysis methods based on inertial sensors and adaptive algorithms," *Gait & Posture*, vol. 57, pp. 204–210, 2017, ISSN: 0966-6362. DOI: `https://doi.org/10.1016/j.gaitpost.2017.06.019`. [Online]. Available: `https://www.sciencedirect.com/science/article/pii/S0966636217302424`.

[38] D. B. Kowalsky, J. R. Rebula, L. V. Ojeda, P. G. Adamczyk, and A. D. Kuo, "Human walking in the real world: Interactions between terrain type, gait parameters, and energy expenditure," *PLOS ONE*, vol. 16, no. 1, pp. 1–14, Jan. 2021. DOI: `10.1371/journal.pone.0228682`. [Online]. Available: `https://doi.org/10.1371/journal.pone.0228682`.

[39] D. S. Marigold and A. E. Patla, "Age-related changes in gait for multi-surface terrain," *Gait & Posture*, vol. 27, no. 4, pp. 689–696, 2008, ISSN: 0966-6362. DOI: `https://doi.org/10.1016/j.gaitpost.2007.09.005`. [Online]. Available: `https://www.sciencedirect.com/science/article/pii/S096663620700238X`.

[40] J. C. Mitchell, A. A. Dehghani-Sanij, S. Q. Xie, and R. J. O'Connor, "Analysis of multimodal sensor systems for identifying basic walking activities," *Technologies*, vol. 13, no. 4, 2025, ISSN: 2227-7080. DOI: `10.3390/technologies13040152`. [Online]. Available: `https://www.mdpi.com/2227-7080/13/4/152`.

[41] J. C. Mitchell, A. A. Dehghani-Sanij, S. Q. Xie, and R. J. O'Connor, "Machine learn-
      ing techniques for context-aware human activity recognition: A feasibility study," in
      *2024 30th International Conference on Mechatronics and Machine Vision in Practice
      (M2VIP)*, 2024, pp. 1–6. DOI: `10.1109/M2VIP62491.2024.10746162`.

[42] M. E. Mlinac and M. C. Feng, "Assessment of activities of daily living, self-care, and
      independence," *Arch. Clin. Neuropsychol.*, vol. 31, no. 6, pp. 506–516,

[43] G. A. Broe *et al.*, "Impact of chronic systemic and neurological disorders on disability,
      depression and life satisfaction," *International Journal of Geriatric Psychiatry*, vol. 13,
      no. 10, pp. 667–673, Oct. 1998, ISSN: 1099-1166. DOI: `10.1002/(sici)1099-1166(1998100)`
      `13:10<667::aid-gps839>3.0.co;2-g`. [Online]. Available: `http://dx.doi.org/10.`
      `1002/(sici)1099-1166(1998100)13:10%3C667::aid-gps839%3E3.0.co;2-g`.

[44] W. Lyu and F. D. Wolinsky, "The onset of adl difficulties and changes in health-related
      quality of life," *Health and Quality of Life Outcomes*, vol. 15, no. 1, Nov. 2017, ISSN:
      1477-7525. DOI: `10.1186/s12955-017-0792-8`. [Online]. Available: `http://dx.doi.`
      `org/10.1186/s12955-017-0792-8`.

[45] N. Petersen, H.-H. König, and A. Hajek, "The link between falls, social isolation and lone-
      liness: A systematic review," *Archives of Gerontology and Geriatrics*, vol. 88, p. 104 020,
      May 2020, ISSN: 0167-4943. DOI: `10.1016/j.archger.2020.104020`. [Online]. Available:
      `http://dx.doi.org/10.1016/j.archger.2020.104020`.

[46] J. C. Millán-Calenti *et al.*, "Prevalence of functional disability in activities of daily living
      (adl), instrumental activities of daily living (iadl) and associated factors, as predictors
      of morbidity and mortality," *Archives of Gerontology and Geriatrics*, vol. 50, no. 3,
      pp. 306–310, May 2010, ISSN: 0167-4943. DOI: `10.1016/j.archger.2009.04.017`.
      [Online]. Available: `http://dx.doi.org/10.1016/j.archger.2009.04.017`.

[47] N. Digital, *Health survey for england 2021: Social care*, Accessed: 2024-06-25, May
      2021. [Online]. Available: `https://digital.nhs.uk/data-and-information/`
      `publications/statistical/health-survey-for-england/2021-part-2/social-`
      `care`.

[48] N. Bleijenberg, N. P. A. Zuithoff, A. K. Smith, N. J. de Wit, and M. J. Schuurmans,
      "Disability in the individual adl, iadl, and mobility among older adults: A prospective
      cohort study," *The journal of nutrition, health $; aging*, vol. 21, no. 8, pp. 897–903,

Feb. 2017, ISSN: 1760-4788. DOI: 10.1007/s12603-017-0891-6. [Online]. Available: http://dx.doi.org/10.1007/s12603-017-0891-6.

[49] E. Lunt, T. Ong, A. L. Gordon, P. L. Greenhaff, and J. R. F. Gladman, "The clinical usefulness of muscle mass and strength measures in older people: A systematic review," en, *Age Ageing*, vol. 50, no. 1, pp. 88–95, Jan. 2021.

[50] R. Hacihasanoğlu, A. Yildirim, and P. Karakurt, "Loneliness in elderly individuals, level of dependence in activities of daily living (adl) and influential factors," *Archives of Gerontology and Geriatrics*, vol. 54, no. 1, pp. 61–66, 2012, ISSN: 0167-4943. DOI: https://doi.org/10.1016/j.archger.2011.03.011. [Online]. Available: https://www.sciencedirect.com/science/article/pii/S0167494311000793.

[51] D. Schoene, C. Heller, Y. N. Aung, C. C. Sieber, W. Kemmler, and E. Freiberger, "A systematic review on the influence of fear of falling on quality of life in older people: Is there a role for falls?" en, *Clin. Interv. Aging*, vol. 14, pp. 701–719, Apr. 2019.

[52] U. B. of Labor Statistics, *American time use survey - 2019 results*, Accessed: 2024-06-25, Jun. 2020. [Online]. Available: https://www.bls.gov/news.release/archives/atus_06252020.pdf.

[53] O. for National Statistics, *Time use in the uk: March 2023*, https://www.ons.gov.uk, Statistical Bulletin, released 04 July 2023, Jul. 2023.

[54] A. A. Schmid, M. Van Puymbroeck, and D. M. Koceja, "Effect of a 12-week yoga intervention on fear of falling and balance in older adults: A pilot study," *Archives of physical medicine and rehabilitation*, vol. 91, no. 4, pp. 576–583, 2010.

[55] O. A. Coubard, L. Ferrufino, T. Nonaka, O. Zelada, B. Bril, and G. Dietrich, "One month of contemporary dance modulates fractal posture in aging," *Frontiers in aging neuroscience*, vol. 6, p. 17, 2014.

[56] G. Pliske, P. Emmermacher, V. Weinbeer, and K. Witte, "Changes in dual-task performance after 5 months of karate and fitness training for older adults to enhance fall prevention," *Aging clinical and experimental research*, vol. 28, pp. 1179–1186, 2016.

[57] M. Grimmer, R. Riener, C. J. Walsh, and A. Seyfarth, "Mobility related physical and functional losses due to aging and disease - a motivation for lower limb exoskeletons," *Journal of NeuroEngineering and Rehabilitation*, vol. 16, no. 1, Jan. 2019, ISSN: 1743-

0003. DOI: `10.1186/s12984-018-0458-8`. [Online]. Available: `http://dx.doi.org/10.1186/s12984-018-0458-8`.

[58] M. Appeadu and B. Bordoni, *Falls and Fall Prevention in Older Adults* (StatPearls), Updated 2023 Jun 4. Treasure Island (FL): StatPearls Publishing, Jun. 2023, Available from: https://www.ncbi.nlm.nih.gov/books/NBK560761/. [Online]. Available: `https://www.ncbi.nlm.nih.gov/books/NBK560761/`.

[59] K. Devinuwara, A. Dworak-Kula, and R. J. O'Connor, "Rehabilitation and prosthetics post-amputation," *Orthopaedics and Trauma*, vol. 32, no. 4, pp. 234–240, Aug. 2018, ISSN: 1877-1327. DOI: `10.1016/j.mporth.2018.05.007`. [Online]. Available: `http://dx.doi.org/10.1016/j.mporth.2018.05.007`.

[60] S. Association, *Balance problems after stroke: A guide*, Accessed: 2024-06-25, Jan. 2024. [Online]. Available: `https://www.stroke.org.uk/balance_problems_after_stroke_guide.pdf`.

[61] N. E. Fritz *et al.*, "Motor performance differentiates individuals with lewy body dementia, parkinson's and alzheimer's disease," *Gait &; Posture*, vol. 50, pp. 1–7, Oct. 2016, ISSN: 0966-6362. DOI: `10.1016/j.gaitpost.2016.08.009`. [Online]. Available: `http://dx.doi.org/10.1016/j.gaitpost.2016.08.009`.

[62] W. H. Organization, *Worldwide prevalence of anaemia 1993-2005: WHO global database on anaemia*. World Health Organization, 2008, Accessed: 2024-06-25. [Online]. Available: `https://iris.who.int/bitstream/handle/10665/43811/9789241563536_eng.pdf?sequence=1`.

[63] O. for Health Improvement and Disparities, *Public health profiles*, `https://fingertips.phe.org.uk/search/falls`, Accessed: 2024-06-26, 2024.

[64] K. Christensen, G. Doblhammer, R. Rau, and J. W. Vaupel, "Ageing populations: The challenges ahead," en, *Lancet*, vol. 374, no. 9696, pp. 1196–1208, Oct. 2009.

[65] L. B. Murphy *et al.*, "One in four people may develop symptomatic hip osteoarthritis in his or her lifetime," en, *Osteoarthritis Cartilage*, vol. 18, no. 11, pp. 1372–1379, Nov. 2010.

REFERENCES

[66] A. UK, *Later life in the united kingdom*, `https://www.ageuk.org.uk/globalassets/age-uk/documents/reports-and-publications/later_life_uk_factsheet.pdf`, Accessed: 2024-06-26, May 2019.

[67] B. R. Bloem, J. A. G. Steijns, and B. C. Smits-Engelsman, "An update on falls," en, *Curr. Opin. Neurol.*, vol. 16, no. 1, pp. 15–26, Feb. 2003.

[68] M. Sandberg, J. Kristensson, P. Midlöv, C. Fagerström, and U. Jakobsson, "Prevalence and predictors of healthcare utilization among older people (60+): Focusing on ADL dependency and risk of depression," en, *Arch. Gerontol. Geriatr.*, vol. 54, no. 3, e349–63, May 2012.

[69] D. A. Ganz, Y. Bao, P. G. Shekelle, and L. Z. Rubenstein, "Will my patient fall?" en, *JAMA*, vol. 297, no. 1, pp. 77–86, Jan. 2007.

[70] GBD 2016 Stroke Collaborators, "Global, regional, and national burden of stroke, 1990-2016: A systematic analysis for the global burden of disease study 2016," en, *Lancet Neurol.*, vol. 18, no. 5, pp. 439–458, May 2019.

[71] S. Association, *Stroke statistics*, `https://www.stroke.org.uk/stroke/statistics`, Accessed: 2024-06-26, 2024.

[72] A.-L. Hsu, P.-F. Tang, and M.-H. Jan, "Analysis of impairments influencing gait velocity and asymmetry of hemiplegic patients after mild to moderate stroke11no commercial party having a direct financial interest in the results of the research supporting this article has or will confer a benefit upon the authors(s) or upon any organization with which the author(s) is/are associated," en, *Arch. Phys. Med. Rehabil.*, vol. 84, no. 8, pp. 1185–1193, Aug. 2003.

[73] M. D. Lewek, C. E. Bradley, C. J. Wutzke, and S. M. Zinder, "The relationship between spatiotemporal gait asymmetry and balance in individuals with chronic stroke," en, *J. Appl. Biomech.*, vol. 30, no. 1, pp. 31–36, Feb. 2014.

[74] K. K. Patterson *et al.*, "Gait asymmetry in community-ambulating stroke survivors," en, *Arch. Phys. Med. Rehabil.*, vol. 89, no. 2, pp. 304–310, Feb. 2008.

[75] R. Mc Ardle, R. Morris, J. Wilson, B. Galna, A. J. Thomas, and L. Rochester, "What can quantitative gait analysis tell us about dementia and its subtypes? a structured review," *J. Alzheimers. Dis.*, vol. 60, no. 4, pp. 1295–1312, Nov. 2017.

[76] J. Verghese, R. B. Lipton, C. B. Hall, G. Kuslansky, M. J. Katz, and H. Buschke, "Abnormality of gait as a predictor of non-alzheimer's dementia," en, *N. Engl. J. Med.*, vol. 347, no. 22, pp. 1761–1768, Nov. 2002.

[77] M. Prince, A. Wimo, M. Guerchet, G.-C. Ali, Y.-T. Wu, and M. Prina, "World alzheimer report 2015: The global impact of dementia - an analysis of prevalence, incidence, cost and trends," Alzheimer's Disease International (ADI), 2015. [Online]. Available: `https://www.alzint.org/u/WorldAlzheimerReport2015.pdf`.

[78] R. Mc Ardle, S. Del Din, B. Galna, A. Thomas, and L. Rochester, "Differentiating dementia disease subtypes with gait analysis: Feasibility of wearable sensors?" en, *Gait Posture*, vol. 76, pp. 372–376, Feb. 2020.

[79] O. Beauchet *et al.*, "Poor gait performance and prediction of dementia: Results from a meta-analysis," en, *J. Am. Med. Dir. Assoc.*, vol. 17, no. 6, pp. 482–490, Jun. 2016.

[80] O. Beauchet, G. Allali, G. Berrut, C. Hommet, V. Dubost, and F. Assal, "Gait analysis in demented subjects: Interests and perspectives," en, *Neuropsychiatr. Dis. Treat.*, vol. 4, no. 1, pp. 155–160, Feb. 2008.

[81] L. M. Allan, C. G. Ballard, E. N. Rowan, and R. A. Kenny, "Incidence and prediction of falls in dementia: A prospective study in older people," en, *PLoS One*, vol. 4, no. 5, e5521, May 2009.

[82] N. Ghasemi, S. Razavi, and E. Nikzad, "Multiple sclerosis: Pathogenesis, symptoms, diagnoses and cell-based therapy," en, *Cell J.*, vol. 19, no. 1, pp. 1–10, Apr. 2017.

[83] R. Mazumder, C. Murchison, D. Bourdette, and M. Cameron, "Falls in people with multiple sclerosis compared with falls in healthy controls," en, *PLoS One*, vol. 9, no. 9, e107620, Sep. 2014.

[84] S. Coote, J. J. Sosnoff, and H. Gunn, "Fall incidence as the primary outcome in multiple sclerosis falls-prevention trials: Recommendation from the international MS falls prevention research network," en, *Int. J. MS Care*, vol. 16, no. 4, pp. 178–184, 2014.

[85] M. H. Cameron, A. J. Poel, J. K. Haselkorn, A. Linke, and D. Bourdette, "Falls requiring medical attention among veterans with multiple sclerosis: A cohort study," en, *J. Rehabil. Res. Dev.*, vol. 48, no. 1, pp. 13–20, 2011.

REFERENCES

[86] P. N. Matsuda, A. Shumway-Cook, A. M. Bamer, S. L. Johnson, D. Amtmann, and G. H. Kraft, "Falls in multiple sclerosis," en, *PM R*, vol. 3, no. 7, 624–32, quiz 632, Jul. 2011.

[87] E. W. Peterson, C. C. Cho, L. von Koch, and M. L. Finlayson, "Injurious falls among middle aged and older adults with multiple sclerosis," en, *Arch. Phys. Med. Rehabil.*, vol. 89, no. 6, pp. 1031–1037, Jun. 2008.

[88] F. N. Emamzadeh and A. Surguchov, "Parkinson's disease: Biomarkers, treatment, and risk factors," en, *Front. Neurosci.*, vol. 12, p. 612, Aug. 2018.

[89] R. B. Postuma, A. E. Lang, J. F. Gagnon, A. Pelletier, and J. Y. Montplaisir, "How does parkinsonism start? prodromal parkinsonism motor changes in idiopathic REM sleep behaviour disorder," en, *Brain*, vol. 135, no. Pt 6, pp. 1860–1870, Jun. 2012.

[90] S. Del Din *et al.*, "Gait analysis with wearables predicts conversion to parkinson disease," en, *Ann. Neurol.*, vol. 86, no. 3, pp. 357–367, Sep. 2019.

[91] C. G. Canning, S. S. Paul, and A. Nieuwboer, "Prevention of falls in parkinson's disease: A review of fall risk factors and the role of physical interventions," en, *Neurodegener. Dis. Manag.*, vol. 4, no. 3, pp. 203–221, 2014.

[92] J. G. Nutt, B. R. Bloem, N. Giladi, M. Hallett, F. B. Horak, and A. Nieuwboer, "Freezing of gait: Moving forward on a mysterious clinical phenomenon," en, *Lancet Neurol.*, vol. 10, no. 8, pp. 734–744, Aug. 2011.

[93] J. D. Schaafsma, Y. Balash, T. Gurevich, A. L. Bartels, J. M. Hausdorff, and N. Giladi, "Characterization of freezing of gait subtypes and the response of each to levodopa in parkinson's disease," en, *Eur. J. Neurol.*, vol. 10, no. 4, pp. 391–398, Jul. 2003.

[94] M. Bächlin *et al.*, "Wearable assistant for parkinson's disease patients with the freezing of gait symptom," en, *IEEE Trans. Inf. Technol. Biomed.*, vol. 14, no. 2, pp. 436–446, Mar. 2010.

[95] N. Giladi and A. Nieuwboer, "Understanding and treating freezing of gait in parkinsonism, proposed working definition, and setting the stage," en, *Mov. Disord.*, vol. 23 Suppl 2, no. S2, S423–5, 2008.

[96] A. Sabzi Sarvestani and A. Taheri Azam, "Amputation: A ten-year survey," en, *Trauma Mon.*, vol. 18, no. 3, pp. 126–129, Dec. 2013.

[97] J. M. van Velzen, C. A. M. van Bennekom, W. Polomski, J. R. Slootman, L. H. V. van der Woude, and H. Houdijk, "Physical capacity and walking ability after lower limb amputation: A systematic review," en, *Clin. Rehabil.*, vol. 20, no. 11, pp. 999–1016, Nov. 2006.

[98] P. M. Stevens and S. R. Wurdeman, "Prosthetic knee selection for individuals with unilateral transfemoral amputation: A clinical practice guideline," en, *J. Prosthet. Orthot.*, vol. 31, no. 1, pp. 2–8, Jan. 2019.

[99] H. R. Batten, S. M. McPhail, A. M. Mandrusiak, P. N. Varghese, and S. S. Kuys, "Gait speed as an indicator of prosthetic walking potential following lower limb amputation," en, *Prosthet. Orthot. Int.*, vol. 43, no. 2, pp. 196–203, Apr. 2019.

[100] D. E. Hurwitz, D. R. Sumner, and J. A. Block, "Bone density, dynamic joint loading and joint degeneration. a review," en, *Cells Tissues Organs*, vol. 169, no. 3, pp. 201–209, 2001.

[101] J. S. Brach, S. A. Studenski, S. Perera, J. M. VanSwearingen, and A. B. Newman, "Gait variability and the risk of incident mobility disability in community-dwelling older adults," *J. Gerontol. A Biol. Sci. Med. Sci.*, vol. 62, no. 9, pp. 983–988, Sep. 2007.

[102] S. W. Hunter, F. Batchelor, K. D. Hill, A.-M. Hill, S. Mackintosh, and M. Payne, "Risk factors for falls in people with a lower limb amputation: A systematic review," en, *PM R*, vol. 9, no. 2, p. 170, Feb. 2017.

[103] C. M. Kim and J. J. Eng, "Symmetry in vertical ground reaction force is accompanied by symmetry in temporal but not distance variables of gait in persons with stroke," en, *Gait Posture*, vol. 18, no. 1, pp. 23–28, Aug. 2003.

[104] L. Z. Rubenstein, "Falls in older people: Epidemiology, risk factors and strategies for prevention," en, *Age Ageing*, vol. 35 Suppl 2, no. suppl_2, pp. ii37–ii41, Sep. 2006.

[105] B. R. Connell and S. L. Wolf, "Environmental and behavioral circumstances associated with falls at home among healthy elderly individuals," *Archives of Physical Medicine and Rehabilitation*, vol. 78, no. 2, pp. 179–186, 1997, ISSN: 0003-9993. DOI: https://doi.org/10.1016/S0003-9993(97)90261-6. [Online]. Available: https://www.sciencedirect.com/science/article/pii/S0003999397902616.

REFERENCES

[106] C. Brundle *et al.*, "The causes of falls: Views of older people with visual impairment," *Health Expectations*, vol. 18, no. 6, pp. 2021–2031, 2015. DOI: `https://doi.org/10.1111/hex.12355`. eprint: `https://onlinelibrary.wiley.com/doi/pdf/10.1111/hex.12355`. [Online]. Available: `https://onlinelibrary.wiley.com/doi/abs/10.1111/hex.12355`.

[107] E. Gibson, G. Douglas, K. Jeffries, J. Delaurier, T. Chestnut, and J. M. Charlton, "Foot orientation and trajectory variability in locomotion: Effects of real-world terrain," *PLOS ONE*, vol. 19, no. 5, pp. 1–17, May 2024. DOI: `10.1371/journal.pone.0293691`. [Online]. Available: `https://doi.org/10.1371/journal.pone.0293691`.

[108] M.-S. Kang *et al.*, "Effect of surface properties on gait characteristics," *Indian Journal of Science and Technology*, vol. 9, no. 46, pp. 1–5, 2016.

[109] S. B. Thies, J. K. Richardson, and J. A. Ashton-Miller, "Effects of surface irregularity and lighting on step variability during gait: A study in healthy young and older women," *Gait & Posture*, vol. 22, no. 1, pp. 26–31, 2005, ISSN: 0966-6362. DOI: `https://doi.org/10.1016/j.gaitpost.2004.06.004`. [Online]. Available: `https://www.sciencedirect.com/science/article/pii/S0966636204001110`.

[110] J. C. Menant, J. R. Steele, H. B. Menz, B. J. Munro, and S. R. Lord, "Effects of walking surfaces and footwear on temporo-spatial gait parameters in young and older people," *Gait & Posture*, vol. 29, no. 3, pp. 392–397, 2009, ISSN: 0966-6362. DOI: `https://doi.org/10.1016/j.gaitpost.2008.10.057`. [Online]. Available: `https://www.sciencedirect.com/science/article/pii/S096663620800355X`.

[111] S. Demura, S. Shin, S. Takahashi, and S. Yamaji, "Relationships between gait properties on soft surfaces, physical function, and fall risk for the elderly," *Adv. Aging Res.*, vol. 02, no. 02, pp. 57–64, 2013.

[112] R. J. Downey *et al.*, "Uneven terrain treadmill walking in younger and older adults," *PLOS ONE*, vol. 17, no. 12, pp. 1–21, Dec. 2022. DOI: `10.1371/journal.pone.0278646`. [Online]. Available: `https://doi.org/10.1371/journal.pone.0278646`.

[113] R. J. O'Connor and M. U. Kini, "Non-pharmacological and non-surgical interventions for tremor: A systematic review," *Parkinsonism & Related Disorders*, vol. 17, no. 7, pp. 509–515, Aug. 2011, ISSN: 1353-8020. DOI: `10.1016/j.parkreldis.2010.12.016`. [Online]. Available: `http://dx.doi.org/10.1016/j.parkreldis.2010.12.016`.

[114] B. Kwolek and M. Kepski, "Human fall detection on embedded platform using depth maps and wireless accelerometer," *Computer Methods and Programs in Biomedicine*, vol. 117, no. 3, pp. 489–501, 2014, ISSN: 0169-2607. DOI: `https://doi.org/10.1016/j.cmpb.2014.09.005`. [Online]. Available: `https://www.sciencedirect.com/science/article/pii/S0169260714003447`.

[115] I. Charfi, J. Miteran, J. Dubois, M. Atri, and R. Tourki, "Definition and performance evaluation of a robust svm based fall detection solution," in *2012 Eighth International Conference on Signal Image Technology and Internet Based Systems*, 2012, pp. 218–224. DOI: `10.1109/SITIS.2012.155`.

[116] E. Auvinet, F. Multon, A. Saint-Arnaud, J. Rousseau, and J. Meunier, "Fall detection with multiple cameras: An occlusion-resistant method based on 3-d silhouette vertical distribution," *IEEE Transactions on Information Technology in Biomedicine*, vol. 15, no. 2, pp. 290–300, 2011. DOI: `10.1109/TITB.2010.2087385`.

[117] C. Dhiman and D. K. Vishwakarma, "A robust framework for abnormal human action recognition using r-transform and zernike moments in depth videos," *Ieee Sensors Journal*, vol. 19, no. 13, pp. 5195–5203, 2019, 766, fall detection, ISSN: 1530-437X. DOI: `10.1109/jsen.2019.2903645`. [Online]. Available: `https://ieeexplore.ieee.org/document/8662635/`.

[118] F. Harrou, N. Zerrouki, Y. Sun, and A. Houacine, "Vision-based fall detection system for improving safety of elderly people," *IEEE Instrumentation & Measurement Magazine*, vol. 20, no. 6, pp. 49–55, 2017, ISSN: 1941-0123. DOI: `10.1109/MIM.2017.8121952`. [Online]. Available: `https://ieeexplore.ieee.org/document/8121952/`.

[119] L. Panahi and V. Ghods, "Human fall detection using machine vision techniques on rgb-d images," *Biomedical Signal Processing and Control*, vol. 44, pp. 146–153, 2018, 2472, fall detection, ISSN: 1746-8094. DOI: `10.1016/j.bspc.2018.04.014`.

[120] T. H. Tran, T. L. Le, V. N. Hoang, and H. Vu, "Continuous detection of human fall using multimodal features from kinect sensors in scalable environment," *Computer Methods and Programs in Biomedicine*, vol. 146, pp. 151–165, 2017, 3312, fall detection, ISSN: 0169-2607. DOI: `10.1016/j.cmpb.2017.05.007`.

[121] T. Vaiyapuri, E. L. Lydia, M. Y. Sikkandar, V. G. Díaz, I. V. Pustokhina, and D. A. Pustokhin, "Internet of things and deep learning enabled elderly fall detection model

for smart homecare," *IEEE Access*, vol. 9, pp. 113 879–113 888, 2021. DOI: `10.1109/`
`ACCESS.2021.3094243`.

[122] X. Xiong, W. D. Min, W. S. Zheng, P. Liao, H. Yang, and S. Wang, "S3d-cnn: Skeleton-based 3d consecutive-low-pooling neural network for fall detection," *Applied Intelligence*, vol. 50, no. 10, pp. 3521–3534, 2020, 3584, fall detection, ISSN: 0924-669X. DOI: `10.1007/` `s10489-020-01751-y`. [Online]. Available: `https://link.springer.com/article/10.` `1007/s10489-020-01751-y`.

[123] Y. X. Yun and I. Y. H. Gu, "Human fall detection in videos by fusing statistical features of shape and motion dynamics on riemannian manifolds," *Neurocomputing*, vol. 207, pp. 726–734, 2016, 3699, fall detection, ISSN: 0925-2312. DOI: `10.1016/j.neucom.2016.` `05.058`.

[124] Y. X. Yun and I. Y. H. Gu, "Human fall detection in videos via boosting and fusing statistical features of appearance, shape and motion dynamics on riemannian manifolds with applications to assisted living," *Computer Vision and Image Understanding*, vol. 148, pp. 111–122, 2016, 3700, fall detection, ISSN: 1077-3142. DOI: `10.1016/j.cviu.2015.` `12.002`.

[125] Y. Wang and T. Deng, "Enhancing elderly care: Efficient and reliable real-time fall detection algorithm," *DIGITAL HEALTH*, vol. 10, Jan. 2024, ISSN: 2055-2076. DOI: `10.1177/20552076241233690`. [Online]. Available: `http://dx.doi.org/10.1177/` `20552076241233690`.

[126] J. Klenk *et al.*, "The farseeing real-world fall repository: A large-scale collaborative database to collect and share sensor signals from real-world falls," *European Review of Aging and Physical Activity*, vol. 13, no. 1, Oct. 2016, ISSN: 1861-6909. DOI: `10.1186/` `s11556-016-0168-9`. [Online]. Available: `http://dx.doi.org/10.1186/s11556-016-` `0168-9`.

[127] M. S. Alzahrani, S. K. Jarraya, M. A. Salamah, and H. Ben-Abdallah, "Fallfree: Multiple fall scenario dataset of cane users for monitoring applications using kinect," in *2017 13th International Conference on Signal-Image Technology & Internet-Based Systems (SITIS)*, 2017, pp. 327–333. DOI: `10.1109/SITIS.2017.61`.

[128] A. Sucerquia, J. D. López, and J. F. Vargas-Bonilla, "SisFall: A fall and movement dataset," en, *Sensors (Basel)*, vol. 17, no. 1, Jan. 2017.

[129] E. Casilari, J. A. Santoyo-Ramón, and J. M. Cano-García, "Umafall: A multisensor dataset for the research on automatic fall detection," *Procedia Computer Science*, vol. 110, pp. 32–39, 2017, 14th International Conference on Mobile Systems and Pervasive Computing (MobiSPC 2017) / 12th International Conference on Future Networks and Communications (FNC 2017) / Affiliated Workshops, ISSN: 1877-0509. DOI: `https://doi.org/10.1016/j.procs.2017.06.110`. [Online]. Available: `https://www.sciencedirect.com/science/article/pii/S1877050917312899`.

[130] A. T. Özdemir and B. Barshan, "Detecting falls with wearable sensors using machine learning techniques," *Sensors*, vol. 14, no. 6, pp. 10 691–10 708, 2014, ISSN: 1424-8220. DOI: `10.3390/s140610691`. [Online]. Available: `https://www.mdpi.com/1424-8220/14/6/10691`.

[131] M. Saleh, M. Abbas, and R. B. L. Jeannès, "Fallalld: An open dataset of human falls and activities of daily living for classical and deep learning applications," *IEEE Sensors Journal*, vol. 21, no. 2, pp. 1849–1858, 2021, ISSN: 1558-1748. DOI: `10.1109/JSEN.2020.3018335`. [Online]. Available: `https://ieeexplore.ieee.org/document/9171857/`.

[132] S. Gaglio, G. L. Re, and M. Morana, "Human activity recognition process using 3-d posture data," *IEEE Transactions on Human-Machine Systems*, vol. 45, no. 5, pp. 586–597, 2015. DOI: `10.1109/THMS.2014.2377111`.

[133] I. Charfi, J. Miteran, J. Dubois, M. Atri, and R. Tourki, "Optimised spatio-temporal descriptors for real-time fall detection : Comparison of svm and adaboost based classification," Oct. 2013.

[134] J. wang, X. Nie, Y. Xia, Y. Wu, and S.-C. Zhu, *Cross-view action modeling, learning and recognition*, 2014. arXiv: `1405.2941 [cs.CV]`.

[135] E. Auvinet, L. Reveret, A. St-Arnaud, J. Rousseau, and J. Meunier, "Fall detection using multiple cameras," in *2008 30th Annual International Conference of the IEEE Engineering in Medicine and Biology Society*, 2008, pp. 2554–2557. DOI: `10.1109/IEMBS.2008.4649721`.

[136] G. Baldewijns, G. Debard, G. Mertes, B. Vanrumste, and T. Croonenborghs, "Bridging the gap between real-life data and simulated data by providing a highly realistic fall dataset for evaluating camera-based fall detection algorithms," *Healthcare Technology Letters*, vol. 3, no. 1, pp. 6–11, 2016. DOI: `https://doi.org/10.1049/htl.2015.0047`.

eprint: `https://ietresearch.onlinelibrary.wiley.com/doi/pdf/10.1049/htl.2015.0047`. [Online]. Available: `https://ietresearch.onlinelibrary.wiley.com/doi/abs/10.1049/htl.2015.0047`.

[137] X. Ma, H. Wang, B. Xue, M. Zhou, B. Ji, and Y. Li, "Depth-based human fall detection via shape features and improved extreme learning machine," *IEEE Journal of Biomedical and Health Informatics*, vol. 18, no. 6, pp. 1915–1922, 2014. DOI: `10.1109/JBHI.2014.2304357`.

[138] L. Martínez-Villaseñor, H. Ponce, J. Brieva, E. Moya-Albor, J. Núñez-Martínez, and C. Peñafort-Asturiano, "UP-Fall detection dataset: A multimodal approach," en, *Sensors (Basel)*, vol. 19, no. 9, Apr. 2019.

[139] P. Mazurek, J. Wagner, and R. Z. Morawski, "Use of kinematic and mel-cepstrum-related features for fall detection based on data from infrared depth sensors," *Biomedical Signal Processing and Control*, vol. 40, pp. 102–110, 2018, 2119, fall detection, ISSN: 1746-8094. DOI: `10.1016/j.bspc.2017.09.006`.

[140] S. Gasparrini *et al.*, "Proposal and experimental evaluation of fall detection solution based on wearable and depth data fusion," in *ICT Innovations 2015*, S. Loshkovska and S. Koceski, Eds., Cham: Springer International Publishing, 2016, pp. 99–108, ISBN: 978-3-319-25733-4.

[141] M. Saleh, M. Abbas, J. Prud'Homm, D. Somme, and R. L. B. Jeannès, "A reliable fall detection system based on analyzing the physical activities of older adults living in long-term care facilities," *IEEE Transactions on Neural Systems and Rehabilitation Engineering*, vol. 29, pp. 2587–2594, 2021, ISSN: 1558-0210. DOI: `10.1109/TNSRE.2021.3133616`. [Online]. Available: `https://ieeexplore.ieee.org/ielx7/7333/9363468/09641843.pdf?tp=%5C&arnumber=9641843%5C&isnumber=9363468%5C&ref=`.

[142] S. Saurav, R. Saini, and S. Singh, "Vision-based techniques for fall detection in 360 degrees videos using deep learning: Dataset and baseline results," *Multimedia Tools and Applications*, 2859, fall detection, ISSN: 1380-7501. DOI: `10.1007/s11042-022-12366-5`. [Online]. Available: `https://link.springer.com/article/10.1007/s11042-022-12366-5`.

[143] C. Medrano, R. Igual, I. Plaza, and M. Castro, "Detecting falls as novelties in acceleration patterns acquired with smartphones," *PLOS ONE*, vol. 9, no. 4, pp. 1–9, Apr. 2014. DOI:

`10.1371/journal.pone.0094811`. [Online]. Available: `https://doi.org/10.1371/journal.pone.0094811`.

[144] L. Xia, C.-C. Chen, and J. K. Aggarwal, "View invariant human action recognition using histograms of 3d joints," in *2012 IEEE Computer Society Conference on Computer Vision and Pattern Recognition Workshops*, 2012, pp. 20–27. DOI: `10.1109/CVPRW.2012.6239233`.

[145] Z. Cheng, L. Qin, Y. Ye, Q. Huang, and Q. Tian, "Human daily action analysis with multi-view and color-depth data," in *Computer Vision – ECCV 2012. Workshops and Demonstrations*, A. Fusiello, V. Murino, and R. Cucchiara, Eds., Berlin, Heidelberg: Springer Berlin Heidelberg, 2012, pp. 52–61, ISBN: 978-3-642-33868-7.

[146] O. Aziz, E. J. Park, G. Mori, and S. N. Robinovitch, "Distinguishing the causes of falls in humans using an array of wearable tri-axial accelerometers," *Gait & Posture*, vol. 39, no. 1, pp. 506–512, 2014, 200, fall prevention, ISSN: 0966-6362. DOI: `10.1016/j.gaitpost.2013.08.034`.

[147] F. S. Butt, L. L. Blunda, M. F. Wagner, J. Schafer, I. Medina-Bulo, and D. Gomez-Ullate, "Fall detection from electrocardiogram (ecg) signals and classification by deep transfer learning," *Information*, vol. 12, no. 2, 2021, 411, fall prevention. DOI: `10.3390/info12020063`. [Online]. Available: `https://mdpi-res.com/d_attachment/information/information-12-00063/article_deploy/information-12-00063-v2.pdf?version=1612678501`.

[148] K. H. Chen, Y. W. Hsu, J. J. Yang, and F. S. Jaw, "Evaluating the specifications of built-in accelerometers in smartphones on fall detection performance," *Instrumentation Science & Technology*, vol. 46, no. 2, pp. 194–206, 2018, 514, fall detection, ISSN: 1073-9149. DOI: `10.1080/10739149.2017.1363054`.

[149] C. Garripoli *et al.*, "Embedded dsp-based telehealth radar system for remote in-door fall detection," *IEEE J Biomed Health Inform*, vol. 19, no. 1, pp. 92–101, 2015, ISSN: 2168-2194. DOI: `10.1109/jbhi.2014.2361252`. [Online]. Available: `https://ieeexplore.ieee.org/document/6914524/`.

[150] R. Narasimhan, "Skin-contact sensor for automatic fall detection," *Annu Int Conf IEEE Eng Med Biol Soc*, vol. 2012, pp. 4038–41, 2012, ISSN: 2375-7477. DOI: `10.1109/embc.`

REFERENCES

2012.6346853. [Online]. Available: `https : / / ieeexplore . ieee . org / document / 6346853/`.

[151] M. Yu, Y. Yu, A. Rhuma, S. M. Naqvi, L. Wang, and J. A. Chambers, "An online one class support vector machine-based person-specific fall detection system for monitoring an elderly individual in a room environment," *IEEE J Biomed Health Inform*, vol. 17, no. 6, pp. 1002–14, 2013, ISSN: 2168-2194. DOI: `10.1109/jbhi.2013.2274479`. [Online]. Available: `https://ieeexplore.ieee.org/document/6566012/`.

[152] A. E. Attaoui, S. Largo, S. Kaissari, A. Benba, A. Jilbab, and A. Bourouhou, "Machine learning-based edge-computing on a multi-level architecture of wsn and iot for real-time fall detection," *Iet Wireless Sensor Systems*, vol. 10, no. 6, pp. 320–332, 2020, 861, fall detection, ISSN: 2043-6386. DOI: `10.1049/iet-wss.2020.0091`.

[153] E. A. de la Cal, M. Fanez, M. Villar, J. R. Villar, and V. M. Gonzalez, "A low-power har method for fall and high-intensity adls identification using wrist-worn accelerometer devices," *Logic Journal of the IGPL*, 716, fall intervention, ISSN: 1367-0751. DOI: `10.1093/jigpal/jzac025`. [Online]. Available: `https://academic.oup.com/jigpal/advance-article - abstract / doi / 10 . 1093 / jigpal / jzac025 / 6539735 ? redirectedFrom = fulltext`.

[154] S. S. Kambhampati, V. Singh, M. S. Manikandan, and B. Ramkumar, "Unified framework for triaxial accelerometer-based fall event detection and classification using cumulants and hierarchical decision tree classifier," *Healthc Technol Lett*, vol. 2, no. 4, pp. 101–7, 2015, ISSN: 2053-3713 (Print). [Online]. Available: `https://www.ncbi.nlm.nih.gov/pmc/articles/PMC4612541/pdf/HTL.2015.0018.pdf`.

[155] C. H. Li, M. Lin, L. T. Yang, and C. Ding, "Integrating the enriched feature with machine learning algorithms for human movement and fall detection," *Journal of Supercomputing*, vol. 67, no. 3, pp. 854–865, 2014, 1797, fall detection, ISSN: 0920-8542. DOI: `10.1007/s11227-013-1056-y`. [Online]. Available: `https://link.springer.com/article/10.1007/s11227-013-1056-y`.

[156] G. Sengul, M. Karakaya, S. Misra, O. O. Abayomi-Alli, and R. Damasevicius, "Deep learning based fall detection using smartwatches for healthcare applications," *Biomedical Signal Processing and Control*, vol. 71, 2022, 2913, fall detection, ISSN: 1746-8094. DOI: `10.1016/j.bspc.2021.103242`.

[157] R. Shrivastava and M. Pandey, "Real time fall detection in fog computing scenario," *Cluster Computing*, vol. 23, no. 4, pp. 2861–2870, Jan. 2020, ISSN: 1573-7543. DOI: `10.1007/s10586-020-03051-z`. [Online]. Available: `http://dx.doi.org/10.1007/s10586-020-03051-z`.

[158] F. Wu, H. Zhao, Y. Zhao, and H. Zhong, "Development of a wearable-sensor-based fall detection system," *Int J Telemed Appl*, vol. 2015, p. 576 364, 2015, ISSN: 1687-6415 (Print). [Online]. Available: `https://www.ncbi.nlm.nih.gov/pmc/articles/PMC4346101/pdf/IJTA2015-576364.pdf`.

[159] A. Alarifi and A. Alwadain, "Killer heuristic optimized convolution neural network-based fall detection with wearable iot sensor devices," *Measurement*, vol. 167, 2021, 73, fall detection, ISSN: 0263-2241. DOI: `10.1016/j.measurement.2020.108258`.

[160] Y. F. Wu, Y. W. Su, R. J. Feng, N. Yu, and X. Zang, "Wearable-sensor-based pre-impact fall detection system with a hierarchical classifier," *Measurement*, vol. 140, pp. 283–292, 2019, 3564, fall detection, ISSN: 0263-2241. DOI: `10.1016/j.measurement.2019.04.002`.

[161] Y. Lee, S. Pokharel, A. A. Muslim, D. B. KC, K. H. Lee, and W.-H. Yeo, "Experimental study: Deep learning-based fall monitoring among older adults with skin-wearable electronics," *Sensors*, vol. 23, no. 8, 2023, ISSN: 1424-8220. DOI: `10.3390/s23083983`. [Online]. Available: `https://www.mdpi.com/1424-8220/23/8/3983`.

[162] O. Ribeiro, L. Gomes, and Z. Vale, "Iot-based human fall detection system," *Electronics*, vol. 11, no. 4, 2022, 2696, fall prevention. DOI: `10.3390/electronics11040592`. [Online]. Available: `https://mdpi-res.com/d_attachment/electronics/electronics-11-00592/article_deploy/electronics-11-00592.pdf?version=1644917636`.

[163] M. S. Alzahrani, S. K. Jarraya, H. Ben-Abdallah, and M. S. Ali, "Comprehensive evaluation of skeleton features-based fall detection from microsoft kinect v2," *Signal Image and Video Processing*, vol. 13, no. 7, pp. 1431–1439, 2019, 107, fall detection.

[164] B. Kwolek and M. Kepski, "Human fall detection on embedded platform using depth maps and wireless accelerometer," *Computer Methods and Programs in Biomedicine*, vol. 117, no. 3, pp. 489–501, 2014, 1710, fall detection, ISSN: 0169-2607. DOI: `10.1016/j.cmpb.2014.09.005`.

REFERENCES

[165] B. Kwolek and M. Kepski, "Improving fall detection by the use of depth sensor and accelerometer," *Neurocomputing*, vol. 168, pp. 637–645, 2015, 1711, fall detection, ISSN: 0925-2312. DOI: `10.1016/j.neucom.2015.05.061`.

[166] B. Kwolek and M. Kepski, "Fuzzy inference-based fall detection using kinect and body-worn accelerometer," *Applied Soft Computing*, vol. 40, pp. 305–318, 2016, 1712, fall detection, ISSN: 1568-4946. DOI: `10.1016/j.asoc.2015.11.031`.

[167] M. Mansoor, R. Amin, Z. Mustafa, S. Sengan, H. Aldabbas, and M. T. Alharbi, "A machine learning approach for non-invasive fall detection using kinect," *Multimedia Tools and Applications*, 2052, fall detection, ISSN: 1380-7501. DOI: `10.1007/s11042-022-12113-w`. [Online]. Available: `https://link.springer.com/article/10.1007/s11042-022-12113-w`.

[168] W. D. Min, L. Y. Yao, Z. R. Lin, and L. Liu, "Support vector machine approach to fall recognition based on simplified expression of human skeleton action and fast detection of start key frame using torso angle," *Iet Computer Vision*, vol. 12, no. 8, pp. 1133–1140, 2018, 2192, fall detection, ISSN: 1751-9632. DOI: `10.1049/iet-cvi.2018.5324`. [Online]. Available: `https://ietresearch.onlinelibrary.wiley.com/doi/pdfdirect/10.1049/iet-cvi.2018.5324?download=true`.

[169] L. Y. Yao, W. Yang, and W. Huang, "A fall detection method based on a joint motion map using double convolutional neural networks," *Multimedia Tools and Applications*, vol. 81, no. 4, pp. 4551–4568, 2022, 3655, fall detection, ISSN: 1380-7501. DOI: `10.1007/s11042-020-09181-1`. [Online]. Available: `https://link.springer.com/article/10.1007/s11042-020-09181-1`.

[170] Y. X. Fan, M. D. Levine, G. J. Wen, and S. H. Qiu, "A deep neural network for real-time detection of falling humans in naturally occurring scenes," *Neurocomputing*, vol. 260, pp. 43–58, 2017, 910, fall detection, ISSN: 0925-2312. DOI: `10.1016/j.neucom.2017.02.082`.

[171] S. Ezatzadeh, M. R. Keyvanpour, and S. V. Shojaedini, "A human fall detection framework based on multi-camera fusion," *Journal of Experimental & Theoretical Artificial Intelligence*, 891, fall detection, ISSN: 0952-813X. DOI: `10.1080/0952813x.2021.1938696`.

[172] R. Espinosa, H. Ponce, S. Gutierrez, L. Martinez-Villasenor, J. Brieva, and E. Moya-Albor, "A vision-based approach for fall detection using multiple cameras and convo-

lutional neural networks: A case study using the up-fall detection dataset," *Computers in Biology and Medicine*, vol. 115, 2019, 887, fall detection, ISSN: 0010-4825. DOI: `10.1016/j.compbiomed.2019.103520`.

[173] K. B. Fan, P. Wang, and S. Zhuang, "Human fall detection using slow feature analysis," *Multimedia Tools and Applications*, vol. 78, no. 7, pp. 9101–9128, 2019, 907, fall detection, ISSN: 1380-7501. DOI: `10.1007/s11042-018-5638-9`. [Online]. Available: `https://link.springer.com/article/10.1007/s11042-018-5638-9`.

[174] B. Hadjadji, M. Saumard, and M. Aron, "Multi-oriented run length based static and dynamic features fused with choquet fuzzy integral for human fall detection in videos," *Journal of Visual Communication and Image Representation*, vol. 82, 2022, 1169, fall detection, ISSN: 1047-3203. DOI: `10.1016/j.jvcir.2021.103375`. [Online]. Available: `https://www.sciencedirect.com/science/article/pii/S1047320321002480?via%3Dihub`.

[175] S. Z. Su, S. S. Wu, S. Y. Chen, D. J. Duh, and S. Z. Li, "Multi-view fall detection based on spatio-temporal interest points," *Multimedia Tools and Applications*, vol. 75, no. 14, pp. 8469–8492, 2016, 3133, fall detection, ISSN: 1380-7501. DOI: `10.1007/s11042-015-2766-3`. [Online]. Available: `https://link.springer.com/article/10.1007/s11042-015-2766-3`.

[176] D. N. Olivieri, I. G. Conde, and X. A. V. Sobrino, "Eigenspace-based fall detection and activity recognition from motion templates and machine learning," *Expert Systems with Applications*, vol. 39, no. 5, pp. 5935–5945, 2012, 2426, fall detection, ISSN: 0957-4174. DOI: `10.1016/j.eswa.2011.11.109`.

[177] F. Jin, A. Sengupta, and S. Cao, "Mmfall: Fall detection using 4-d mmwave radar and a hybrid variational rnn autoencoder," *IEEE Transactions on Automation Science and Engineering*, vol. 19, no. 2, pp. 1245–1257, 2022, ISSN: 1558-3783. DOI: `10.1109/TASE.2020.3042158`. [Online]. Available: `https://ieeexplore.ieee.org/document/9305931/`.

[178] J. D. Cardenas, C. A. Gutierrez, and R. Aguilar-Ponce, "Deep learning multi-class approach for human fall detection based on doppler signatures," *International Journal of Environmental Research and Public Health*, vol. 20, no. 2, 2023, ISSN: 1660-4601. DOI: `10.3390/ijerph20021123`. [Online]. Available: `https://www.mdpi.com/1660-4601/20/2/1123`.

REFERENCES

[179] D. Haider, X. D. Yang, and Q. H. Abbasi, "Post-surgical fall detection by exploiting the 5 g c-band technology for ehealth paradigm," *Applied Soft Computing*, vol. 81, 2019, 1180, fall detection, ISSN: 1568-4946. DOI: `10.1016/j.asoc.2019.105537`.

[180] T. Liu, X. M. Guo, and G. L. Wang, "Elderly-falling detection using distributed direction-sensitive pyroelectric infrared sensor arrays," *Multidimensional Systems and Signal Processing*, vol. 23, no. 4, pp. 451–467, 2012, 1921, fall detection, ISSN: 0923-6082. DOI: `10.1007/s11045-011-0161-4`. [Online]. Available: `https://link.springer.com/article/10.1007/s11045-011-0161-4`.

[181] X. M. Luo, T. Liu, J. Liu, X. M. Guo, and G. L. Wang, "Design and implementation of a distributed fall detection system based on wireless sensor networks," *Eurasip Journal on Wireless Communications and Networking*, pp. 1–13, 2012, 1973, fall detection, ISSN: 1687-1472. DOI: `10.1186/1687-1499-2012-118`. [Online]. Available: `https://jwcn-eurasipjournals.springeropen.com/counter/pdf/10.1186/1687-1499-2012-118.pdf`.

[182] J. Haffner, C. Margo, Y. Oussar, S. Hole, J. Casimiro, and P. Mabire, "A smart capacitive measurement system for fall detection," *Journal of Electrostatics*, vol. 92, pp. 45–53, 2018, 1172, fall detection, ISSN: 0304-3886. DOI: `10.1016/j.elstat.2018.01.005`.

[183] G. M. Bertolotti *et al.*, "A wearable and modular inertial unit for measuring limb movements and balance control abilities," *IEEE Sensors Journal*, vol. 16, no. 3, pp. 790–797, 2016. DOI: `10.1109/JSEN.2015.2489381`.

[184] A. Anwary, H. Yu, and M. Vassallo, "An automatic gait feature extraction method for identifying gait asymmetry using wearable sensors," *Sensors*, vol. 18, no. 3, p. 676, Feb. 2018, ISSN: 1424-8220. DOI: `10.3390/s18020676`. [Online]. Available: `http://dx.doi.org/10.3390/s18020676`.

[185] X. Cai, G. Han, X. Song, and J. Wang, "Single-camera-based method for step length symmetry measurement in unconstrained elderly home monitoring," *IEEE Transactions on Biomedical Engineering*, vol. 64, no. 11, pp. 2618–2627, 2017. DOI: `10.1109/TBME.2017.2653246`.

[186] Z. Chen, H. Zhang, A. Zaferiou, D. Zanotto, and Y. Guo, "Mobile robot assisted gait monitoring and dynamic margin of stability estimation," *IEEE Transactions on Medical*

Robotics and Bionics, vol. 4, no. 2, pp. 460–471, 2022. DOI: `10.1109/TMRB.2022.3162148`.

[187] P. E. Cuddihy *et al.*, "Radar walking speed measurements of seniors in their apartments: Technology for fall prevention," in *2012 Annual International Conference of the IEEE Engineering in Medicine and Biology Society*, IEEE, Aug. 2012. DOI: `10.1109/embc.2012.6345919`. [Online]. Available: `http://dx.doi.org/10.1109/EMBC.2012.6345919`.

[188] R. Das and N. Kumar, "Investigations on postural stability and spatiotemporal parameters of human gait using developed wearable smart insole," *Journal of Medical Engineering & Technology*, vol. 39, no. 1, pp. 75–78, Oct. 2014, ISSN: 1464-522X. DOI: `10.3109/03091902.2014.968676`. [Online]. Available: `http://dx.doi.org/10.3109/03091902.2014.968676`.

[189] R. Eguchi and M. Takahashi, "Insole-based estimation of vertical ground reaction force using one-step learning with probabilistic regression and data augmentation," *IEEE Transactions on Neural Systems and Rehabilitation Engineering*, vol. 27, no. 6, pp. 1217–1225, 2019. DOI: `10.1109/TNSRE.2019.2916476`.

[190] H. Abou Ghaida, S. Mottet, and J.-M. Goujon, "A real time study of the human equilibrium using an instrumented insole with 3 pressure sensors," in *2014 36th Annual International Conference of the IEEE Engineering in Medicine and Biology Society*, IEEE, Aug. 2014. DOI: `10.1109/embc.2014.6944739`. [Online]. Available: `http://dx.doi.org/10.1109/EMBC.2014.6944739`.

[191] A. González, M. Hayashibe, and P. Fraisse, "Estimation of the center of mass with kinect and wii balance board," in *2012 IEEE/RSJ International Conference on Intelligent Robots and Systems*, 2012, pp. 1023–1028. DOI: `10.1109/IROS.2012.6385665`.

[192] V. Gutta, P. Fallavollita, N. Baddour, and E. D. Lemaire, "Development of a smart hallway for marker-less human foot tracking and stride analysis," *IEEE Journal of Translational Engineering in Health and Medicine*, vol. 9, pp. 1–12, 2021, ISSN: 2168-2372. DOI: `10.1109/jtehm.2021.3069353`. [Online]. Available: `http://dx.doi.org/10.1109/JTEHM.2021.3069353`.

[193] Y. Horiuchi, Y. Makino, and H. Shinoda, "Computational foresight: Forecasting human body motion in real-time for reducing delays in interactive system," in *Proceedings of the 2017 ACM International Conference on Interactive Surfaces and Spaces*, ser. ISS

'17, Brighton, United Kingdom: Association for Computing Machinery, 2017, pp. 312–317, ISBN: 9781450346917. DOI: `10.1145/3132272.3135076`. [Online]. Available: `https://doi.org/10.1145/3132272.3135076`.

[194] M. Single *et al.*, "A transferable lidar-based method to conduct contactless assessments of gait parameters in diverse home-like environments," *Sensors*, vol. 24, no. 4, p. 1172, Feb. 2024, ISSN: 1424-8220. DOI: `10.3390/s24041172`. [Online]. Available: `http://dx.doi.org/10.3390/s24041172`.

[195] X. Liu, X. Zhang, B. Zhang, B. Zhou, Z. He, and T. Liu, "An imu-based ground reaction force estimation method and its application in walking balance assessment," *IEEE Transactions on Neural Systems and Rehabilitation Engineering*, vol. PP, pp. 1–1, Dec. 2023. DOI: `10.1109/TNSRE.2023.3347729`.

[196] P. Colagiorgio *et al.*, "Affordable, automatic quantitative fall risk assessment based on clinical balance scales and kinect data," in *2014 36th Annual International Conference of the IEEE Engineering in Medicine and Biology Society*, IEEE, Aug. 2014. DOI: `10.1109/embc.2014.6944377`. [Online]. Available: `http://dx.doi.org/10.1109/EMBC.2014.6944377`.

[197] Y. Deguchi, D. Takayama, S. Takano, V.-M. Scuturici, J.-M. Petit, and E. Suzuki, "Skeleton clustering by multi-robot monitoring for fall risk discovery," *Journal of Intelligent Information Systems*, vol. 48, no. 1, pp. 75–115, Dec. 2015, ISSN: 1573-7675. DOI: `10.1007/s10844-015-0392-1`. [Online]. Available: `http://dx.doi.org/10.1007/s10844-015-0392-1`.

[198] A. Dubois, T. Bihl, and J.-P. Bresciani, "Identifying fall risk predictors by monitoring daily activities at home using a depth sensor coupled to machine learning algorithms," *Sensors*, vol. 21, no. 6, p. 1957, Mar. 2021, ISSN: 1424-8220. DOI: `10.3390/s21061957`. [Online]. Available: `http://dx.doi.org/10.3390/s21061957`.

[199] N. Eichler, S. Raz, A. Toledano-Shubi, D. Livne, I. Shimshoni, and H. Hel-Or, "Automatic and efficient fall risk assessment based on machine learning," *Sensors*, vol. 22, no. 4, p. 1557, Feb. 2022, ISSN: 1424-8220. DOI: `10.3390/s22041557`. [Online]. Available: `http://dx.doi.org/10.3390/s22041557`.

[200] M. Haescher *et al.*, "Automated fall risk assessment of elderly using wearable devices," *Journal of Rehabilitation and Assistive Technologies Engineering*, vol. 7, p. 205 566 832 094 620,

Jan. 2020, ISSN: 2055-6683. DOI: 10.1177/2055668320946209. [Online]. Available: http://dx.doi.org/10.1177/2055668320946209.

[201] L. Johnson *et al.*, "An automated, electronic assessment tool can accurately classify older adult postural stability," *Journal of Biomechanics*, vol. 93, pp. 6–10, 2019, ISSN: 0021-9290. DOI: https://doi.org/10.1016/j.jbiomech.2019.06.001. [Online]. Available: https://www.sciencedirect.com/science/article/pii/S0021929019303975.

[202] K. McManus, B. R. Greene, L. G. M. Ader, and B. Caulfield, "Development of data-driven metrics for balance impairment and fall risk assessment in older adults," *IEEE Transactions on Biomedical Engineering*, vol. 69, no. 7, pp. 2324–2332, Jul. 2022, ISSN: 1558-2531. DOI: 10.1109/tbme.2022.3142617. [Online]. Available: http://dx.doi.org/10.1109/TBME.2022.3142617.

[203] M. Nouredanesh, S. L. Kukreja, and J. Tung, "Detection of compensatory balance responses using wearable electromyography sensors for fall-risk assessment," in *2016 38th Annual International Conference of the IEEE Engineering in Medicine and Biology Society (EMBC)*, IEEE, Aug. 2016. DOI: 10.1109/embc.2016.7591038. [Online]. Available: http://dx.doi.org/10.1109/EMBC.2016.7591038.

[204] M. Savadkoohi, T. Oladunni, and L. Thompson, "Deep neural networks for human's fall-risk prediction using force-plate time series signal," *Expert Systems with Applications*, vol. 182, p. 115 220, Nov. 2021, ISSN: 0957-4174. DOI: 10.1016/j.eswa.2021.115220. [Online]. Available: http://dx.doi.org/10.1016/j.eswa.2021.115220.

[205] A.-K. Seifert, A. M. Zoubir, and M. G. Amin, "Detection of gait asymmetry using indoor doppler radar," in *2019 IEEE Radar Conference (RadarConf)*, 2019, pp. 1–6. DOI: 10.1109/RADAR.2019.8835611.

[206] R.-K. Shen, C.-Y. Yang, V. R. L. Shen, and W.-C. Chen, "A novel fall prediction system on smartphones," *IEEE Sensors Journal*, vol. 17, no. 6, pp. 1865–1871, 2017. DOI: 10.1109/JSEN.2016.2598524.

[207] S. Wang, G. Varas-Diaz, S. Dusane, Y. Wang, and T. Bhatt, "Slip-induced fall-risk assessment based on regular gait pattern in older adults," *Journal of Biomechanics*, vol. 96, p. 109 334, Nov. 2019, ISSN: 0021-9290. DOI: 10.1016/j.jbiomech.2019.109334. [Online]. Available: http://dx.doi.org/10.1016/j.jbiomech.2019.109334.

[208]   P. Antonellis, S. Galle, D. De Clercq, and P. Malcolm, "Altering gait variability with an ankle exoskeleton," *PLOS ONE*, vol. 13, no. 10, A. Grabowski, Ed., e0205088, Oct. 2018, ISSN: 1932-6203. DOI: `10.1371/journal.pone.0205088`. [Online]. Available: `http://dx.doi.org/10.1371/journal.pone.0205088`.

[209]   M.-y. Deng *et al.*, "Fall preventive gait trajectory planning of a lower limb rehabilitation exoskeleton based on capture point theory," *Frontiers of Information Technology & Electronic Engineering*, vol. 20, no. 10, pp. 1322–1330, Oct. 2019, ISSN: 2095-9230. DOI: `10.1631/fitee.1800777`. [Online]. Available: `http://dx.doi.org/10.1631/FITEE.1800777`.

[210]   M. Geravand, W. Rampeltshammer, and A. Peer, "Control of mobility assistive robot for human fall prevention," in *2015 IEEE International Conference on Rehabilitation Robotics (ICORR)*, 2015, pp. 882–887. DOI: `10.1109/ICORR.2015.7281314`.

[211]   K. Hirota and T. Murakami, "Imu sensor based human motion detection and its application to braking control of electric wheeled walker for fall-prevention," *IEEJ Journal of Industry Applications*, vol. 5, no. 4, pp. 347–354, 2016. DOI: `10.1541/ieejjia.5.347`.

[212]   X. Hu *et al.*, "A soft robotic intervention for gait enhancement in older adults," *IEEE Transactions on Neural Systems and Rehabilitation Engineering*, vol. 29, pp. 1838–1847, 2021. DOI: `10.1109/TNSRE.2021.3109729`.

[213]   P. Van Lam and Y. Fujimoto, "A robotic cane for balance maintenance assistance," *IEEE Transactions on Industrial Informatics*, vol. 15, no. 7, pp. 3998–4009, 2019. DOI: `10.1109/TII.2019.2903893`.

[214]   K. Nomura, T. Yonezawa, T. Ogitsu, H. Mizoguchi, and H. Takemura, "Development of stewart platform type ankle-foot device for trip prevention support," in *2015 37th Annual International Conference of the IEEE Engineering in Medicine and Biology Society (EMBC)*, 2015, pp. 4808–4811. DOI: `10.1109/EMBC.2015.7319469`.

[215]   P. Romtrairat, C. Virulsri, and P. Tangpornprasert, "An application of scissored-pair control moment gyroscopes in a design of wearable balance assistance device for the elderly," *Journal of Biomechanics*, vol. 87, pp. 183–188, Apr. 2019, ISSN: 0021-9290. DOI: `10.1016/j.jbiomech.2019.03.015`. [Online]. Available: `http://dx.doi.org/10.1016/j.jbiomech.2019.03.015`.

[216] Q. Yan, J. Huang, and Z. Luo, "Human-robot coordination stability for fall detection and prevention using cane robot," in *2016 International Symposium on Micro-NanoMechatronics and Human Science (MHS)*, 2016, pp. 1–7. DOI: `10.1109/MHS.2016.7824171`.

[217] S. Taghvaei and K. Kosuge, "Image-based fall detection and classification of a user with a walking support system," *Frontiers of Mechanical Engineering*, vol. 13, no. 3, pp. 427–441, Oct. 2017, ISSN: 2095-0241. DOI: `10.1007/s11465-017-0465-7`. [Online]. Available: `http://dx.doi.org/10.1007/s11465-017-0465-7`.

[218] C. Zhu and J. Yi, "Knee exoskeleton-enabled balance control of human walking gait with unexpected foot slip," *IEEE Robotics and Automation Letters*, vol. 8, no. 11, pp. 7751–7758, 2023. DOI: `10.1109/LRA.2023.3322082`.

[219] V. Monaco *et al.*, "An ecologically-controlled exoskeleton can improve balance recovery after slippage," *Scientific Reports*, vol. 7, no. 1, May 2017, ISSN: 2045-2322. DOI: `10.1038/srep46721`. [Online]. Available: `http://dx.doi.org/10.1038/srep46721`.

[220] W. Verrusio, V. Gianturco, M. Cacciafesta, V. Marigliano, G. Troisi, and M. Ripani, "Fall prevention in the young old using an exoskeleton human body posturizer: A randomized controlled trial," *Aging Clinical and Experimental Research*, vol. 29, no. 2, pp. 207–214, Feb. 2016, ISSN: 1720-8319. DOI: `10.1007/s40520-016-0540-7`. [Online]. Available: `http://dx.doi.org/10.1007/s40520-016-0540-7`.

[221] A. A. Schmid, M. Van Puymbroeck, and D. M. Koceja, "Effect of a 12-week yoga intervention on fear of falling and balance in older adults: A pilot study," *Archives of physical medicine and rehabilitation*, vol. 91, no. 4, pp. 576–583, 2010.

[222] G. Duque *et al.*, "Effects of balance training using a virtual-reality system in older fallers," *Clinical interventions in aging*, pp. 257–263, 2013.

[223] O. A. Coubard, L. Ferrufino, T. Nonaka, O. Zelada, B. Bril, and G. Dietrich, "One month of contemporary dance modulates fractal posture in aging," *Frontiers in aging neuroscience*, vol. 6, p. 17, 2014.

[224] D. M. Koceja and J. S. Greiwe, *Novel balance rehabilitation and training apparatus to improve functional balance*, 2014.

REFERENCES

[225] M. Schwenk *et al.*, "Interactive balance training integrating sensor-based visual feedback of movement performance: A pilot study in older adults," *Journal of neuroengineering and rehabilitation*, vol. 11, pp. 1–13, 2014.

[226] K. Freyler, A. Krause, A. Gollhofer, and R. Ritzmann, "Specific stimuli induce specific adaptations: Sensorimotor training vs. reactive balance training," *PLoS One*, vol. 11, no. 12, e0167557, 2016.

[227] C.-J. Kwak, Y. L. Kim, and S. M. Lee, "Effects of elastic-band resistance exercise on balance, mobility and gait function, flexibility and fall efficacy in elderly people," *Journal of physical therapy science*, vol. 28, no. 11, pp. 3189–3196, 2016.

[228] G. Pliske, P. Emmermacher, V. Weinbeer, and K. Witte, "Changes in dual-task performance after 5 months of karate and fitness training for older adults to enhance fall prevention," *Aging clinical and experimental research*, vol. 28, pp. 1179–1186, 2016.

[229] L. K. Allison, T. Kiemel, and J. J. Jeka, "Sensory-challenge balance exercises improve multisensory reweighting in fall-prone older adults," *Journal of neurologic physical therapy*, vol. 42, no. 2, pp. 84–93, 2018.

[230] T. Liu-Ambrose *et al.*, "Effect of a home-based exercise program on subsequent falls among community-dwelling high-risk older adults after a fall: A randomized clinical trial," *Jama*, vol. 321, no. 21, pp. 2092–2100, 2019.

[231] S. Phu, S. Vogrin, A. Al Saedi, and G. Duque, "Balance training using virtual reality improves balance and physical performance in older adults at high risk of falls," *Clinical interventions in aging*, pp. 1567–1577, 2019.

[232] J. Chittrakul, P. Siviroj, S. Sungkarat, and R. Sapbamrer, "Multi-system physical exercise intervention for fall prevention and quality of life in pre-frail older adults: A randomized controlled trial," *International Journal of Environmental Research and Public Health*, vol. 17, no. 9, 2020, ISSN: 1660-4601. DOI: `10.3390/ijerph17093102`. [Online]. Available: `https://www.mdpi.com/1660-4601/17/9/3102`.

[233] N. Zahedian-Nasab, A. Jaberi, F. Shirazi, and S. Kavousipor, "Effect of virtual reality exercises on balance and fall in elderly people with fall risk: A randomized controlled trial," *BMC Geriatrics*, vol. 21, no. 1, Sep. 2021, ISSN: 1471-2318. DOI: `10.1186/s12877-021-02462-w`. [Online]. Available: `http://dx.doi.org/10.1186/s12877-021-02462-w`.

[234] D. L. Sturnieks *et al.*, "Exergame and cognitive training for preventing falls in community-dwelling older people: A randomized controlled trial," *Nature Medicine*, vol. 30, no. 1, pp. 98–105, Jan. 2024, ISSN: 1546-170X. DOI: `10.1038/s41591-023-02739-0`. [Online]. Available: `http://dx.doi.org/10.1038/s41591-023-02739-0`.

[235] O. Dehzangi, Z. Zhao, M.-M. Bidmeshki, J. Biggan, C. Ray, and R. Jafari, "The impact of vibrotactile biofeedback on the excessive walking sway and the postural control in elderly," in *Proceedings of the 4th Conference on Wireless Health*, ser. WH '13, ACM, Nov. 2013. DOI: `10.1145/2534088.2534110`. [Online]. Available: `http://dx.doi.org/10.1145/2534088.2534110`.

[236] M. Karim, S. Khalid, A. Aleryani, J. Khan, I. Ullah, and Z. Ali, "Human action recognition systems: A review of the trends and state-of-the-art," *IEEE Access*, vol. 12, pp. 36 372–36 390, 2024. DOI: `10.1109/ACCESS.2024.3373199`.

[237] L. Xia, C.-C. Chen, and J. K. Aggarwal, "View invariant human action recognition using histograms of 3d joints," in *2012 IEEE Computer Society Conference on Computer Vision and Pattern Recognition Workshops*, 2012, pp. 20–27. DOI: `10.1109/CVPRW.2012.6239233`.

[238] M. Zhang and A. A. Sawchuk, "Usc-had: A daily activity dataset for ubiquitous activity recognition using wearable sensors," in *Proceedings of the 2012 ACM Conference on Ubiquitous Computing*, ser. UbiComp '12, Pittsburgh, Pennsylvania: Association for Computing Machinery, 2012, pp. 1036–1043, ISBN: 9781450312240. DOI: `10.1145/2370216.2370438`. [Online]. Available: `https://doi.org/10.1145/2370216.2370438`.

[239] R. Chereshnev and A. Kertesz-Farkas, *Hugadb: Human gait database for activity recognition from wearable inertial sensor networks*, 2017. arXiv: `1705.08506 [cs.CY]`.

[240] H. Liu, Y. Hartmann, and T. Schultz, "Csl-share: A multimodal wearable sensor-based human activity dataset," *Frontiers in Computer Science*, vol. 3, p. 90, Oct. 2021. DOI: `10.3389/fcomp.2021.759136`.

[241] J. Mitchell, A. Dehghani-Sanij, S. Xie, and R. O'Connor, *Context-Aware Human Activity Recognition (CAHAR) Dataset*, 2024. DOI: `10.21227/bwee-bv18`. [Online]. Available: `https://dx.doi.org/10.21227/bwee-bv18`.

[242] C. Morbidoni, A. Cucchiarelli, S. Fioretti, and F. Di Nardo, "A deep learning approach to EMG-based classification of gait phases during level ground walking," en, *Electronics (Basel)*, vol. 8, no. 8, p. 894, Aug. 2019.

[243] T. Hussain, N. Iqbal, H. F. Maqbool, M. Khan, M. I. Awad, and A. A. Dehghani-Sanij, "Intent based recognition of walking and ramp activities for amputee using sEMG based lower limb prostheses," en, *Biocybern. Biomed. Eng.*, vol. 40, no. 3, pp. 1110–1123, Jul. 2020.

[244] M. Islam and E. T. Hsiao-Wecksler, "Detection of gait modes using an artificial neural network during walking with a powered ankle-foot orthosis," *Journal of Biophysics*, vol. 2016, pp. 1–9, Dec. 2016, ISSN: 1687-8019. DOI: 10.1155/2016/7984157. [Online]. Available: http://dx.doi.org/10.1155/2016/7984157.

[245] J. Yang *et al.*, "Machine learning based adaptive gait phase estimation using inertial measurement sensors," in *2019 Design of Medical Devices Conference*, ser. DMD2019, American Society of Mechanical Engineers, Apr. 2019. DOI: 10.1115/dmd2019-3266. [Online]. Available: http://dx.doi.org/10.1115/DMD2019-3266.

[246] A. J. Young and L. J. Hargrove, "A classification method for user-independent intent recognition for transfemoral amputees using powered lower limb prostheses," *IEEE Transactions on Neural Systems and Rehabilitation Engineering*, vol. 24, no. 2, pp. 217–225, Feb. 2016, ISSN: 1558-0210. DOI: 10.1109/tnsre.2015.2412461. [Online]. Available: http://dx.doi.org/10.1109/TNSRE.2015.2412461.

[247] F. Fereidoonian, F. Firouzi, and B. Farahani, "Human activity recognition: From sensors to applications," in *2020 International Conference on Omni-layer Intelligent Systems (COINS)*, Barcelona, Spain: IEEE, Aug. 2020.

[248] S. Zia, A. N. Khan, M. Mukhtar, S. E. Ali, J. Shahid, and M. Sohail, "Detection of motor seizures and falls in mobile application using machine learning classifiers," in *2020 IEEE International Conference on Industry 4.0, Artificial Intelligence, and Communications Technology (IAICT)*, Bali, Indonesia: IEEE, Jul. 2020.

[249] M. Shoaib, S. Bosch, O. D. Incel, H. Scholten, and P. J. M. Havinga, "A survey of online activity recognition using mobile phones," en, *Sensors (Basel)*, vol. 15, no. 1, pp. 2059–2085, Jan. 2015.

[250] H. Wang, W. Yan, and S. Liu, "Physical activity recognition using multi-sensor fusion and extreme learning machines," in *2019 International Joint Conference on Neural Networks (IJCNN)*, IEEE, Jul. 2019. DOI: `10.1109/ijcnn.2019.8852175`. [Online]. Available: `http://dx.doi.org/10.1109/IJCNN.2019.8852175`.

[251] K. Bhakta, J. Camargo, L. Donovan, K. Herrin, and A. Young, "Machine learning model comparisons of user independent & dependent intent recognition systems for powered prostheses," *IEEE Robotics and Automation Letters*, vol. 5, no. 4, pp. 5393–5400, Oct. 2020, ISSN: 2377-3774. DOI: `10.1109/lra.2020.3007480`. [Online]. Available: `http://dx.doi.org/10.1109/LRA.2020.3007480`.

[252] A. Halim, A. A. Ibrahim, M. I. Awad, and M. R. A. Atia, "Optimization of sensor number for lower limb prosthetics using genetic algorithm," in *2020 International Conference on Innovative Trends in Communication and Computer Engineering (ITCE)*, Aswan, Egypt: IEEE, Feb. 2020.

[253] N. Sikder and A.-A. Nahid, "Ku-har: An open dataset for heterogeneous human activity recognition," *Pattern Recognition Letters*, vol. 146, pp. 46–54, Jun. 2021, ISSN: 0167-8655. DOI: `10.1016/j.patrec.2021.02.024`. [Online]. Available: `http://dx.doi.org/10.1016/j.patrec.2021.02.024`.

[254] J. Camargo, A. Ramanathan, W. Flanagan, and A. Young, "A comprehensive, open-source dataset of lower limb biomechanics in multiple conditions of stairs, ramps, and level-ground ambulation and transitions," *Journal of Biomechanics*, vol. 119, p. 110 320, 2021, ISSN: 0021-9290. DOI: `https://doi.org/10.1016/j.jbiomech.2021.110320`. [Online]. Available: `https://www.sciencedirect.com/science/article/pii/S0021929021001007`.

[255] Y. Duan and K. Fujinami, "Effect of combinations of sensor positions on wearable-sensor-based human activity recognition," *Sensors and Materials*, vol. 35, pp. 2175–2193, Jul. 2023. DOI: `10.18494/SAM4421`.

[256] O. Baños, M. Damas, H. Pomares, I. Rojas, M. A. Tóth, and O. Amft, "A benchmark dataset to evaluate sensor displacement in activity recognition," in *Proceedings of the 2012 ACM Conference on Ubiquitous Computing*, ser. UbiComp '12, Pittsburgh, Pennsylvania: Association for Computing Machinery, 2012, pp. 1026–1035, ISBN: 9781450312240.

DOI: `10.1145/2370216.2370437`. [Online]. Available: `https://doi.org/10.1145/2370216.2370437`.

[257] W. Taylor, S. A. Shah, K. Dashtipour, A. Zahid, Q. H. Abbasi, and M. A. Imran, "An intelligent non-invasive real-time human activity recognition system for next-generation healthcare," *Sensors*, vol. 20, no. 9, p. 2653, May 2020, ISSN: 1424-8220. DOI: `10.3390/s20092653`. [Online]. Available: `http://dx.doi.org/10.3390/s20092653`.

[258] Z. Meng *et al.*, "Recent progress in sensing and computing techniques for human activity recognition and motion analysis," en, *Electronics (Basel)*, vol. 9, no. 9, p. 1357, Aug. 2020.

[259] K. Wang, J. He, and L. Zhang, "Attention-based convolutional neural network for weakly labeled human activities' recognition with wearable sensors," *IEEE Sensors Journal*, vol. 19, no. 17, pp. 7598–7604, Sep. 2019, ISSN: 2379-9153. DOI: `10.1109/jsen.2019.2917225`. [Online]. Available: `http://dx.doi.org/10.1109/JSEN.2019.2917225`.

[260] J. Perry and J. Burnfield, *Gait Analysis: Normal and Pathological Function.* Feb. 2010, ISBN: 978-1556427664. DOI: `10.1201/9781003525592`.

[261] A. S. Alharthi, S. U. Yunas, and K. B. Ozanyan, "Deep learning for monitoring of human gait: A review," *IEEE Sens. J.*, vol. 19, no. 21, pp. 9575–9591, Nov. 2019.

[262] H.-C. Chang, Y.-L. Hsu, S.-C. Yang, J.-C. Lin, and Z.-H. Wu, "A wearable inertial measurement system with complementary filter for gait analysis of patients with stroke or parkinson's disease," *IEEE Access*, vol. 4, pp. 8442–8453, 2016, ISSN: 2169-3536. DOI: `10.1109/access.2016.2633304`. [Online]. Available: `http://dx.doi.org/10.1109/ACCESS.2016.2633304`.

[263] J. C. Perez-Ibarra, A. A. G. Siqueira, and H. I. Krebs, "Identification of gait events in healthy subjects and with parkinson's disease using inertial sensors: An adaptive unsupervised learning approach," en, *IEEE Trans. Neural Syst. Rehabil. Eng.*, vol. 28, no. 12, pp. 2933–2943, Dec. 2020.

[264] W.-C. Hsu *et al.*, "Multiple-wearable-sensor-based gait classification and analysis in patients with neurological disorders," *Sensors*, vol. 18, no. 10, p. 3397, Oct. 2018, ISSN: 1424-8220. DOI: `10.3390/s18103397`. [Online]. Available: `http://dx.doi.org/10.3390/s18103397`.

[265] J. S. Park, C. M. Lee, S.-M. Koo, and C. H. Kim, "Gait phase detection using force sensing resistors," *IEEE Sensors Journal*, vol. 20, no. 12, pp. 6516–6523, 2020. DOI: `10.1109/JSEN.2020.2975790`.

[266] H. T. T. Vu *et al.*, "A review of gait phase detection algorithms for lower limb prostheses," *Sensors*, vol. 20, no. 14, p. 3972, Jul. 2020, ISSN: 1424-8220. DOI: `10.3390/s20143972`. [Online]. Available: `http://dx.doi.org/10.3390/s20143972`.

[267] H. F. Maqbool, M. A. B. Husman, M. I. Awad, A. Abouhossein, N. Iqbal, and A. A. Dehghani-Sanij, "A real-time gait event detection for lower limb prosthesis control and evaluation," *IEEE Transactions on Neural Systems and Rehabilitation Engineering*, vol. 25, no. 9, pp. 1500–1509, Sep. 2017, ISSN: 1558-0210. DOI: `10.1109/tnsre.2016.2636367`. [Online]. Available: `http://dx.doi.org/10.1109/TNSRE.2016.2636367`.

[268] D. Quintero, D. J. Lambert, D. J. Villarreal, and R. D. Gregg, "Real-time continuous gait phase and speed estimation from a single sensor," in *2017 IEEE Conference on Control Technology and Applications (CCTA)*, IEEE, Aug. 2017. DOI: `10.1109/ccta.2017.8062565`. [Online]. Available: `http://dx.doi.org/10.1109/CCTA.2017.8062565`.

[269] D.-X. Liu, X. Wu, W. Du, C. Wang, and T. Xu, "Gait phase recognition for lower-limb exoskeleton with only joint angular sensors," *Sensors*, vol. 16, no. 10, p. 1579, Sep. 2016, ISSN: 1424-8220. DOI: `10.3390/s16101579`. [Online]. Available: `http://dx.doi.org/10.3390/s16101579`.

[270] S. Qiu *et al.*, "Body sensor network-based robust gait analysis: Toward clinical and at home use," *IEEE Sensors Journal*, vol. 19, no. 19, pp. 8393–8401, Oct. 2019, ISSN: 2379-9153. DOI: `10.1109/jsen.2018.2860938`. [Online]. Available: `http://dx.doi.org/10.1109/JSEN.2018.2860938`.

[271] A. Ferrari, P. Ginis, M. Hardegger, F. Casamassima, L. Rocchi, and L. Chiari, "A mobile kalman-filter based solution for the real-time estimation of spatio-temporal gait parameters," *IEEE Transactions on Neural Systems and Rehabilitation Engineering*, vol. 24, no. 7, pp. 764–773, Jul. 2016, ISSN: 1558-0210. DOI: `10.1109/tnsre.2015.2457511`. [Online]. Available: `http://dx.doi.org/10.1109/TNSRE.2015.2457511`.

[272] P. Ismailidis *et al.*, "Measuring gait kinematics in patients with severe hip osteoarthritis using wearable sensors," *Gait & Posture*, vol. 81, pp. 49–55, Sep. 2020, ISSN: 0966-6362.

DOI: 10.1016/j.gaitpost.2020.07.004. [Online]. Available: http://dx.doi.org/10.1016/j.gaitpost.2020.07.004.

[273] P. Tahafchi and J. W. Judy, "Freezing-of-gait detection using wearable-sensor technology and neural-network classifier," in *2019 IEEE SENSORS*, IEEE, Oct. 2019. DOI: 10.1109/sensors43011.2019.8956548. [Online]. Available: http://dx.doi.org/10.1109/SENSORS43011.2019.8956548.

[274] R. D. Gurchiek, C. P. Garabed, and R. S. McGinnis, "Gait event detection using a thigh-worn accelerometer," *Gait & Posture*, vol. 80, pp. 214–216, Jul. 2020, ISSN: 0966-6362. DOI: 10.1016/j.gaitpost.2020.06.004. [Online]. Available: http://dx.doi.org/10.1016/j.gaitpost.2020.06.004.

[275] J. D. Farah, N. Baddour, and E. D. Lemaire, "Gait phase detection from thigh kinematics using machine learning techniques," in *2017 IEEE International Symposium on Medical Measurements and Applications (MeMeA)*, IEEE, May 2017. DOI: 10.1109/memea.2017.7985886. [Online]. Available: http://dx.doi.org/10.1109/MeMeA.2017.7985886.

[276] W. Heng, G. Pang, F. Xu, X. Huang, Z. Pang, and G. Yang, "Flexible insole sensors with stably connected electrodes for gait phase detection," *Sensors*, vol. 19, no. 23, p. 5197, Nov. 2019, ISSN: 1424-8220. DOI: 10.3390/s19235197. [Online]. Available: http://dx.doi.org/10.3390/s19235197.

[277] Z. Ding *et al.*, "The real time gait phase detection based on long short-term memory," in *2018 IEEE Third International Conference on Data Science in Cyberspace (DSC)*, IEEE, Jun. 2018. DOI: 10.1109/dsc.2018.00014. [Online]. Available: http://dx.doi.org/10.1109/DSC.2018.00014.

[278] R. Evans and D. Arvind, "Detection of gait phases using orient specks for mobile clinical gait analysis," in *2014 11th International Conference on Wearable and Implantable Body Sensor Networks*, IEEE, Jun. 2014. DOI: 10.1109/bsn.2014.22. [Online]. Available: http://dx.doi.org/10.1109/BSN.2014.22.

[279] K. A. Hawkins, D. J. Clark, C. K. Balasubramanian, and E. J. Fox, "Walking on uneven terrain in healthy adults and the implications for people after stroke," *NeuroRehabilitation*, vol. 41, no. 4, pp. 765–774, 2017, PMID: 28946584. DOI: 10.3233/NRE-172154. eprint: https://journals.sagepub.com/doi/pdf/10.3233/NRE-172154. [Online]. Available: https://journals.sagepub.com/doi/abs/10.3233/NRE-172154.

[280] P. Kozlowski and K. Walas, "Deep neural networks for terrain recognition task," in *2018 Baltic URSI Symposium (URSI)*, 2018, pp. 283–286. DOI: `10.23919/URSI.2018.8406736`.

[281] K. Walas, "Terrain classification and negotiation with a walking robot," en, *J. Intell. Robot. Syst.*, vol. 78, no. 3-4, pp. 401–423, Jun. 2015.

[282] P. Ewen, A. Li, Y. Chen, S. Hong, and R. Vasudevan, "These maps are made for walking: Real-time terrain property estimation for mobile robots," *IEEE Robotics and Automation Letters*, vol. 7, no. 3, pp. 7083–7090, 2022. DOI: `10.1109/LRA.2022.3180439`.

[283] R. L. Medrano, G. C. Thomas, C. G. Keais, E. J. Rouse, and R. D. Gregg, "Real-time gait phase and task estimation for controlling a powered ankle exoskeleton on extremely uneven terrain," *IEEE Transactions on Robotics*, vol. 39, no. 3, pp. 2170–2182, 2023. DOI: `10.1109/TRO.2023.3235584`.

[284] J. P. Diaz, R. L. da Silva, B. Zhong, H. H. Huang, and E. Lobaton, "Visual terrain identification and surface inclination estimation for improving human locomotion with a lower-limb prosthetic," in *2018 40th Annual International Conference of the IEEE Engineering in Medicine and Biology Society (EMBC)*, 2018, pp. 1817–1820. DOI: `10.1109/EMBC.2018.8512614`.

[285] D. B. Das, O. Das, and M. Inalpolat, "A multi-modal sensing based terrain identification approach for active lower limb exoskeletons," *Expert Systems with Applications*, vol. 275, p. 126 862, 2025, ISSN: 0957-4174. DOI: `https://doi.org/10.1016/j.eswa.2025.126862`. [Online]. Available: `https://www.sciencedirect.com/science/article/pii/S0957417425004841`.

[286] J. Moore *et al.*, "Toward enhanced free-living fall risk assessment: Data mining and deep learning for environment and terrain classification," *Intelligence-Based Medicine*, vol. 8, p. 100 103, 2023, ISSN: 2666-5212. DOI: `https://doi.org/10.1016/j.ibmed.2023.100103`. [Online]. Available: `https://www.sciencedirect.com/science/article/pii/S2666521223000170`.

[287] M. Nouredanesh, A. Godfrey, D. Powell, and J. Tung, "Egocentric vision-based detection of surfaces: Towards context-aware free-living digital biomarkers for gait and fall risk assessment," en, *J. Neuroeng. Rehabil.*, vol. 19, no. 1, p. 79, Jul. 2022.

[288] B. Zhong, R. L. d. Silva, M. Li, H. Huang, and E. Lobaton, "Environmental context prediction for lower limb prostheses with uncertainty quantification," *IEEE Transactions on Automation Science and Engineering*, vol. 18, no. 2, pp. 458–470, 2021. DOI: `10.1109/TASE.2020.2993399`.

[289] M. Z. U. H. Hashmi, Q. Riaz, M. Hussain, and M. Shahzad, "What lies beneath one's feet? terrain classification using inertial data of human walk," *Applied Sciences*, vol. 9, no. 15, 2019, ISSN: 2076-3417. DOI: `10.3390/app9153099`. [Online]. Available: `https://www.mdpi.com/2076-3417/9/15/3099`.

[290] P. Dixon *et al.*, "Machine learning algorithms can classify outdoor terrain types during running using accelerometry data," *Gait & Posture*, vol. 74, pp. 176–181, 2019, ISSN: 0966-6362. DOI: `https://doi.org/10.1016/j.gaitpost.2019.09.005`. [Online]. Available: `https://www.sciencedirect.com/science/article/pii/S0966636219307064`.

[291] B. Hu, P. Dixon, J. Jacobs, J. Dennerlein, and J. Schiffman, "Machine learning algorithms based on signals from a single wearable inertial sensor can detect surface- and age-related differences in walking," *Journal of Biomechanics*, vol. 71, pp. 37–42, 2018, ISSN: 0021-9290. DOI: `https://doi.org/10.1016/j.jbiomech.2018.01.005`. [Online]. Available: `https://www.sciencedirect.com/science/article/pii/S0021929018300198`.

[292] P. Dixon, K. Schütte, B. Vanwanseele, J. Jacobs, J. Dennerlein, and J. Schiffman, "Gait adaptations of older adults on an uneven brick surface can be predicted by age-related physiological changes in strength," *Gait & Posture*, vol. 61, pp. 257–262, 2018, ISSN: 0966-6362. DOI: `https://doi.org/10.1016/j.gaitpost.2018.01.027`. [Online]. Available: `https://www.sciencedirect.com/science/article/pii/S0966636218300389`.

[293] S. Laible, Y. N. Khan, K. Bohlmann, and A. Zell, "3D LIDAR- and camera-based terrain classification under different lighting conditions," in *Informatik aktuell*, Berlin, Heidelberg: Springer Berlin Heidelberg, 2012, pp. 21–29.

[294] S. Siva, M. Wigness, J. G. Rogers, L. Quang, and H. Zhang, "Self-reflective terrain-aware robot adaptation for consistent off-road ground navigation," *The International Journal of Robotics Research*, vol. 43, no. 7, pp. 1003–1023, 2024. DOI: `10.1177/02783649231225243`. eprint: `https://doi.org/10.1177/02783649231225243`. [Online]. Available: `https://doi.org/10.1177/02783649231225243`.

[295] Y.-J. Lee, M.-Y. Wei, and Y.-J. Chen, "Multiple inertial measurement unit combination and location for recognizing general, fatigue, and simulated-fatigue gait," en, *Gait Posture*, vol. 96, pp. 330–337, Jul. 2022.

[296] Y. Yin, L. Xie, Z. Jiang, F. Xiao, J. Cao, and S. Lu, "A systematic review of human activity recognition based on mobile devices: Overview, progress and trends," *IEEE Communications Surveys & Tutorials*, vol. 26, no. 2, pp. 890–929, 2024. DOI: 10.1109/COMST.2024.3357591.

[297] E. Martini *et al.*, "Pressure-sensitive insoles for real-time gait-related applications," *Sensors*, vol. 20, no. 5, 2020, ISSN: 1424-8220. [Online]. Available: https://www.mdpi.com/1424-8220/20/5/1448.

[298] N. Carbonaro, F. Lorussi, and A. Tognetti, "Assessment of a smart sensing shoe for gait phase detection in level walking," *Electronics*, vol. 5, no. 4, 2016, ISSN: 2079-9292. DOI: 10.3390/electronics5040078. [Online]. Available: https://www.mdpi.com/2079-9292/5/4/78.

[299] J. Kim, M.-N. Bae, K. B. Lee, and S. G. Hong, "Gait event detection algorithm based on smart insoles," *ETRI Journal*, vol. 42, no. 1, pp. 46–53, 2020. DOI: https://doi.org/10.4218/etrij.2018-0639. eprint: https://onlinelibrary.wiley.com/doi/pdf/10.4218/etrij.2018-0639. [Online]. Available: https://onlinelibrary.wiley.com/doi/abs/10.4218/etrij.2018-0639.

[300] J. Moore *et al.*, "Enhancing free-living fall risk assessment: Contextualizing mobility based imu data," *Sensors*, vol. 23, no. 2, 2023, ISSN: 1424-8220. DOI: 10.3390/s23020891. [Online]. Available: https://www.mdpi.com/1424-8220/23/2/891.

[301] D. Renggli *et al.*, "Wearable inertial measurement units for assessing gait in real-world environments," *Frontiers in Physiology*, vol. 11, Feb. 2020, ISSN: 1664-042X. DOI: 10.3389/fphys.2020.00090. [Online]. Available: http://dx.doi.org/10.3389/fphys.2020.00090.

[302] S. Vítečková, H. Horáková, K. Poláková, R. Krupička, E. Růžička, and H. Brožová, "Agreement between the GAITRite® system and the wearable sensor BTS G-Walk® for measurement of gait parameters in healthy adults and parkinson's disease patients," en, *PeerJ*, vol. 8, no. e8835, e8835, May 2020.

[303] G. Kumari, J. Chakraborty, and A. Nandy, "Effect of reduced dimensionality on deep learning for human activity recognition," in *2020 11th International Conference on Computing, Communication and Networking Technologies (ICCCNT)*, IEEE, Jul. 2020. DOI: `10.1109/icccnt49239.2020.9225419`. [Online]. Available: `http://dx.doi.org/10.1109/ICCCNT49239.2020.9225419`.

[304] M. Gil-Martín, R. San-Segundo, F. Fernández-Martínez, and J. Ferreiros-López, "Time analysis in human activity recognition," *Neural Processing Letters*, vol. 53, no. 6, pp. 4507–4525, Aug. 2021, ISSN: 1573-773X. DOI: `10.1007/s11063-021-10611-w`. [Online]. Available: `http://dx.doi.org/10.1007/s11063-021-10611-w`.

[305] H. Yang, X. Wen, Y. Geng, Y. Wang, X. Wang, and C. Lu, "Mpja-had: A multi-position joint angle dataset for human activity recognition using wearable sensors," in *2022 International Conference on Advanced Mechatronic Systems (ICAMechS)*, IEEE, Dec. 2022. DOI: `10.1109/icamechs57222.2022.10003441`. [Online]. Available: `http://dx.doi.org/10.1109/ICAMechS57222.2022.10003441`.

[306] S. Ramasamy Ramamurthy and N. Roy, "Recent trends in machine learning for human activity recognition—a survey," *WIREs Data Mining and Knowledge Discovery*, vol. 8, no. 4, Mar. 2018, ISSN: 1942-4795. DOI: `10.1002/widm.1254`. [Online]. Available: `http://dx.doi.org/10.1002/widm.1254`.

[307] L. Bao and S. S. Intille, "Activity recognition from user-annotated acceleration data," in *Pervasive Computing*. Springer Berlin Heidelberg, 2004, pp. 1–17, ISBN: 9783540246466. DOI: `10.1007/978-3-540-24646-6_1`. [Online]. Available: `http://dx.doi.org/10.1007/978-3-540-24646-6_1`.

[308] E. M. Tapia *et al.*, "Real-time recognition of physical activities and their intensities using wireless accelerometers and a heart rate monitor," in *2007 11th IEEE International Symposium on Wearable Computers*, IEEE, Oct. 2007. DOI: `10.1109/iswc.2007.4373774`. [Online]. Available: `http://dx.doi.org/10.1109/ISWC.2007.4373774`.

[309] Ó. D. Lara, A. J. Pérez, M. A. Labrador, and J. D. Posada, "Centinela: A human activity recognition system based on acceleration and vital sign data," *Pervasive and Mobile Computing*, vol. 8, no. 5, pp. 717–729, Oct. 2012, ISSN: 1574-1192. DOI: `10.1016/j.pmcj.2011.06.004`. [Online]. Available: `http://dx.doi.org/10.1016/j.pmcj.2011.06.004`.

[310] D. Minnen, T. Westeyn, D. Ashbrook, P. Presti, and T. Starner, "Recognizing soldier activities in the field," in *IFMBE Proceedings*. Springer Berlin Heidelberg, 2007, pp. 236–241, ISBN: 9783540709947. DOI: `10.1007/978-3-540-70994-7_40`. [Online]. Available: `http://dx.doi.org/10.1007/978-3-540-70994-7_40`.

[311] O. Banos, J.-M. Galvez, M. Damas, H. Pomares, and I. Rojas, "Window size impact in human activity recognition," *Sensors*, vol. 14, no. 4, pp. 6474–6499, Apr. 2014, ISSN: 1424-8220. DOI: `10.3390/s140406474`. [Online]. Available: `http://dx.doi.org/10.3390/s140406474`.

[312] S. Gupta, "Deep learning based human activity recognition (har) using wearable sensor data," *International Journal of Information Management Data Insights*, vol. 1, no. 2, p. 100 046, Nov. 2021, ISSN: 2667-0968. DOI: `10.1016/j.jjimei.2021.100046`. [Online]. Available: `http://dx.doi.org/10.1016/j.jjimei.2021.100046`.

[313] M. Jaén-Vargas *et al.*, "Effects of sliding window variation in the performance of acceleration-based human activity recognition using deep learning models," *PeerJ Computer Science*, vol. 8, e1052, Aug. 2022, ISSN: 2376-5992. DOI: `10.7717/peerj-cs.1052`. [Online]. Available: `http://dx.doi.org/10.7717/peerj-cs.1052`.

[314] M. Bock, A. Hölzemann, M. Moeller, and K. Van Laerhoven, "Improving deep learning for har with shallow lstms," in *2021 International Symposium on Wearable Computers*, ser. UbiComp '21, ACM, Sep. 2021. DOI: `10.1145/3460421.3480419`. [Online]. Available: `http://dx.doi.org/10.1145/3460421.3480419`.

[315] A. Dehghani, O. Sarbishei, T. Glatard, and E. Shihab, "A quantitative comparison of overlapping and non-overlapping sliding windows for human activity recognition using inertial sensors," *Sensors*, vol. 19, no. 22, p. 5026, Nov. 2019, ISSN: 1424-8220. DOI: `10.3390/s19225026`. [Online]. Available: `http://dx.doi.org/10.3390/s19225026`.

[316] O. Baños, M. Damas, H. Pomares, I. Rojas, M. A. Tóth, and O. Amft, "A benchmark dataset to evaluate sensor displacement in activity recognition," in *Proceedings of the 2012 ACM Conference on Ubiquitous Computing*, ser. Ubicomp '12, ACM, Sep. 2012. DOI: `10.1145/2370216.2370437`. [Online]. Available: `http://dx.doi.org/10.1145/2370216.2370437`.

[317] D. Morris, T. S. Saponas, A. Guillory, and I. Kelner, "Recofit: Using a wearable sensor to find, recognize, and count repetitive exercises," in *Proceedings of the SIGCHI Conference*

on Human Factors in Computing Systems, ser. CHI '14, ACM, Apr. 2014. DOI: `10.1145/2556288.2557116`. [Online]. Available: `http://dx.doi.org/10.1145/2556288.2557116`.

[318] S. K. Yadav, K. Tiwari, H. M. Pandey, and S. A. Akbar, "A review of multimodal human activity recognition with special emphasis on classification, applications, challenges and future directions," *Knowledge-Based Systems*, vol. 223, p. 106 970, Jul. 2021, ISSN: 0950-7051. DOI: `10.1016/j.knosys.2021.106970`. [Online]. Available: `http://dx.doi.org/10.1016/j.knosys.2021.106970`.

[319] I. A. Bustoni, I. Hidayatulloh, A. M. Ningtyas, A. Purwaningsih, and S. N. Azhari, "Classification methods performance on human activity recognition," *Journal of Physics: Conference Series*, vol. 1456, no. 1, p. 012 027, Jan. 2020, ISSN: 1742-6596. DOI: `10.1088/1742-6596/1456/1/012027`. [Online]. Available: `http://dx.doi.org/10.1088/1742-6596/1456/1/012027`.

[320] A. Hayat, F. Morgado-Dias, B. Bhuyan, and R. Tomar, "Human activity recognition for elderly people using machine and deep learning approaches," *Information*, vol. 13, no. 6, p. 275, May 2022, ISSN: 2078-2489. DOI: `10.3390/info13060275`. [Online]. Available: `http://dx.doi.org/10.3390/info13060275`.

[321] A. H. Niazi *et al.*, "Statistical analysis of window sizes and sampling rates in human activity recognition.," in *HEALTHINF*, 2017, pp. 319–325.

[322] H. Li, G. D. Abowd, and T. Plötz, "On specialized window lengths and detector based human activity recognition," in *Proceedings of the 2018 ACM International Symposium on Wearable Computers*, ser. ISWC '18, Singapore, Singapore: Association for Computing Machinery, 2018, pp. 68–71, ISBN: 9781450359672. DOI: `10.1145/3267242.3267246`. [Online]. Available: `https://doi.org/10.1145/3267242.3267246`.

[323] J. Kulchyk and A. Etemad, "Activity recognition with wearable accelerometers using deep convolutional neural network and the effect of sensor placement," in *2019 IEEE SENSORS*, 2019, pp. 1–4. DOI: `10.1109/SENSORS43011.2019.8956668`.

[324] M. U. S. Khan *et al.*, "On the correlation of sensor location and human activity recognition in body area networks (bans)," *IEEE Systems Journal*, vol. 12, no. 1, pp. 82–91, 2018. DOI: `10.1109/JSYST.2016.2610188`.

[325] U. Maurer, A. Smailagic, D. Siewiorek, and M. Deisher, "Activity recognition and monitoring using multiple sensors on different body positions," in *International Workshop on Wearable and Implantable Body Sensor Networks (BSN'06)*, 2006, 4 pp.–116. DOI: `10.1109/BSN.2006.6`.

[326] I. Orha and S. Oniga, "Study regarding the optimal sensors placement on the body for human activity recognition," in *2014 IEEE 20th International Symposium for Design and Technology in Electronic Packaging (SIITME)*, 2014, pp. 203–206. DOI: `10.1109/SIITME.2014.6967028`.

[327] H. D. Nguyen, K. P. Tran, X. Zeng, L. Koehl, and G. Tartare, *Wearable sensor data based human activity recognition using machine learning: A new approach*, 2019. DOI: `10.48550/ARXIV.1905.03809`. [Online]. Available: `https://arxiv.org/abs/1905.03809`.

[328] C. Han, L. Zhang, Y. Tang, W. Huang, F. Min, and J. He, "Human activity recognition using wearable sensors by heterogeneous convolutional neural networks," *Expert Systems with Applications*, vol. 198, p. 116 764, Jul. 2022, ISSN: 0957-4174. DOI: `10.1016/j.eswa.2022.116764`. [Online]. Available: `http://dx.doi.org/10.1016/j.eswa.2022.116764`.

[329] J. L. Gay, S. A. Cherof, C. C. LaFlamme, and P. J. O'Connor, "Psychological aspects of stair use: A systematic review," *American Journal of Lifestyle Medicine*, vol. 16, no. 1, pp. 109–121, Aug. 2019, ISSN: 1559-8284. DOI: `10.1177/1559827619870104`. [Online]. Available: `http://dx.doi.org/10.1177/1559827619870104`.

[330] S. A. Bridenbaugh and R. W. Kressig, "Laboratory review: The role of gait analysis in seniors' mobility and fall prevention," *Gerontology*, vol. 57, no. 3, pp. 256–264, Oct. 2010, ISSN: 1423-0003. DOI: `10.1159/000322194`. [Online]. Available: `http://dx.doi.org/10.1159/000322194`.

[331] M. Straczkiewicz, P. James, and J.-P. Onnela, "A systematic review of smartphone-based human activity recognition methods for health research," *npj Digital Medicine*, vol. 4, no. 1, Oct. 2021, ISSN: 2398-6352. DOI: `10.1038/s41746-021-00514-4`. [Online]. Available: `http://dx.doi.org/10.1038/s41746-021-00514-4`.

[332] M. Zhang and A. Sawchuk, "A feature selection-based framework for human activity recognition using wearable multimodal sensors," in *Proceedings of the 6th International ICST Conference on Body Area Networks*, ser. BODYNETS, ACM, 2011. DOI: `10.4108/`

`icst.bodynets.2011.247018.` [Online]. Available: `http://dx.doi.org/10.4108/` `icst.bodynets.2011.247018.`

[333] F. Li, K. Shirahama, M. Nisar, L. Köping, and M. Grzegorzek, "Comparison of feature learning methods for human activity recognition using wearable sensors," *Sensors*, vol. 18, no. 2, p. 679, Feb. 2018, ISSN: 1424-8220. DOI: `10.3390/s18020679`. [Online]. Available: `http://dx.doi.org/10.3390/s18020679`.

[334] N. Zurbuchen, P. Bruegger, and A. Wilde, "A comparison of machine learning algorithms for fall detection using wearable sensors," in *2020 International Conference on Artificial Intelligence in Information and Communication (ICAIIC)*, Fukuoka, Japan: IEEE, Feb. 2020.

[335] U. ZIA, W. KHALIL, S. KHAN, I. AHMAD, and M. N. KHAN, "Towards human activity recognition for ubiquitous health care using data from awaist-mounted smartphone," *TURKISH JOURNAL OF ELECTRICAL ENGINEERING & COMPUTER SCIENCES*, vol. 28, no. 2, pp. 646–663, Mar. 2020, ISSN: 1303-6203. DOI: `10.3906/elk-1901-31`. [Online]. Available: `http://dx.doi.org/10.3906/elk-1901-31`.

[336] H. Zhang, Z. Chen, D. Zanotto, and Y. Guo, "Robot-assisted and wearable sensor-mediated autonomous gait analysis," in *2020 IEEE International Conference on Robotics and Automation (ICRA)*, IEEE, May 2020. DOI: `10.1109/icra40945.2020.9197571`. [Online]. Available: `http://dx.doi.org/10.1109/ICRA40945.2020.9197571`.

[337] T. Reches *et al.*, "Using wearable sensors and machine learning to automatically detect freezing of gait during a fog-provoking test," *Sensors*, vol. 20, no. 16, p. 4474, Aug. 2020, ISSN: 1424-8220. DOI: `10.3390/s20164474`. [Online]. Available: `http://dx.doi.org/10.3390/s20164474`.

[338] Z. Chen, L. Zhang, Z. Cao, and J. Guo, "Distilling the knowledge from handcrafted features for human activity recognition," *IEEE Transactions on Industrial Informatics*, vol. 14, no. 10, pp. 4334–4342, Oct. 2018, ISSN: 1941-0050. DOI: `10.1109/tii.2018.2789925`. [Online]. Available: `http://dx.doi.org/10.1109/TII.2018.2789925`.

[339] M. M. Hassan, M. Z. Uddin, A. Mohamed, and A. Almogren, "A robust human activity recognition system using smartphone sensors and deep learning," *Future Generation Computer Systems*, vol. 81, pp. 307–313, Apr. 2018, ISSN: 0167-739X. DOI: `10.1016/j.`

future.2017.11.029. [Online]. Available: http://dx.doi.org/10.1016/j.future.2017.11.029.

[340] G. J. Rani, M. F. Hashmi, and A. Gupta, "Surface electromyography and artificial intelligence for human activity recognition—a systematic review on methods, emerging trends applications, challenges, and future implementation," *IEEE Access*, vol. 11, pp. 105 140–105 169, 2023. DOI: 10.1109/ACCESS.2023.3316509.

[341] S. S. Bangaru, C. Wang, S. A. Busam, and F. Aghazadeh, "Ann-based automated scaffold builder activity recognition through wearable emg and imu sensors," *Automation in Construction*, vol. 126, p. 103 653, 2021, ISSN: 0926-5805. DOI: https://doi.org/10.1016/j.autcon.2021.103653. [Online]. Available: https://www.sciencedirect.com/science/article/pii/S0926580521001047.

[342] N. Anantrasirichai, J. Burn, and D. Bull, "Terrain classification from body-mounted cameras during human locomotion," *IEEE Transactions on Cybernetics*, vol. 45, no. 10, pp. 2249–2260, 2015. DOI: 10.1109/TCYB.2014.2368353.

[343] F. Demrozi, G. Pravadelli, A. Bihorac, and P. Rashidi, "Human activity recognition using inertial, physiological and environmental sensors: A comprehensive survey," *IEEE Access*, vol. 8, pp. 210 816–210 836, 2020. DOI: 10.1109/ACCESS.2020.3037715.

[344] C. Hou, "A study on imu-based human activity recognition using deep learning and traditional machine learning," in *2020 5th International Conference on Computer and Communication Systems (ICCCS)*, 2020, pp. 225–234. DOI: 10.1109/ICCCS49078.2020.9118506.

[345] N. G. Nia, E. Kaplanoglu, A. Nasab, and H. Qin, "Human activity recognition using machine learning algorithms based on imu data," in *2023 5th International Conference on Bio-engineering for Smart Technologies (BioSMART)*, 2023, pp. 1–8. DOI: 10.1109/BioSMART58455.2023.10162095.

[346] D. Yang, J. Huang, X. Tu, G. Ding, T. Shen, and X. Xiao, "A wearable activity recognition device using air-pressure and imu sensors," *IEEE Access*, vol. 7, pp. 6611–6621, 2019. DOI: 10.1109/ACCESS.2018.2890004.

[347] S. Zhang *et al.*, "Deep learning in human activity recognition with wearable sensors: A review on advances," *Sensors*, vol. 22, no. 4, 2022, ISSN: 1424-8220. DOI: 10.3390/s22041476. [Online]. Available: https://www.mdpi.com/1424-8220/22/4/1476.

REFERENCES

[348] *World's lowest power 9-axis mems motiontracking™ device*, DS-000189, Rev. 1.5, InvenSense, Sep. 2021.

[349] *Color light-to-digital converter with ir filter*, TAOS135, Texas Advanced Optoelectronic Solutions Inc., Aug. 2012.

[350] *A new generation, long distance ranging time-of-flight sensor based on st's flightsense™ technology*, DocID031281, Rev. 3, STMicroelectronics, Nov. 2018.

[351] R. Das and N. Kumar, "Investigations on postural stability and spatiotemporal parameters of human gait using developed wearable smart insole," *Journal of Medical Engineering &; Technology*, vol. 39, no. 1, pp. 75–78, Oct. 2014, ISSN: 1464-522X. DOI: `10.3109/03091902.2014.968676`. [Online]. Available: `http://dx.doi.org/10.3109/03091902.2014.968676`.

[352] R. Eguchi and M. Takahashi, "Insole-based estimation of vertical ground reaction force using one-step learning with probabilistic regression and data augmentation," *IEEE Transactions on Neural Systems and Rehabilitation Engineering*, vol. 27, no. 6, pp. 1217–1225, 2019. DOI: `10.1109/TNSRE.2019.2916476`.

[353] A. M. Howell, T. Kobayashi, H. A. Hayes, K. B. Foreman, and S. J. M. Bamberg, "Kinetic gait analysis using a low-cost insole," *IEEE Transactions on Biomedical Engineering*, vol. 60, no. 12, pp. 3284–3290, Dec. 2013, ISSN: 1558-2531. DOI: `10.1109/tbme.2013.2250972`. [Online]. Available: `http://dx.doi.org/10.1109/TBME.2013.2250972`.

[354] U. Pant, S. Baral, A. Gupta, and P. L. Shrestha, "Design of force sensitive resistor (fsr) embedded insole for phase detection during human gait and its classification," *IOP Conference Series: Materials Science and Engineering*, vol. 1314, no. 1, p. 012008, Sep. 2024, ISSN: 1757-899X. DOI: `10.1088/1757-899x/1314/1/012008`. [Online]. Available: `http://dx.doi.org/10.1088/1757-899X/1314/1/012008`.

[355] H. Prasanth *et al.*, "Wearable sensor-based real-time gait detection: A systematic review," *Sensors*, vol. 21, no. 8, 2021, ISSN: 1424-8220. DOI: `10.3390/s21082727`. [Online]. Available: `https://www.mdpi.com/1424-8220/21/8/2727`.

[356] V. M. Santos, B. B. Gomes, M. A. Neto, and A. M. Amaro, "A systematic review of insole sensor technology: Recent studies and future directions," *Applied Sciences*, vol. 14, no. 14, 2024, ISSN: 2076-3417. DOI: `10.3390/app14146085`. [Online]. Available: `https://www.mdpi.com/2076-3417/14/14/6085`.

[357] *Fsr 402 data sheet*, 30-81794, Rev. A, Interlink Electronics, Oct. 2010.

[358] *Arduino® nano 33 ble product reference manual*, Arduino, Feb. 2024.

[359] V. Losing and M. Hasenjäger, "A multi-modal gait database of natural everyday-walk in an urban environment," *Scientific Data*, vol. 9, no. 1, Aug. 2022, ISSN: 2052-4463. DOI: 10.1038/s41597-022-01580-3. [Online]. Available: http://dx.doi.org/10.1038/s41597-022-01580-3.

[360] D. Roggen *et al.*, "Collecting complex activity datasets in highly rich networked sensor environments," in *2010 Seventh International Conference on Networked Sensing Systems (INSS)*, 2010, pp. 233–240. DOI: 10.1109/INSS.2010.5573462.

[361] S. Khandelwal and N. Wickström, "Evaluation of the performance of accelerometer-based gait event detection algorithms in different real-world scenarios using the marea gait database," *Gait & Posture*, vol. 51, pp. 84–90, 2017, ISSN: 0966-6362. DOI: https://doi.org/10.1016/j.gaitpost.2016.09.023. [Online]. Available: https://www.sciencedirect.com/science/article/pii/S0966636216305859.

[362] S. R. Simon, "Quantification of human motion: Gait analysis—benefits and limitations to its application to clinical problems," *Journal of Biomechanics*, vol. 37, no. 12, pp. 1869–1880, 2004, ISSN: 0021-9290. DOI: https://doi.org/10.1016/j.jbiomech.2004.02.047. [Online]. Available: https://www.sciencedirect.com/science/article/pii/S0021929004001228.

[363] W. Tao, T. Liu, R. Zheng, and H. Feng, "Gait analysis using wearable sensors," *Sensors*, vol. 12, no. 2, pp. 2255–2283, 2012, ISSN: 1424-8220. DOI: 10.3390/s120202255. [Online]. Available: https://www.mdpi.com/1424-8220/12/2/2255.

[364] J. Antonio Santoyo-Ramón, E. Casilari, and J. Manuel Cano-García, "A study of the influence of the sensor sampling frequency on the performance of wearable fall detectors," *Measurement*, vol. 193, p. 110 945, 2022, ISSN: 0263-2241. DOI: https://doi.org/10.1016/j.measurement.2022.110945. [Online]. Available: https://www.sciencedirect.com/science/article/pii/S0263224122002226.

[365] S. Wang, L. Zhang, X. Wang, W. Huang, H. Wu, and A. Song, "Patchhar: A mlp-like architecture for efficient activity recognition using wearables," *IEEE Transactions on Biometrics, Behavior, and Identity Science*, vol. 6, no. 2, pp. 169–181, 2024. DOI: 10.1109/TBIOM.2024.3354261.

REFERENCES

[366] G. Park, K. M. Lee, and S. Koo, "Uniqueness of gait kinematics in a cohort study," en, *Sci. Rep.*, vol. 11, no. 1, p. 15 248, Jul. 2021.

[367] F. Hug *et al.*, "Individuals have unique muscle activation signatures as revealed during gait and pedaling," *Journal of Applied Physiology*, vol. 127, no. 4, pp. 1165–1174, 2019, PMID: 31589090. DOI: 10.1152/japplphysiol.01101.2018. eprint: https://doi.org/10.1152/japplphysiol.01101.2018. [Online]. Available: https://doi.org/10.1152/japplphysiol.01101.2018.

[368] T. Gujarathi and K. Bhole, "Gait analysis using imu sensor," in *2019 10th International Conference on Computing, Communication and Networking Technologies (ICCCNT)*, 2019, pp. 1–5. DOI: 10.1109/ICCCNT45670.2019.8944545.

[369] A. R. Anwary, H. Yu, and M. Vassallo, "Optimal foot location for placing wearable imu sensors and automatic feature extraction for gait analysis," *IEEE Sensors Journal*, vol. 18, no. 6, pp. 2555–2567, 2018. DOI: 10.1109/JSEN.2017.2786587.

[370] A. Küderle, N. Roth, J. Zlatanovic, M. Zrenner, B. Eskofier, and F. Kluge, "The placement of foot-mounted imu sensors does affect the accuracy of spatial parameters during regular walking," *PLOS ONE*, vol. 17, no. 6, pp. 1–29, Jun. 2022. DOI: 10.1371/journal.pone.0269567. [Online]. Available: https://doi.org/10.1371/journal.pone.0269567.

[371] M. Song and J. Kim, "An ambulatory gait monitoring system with activity classification and gait parameter calculation based on a single foot inertial sensor," *IEEE Transactions on Biomedical Engineering*, vol. 65, no. 4, pp. 885–893, 2018. DOI: 10.1109/TBME.2017.2724543.

[372] M. V. Potter, L. V. Ojeda, N. C. Perkins, and S. M. Cain, "Effect of imu design on imu-derived stride metrics for running," *Sensors*, vol. 19, no. 11, 2019, ISSN: 1424-8220. DOI: 10.3390/s19112601. [Online]. Available: https://www.mdpi.com/1424-8220/19/11/2601.

[373] A. Mannini, V. Genovese, and A. Maria Sabatini, "Online decoding of hidden markov models for gait event detection using foot-mounted gyroscopes," *IEEE Journal of Biomedical and Health Informatics*, vol. 18, no. 4, pp. 1122–1130, 2014. DOI: 10.1109/JBHI.2013.2293887.

[374] A. Sabatini, C. Martelloni, S. Scapellato, and F. Cavallo, "Assessment of walking features from foot inertial sensing," *IEEE Transactions on Biomedical Engineering*, vol. 52, no. 3, pp. 486–494, 2005. DOI: 10.1109/TBME.2004.840727.

[375] G. Bailey and R. Harle, "Assessment of foot kinematics during steady state running using a foot-mounted imu," *Procedia Engineering*, vol. 72, pp. 32–37, 2014, The Engineering of Sport 10, ISSN: 1877-7058. DOI: https://doi.org/10.1016/j.proeng.2014.06.009. [Online]. Available: https://www.sciencedirect.com/science/article/pii/S1877705814005256.

[376] M. Narasimhappa, A. D. Mahindrakar, V. C. Guizilini, M. H. Terra, and S. L. Sabat, "Mems-based imu drift minimization: Sage husa adaptive robust kalman filtering," *IEEE Sensors Journal*, vol. 20, no. 1, pp. 250–260, 2020. DOI: 10.1109/JSEN.2019.2941273.

[377] K. L. Roeing, K. L. Hsieh, and J. J. Sosnoff, "A systematic review of balance and fall risk assessments with mobile phone technology," *Archives of Gerontology and Geriatrics*, vol. 73, pp. 222–226, 2017, ISSN: 0167-4943. DOI: https://doi.org/10.1016/j.archger.2017.08.002. [Online]. Available: https://www.sciencedirect.com/science/article/pii/S0167494317302698.

[378] R. Sun and J. J. Sosnoff, "Novel sensing technology in fall risk assessment in older adults: A systematic review," en, *BMC Geriatr.*, vol. 18, no. 1, Dec. 2018.

[379] C. Eost-Telling *et al.*, "Digital technologies to prevent falls in people living with dementia or mild cognitive impairment: A rapid systematic overview of systematic reviews," en, *Age Ageing*, vol. 53, no. 1, Jan. 2024.

[380] L. Ren and Y. Peng, "Research of fall detection and fall prevention technologies: A systematic review," *IEEE Access*, vol. 7, pp. 77 702–77 722, 2019. DOI: 10.1109/ACCESS.2019.2922708.

[381] R. Tanwar, N. Nandal, M. Zamani, and A. A. Manaf, "Pathway of trends and technologies in fall detection: A systematic review," *Healthcare*, vol. 10, no. 1, 2022, ISSN: 2227-9032. DOI: 10.3390/healthcare10010172. [Online]. Available: https://www.mdpi.com/2227-9032/10/1/172.

Appendix A

Systematic Review Tables

The following appendix contains the full tables detailing the summaries for each of the 104 studies included in the systematic review performed in Chapter 2. Tables A.1-A.3, A.4-A.5, A.6-A.7, and A.8-A.10 contain the summaries of each fall detection, prediction, prevention, and intervention study, respectively.

Authors & Year	Sensor(s)	Sensor Locations	Dataset	Activities	Classification Methods	Results
Alarifi and Alwadain [159] 2020	6x 9-DoF Inertial Measurement Unit (IMU)	Chest, waist, head, right wrist, right ankle, and right thigh.	New dataset - 14 participants	16 Activity of Daily Living (ADL) and 20 falls, repeated 5 times each.	**Convolutional Neural Network (CNN)**, Support Vector Machine (SVM), Artificial Neural Network (ANN), and Recurrent Neural Network (RNN).	Acc: 99.5%, Prec: 99.6%, Rec: 99.8%, F1: 99.7%.
Alzahrani et al. [163] 2019	Kinect V2	Ambient	FallFree	N/A	Decision Tree (DT), **Random Forest (RF)**, **ANN**, SVM.	Acc: 99.5%.
Attaoui et al. [152] 2020	1x 6-DoF IMU	Chest	SisFall, New dataset for testing - 6 participants	19 ADLs and 15 falls	**SVM**, RF, **K-Nearest Neighbours (KNN)** ANN.	Scenario A: Acc 99.9% Scenario B: Acc 97.6% Real-World: Acc: 94.42%
Aziz et al. [146] 2014	4x Accelerometer	Left and right lateral malleoli, anterior waist, and sternum.	New dataset - 12 participants	Recreate a recording of a fall onto a mattress.	**Linear Discriminant Analysis (LDA)**	Acc: 78% Spec: 97%
Butt et al. [147] 2021	1x 3-lead Electrocardiogram (ECG)	Chest	New dataset - 6 participants	30 trials consisting of a 10 second rest followed by a fall and laying.	**CNN**	Acc: 97.36%
Cal et al. [153] 2022	1x accelerometer	Wrist	UMAFall, UCIFall, and FallAllD	N/A	KNN, **EKMeans (ensemble of KNN and K-means**	Fall vs No-Fall Acc: 56.7% Multiclass ADL: Acc: 58.0%
Chen et al. [148] 2017	IMU	Smartphone in right-side trouser pocket	New Dataset - 10 participants	8 ADLs and 6 falls	**SVM**	Sens: 93.3% Spec: 95.71%
Dhiman and Vishwakarma [117] 2019	Kinect	Ambient	URFall, KARD, NUCLA, and a new dataset dubbed 'AbHA' featuring 8 participants	5 ailment-based activities such as headache, fainting, chest pain, backwards fall, and forwards fall.	**KNN, SVM**	URFall: Acc: 96.5% KARD: Acc: 96.6% NUCLA: Acc: 86.4% AbHA: Acc: 95.9%

Table A.2: Fall Detection Studies — continued

Authors & Year	Sensor(s)	Sensor Locations	Dataset	Activities	Classification Methods	Results
Dhiman and Vishwakarma [117] 2019	Kinect	Ambient	URFall, KARD, NUCLA, and a new dataset dubbed 'AbHA' featuring 8 participants	5 ailment-based activities such as headache, fainting, chest pain, backwards fall, and forwards fall.	**KNN, SVM**	URFall: Acc: 96.5% KARD: Acc: 96.6% NUCLA: Acc: 86.4% AbHA: Acc: 95.9%
Fan et al. [170] 2017	RGB Camera	Ambient	Le2i, Multiple Cameras Fall (MCF) dataset, High Quality Fall Simulation (HQFS) dataset, new 'YouTube Fall Dataset'	430 videos containing a fall and 176 videos featuring normal activities	**CNN**	Le2i: Sens: 98.4% Spec: 100% MCF: Sens: 97.1% Spec: 97.9% HQFS: Sens: 74.2% Spec: 68.6% Youtube Fall: Sens: 63.7% Spec: 68.1%
Ezatzadeh et al. [171] 2021	RGB Camera	Ambient	MCF dataset	N/A	SVM, **Hidden Markov Model (HMM)**	Acc: 98.7% Sens: 98.7% Spec: 98.6%
Espinosa et al. [172] 2019	RGB Camera	Ambient	2 cameras from the UP-Fall dataset	N/A	**CNN**, SVM, RF, ANN, KNN	Acc: 95.6% Prec: 96.9% Sens: 98.0% Spec: 83.1% F1: 97.4%
Fan et al. [173] 2016	RGB Camera	Ambient	MCF dataset and RGB data from SDUFall	N/A	**DAGSVM (Ensemble SVM)**	MCF: Acc: 98.3% SDUFall: Acc: 81.3%
Garripoli et al. [149] 2015	RaDAR	Ambient	New dataset - 16 participants	40 random walking activities, 30 sitting and standing activities, and 40 fall activities.	**SVM**	Sens: 100%
Hadjadji et al. [174] 2022	RGB Camera	Ambient	MCF, HQFS, and URFall datasets	N/A	SVM, **One class-Principal Component Analysis (PCA)**	MCF: Acc: 99.6% Sens: 100% Spec: 99.2% HQFS: Acc: 87.9% Sens: 89.9% Spec: 99.2% URFall: Acc: 100% Sens: 100% Spec: 100%
Haffner et al. [182] 2018	Flooring augmented with capacitive sensors	Ambient (system 1), portable version (system 2).	New dataset - 4 participants	System 1: 2 falls, 4 static non-fall events. System 2: 1 fall, 1 static non-fall event.	**Least Squares (LS)**, KNN, SVM	System 1: Acc: 92.6% System 2: Acc: 100%
Haider et al. [179] 2019	5G C-band wireless channel information	Ambient	New dataset - 8 participants	5 ADLs and 1 fall.	**SVM**, Naïve Bayes, DT	Kappa score: 0.98
Harrou et al. [118] 2017	RGB Camera	Ambient	URFall, Fall Detection Dataset (FDD)	N/A	**Multivariate, exponentially-weighted moving-average SVM**, KNN, ANN, Naïve Bayes	Acc: 96.7% Sens: 100% Spec: 94.9% Prec: 93.6% F1: 95.2% AUC: 95.3%
Jin et al. [177] 2022	mmWave RaDAR	Ambient	New dataset - 2 participants	5 ADLs and 4 falls	**RNN-based autoencoder dubbed HVRAE**	Detection rate: 98%
Kambhampati et al. [154] 2015	IMU	Smartphone mounted to the waist.	New dataset - 6 participants	5 ADLs and 4 falls along with transitions	**SVM**, Naïve Bayes, DT, ANN	Fall detection: Acc: 97.3% Activity recognition: Acc: 95.6% Falls and activities: Acc: 96.1%

Authors & Year	Sensor(s)	Sensor Locations	Dataset	Spatiotemporal Gait Parameters	Classification Methods	Results
Kwolek and Kepski [164] 2014 Kwolek and Kepski [165] 2015 Kwolek and Kepski [166] 2016	6-axis IMU & Kinect	Pelvis (IMU) and ambient	URFall and new dataset - 5 participants	URFall with 3 additional falls and 6 additional ADLs including IMU data	**SVM, KNN, Fuzzy Logic**	Study 1: Acc: 98.3% Prec: 96.8% Sens: 100% Spec: 96.7% Study 2: Acc: 95.8% Prec: 90.1% Sens: 100% Spec: 92.9% Study 3: Acc: 97.1% Prec: 93.7% Sens: 100% Spec: 95.0%
Li *et al.* [155] 2013	Accelerometer	Waist	New dataset - 5 participants	6 ADLs	**ANN**, KNN	Acc: 98.3%
Liu *et al.* [180] 2011	3x Pyro-electric Infrared (PIR) sensors	Ambient	New dataset - 4 participants	7 ADLs and 1 fall	**HMM**	Acc: 93.1% Prec: 92.6% Sens: 93.7% Spec: 92.5%
Luo *et al.* [181] 2012	7x PIR sensors	Ambient	New dataset - 8 participants	4 ADLs and 1 fall	**HMM**	Acc: 92.2% Prec: 97.7% Sens: 86.5% Spec: 98.0%
Mansoor *et al.* [167] 2022	Kinect	Ambient	New dataset - 5 participants	7 ADLs and 3 falls	**KNN**	Acc: 90.8%
Mazurek *et al.* [139] 2018	Kinect	Ambient	IRMTv1 and TSTv2 datasets	N/A	**SVM**, ANN, Naïve Bayes	IRMTv1: False Negative (FN): 0.0% False Negative Rate (FNR): 0.0% False Positive (FP): 1.0% False Positive Rate (FPR): 1.25% TSTv2: FN: 3.0% FNR: 2.27% FP: 16.0% FPR: 12.1%
Min *et al.* [168] 2018	Kinect	Ambient	TSTv2 dataset	N/A	**SVM**	Acc: 92.1%
Narasimhan [150] 2012	Accelerometer	Torso	ADLs: New dataset - 15 participants Falls: New dataset - 10 participants	11 ADLs and 10 falls	**Threshold algorithm**	ADLs: Sens: 100% Falls: Sens: 99%
Olivieri *et al.* [176] 2012	RGB Camera	Ambient	New dataset - 12 participants	5 ADLs and 1 fall	**KNN**	Acc: 98.28%
Panahi and Ghods [119] 2018	Kinect	Ambient	URFall and new dataset - 5 participants	URFall with 3 additional falls and 6 additional ADLs	**SVM, threshold algorithm**	Sens: 100% Spec: 97.5%
Ribeiro *et al.* [162] 2022	IMU and Doppler RaDAR	Nodes containing both sensors are placed in various locations on the floor	New dataset - number of participants not listed	1 fall and 4 noise classes	**Mortlet Wavelet**, ANN	Acc: 92.5%
Saleh *et al.* [131] 2021	IMU and barometer	Neck, waist, and wrist	Sisfall, UMA-Fall, AllFallD	N/A	**CNN, ANN, autoencoder**,Long Short-Term Memory (LSTM), SVM, KNN,RF	Sisfall: Acc: 99.5% UMA-Fall: Acc: 98.49% FallAllD: Acc: 93.46%
Saleh *et al.* [141] 2021	IMU and barometer	Neck and wrist	AllFallD and RealAct	N/A	**Gradient Boosting**,SVM, RF, Adaboost,DT, KNN, LDA, Quadratic Discrimenant Analysis (QDA), Naïve Bayes	Neck Sensor: Acc: 99.0% Sens: 100% Spec: 98.5% Wrist Sensor: Acc: 96.9% Sens: 100% Spec: 96.7%

Table A.3: Fall Detection Studies — continued

Authors & Year	Sensor(s)	Sensor Locations	Dataset	Activities	Classification Methods	Results
Saurav *et al.* [142] 2022	360-degree RGB Camera	Ambient	UPFall, Kinetics-400, UCF101, Fall360	N/A	**Multiple hybrid CNN and LSTM model architectures.**	Fall360: Acc: 98.42% UPFall: Acc: 100%
Sengul *et al.* [156] 2022	IMU	Wrist-mounted smartwatch	New dataset - 15 participants	4 ADLs and 2 falls	KNN, SVM, RF, **Bidirectional LSTM**	Leave-one-activity-out: Acc: 99.69% Leave-one-subject-out: Acc: 100%
Shrivastava and Pandey [157] 2019	IMU	Smartphone in a pocket	Medrano et al's dataset, FARSEEING	N/A	**SVM**	Acc: 99.25% Sens: 100% Spec: 98.77% F1: 99.53%
Su *et al.* [175] 2015	RGB Camera	Ambient	MCF	N/A	**Ensemble SVM**	Acc: 98.00% Sens: 85.00% Spec: 100% F1: 92.00%
Tran *et al.* [120] 2017	Kinect	Ambient	URFall, LE2I, New datasets - 20 participants dubbed "MICAFALL-1" and 4 participants	MICAFALL-1: 200 ADLs & 40 falls, Unnamed: 206 ADLs & 95 falls.	**Threshold algorithm, SVM**	Skeleton-based: Acc: 93.02% Sens: 81.25% Spec: 100% Prec: 100% URFall: Acc: 99.37% Sens: 100% Spec: 99.23% Prec: 96.77% LE2I: Acc: 99.61% Sens: 98.00% Spec: 99.69% Prec: 94.32% MICAFALL-1: Acc: 98.75% Sens: 95.24% Spec: 100% Prec: 100% Unnamed: Acc: 96.01% Sens: 88.42% Spec: 99.51% Prec: 98.82%
Vaiyapuri *et al.* [121] 2021	RGB Camera	Ambient	MCF, URFall	N/A	**CNN**	Multiple cameras fall: Acc: 99.76% Spec: 99.29% Prec: 99.68% Rec: 99.85% F1: 99.65% URFall: Acc: 99.57% Spec: 99.52% Prec: 99.72% Rec: 99.55% F1: 99.38%
Wu *et al.* [158] 2015	IMU	Waist	New dataset - 3 participants	5 ADLs, 4 falls	**Threshold algorithm**	Acc: 96.25%
Wu *et al.* [160] 2019	IMU	Waist and right thigh	New dataset - 15 participants	7 ADLs, 2 falls	**Fisher discriminant analysis**	Sens: 95.50% Spec: 97.30%
Xiong *et al.* [122] 2020	RGB Camera	Ambient	URFall, FDD, MCF, New dataset - 12 participants	4 ADLs, 1 fall	**CNN**	URFall: Acc: 100% FDD: Acc: 100% MCF: 100%, Unnamed: Acc: 98.18%
Yao *et al.* [169] 2022	Kinect	Ambient	TSTv2, UT-A3D	N/A	**CNN**	TSTv2: Acc: 97.35% UT-A3D: Acc: 100%
Yu *et al.* [151] 2013	RGB Camera	Ambient	New dataset - 12 participants	38 ADLs, 18 falls	**One-class, unsupervised SVM**	True Positive Rate (TPR): 100% FPR: 3%
Yun and Gu [123] 2016 Yun and Gu [124] 2016	RGB Camera	Ambient	MCF, URFall, ACT4^2	N/A	AdaBoost, **SVM**	MCF: Sens: 100% Spec: 100% URFall: Sens: 100% Spec: 100% ACT4^2: Sens: 98.13% Spec: 94.48%

Table A.3: Fall Detection Studies — continued

Authors & Year	Sensor(s)	Sensor Locations	Dataset	Activities	Classification Methods	Results
Lee *et al.* [161] 2023	IMU	Chest, wrist, necklace/-torso	New dataset - 20 participants	4 ADLs, 1 fall	**LSTM**, CNN, Bidirectional LSTM, Hybrid CNN and LSTM	Acc: 93.26% Prec: 97.57% Rec: 96.06% F1: 96.74%
Cardenas *et al.* [178] 2023	Continuous-Wave Doppler RaDAR	Ambient	New dataset - 11 participants	2 ADLs, 1 fall. Later reduced to 1 ADL, 1 fall	**LSTM**, CNN	With stairs: Acc: 82.20% Without stairs: Acc: 94.95% Prec: 92.1% Rec: 82.00%
Wang and Deng [125] 2024	RGB Camera	Ambient	URFall, Le2i	N/A	**RF**	Acc: 89.99%, Sens: 90.33%, Spec: 89.66%, Prec: 89.73%, F1: 90.02%.

Table A.4: Fall Prediction Studies

Authors & Year	Sensor(s)	Sensor Locations	Dataset	Spatiotemporal Gait Parameters	Classification Methods	Results
Bertolotti *et al.* [183] 2015	IMU	Waist	Two new datasets - 10 participants, 8 participants (healthy)	Centre of Pressure (CoP)/Centre of Mass (CoM)	N/A	IMU found to produce reliable estimates for CoP/CoM when compared with the gold standard Wii Balance Board (WBB).
Anwary *et al.* [184] 2018	IMU	Feet	New dataset - 20 participants (10 healthy, 10 with gait-affecting conditions)	Stride Length, Stride Time, Stride Velocity, Step Length, Step Time, Cadence, Step Velocity, Step Length Ratio, Stance Length, Stance Time, Stance Velocity, Swing Length, Swing Time, Swing Velocity	**Threshold algorithm**	Extracted gait parameters exhibit 97.73%-100% agreement with the Qualiysis motion capture device for healthy participants, and 88.71%-92.67% agreement for those with gait-affecting conditions.
Cai *et al.* [185] 2017	RGB Camera	Ambient	New dataset - 15 participants (healthy, simulated gait-affecting conditions)	Step Length, Step Length Ratio	**Threshold algorithm**	Mean Absolute Error (MAE) between the calculated parameters and measurements taken from footprints in sand was 1.95%, 2.40%, and 3.97% for 90, 45, and 30 degree views respectively.
Chen *et al.* [186] 2022	Robot-mounted Kinect, IMU, and force-sensing insoles	Ambient and Feet	New dataset - 10 participants (all healthy)	Margin of Stability (MoS), CoP/CoM, Stride Length, Step Length, Step Width, Stride Velocity	**Threshold algorithm**	Intra-class correlation coefficient (ICC) between calculated parameters and those captured with an Optitrack motion capture system: Anterioposterior MoS: 0.98, MoS: 0.92, Mediolateral MoS: 0.26, Stride Length: 1.0, Step Length: 1.0, Stride Velocity: 1.0, Step Width: 0.77
Colagiorgio *et al.* [196] 2014	Kinect	Ambient	New dataset - 79 participants (13 young, 66 older people)	N/A	Majority Classifier, DT, **SVM**, KNN, Naïve Bayes	Participants classified as at risk of falling or not. SVM was the highest performing with Acc: 84.3% Sens: 91.3%.
Cuddihy *et al.* [187] 2012	Pulse-Doppler Range Control Radar (RCR), Kinect	Ambient	New dataset - 13 participants (healthy)	Gait Speed	N/A	MAE used to find the similarity between manual timing, a Kinect, and the RCR. RCR alone: 14.5%, Kinect-corrected RCR: 11.9%, calibrated, Kinect-corrected RCR: 10.9%

Table A.5: Fall Prediction Studies — continued

Authors & Year	Sensor(s)	Sensor Locations	Dataset	Spatiotemporal Gait Parameters	Classification Methods	Results
Das and Kumar [188] 2015	Force-sensing insole	Feet	New dataset - 3 participants (healthy)	Stride time, swing phase, stance time, single support	N/A	Mean error for temporal parameters when compared to the Zebris pressure mat is 0.01s
Deguchi *et al.* [197] 2017	Robot-mounted Kinect	Ambient	New dataset - 4 participants (healthy)	N/A	**Balanced Iterative Reducing and Clustering using Hierarchies (BIRCH) Clustering**	Normal and abnormal gaits are clustered and then observed for similarity. Abnormal gait can be adequately seperated from healthy gait after 500 skeletons are observed, which took around 2 minutes.
Dubois *et al.* [198] 2021	Kinect	Ambient	New dataset - 30 participants (healthy)	Step length, step length variation, step time, step time variation, cadence, cadence variation, and gait speed	DT, AdaBoost, **ANN, Naïve Bayes, KNN**, SVM, RF, QDA	Participants are classified as high-risk or low-risk fallers. ANN, Naïve Bayes, and KNN achieve 100% mean accuracy.
Eguchi and Takahashi [189] 2019	Force-sensing insole	Feet	New dataset - 6 participants (healthy)	Ground Reaction Force (GRF)	**Gaussian Process Regression**	Mean error between insole and ground truth measured on force plates was 8%.
Eichler *et al.* [199] 2022	Kinect	Ambient	New dataset - 130 participants (100 in-patents, 30 carers)	N/A	**RF, SVM**	RF is used to predict the score of each Berg Balance Scale (BBS) task with accuracy ranging between 52% and 100%. For predicting fall risk, the SVM classifies subjects into low, medium, and high risk, with a physiotherapist's decision as the ground truth.
Abou Ghaida *et al.* [190] 2014	Force-sensing insole	Feet	New dataset - 8 participants (healthy)	CoP/CoM	N/A	Root Mean Square (RMS) error between the proposed system and the commercial F-SCAN system. Mediolateral displacement error: 4.3-7.8mm, anteroposterior displacement error: 2.4-5.9mm, mediolateral CoP RMS error: 3±2mm, anteroposterior CoP RMS error: 2±1.5mm.
González *et al.* [191] 2012	WBB, Kinect	Underfoot and ambient	New dataset - 5 participants (healthy)	CoP/CoM	N/A	RMS error for each subject between 13.00mm and 37.83mm
Gutta *et al.* [192] 2021	Depth Camera	Ambient	New dataset - 22 participants (healthy)	Stride length, stride time, stride speed, step length, step width, step time, cadence, stance time, swing time, stance to swing ratio, double support time, foot angle, maximum velocity, foot clearance	N/A	Mean error is used to compare the system to a Vicon motioncapture system. Error is extremely low for all parameters except for step width and foot angle. Over 90% of parameters are inliers.
Haescher *et al.* [200] 2020	IMU	Wrist	New dataset - 13 participants (healthy, older people)	Stride length	**Threshold algorithm**	A questionnaire and literature guidelines are used to determine if an individual is at high risk of falling. Then the system predicts the risk of falling after each of 3 tests is performed: 6-minute walking: 96.55%, Timed up and go: 86.43% 30-second sit to stand test: 78.15%.

Authors & Year	Sensor(s)	Sensor Locations	Dataset	Spatiotemporal Gait Parameters	Classification Methods	Results
Horiuchi *et al.* [193] 2017	Kinect	Ambient	New dataset - 11 participants (healthy)	CoP/CoM	**ANN**	RMS error of 154mm for body position prediction and 79mm for Centre of Gravity (CoG) position prediction.
Johnson *et al.* [201] 2019	Kinect	Ambient	New dataset - 74 participants (healthy and with gait-affecting conditions)	N/A	**ANN**	Median absolute error when predicting fall risk using the BBS score was 0.93.
McManus *et al.* [202] 2022	IMU	Lower back	New datasets - 39 and 248 participants (healthy, older people)	Postural sway	**Logistic regression**	Study 1 acts as a validation of the systems, study 2 classifies between fallers and non-fallers: Acc: 65.83% Sens: 90.59% Spec: 29.29% Positive Predicted Value (PPV): 68.75% Negative Predicted Value (NPV): 64.44%
Nouredanesh *et al.* [203] 2016	IMU, ECG, Electromyography (EMG)	rectus femoris, biceps femoris, tibialis anterior, gastrocnemius	New dataset - 5 participants (healthy)	N/A	KNN, SVM, **RF**	Compensatory balance responses predicted with an accuracy of 92.35%.
Savadkoohi *et al.* [204] 2021	Force plate	Underfoot	New dataset - 163 participants (various gait-affecting conditions)	CoP/CoM	**Hybrid CNN, LSTM, ANN**, RNN	Fall risk automatically determined by predicting fear of falling with Sens: 100%, Spec: 99.9%, Prec: 100%.
Seifert *et al.* [205] 2019	Micro-Doppler RaDAR	Ambient	New dataset - 14 participants (10 healthy, 4 with gait-affecting conditions)	N/A	Bayesian information criterion	Gait is classified as symmetric or asymmetric when walking towards (Mean Acc: 96.43%), and away (Mean Acc: 82.22%) from the sensor.
Shen *et al.* [206] 2016	IMU	Smartphone in pocket	New dataset - 6 participants (4 older people, 2 amputees)	N/A	High-Level Fuzzy Petri Net	Falls predicted one step before occurring. Forward fall: Rec: 91.60% Prec: 78.57% Backwards Fall: Rec: 87.5%, Prec: 77.78% Sideways Fall: Rec: 95.83%, Prec: 79.31%
Wang *et al.* [207] 2019	Motion capture system, force plates	Full-body and underfoot	New dataset - 112 participants (older people)	Step length, step width, gait speed, CoP/CoM, segment angles, segment velocity, for all trunk, thigh, shank, and foot. GRF, CoM velocity	**Logistic regression**	Body weight, step length, relative CoM position at heel strike, momentum change from heel strike to toe-off, right thigh angle, and angular velocity at heel strike can predict fall risk with greater than 60% accuracy.
Single *et al.* [194] 2024	LiDAR, IMU, GAITRite	Ambient, IMUs on feet, GAITRite underfoot	New dataset - 45 participants (healthy, some older people)	Step length, step time, stride length, stride time, cadence, velocity	N/A	The novel LiDAR approach is validated against the GAITRite and IMU approaches. The extracted spatiotemporal gait parameters from each of the systems are found to have no significant statistical differences.
Liu *et al.* [195] 2024	IMU, force-sensing shoes	Shank and instrumented shoes	New dataset - 31 participants (10 healthy, 11 Parkinsons, 10 stroke)	GRF	N/A	GRF is calcualted with a maximum error of around 20% and mean error of around 6%. Dynamic fall risk factor is caculated for each participant allowing fall risk to be quanitfied.

continued on the next page

Table A.6: Fall Prevention

Authors & Year	Device	Sensors	Prevention Method	Device Location	Number of Participants	Results
Antonellis *et al.* [208] 2018	Bilateral ankle exoskeleton	load cells and linear displacement sensors	Torque applied to the ankle to aid with ankle flexion.	Ankle	10 participants (healthy)	Lyapunov exponent decreased at higher values of exoskeleton power, whilst the Floquet multiplier was found to increase. As such, whether the exoskeleton aided in reducing variability is uncertain.
Deng *et al.* [209] 2019	Lower-limb exoskeleton	IMU & force-sensors in shoes.	Torque applied to the hip and knee joints.	Full lower-limb exoskeleton attached to the waist, thighs, shanks, and feet.	10 participants (healthy)	The system is reported to have helped improve balance and reduce the instability caused by upper body tilt.
Geravand *et al.* [210] 2015	Assistive robot walker	A range of sensors including 6-DOF force sensors	User holds a handle mounted to the robot via actuated arms. This arm is manipulated according to the user's extrapolated CoM	User manipulates the device with their hands.	1 participant (healthy)	Device reacted appropriately to provoked falls.
Hirota and Murakami [211] 2016	Assistive robot walker	IMU	Falls are detected using the IMU, and an algorithm brings the walker to a stop intelligently such that the fall is prevented.	User manipulates the device with their hands.	1 participant (healthy)	The device is tested in 3 different experiments, each of which was successful, with the walker autonomously adapting to the situation and returning the user to a state of balance.
Hu *et al.* [212] 2021	Soft robotic orthotic	N/A	Assistive torque is appled to ankle dorsiflexion to reduce gait variability	Ankle	24 participants (older people, 12 low, and 12 medium risk of fall)	Step width and step length variability decreased at all 3 speeds of walking that the device was tested at, becoming more promenant at lower speeds. The device was also found to reduce variability, although by a lesser amount, when attached but deactivated.
Van Lam and Fujimoto [213] 2019	Robotic walking cane	Gyroscope and touch sensor	Wheeled robotic walking cane which can adjust the output torque of the wheels to restore balance and prevent falls.	User manipulates the device with their hands.	7 participants (healthy)	Body vibration is measured when using no support, a traditional cane, and the robotic cane. Vibrations are significantly reduced with the robotic cane, with a larger difference between a traditional cane and robotic cane than no cane and a traditional cane.
Nomura *et al.* [214] 2015	Ankle exoskeleton	Force-sensing insole	6-DOF parallel bar active orthotic exoskeleton to increase foot clearence	Ankle	3 participants (healthy)	Foot clearance was reported to increase when the device is active.
Romtrairat *et al.* [215] 2019	Gyroscopic balance correction backpack	2-axis inclination sensor	2 gyroscopic flywheels generate torque to counteract postural sway, increasing balance and stability.	Lower back	1 simulated participant	The device performs well in a simulated environment and is below the recommended backpack weight.

Authors & Year	Device	Sensors	Prevention Method	Device Location	Number of Partici-pants	Results
Yan *et al.* [216] 2016	Robotic walking cane	Force sensors, laser range finder	The cane calculates the user's stability and can adapt and reposition itself to prevent falls.	User ma-nipulates the device with their hands.	N/A	Device appears to have been tested and responds accordingly to fall-like scenarios, acting to prevent the fall.
Taghvaei and Kosuge [217] 2018	Passive robot walker	Kinect	The user is watched by the Kinect while using the walker. If a fall is detected, a servo break is enabled to stabalise the user.	User ma-nipulates the device with their hands.	4 partici-pants (healthy)	Falls are detected with 98.75% accuracy, enabling the device to detect and prevent different types of fall.
Zhu and Yi [218] 2023	Bilateral knee ex-oskeleton	7 IMUs	Torque applied to the knee to aid in slip recovery.	Knee	6 partici-pants (healthy)	The group wearing the exoskeleton with the proposed slip prevention controller recovered in all 16 of the fall trials, whereas the control group without an exoskeleton recovered in only 6/16 trials.
Monaco *et al.* [219] 2017	Active pelvis orthosis	Torque-calculating actuators	A threshold algorithm detects perturbations and uses complient actuators to apply torques to the hip joints.	Pelvis	10 partici-pants (all older people, 2 amputees)	The device detects a perturbation in 350ms and successfully reduces the range of motion in the hip joint and keeps the wearer's CoM within a region of stability.

Table A.8: Fall Intervention

Authors and Year	Intervention	Duration of Pro-gram	Number of Partici-pants	Testing Method	Results
Schmid *et al.* [221] 2010	Yoga	12 weeks	14	Illinois Fear of Falling (FoF) measure, BBS, back scratch test, chair sit and reach test	decreased FoF (6%), increased static balance (4%) and lower-body flexibility (34%)
Duque *et al.* [222] 2013	Virtual Reality (VR)-based Balance training (BT)	6 weeks	60	VR based balance test, Survey of Activities and Fear of Falling (SAFFE)	increased balance parameters and reduced FoF
Coubard *et al.* [223] 2014	Contemporary dance	4 weeks	38	Upright Stance Posturography (USS)	increased alpha component in a Detrended Fluctuation Analysis (DFA)
Koceja and Greiwe [224] 2014	BT using a self-developed apparatus	4 weeks	1	Postural stability during the training	decreased sway area, lateral sway and anterior sway
Schwenk *et al.* [225] 2014	BT with IMU sensors and visual feedback	4 weeks	33	Reciprocal Compensatory Index (RCI), Alternate Step Test (AST), Timed Up and Go (TUG), user experience questionnaire	reduced CoM sway, ankle and hip sway. Improved AST and TUG score and gait speed
Freyler *et al.* [226] 2016	Sensorimotor training and reactive BT	4 weeks	38	Spinning top test, swinging platform test, transfer task with cognitive interference	improved postural sway and co-contraction index

Table A.9: Fall Intervention — continued

Authors and Year	Intervention	Duration of Program	Number of Participants	Testing Method	Results
Kwak *et al.* [227] 2016	Elastic-band resistance exercise	8 weeks	45	Functional Reach Test (FRT), BBS, TUG, Sit and Reach Test (SRT), and Activities-specific Balance Confidence Scale (ABC)	improved scores for FRT, BBS, TUG, SRT, and ABC
Pliske *et al.* [228] 2016	Karate and fitness training	20 weeks	68	Gait test and dual-task test	reduced single-step time, increased step frequency and step length and improved cognitive performance
Allison *et al.* [229] 2018	Sensory challenge BT	8 weeks	20	ABC, BBS, Sensory Organization Test (SOT), Lower Extremity Strength Score (LESS)	improved CoM gain and phase, BBS, SOT and LESS
Liu-Ambrose *et al.* [230] 2019	Otago training	52 weeks	345	Physiological Profile Assessment Scores (PPAS), TUG, Short Physical Performance Battery Scores (SPPBS), Self-reported Number of Falls (SNF)	improved SNF and no significant differences in physical performance
Phu *et al.* [231] 2019	VR-based BT	6 weeks	195	Sit to stand (STS), TUG, USS, Falls Efficacy Scale (FES), gait speed, handgrip strength	improved gait speed, FES, handgrip strength, and TUG
Dehzangi *et al.* [235] 2013	IMU-based Vibrotactile feedback nodes	20 minutes	12	Randomized controlled trial in which the experimental group and control group have their gait parameters compared before and after the training period.	Improved lateral sway and posture control. The experimental group maintained pre-training scores for parameters like cadence and gait velocity, whilst the control group exhibited increased variability over the same period.
Verrusio *et al.* [220] 2016	Full body passive exoskeleton	52 weeks	150	Tinetti Gait and Balance, Tinetti Gait, Tinetti Balance, SPPBS, a Numeric Rating Scale (NRS) for pain, and SF-36 QoL	Improved scores in the Tinetti Gait and Balance, Tinetti Balance, SPPBS, NRS, and SF-36 QoL.
Chittrakul *et al.* [232] 2020	Multi-system Physical Exercise (MPE)	12 weeks	72	Physiological Profile Assessment (PPA), Thai Fall Efficacy Scale (TFES), Thai Geriatric Depression Scale (TGDS), Health-Related Quality of Life (HRQOL)	MPE group exhibited reduced fall risk, fear of falling, depression score, and increased HRQOL after 12 weeks. At 24 weeks, depression score and HRQOL returned to pre-trial levels.
Zahedian-Nasab *et al.* [233] 2021	Simulated balance exercises using Xbox Kinect	6 weeks	60	FES, TUG, BBS	BBS, FES, and TUG scores improved in the intervention group and were unchanged in the control group.
Rikkonen *et al.* [4] 2023	26 weeks of a 1-hour circuit gym session and 1-hour Tai Chi session each week, with warm-ups 50 minutes of training, followed by a year of unlimited access to facilities.	26 weeks/12 months.	914 (recruited), 850 (12-months), 838 (24-months)	TUG and fall rate	Slight improvements in leg extension strength and one leg stance time, improved TUG speed. 14.3% reduction in fall rate among the exercise group after 24 months.

Table A.10: Fall Intervention — continued

Authors and Year	Intervention	Duration of Program	Number of Participants	Testing Method	Results
Sturnieks *et al.* [234] 2024	Goal of 120 (79.7 mean, actual) minutes of exergame step training or cognitive training per week	52 weeks	716	Fall rate, postural sway, coordinated stability, single task gait velocity, single task gait variability, dual-task gait velocity, dual-task gait variability, short physical performance battery, TUG, hand reaction time, choice stepping reaction time, inhibitory choice stepping reaction time, stroop choice stepping reaction time, trail making test B minus A, controlled oral word association test, digit span test forwards, digit span test backwards, Victoria Stroop test interference effect, Victoria Stroop test errors, Addenbrooke's Cognitive Examination-Revised (ACE-R), Patient Health Questionnaire 9 (PHQ-9), Generalized Anxiety Disorder Scale (GADS), Iconographical Falls Efficacy Scale (IFES), World Health Organisation Disability Assessment Schedule v2.0 (WHODAS v.2.0), Late Life Function and Disability Instrument (LLFDI)	Exergame group exhibited 26% reduction in self-reported fall rate along with improvements in the PHQ-9, IFES, and LLFDI tests, whereas cognitive training was found to be relatively ineffective.

Appendix B

Ethical Approval Documentation

The following appendix includes the documentation pertaining to the ethical approval of the study conducted in Chapter 4. All personal information such as email addresses, names, etc. which refer to anyone other than the author of this work have been redacted. Included in this section are: the initial ethical approval from University of Leeds (UoL); approval of an amendment to increase the number of participants from 10 to 20; the participant information sheet; the consent form; the risk assessment; and the experimental procedure.

MEEC 21-016 Study Approval

Dear John

MEEC 21-016 - Context- and Terrain-Aware Gait Analysis and Visualisation

NB: All approvals/comments are subject to compliance with current University of Leeds and UK Government advice regarding the Covid-19 pandemic.

I am pleased to inform you that the above research ethics application has been reviewed by the Engineering and Physical Science Ethics (EPS/FREC) Committee and on behalf of the Chair, I can confirm a favourable ethical opinion based on the documentation received at date of this email.

Please retain this email as evidence of approval in your study file.

Please notify the committee if you intend to make any amendments to the original research as submitted and approved to date. This includes recruitment methodology; all changes must receive ethical approval prior to implementation. Please see https://ris.leeds.ac.uk/research-ethics-and-integrity/applying-for-an-amendment/ or contact the Research Ethics Administrator for further information researchthics@leeds.ac.uk if required.

Ethics approval does not infer you have the right of access to any member of staff or student or documents and the premises of the University of Leeds. Nor does it imply any right of access to the premises of any other organisation, including clinical areas. The committee takes no responsibility for you gaining access to staff, students and/or premises prior to, during or following your research activities.

Please note: You are expected to keep a record of all your approved documentation, as well as documents such as sample consent forms, risk assessments and other documents relating to the study. This should be kept in your study file, which should be readily available for audit purposes. You will be given a two week notice period if your project is to be audited.

It is our policy to remind everyone that it is your responsibility to comply with Health and Safety, Data Protection and any other legal and/or professional guidelines there may be.

I hope the study goes well.

Best wishes

On behalf ▓▓▓▓▓▓▓, CHAIR, EPS

~~~~~~

MEEC 21-016 Amendment 1 – May 2023 - Approval confirmation

[REDACTED]

Dear John

MEEC 21-016 Amendment 1 – May 2023 - Context- and Terrain-Aware Gait Analysis and Visualisation

NB: All approvals/comments are subject to compliance with current University of Leeds and UK Government advice regarding the Covid-19 pandemic.

We are pleased to inform you that your amendment to your research ethics application has been reviewed by the Faculty of Engineering and Physical Sciences Faculty Committee (EPS REC) and we can confirm that ethics approval is granted based on the documenta on received at date of this email.

Please retain this email as evidence of approval in your study file.

Please no fy the committee if you intend to make any further amendments to the research as submitted and approved to date. This includes recruitment methodology; all changes must receive ethical approval prior to implementation. Please see h ps://ris.leeds.ac.uk/research-ethics-and-integrity/applying-for-an-amendment/ or contact the Research Ethics & Governance Administrator for further information epsresearchethics@leeds.ac.uk if required.

Ethics approval does not infer you have the right of access to any member of staff or student or documents and the premises of the University of Leeds. Nor does it imply any right of access to the premises of any other organisation, including clinical areas. The committee takes no responsibility for you gaining access to staff, students and/or premises prior to, during or following your research ac vi es.

Please note: You are expected to keep a record of all your approved documenta on, as well as documents such as sample consent forms, risk assessments and other documents relating to the study. This should be kept in your study file, which should be readily available for audit purposes. You will be given a two week notice period if your project is to be audited.

It is our policy to remind everyone that it is your responsibility to comply with Health and Safety, Data Protec on and any other legal and/or professional guidelines there may be.

I hope the study continues to go well.

Best wishes

[REDACTED]

On behalf of [REDACTED] ***CHAIR, EPS FREC***
~~~~~~

[REDACTED]

School of Mechanical Engineering

UNIVERSITY OF LEEDS

Participant Information Sheet
Context and Terrain-Aware Gait Analysis and Visualisation

Please also see the Research Participant Privacy Notice and Experimental Procedure documents included with this information sheet.

Invitation to Participate

We'd like to invite you to participate in a research study. Participation in the research is entirely optional but before you decide, please take the time to read the following information and feel free to discuss it with others. This document will first walk you through the research topic and design of the research. Then we will inform you of what to expect during the study. Should you have any questions or require further information, please reach out using the contact information at the end of this document.

Project Summary

Many studies have been conducted in the past to use wearable sensors to record gait (walking-related) data remotely as users perform activities such as walking, climbing stairs, traversing ramps, and sitting down. It is the hope of these studies that one day the process of gait analysis can be made remote, replacing hospital visits and lengthy camera studies with a minimalistic sensor system that is prescribed to enable clinical decisions to be made from real-world data, rather than that collected in a specialised environment. Unfortunately, many of these studies do not consider how an individual's gait can change based on the terrain that one is walking on, which is crucial to provide context to the collected data and prevent incorrect diagnosis or prognosis.

As a result, this study is part of a 3-year PhD project which will capture both the gait data and the environmental data using additional sensors. This data will then be analysed and used to build a system that captures gait activity, terrain, and environment in real time. This research is a key step in enabling such devices to be adopted in healthcare scenarios which will reduce hospital contact time for patients whilst increasing the efficiency and capacity of healthcare systems which have been increasingly strained in recent years.

Why have I been chosen?

You have been chosen because you meet the requirements for this study (healthy participant with fully functional limbs). There will be 20 participants in this study.

Do I have to take part?

Participation in this research is entirely optional and participants are free to decline the invitation or withdraw from the project at any point. If you decide you want to participate, you will be given this information sheet to keep along with a copy of the experimental procedure and a consent form, which you will be asked to sign and return before the data collection can occur.

What to Expect when Taking Part in this Study

This study will involve participants meeting the research team at Chapel Allerton Hospital, where they will be weighed, measured, and asked for their age before being equipped with a sensor system comprised of sensors on the trunk, shanks, and feet. These sensors come in the form of a belt and some insoles for existing shoes. Participants will meet with the study team at the hospital, where they will equip the sensor system before being escorted to specific areas which feature certain terrains and structures (ramps, stairs, etc). At these locations,

UNIVERSITY OF LEEDS

participants will be asked to perform several activities at a leisurely pace. Breaks will be offered between activities, and participants are encouraged to take them, as fatigue will not only increase risk of falling, but will also diminish the quality of gathered data. More significant breaks will be offered when travelling between activity areas.

Participants will perform the following activities:

Index	Activity	Terrain	Location	Exercise
1	Walking	Grass	Outside 1	2x – Walk for 30 seconds
2	Ramp Ascend	Grass	Outside 1	3x – Walk up the ramp
3	Ramp Descend	Grass	Outside 1	3x – Walk down the ramp
4	Standing	Grass	Outside 1	1x – Stand still for 10 seconds
-	Rest Opportunity	-	-	-
5	Walking	Paving Slabs	Gym (Outdoors)	3x – Walk the length of the walkway
6	Walking	Gravel	Gym (Outdoors)	3x – Walk the length of the walkway
7	Standing	Paving Slabs	Gym (Outdoors)	1x – Stand still for 10 seconds
8	Standing	Gravel	Gym (Outdoors)	1x – Stand still for 10 seconds
9	Sit to Stand	Paving Slabs (Chair)	Gym (Outdoors)	3x – Stand up from an outdoor chair
10	Stand to Sit	Paving Slabs (Chair)	Gym (Outdoors)	3x – Sit down on an outdoor chair
11	Sitting	Paving Slabs (Chair)	Gym (Outdoors)	1x – Stay sitting for 10 seconds
-	Rest Opportunity	-	-	-
12	Walking	Laminated Flooring	Gym (Indoors)	2x – Walk for 30 seconds
13	Standing	Laminated Flooring	Gym (Indoors)	1x – Stand still for 10 seconds
14	Sit to Stand	Laminated Flooring (Chair)	Gym (Indoors)	3x – Stand up from an indoor chair
15	Stand to Sit	Laminated Flooring (Chair)	Gym (Indoors)	3x – Sit down on an indoor chair
16	Sitting	Laminated Flooring (Chair)	Gym (Indoors)	1x – Stay sitting for 10 seconds
17	Stair Ascend	Laminated Flooring	Gym (Indoors)	3x – Walk up a set of stairs
18	Stair Descend	Laminated Flooring	Gym (Indoors)	3x – Walk down a set of stairs
-	Rest Opportunity	-	-	-
19	Sit to Stand	Toilet	OT Bathroom	3x – Stand up from a toilet
20	Stand to Sit	Toilet	OT Bathroom	3x – Sit down on a toilet
21	Sitting	Toilet	OT Bathroom	1x – Stay sitting for 10 seconds
-	Rest Opportunity	-	-	-
22	Stair Ascend	Paving Slabs	Outside 2	3x – Walk up a set of stairs
23	Stair Descend	Paving Slabs	Outside 2	3x – Walk down a set of stairs
24	Ramp Ascend (low incline)	Paving Slabs	Outside 2	3x – Walk up the ramp
25	Ramp Descend (low incline)	Paving Slabs	Outside 2	3x – Walk down the ramp
26	Ramp Ascend	Asphalt	Outside 2	3x – Walk up the ramp
27	Ramp Descend	Asphalt	Outside 2	3x – Walk down the ramp
28	Walking	Asphalt	Outside 2	2x – Walk for 30 seconds
29	Standing	Asphalt	Outside 2	1x – Stand still for 10 seconds
-	Rest Opportunity	-	-	-
30	Elevator Up	Lift	Lift	1x – Travel up in the lift
31	Elevator Down	Lift	Lift	1x – Travel down in the lift
32	Walking	Carpet	Chapel	2x – Walk for 30 seconds
33	Standing	Carpet	Chapel	1x – Stand still for 10 seconds
34	Sit to Stand	Carpet	Chapel	3x – Stand up from an indoor chair
35	Stand to Sit	Carpet	Chapel	3x – Sit down on an indoor chair
36	Sitting	Carpet	Chapel	1x – Stay sitting for 10 seconds
37	Stair Ascend	Hospital Stairs	Hospital Stairs	3x – Walk up a set of stairs
38	Stair Descend	Hospital Stairs	Hospital Stairs	3x – Walk down a set of stairs
-	Rest Opportunity	-	-	-

Amendment 1: 3 activities were removed: sitting to laying, laying to sitting, and laying down. Rows, columns, and numbering was updated to reflect this.

Activity and terrain combinations will not be artificially created so performing activities such as stair navigation on grass or gravel will not be required. The whole procedure should not take more than 1 to 2 hours, depending on the chosen lengths of breaks. Participants should note that the sensors will be clipped onto the users clothing using 3D-printed cases and elastic straps, and that there is a risk of skin abrasion as such. To mitigate this risk, we ask that participants wear the recommended clothing, as found in the experimental procedure document which is provided alongside this information sheet.

Once the data collection has been completed, the study will conclude, the sensor system will be removed, and participants will be free to return home. There are no further requirements

for participants to remain a part of the research or engage in any follow-up after the data collection event.

Benefits of Participating

Whilst individual benefits cannot be guaranteed, the creation of this dataset will enable the implementation of a prototype remote gait analysis system to provide key insights into how terrain and environment data can offer a level of robustness to these devices. The findings of this study may also further the field of remote gait analysis by moving away from pure analysis and focussing more on implementation, which may lead to these devices being adopted by healthcare systems in the future. Furthermore, the publication of this dataset will allow other researchers to make further discoveries and, as this is the first of its kind, this dataset may inspire future research to also consider factors such as terrain and environment, bringing these devices closer to real-world adoption.

Potential Risks of Participating

Participants will come into contact with a silicone insole and an elastic-fibre strap, such as those seen in sporting applications for supporting an injured joint. Regarding the sensor system, the system has been designed with comfort and convenience in mind. As such, there should be no additional risks created by equipping the system and performing activities on common terrains which are encountered frequently in daily life.

Use, publication, and storage of research data

After the data is collected on site, it will be processed, anonymised, and stored on the University of Leeds SharePoint cloud storage. The data in this study also has the potential to be published in journal articles and will be published as part of the thesis at the end of the PhD. Data will be anonymised at the point of collection, meaning that it cannot be traced back or used to identify a participant. During publication, this anonymised data will be made available to third parties.

What will happen to my personal information?

After collection, data will be stored with a participant number, rather than a name, resulting in the anonymisation of the data. Any photos or videos taken on site at the time of data collection will be digitally masked to remove any identifying qualities of the participant such as the face and head. Should participants decide to withdraw from the study, any contact information will be destroyed, whilst anonymised data (age, weight, height, gender, questionnaire answers, and gait data) will be retained for the study.

What will happen to the results of the research project?

All the contact information collected during the study will be kept strictly confidential, encrypted, and stored separately from the research data. Additionally, recorded data will be anonymised at the time of collection, to make participants unidentifiable after publication.

The results from this study will be published within 18 months of recording, and participants can request to receive a copy of the results or a link to the article once published. Data collected in this study may be used or analysed further in future studies, but this data will only be available in a fully anonymised state.

Photos and video recordings made during the research will only be used for illustrative purposes in journal articles, conference papers, and lectures. No other use will be made of these images and videos without explicit written consent and in all cases, these will be

blurred/masked to hide the identity of the participant. Nobody outside the research project will ever have access to the original recordings.

What type of information will be sought from me and why is the collection of this information relevant for achieving the research project's objectives?

The personal information collected will include the age, height, weight, shoe size, and gender of participants as these factors will all contribute towards the manner in which a person walks. If all data was collected from people of above average height, or was all collected from a single gender, the dataset would be biased, resulting in a decrease in quality of the analysis and reducing the scope of potential applications. As a result, we need to record these factors to prove the validity of our dataset and enable it to have a significant real-world impact on the largest population possible. Individual age, weight, height, and gender will be anonymised and assigned a subject number along with the recorded gait data.

Who is organising/funding the research?

This research has been organised by the University of Leeds. There are no external independent bodies or companies associated with this research.

Supporting Information

Contact for further information:

Lead Researcher: John Mitchell. Email: menjmi@leeds.ac.uk

Contact for complaints:

Academic Supervisor: Prof. Rory O'Connor. Email: r.j.o'connor@leeds.ac.uk

Documents provided to participants:

- Signed consent form.
- This Participant Information Sheet
- Participant Experimental Procedure
- Research Privacy Notice
- Testing Risk Assessment

Thank you for taking the time to read this information.

Version Control

Project title	Document type	Version #	Date	Changelog
Context- and Terrain-Aware Gait Analysis and Visualisation	Participant Information Sheet	1	15/02/2022	First version.
Context- and Terrain-Aware Gait Analysis and Visualisation	Participant Information Sheet	1.1	24/01/2023	Updated the table of activities.

School of Mechanical Engineering

UNIVERSITY OF LEEDS

Consent to take part in Context- and Terrain-Aware Gait Analysis and Visualisation Participant Number:	Add your initials next to the statement if you agree
I confirm that I have read and understand the information sheet explaining the above research project and I have had the opportunity to ask questions about the project.	
I understand that my participation is voluntary and that I am free to withdraw at any time without reason without negative consequences. Upon withdrawal personal data will be destroyed however anonymised data could be retained as set out in the Participant Information Sheet. Email: ll15j3cm@leeds.ac.uk	
I give permission for members of the research team to have access to my anonymised responses. I understand that my name will not be linked with the research materials, and I will not be identified or identifiable in the report or reports that result from the research.	
I agree for the data collected from me to be stored and used in relevant future research in an anonymised form.	
I agree that photographs and videos may be taken during testing on the conditions that: media is only used to illustrate the research in papers, presentations, lectures, and conferences; and the participants face will be digitally masked to maintain anonymity.	
I understand that other genuine researchers will have access to this data only if they agree to preserve the confidentiality of the information as requested in this form.	
I understand that other researchers may use information collected in publications, reports, web pages, and other research outputs, only if they agree to preserve the confidentiality of the information as requested in this form.	
I understand that relevant sections of the data collected during the study, may be looked at by auditors from the University of Leeds where it is relevant to my taking part in this research. I give permission for these individuals to have access to my records.	
I agree to take part in the above research project and will inform the lead researcher should my contact details change during the project and, if necessary, afterwards.	
I confirm that I am not allergic to silicone or elastic fibres such as those found in sporting joint supports.	

Name of participant	
Participant's signature	
Date	
Name of lead researcher	John Mitchell
Signature	
Date*	

*To be signed and dated in the presence of the participant.
Once this has been signed by all parties the participant will receive a copy of the signed and dated participant consent form, the letter/ pre-written script/ information sheet and any other written information provided to the participants. A copy of the signed and dated consent form should be kept with the project's main documents which must be kept in a secure location.

Project title	Document type	Version #	Date
Context- and Terrain-Aware Gait Analysis and Visualisation	Consent form	1	12/01/2022

Health and Safety Services   Risk Assessment Form

RISK ASSESSMENT DETAILS

Faculty/School/Service Team	Mechanical Engineering

Risk Assessment Title	Data Collection
Risk Assessment Log Reference	
Date	15/02/2022
Name of Assessors	John Mitchell
Manager Responsible	Prof. Abbas Dehghani-Sanij, Prof. Shane Xie. Prof. Rory O'Connor
Location	Chapel Allerton Hospital

Details of Activity
Use of a sensor system to collect gait data during various walking activities on a range of terrains.

Other assessments which might also be required, ☑ if needed:
- Manual Handling ☐ REF
- COSHH ☐ REF
- Personal Protective Equipment (PPE) ☐ REF
- Noise ☐ REF
- Other ☐ REF

DEGREE OF RISK

LIKELIHOOD (L)

5	Inevitable
4	Highly Likely
3	Possible
2	Unlikely
1	Remote Possibility

SEVERITY (S)

5	Very High -Multiple Deaths
4	High - Death, serious injury, permanent disability
3	Moderate - RIDDOR over 7 days
2	Slight - First Aid treatment
1	Nil - Very Minor

RISK RATING MATRIX

		SEVERITY				
		1	2	3	4	5
LIKELIHOOD	1	1	2	3	4	5
	2	2	4	6	8	10
	3	3	6	9	12	15
	4	4	8	12	16	20
	5	5	10	15	20	25

PERSONS AT RISK

PERSONS AT RISK

Employees
Students
Clients
Contractors
Members of the public
Work Experience students
Other Persons

REVIEW DATES

RISK RATING SCORE	ACTION
1 - 4	Broadly Acceptable - No action required
5 - 9	Moderate - Reduce risks if reasonably practicable
10 -15	High Risk - Priority Action to be undertaken
16 -25	Unacceptable **-Action must be taken IMMEDIATELY**

1

Health and Safety Services　　　　**Risk Assessment Form**　　　　UNIVERSITY OF LEEDS

HAZARD AND RELATED ACTIVITIES e.g. trip, falling objects, fire, explosion, noise, violence etc.	PERSONS AT RISK e.g. Employees, Customers, Contractors, Members of the public	POSSIBLE OUTCOME	RISK RATING BEFORE CONTROLS (LxS)	EXISTING CONTROLS e.g. Guards, Safe Systems of Work, Training, Instruction, Authorised Users, Competent Persons, Personal Protective Equipment (PPE)	RISK RATING AFTER CURRENT CONTROLS (LxS)	FURTHER CONTROLS REQUIRED?	RISK RATING AFTER ADDITIONAL CONTROLS (LxS)
Trip/fall	Participant/Researcher	Fall, potentially down a set of stairs	8	Period of familiarity with the sensor system on safe terrain before data collection. Terrains are chosen to be familiar to participants and safe.	3		
Rash or abrasion caused by sensor system	Participant	Superficial abrasion	2	Participant feedback will be gathered throughout the procedure to monitor comfort. Purchased elastic and flexible materials will be those used for common sporting purposes.	2		
Coronavirus	Participant/Researcher	Contraction of COVID-19	9	Participants are required to take lateral flow tests, young participants are chosen, many activities are in ventilated areas or outside, masks and hand sanitiser will be available, date pushed back to avoid the winter peak in cases.	3		

Health and Safety Services　　　　**Risk Assessment Form**　　　　UNIVERSITY OF LEEDS

MANAGEMENT AGREED ADDITIONAL CONTROL MEASURES REQUIRED		ACTIONED BY			ACTION COMPLETE	
		POSITION	NAME	DATE	MANAGER SIG	DATE

COMMUNICATION OF RISK ASSESSMENT FINDINGS TO STAFF				
	METHOD	YES	DATE	COMMENTS
REFERENCE OF FORMAL COMMUNICATION TO STAFF	Copy of risk assessment issued to staff			
	Controls covered in team procedure issued to staff			
	Staff Handbook issued to staff			
	Other -			
ADDITIONAL METHODS OF COMMUNICATION	Induction			
	Toolbox Talk			
	Team Meeting			
	E-mail circulation			
	Other -			

3

COMMENTS AND INFORMATION
(Use this section to record any dynamic risk assessment comments and information)

Do additional controls adequately lower high risk activities to an acceptable level?	YES / NO	SIGNATURE OF MANAGER "The risks identified in this assessment are controlled so far as is reasonably practicable"	
	If NO explain in comments box above	Signature:	Date:
		Abbas Dehghani	15/2/2022
		Rory J O'Connor	15/02/2022
		Shane Xie	16/02/2022

Health and Safety Services			**Risk Assessment Form**		**UNIVERSITY OF LEEDS**

DATE OF REASSESSMENT (Every two years minimum)	**ARE THERE ANY CHANGES TO THE ACTIVITY SINCE THE LAST ASSESSMENT?**	**SIGNATURE OF MANAGER**

LOCATION OF CURRENT SIGNED RISK ASSESSMENT	

RISK ASSESSMENT LOG											
Directorate:						Area:					
Section/Team	Risk Assessment Title	Version No.	Risk Assessment Category	Code /Location	Risk Assessor	Manager responsible for signing off risk assessment	Date assessment signed off	Review Due	Review Date	Outstanding Controls/Actions Yes/No	Comments

Health and Safety Services   Risk Assessment Form

UNIVERSITY OF LEEDS

UNIVERSITY OF LEEDS

Participant Experimental Procedure

To be supplied along with the participant information sheet.

What Should I Wear?

Shoes and Socks

Participants will have several devices attached to and inserted into their shoes. These shoes will be provided, and a range of sizes will be available. For sanitary reasons, please wear socks.

Avoid Tight Trousers

Baggy/elasticated trousers are advised for comfort and to enable a small box to be fitted to the top of the trousers via a clip. Try to avoid wearing a belt as this may make the clip uncomfortable.

The Sensor System

Foot Sensor

The foot sensor features a silicone insole which is placed within the shoes, a box which attaches to the side of the shoes via a clip, and another box which attaches to the top of the shoe via the laces.

Ankle Sensor

The ankle sensor features a box fitted to the outer side of the leg, along with a small sensor on the back of the ankle.

Waist Sensor

The waist sensor will consist of a small box which clips to the back of the trousers.

Where should I go?

The procedure will take place at Chapel Allerton Hospital in Leeds. Upon arriving the research team will meet you at the entrance and we will make our way down to the bottom floor where a weight and height measurement will be taken.

What Activities Will I Perform?

Participants will perform 38 short activities in 8 different areas of Chapel Allerton Hospital. A full list of activities can be seen below:

Index	Activity	Terrain	Location	Exercise
1	Walking	Grass	Outside 1	2x – Walk for 30 seconds
2	Ramp Ascend	Grass	Outside 1	3x – Walk up the ramp
3	Ramp Descend	Grass	Outside 1	3x – Walk down the ramp
4	Standing	Grass	Outside 1	1x – Stand still for 10 seconds
-	Rest Opportunity	-	-	-
5	Walking	Paving Slabs	Gym (Outdoors)	3x – Walk the length of the walkway
6	Walking	Gravel	Gym (Outdoors)	3x – Walk the length of the walkway
7	Standing	Paving Slabs	Gym (Outdoors)	1x – Stand still for 10 seconds
8	Standing	Gravel	Gym (Outdoors)	1x – Stand still for 10 seconds
9	Sit to Stand	Paving Slabs (Chair)	Gym (Outdoors)	3x – Stand up from an outdoor chair
10	Stand to Sit	Paving Slabs (Chair)	Gym (Outdoors)	3x – Sit down on an outdoor chair
11	Sitting	Paving Slabs (Chair)	Gym (Outdoors)	1x – Stay sitting for 10 seconds
-	Rest Opportunity	-	-	-
12	Walking	Laminated Flooring	Gym (Indoors)	2x – Walk for 30 seconds
13	Standing	Laminated Flooring	Gym (Indoors)	1x – Stand still for 10 seconds
14	Sit to Stand	Laminated Flooring (Chair)	Gym (Indoors)	3x – Stand up from an indoor chair
15	Stand to Sit	Laminated Flooring (Chair)	Gym (Indoors)	3x – Sit down on an indoor chair

16	Sitting	Laminated Flooring (Chair)	Gym (Indoors)	1x – Stay sitting for 10 seconds
17	Stair Ascend	Laminated Flooring	Gym (Indoors)	3x – Walk up a set of stairs
18	Stair Descend	Laminated Flooring	Gym (Indoors)	3x – Walk down a set of stairs
-	Rest Opportunity	-	-	-
19	Sit to Stand	Toilet	OT Bathroom	3x – Stand up from a toilet
20	Stand to Sit	Toilet	OT Bathroom	3x – Sit down on a toilet
21	Sitting	Toilet	OT Bathroom	1x – Stay sitting for 10 seconds
-	Rest Opportunity	-	-	-
22	Stair Ascend	Paving Slabs	Outside 2	3x – Walk up a set of stairs
23	Stair Descend	Paving Slabs	Outside 2	3x – Walk down a set of stairs
24	Ramp Ascend (low incline)	Paving Slabs	Outside 2	3x – Walk up the ramp
25	Ramp Descend (low incline)	Paving Slabs	Outside 2	3x – Walk down the ramp
26	Ramp Ascend	Asphalt	Outside 2	3x – Walk up the ramp
27	Ramp Descend	Asphalt	Outside 2	3x – Walk down the ramp
28	Walking	Asphalt	Outside 2	2x – Walk for 30 seconds
29	Standing	Asphalt	Outside 2	1x – Stand still for 10 seconds
-	Rest Opportunity	-	-	-
30	Elevator Up	Lift	Lift	1x – Travel up in the lift
31	Elevator Down	Lift	Lift	1x – Travel down in the lift
32	Walking	Carpet	Chapel	2x – Walk for 30 seconds
33	Standing	Carpet	Chapel	1x – Stand still for 10 seconds
34	Sit to Stand	Carpet	Chapel	3x – Stand up from an indoor chair
35	Stand to Sit	Carpet	Chapel	3x – Sit down on an indoor chair
36	Sitting	Carpet	Chapel	1x – Stay sitting for 10 seconds
37	Stair Ascend	Hospital Stairs	Hospital Stairs	3x – Walk up a set of stairs
38	Stair Descend	Hospital Stairs	Hospital Stairs	3x – Walk down a set of stairs
-	Rest Opportunity	-	-	-

What if I need a rest outside of the rest opportunities?

If participants need to rest, to visit the toilet, or to stop for any other reason, please inform the researchers and the sensor system will be unequipped for the duration of the rest. Please don't hesitate to let the research team know if a rest is needed, as fatigue or discomfort will diminish the quality of the data and could increase the risk of a fall. On the other hand, if rest opportunities are not needed before moving to a new area, this option is also available. The data collection procedure is flexible as data is only be recorded during an activity, so feel free to give feedback throughout the process.

What can I expect when performing one of the activities?

Before the data recording of an activity, participants will be told or shown where to move and what to do. After this demonstration, a countdown will be given in the form "3, 2, 1, Go". On 'Go' the data collection will begin and participants will be free to perform the activity. Data collection will be automatically stopped upon reaching the end of the activity, or with another countdown in the case of timed events.

What happens when all activities are completed?

When all activities are complete, the sensor system will be removed, and participants are free to leave.

Project title	Document type	Version #	Date	Changelog
Context- and Terrain-Aware Gait Analysis and Visualisation	Participant Experimental Procedure	1	15/02/2022	First version.
Context- and Terrain-Aware Gait Analysis and Visualisation	Participant Experimental Procedure	1.1	24/01/2023	Removed bed activity from activity list.